MycoKeys 54: 1–29 (2019)
doi: 10.3897/mycokeys.54.35018
http://mycokeys.pensoft.net

RESEARCH ARTICLE

A peer-reviewed open-access journal
MycoKeys
Launched to accelerate biodiversity research

Cacaoporus, a new Boletaceae genus, with two new species from Thailand

Santhiti Vadthanarat[1,2,3], Saisamorn Lumyong[1,3,6], Olivier Raspé[4,5]

1 *Department of Biology, Faculty of Science, Chiang Mai University, Chiang Mai, 50200, Thailand* **2** *PhD's Degree Program in Biodiversity and Ethnobiology, Department of Biology, Faculty of Science, Chiang Mai University, Chiang Mai, 50200, Thailand* **3** *Center of Excellence in Microbial Diversity and Sustainable Utilization, Faculty of Science, Chiang Mai University, Chiang Mai, 50200, Thailand* **4** *Meise Botanic Garden, Nieuwelaan 38, 1860 Meise, Belgium* **5** *Fédération Wallonie-Bruxelles, Service général de l'Enseignement universitaire et de la Recherche scientifique, Rue A. Lavallée 1, 1080 Bruxelles, Belgium* **6** *Academy of Science, The Royal Society of Thailand, Bangkok, 10300, Thailand*

Corresponding author: *Olivier Raspé* (olivier.raspe@botanicgardenmeise.be)

Academic editor: *M. P. Martín* | Received 30 March 2019 | Accepted 26 April 2019 | Published 10 June 2019

Citation: Vadthanarat S, Lumyong S, Raspé O (2019) *Cacaoporus*, a new Boletaceae genus, with two new species from Thailand. MycoKeys 54: 1–29. https://doi.org/10.3897/mycokeys.54.35018

Abstract

We introduce a new genus, *Cacaoporus*, characterised by chocolate brown to dark brown basidiomata and hymenophore, tubes not separable from the pileus context, white to off-white basal mycelium, reddening when bruised, amygdaliform to ovoid spores and dark brown spore deposit. Phylogenetic analyses of a four-gene dataset (*atp*6, *tef*1, *rpb*2 and *cox*3) with a wide selection of Boletaceae showed that the new genus is monophyletic and sister to the genera *Cupreoboletus* and *Cyanoboletus* in the *Pulveroboletus* group. Two new species in the genus, *C. pallidicarneus* and *C. tenebrosus* are described from northern Thailand. Full descriptions and illustrations of the new genus and species are presented. The phylogeny also confirmed the reciprocal monophyly of *Neoboletus* and *Sutorius*, which further support the separation of these two genera.

Keywords

3 new taxa, *atp*6, Boletales, *cox*3, Fungal Diversity, multigene phylogeny, *Neoboletus*, *Pulveroboletus* group, Taxonomy

Introduction

In the last decade or so, since molecular techniques and phylogenetic analyses have been used in taxonomy and systematics of the Boletaceae, many new species and genera have been described worldwide (e.g. Halling et al. 2012, 2016; Zeng et al. 2012; Arora and Frank 2014; Gelardi et al. 2014, 2015; Li et al. 2014, Zhao et al. 2014b, Zeng et al. 2014; Wu et al. 2015, 2016; Zhu et al. 2015). In Thailand, although the Boletaceae have been studied for a long time, only a few new Boletaceae species and a new genus have recently been described (Desjardin et al. 2009; Neves et al. 2012; Halling et al. 2014; Raspé et al. 2016; Vadthanarat et al. 2018). At the same time, many new species and genera have been described from southern and south-western China, an area with a climate and forests similar to Thailand (e.g. Li et al. 2011; Wu et al. 2015, 2016; Zhu et al. 2015). Similarly, a high number of new species and possibly new genera are expected to occur in Thailand (Hyde et al. 2018)

During our survey on the diversity of boletes in Thailand, several collections of brown to chocolate to dark brown boletes were obtained. Some collections bearing resemblance to *Sutorius* Halling, Nuhn & N.A. Fechner species, which typically have brown or reddish to purplish-brown basidiomata with reddish to purplish-brown hymenophore, reddish-brown spore deposit and narrowly ellipsoid to ellipsoid basidiospores (Halling et al. 2012). However, our chocolate brown bolete collections also showed differences, in particular in having a darker hymenophore, as well as in some microscopic characters like spore shape. We therefore performed a family-wide phylogeny, which showed that those brown to chocolate to dark brown boletes belong in a generic lineage, different from *Sutorius*. Consequently, we introduce the new Boletaceae genus *Cacaoporus* and describe two new species, *C. pallidicarneus* and *C. tenebrosus*, with full descriptions and illustrations.

Materials and method

Specimens collecting

Fresh basidiomata were collected in Chiang Mai Province, northern Thailand during the rainy season in 2013 to 2018. The specimens were photographed *in situ*, wrapped in aluminium foil and taken to the laboratory. After description of macroscopic characters, the specimens were dried in an electric drier at 45–50 °C. Examined specimens were deposited in the herbaria CMUB, MFLU, BKF and BR (listed in Index Herbariorum; Thiers, continuously updated).

Morphological studies

Macroscopic descriptions were made, based on detailed field notes and photos of fresh basidiomata. Colour codes were taken from Kornerup and Wanscher (1978). Macrochemical reactions (colour reactions) of pileus, pileus context, stipe, stipe context and hy-

menophore were determined using 10% aqueous potassium hydroxide (KOH) and 28–30% ammonium hydroxide (NH_4OH). Microscopic structures were observed from dried specimens, using 5% KOH, NH_4OH, Melzer's reagent or stained with 1% ammoniacal Congo red. A minimum of 50 basidiospores, 20 basidia and 20 cystidia were randomly measured at 1000× with a calibrated ocular micrometer using an Olympus CX51 compound microscope. The notation '[m/n/p]' represents the number of basidiospores "m" measured from "n" basidiomata of "p" collections. Dimensions of microscopic structures are presented in the following format: (a–)b–c–d(–e), in which "c" represents the average, "b" the 5th percentile, "d" the 95th percentile, "a" the minimum and "e" the maximum. *Q*, the length/width ratio, is presented in the same format. A section of the pileus surface was radially and perpendicularly cut to the surface at a point halfway between the centre and margin of the pileus. Sections of stipitipellis were taken from halfway up the stipe and longitudinally cut, perpendicularly to the surface (Hosen et al. 2013; Li et al. 2011). All microscopic features were drawn by free hand using an Olympus Camera Lucida model U–DA fitted to the microscope cited above. For scanning electron microscopy (SEM), a spore print was mounted on to an SEM stub with double-sided tape. The samples were coated with gold, then examined and photographed with a JEOL JSM–5910 LV SEM.

DNA isolation, PCR amplification and DNA sequencing

Genomic DNA was extracted from fresh tissue preserved in CTAB or about 10–15 mg of dried tissue using a CTAB isolation procedure adapted from Doyle and Doyle (1990). Portions of the genes *atp*6, *tef*1, *rpb*2 and *cox*3 were amplified by polymerase chain reaction (PCR) and sequenced by Sanger sequencing. The primer pairs ATP6-1M40F/ATP6-2M (Raspé et al. 2016), EF1-983F/EF1-2218R (Rehner and Buckley 2005) and bRPB2-6F/bRPB2-7.1R (Matheny 2005) were used to amplify *atp*6, *tef*1 and *rpb*2, respectively. Part of the mitochondrial gene *cox*3 was amplified with the newly designed primers COX3M1-F (5'-ATYGGAGCWGTAATGTWYATGC-3') and COX3M1-R (5'-CCWACTAWTACRTGRATWCCATG-3'), using the following PCR programme: 2 min 30 s at 95 °C; 35 cycles of 25 s at 95 °C, 30 s at 48 °C, 30 s at 72 °C; 3 min at 72 °C. PCR products were purified by adding 1 U of Exonuclease I and 0.5 U FastAP Alkaline Phosphatase (Thermo Scientific, St. Leon-Rot, Germany) and incubated at 37 °C for 1 h, followed by inactivation at 80 °C for 15 min. Standard Sanger sequencing was performed in both directions by Macrogen Europe (The Netherlands) with PCR primers, except for *atp*6, for which universal primers M13F-pUC(-40) and M13F(-20) were used; for *tef*1, additional sequencing was performed with two internal primers, EF1-1577F and EF1-1567R (Rehner and Buckley 2005).

Alignment and phylogeny inference

The sequences were assembled in GENEIOUS Pro v. 6.0.6 (Biomatters) and introns were removed prior to alignment based on the amino acid sequence of previously

published sequences. All sequences, including sequences from GenBank, were aligned using MAFFT (Katoh and Standley 2013) on the server accessed at http://mafft.cbrc.jp/alignment/server/.

Maximum Likelihood (ML) phylogenetic inference was performed using RAxML (Stamatakis 2006) on the CIPRES web portal (RAxML-HPC2 on XSEDE; Miller et al. 2009). The phylogenetic tree was inferred by a single analysis with three partitions (one for each gene), using the GTRCAT model with 25 categories, two *Buchwaldoboletus* and nine *Chalciporus* species from sub-family Chalciporoideae were used as outgroup since Chalciporoideae always appeared as sister to the remainder of the Boletaceae in recent phylogenetic analyses (e.g. Nuhn et al. 2013; Wu et al. 2014, 2016). Statistical support of clades was obtained with 1,000 rapid bootstrap replicates.

For Bayesian Inference (BI), the best-fit model of substitution amongst those implementable in MrBayes was estimated separately for each gene using jModeltest (Darriba et al. 2012) on the CIPRES portal, based on the Bayesian Information Criterion (BIC). The selected models were HKY+I+G for *atp*6 and *rpb*2 and GTR+I+G for *cox*3 and *tef*1. Partitioned Bayesian analysis was performed with MrBayes 3.2 (Ronquist et al. 2012) on the CIPRES portal. Two runs of five chains were run for 15,000,000 generations and sampled every 500 generations. The chain temperature was decreased to 0.02 to improve convergence. At the end of the run, the average deviation of split frequencies was 0.008147.

Results

Phylogenetic analysis

A total of 325 sequences were newly generated and deposited in GenBank (Table 1). The alignment contained 1,013 sequences from four genes (186 for *atp*6, 358 for *tef*1, 326 for *rpb*2, 143 for *cox*3) from 362 voucher specimens and was 2946 characters long (TreeBase number 23886).

The four-gene analyses retrieved the six subfamilies (Austroboletoideae, Boletoideae, Chalciporoideae, Leccinoideae, Xerocomoideae, Zangioideae) as monophyletic (Fig. 1). The genera belonging to the *Pulveroboletus* group of Wu et al. (2014, 2016) did not form a monophyletic group. The new genus, *Cacaoporus* was monophyletic (BS=100% and PP=1) within a clade containing the genera *Cupreoboletus* Simonini, Gelardi & Vizzini and *Cyanoboletus* Gelardi, Vizzini & Simonini and one undescribed taxon, *Boletus* p.p. sp., clade 2 (specimen voucher JD0693) with high support (BS=94% and PP=0.99). The macromorphologically most similar genus, *Sutorius*, formed another clade (BS=100% and PP=1) sister to *Neoboletus* Gelardi, Simonini & Vizzini, with 67% BS and 0.97 PP support, in another clade of the *Pulveroboletus* group.

Our phylogeny also showed that thirteen *Sutorius* species including *S. brunneissimus* (W.F. Chiu) G. Wu & Zhu L. Yang, *S. ferrugineus* G. Wu, Fang Li & Zhu L. Yang, *S. flavidus* G. Wu & Zhu L. Yang, *S. hainanensis* (T.H. Li & M. Zang) G. Wu & Zhu L. Yang, *S. junquilleus* (Quél.) G. Wu & Zhu L. Yang, *S. magnificus* (W.F. Chiu) G. Wu &

Table 1. List of collections used for DNA analyses, with origin, GenBank accession numbers and reference(s).

Species	Voucher	Origin	*atp6*	*cox3*	*tef1*	*rpb2*	Reference(s)
Afroboletus aff. *multijugus*	JD671	Burundi	MH614651	MH614794	MH614700	MH614747	This study
Afroboletus costatisporus	ADK4644	Togo	KT823958	MH614795*	KT824024	KT823991	Raspé et al. 2016; *This study
Afroboletus luteolus	ADK4844	Togo	MH614652	MH614796	MH614701	MH614748	This study
Aureoboletus catenarius	HKAS54467	China	–	–	KT990711	KT990349	Wu et al. 2016
Aureoboletus duplicatoporus	HKAS50498	China	–	–	KF112230	KF112754	Wu et al. 2014
Aureoboletus gentilis	ADK4865	Belgium	KT823961	MH614797*	KT824027	KT823994	Raspé et al. 2016; *This study
Aureoboletus mirabilis	HKAS57776	China	–	–	KF112229	KF112743	Wu et al. 2014
Aureoboletus moravicus	VDKO1120	Belgium	MG212528	MH614798*	MG212573	MG212615	Vadthanarat et al. 2018; *This study
Aureoboletus nephrosporus	HKAS67931	China	–	–	KT990720	KT990357	Wu et al. 2016
Aureoboletus projectellus	AFTOL-ID-713	USA	DQ534604*	–	AY879116	AY787218	*Binder and Hibbett 2006; Binder et al., Unpublished
Aureoboletus shichianus	HKAS76852	China	–	–	KF112237	KF112756	Wu et al. 2014
Aureoboletus sp.	HKAS56317	China	–	–	KF112239	KF112753	Wu et al. 2014
Aureoboletus sp.	OR0245	China	MH614653	MH614799	MH614702	MH614749	This study
Aureoboletus sp.	OR0369	Thailand	MH614654	MH614800	MH614703	MH614750	This study
Aureoboletus thibetanus	HKAS76655	China	–	–	KF112236	KF112752	Wu et al. 2014
Aureoboletus thibetanus	AFTOL-ID-450	China	DQ534600*	–	DQ029199	DQ366279	*Binder and Hibbett 2006; Unpublished
Aureoboletus tomentosus	HKAS80485	China	–	–	KT990715	KT990353	Wu et al. 2016
Aureoboletus viscosus	OR0361	Thailand	MH614655	MH614801	MH614704	MH614751	This study
Aureoboletus zangii	HKAS74766	China	–	–	KT990726	KT990363	Wu et al. 2016
Austroboletus cf. *dictyotus*	OR0045	Thailand	KT823966	MH614802*	KT824032	KT823999	Raspé et al. 2016; *This study
Austroboletus cf. *subvirens*	OR0573	Thailand	MH614656	MH614803	MH614705	MH614752	This study
Austroboletus eburneus	REH9487	Australia	–	–	JX889708	–	Halling et al. 2012b
Austroboletus olivaceoglutinosus	HKAS57756	China	–	–	KF112212	KF112764	Wu et al. 2014
Austroboletus sp.	HKAS59624	China	–	–	KF112217	KF112765	Wu et al. 2014
Austroboletus sp.	OR0891	Thailand	MH614657	MH614804	MH614706	MH614753	This study
Baorangia major	OR0209	Thailand	MG897421	MK372295*	MG897431	MG897441	Phookamsak et al. 2019; *This study
Baorangia pseudocalopus	HKAS63607	China	–	–	KF112167	KF112677	Wu et al. 2014
Baorangia pseudocalopus	HKAS75739	China	–	–	KJ184570	KM605179	Wu et al. 2015
Baorangia pseudocalopus	HKAS75081	China	–	–	KF112168	KF112678	Wu et al. 2014
Baorangia rufomaculata	BOTH4144	USA	MG897415	MH614805*	MG897425	MG897435	Phookamsak et al. 2019; *This study
Boletellus ananas	NY815459	Costa Rica	–	–	KF112308	KF112760	Wu et al. 2014
Boletellus ananas	K(M)123769	Belize	MH614658	MH614807	MH614707	MH614754	This study
Boletellus aff. *emodensis*	OR0061	Thailand	KT823970	MH614806*	KT824036	KT824003	Raspé et al. 2016; *This study
Boletellus sp.	HKAS59536	China	–	–	KF112306	KF112758	Wu et al. 2014
Boletellus sp.	OR0621	Thailand	MG212529	MH614808*	MG212574	MG212616	Vadthanarat et al. 2018; *This study
Boletus aereus	VDKO1055	Belgium	MG212530	MH614809*	MG212575	MG212617	Vadthanarat et al. 2018; *This study
Boletus albobrunnescens	OR0131	Thailand	KT823973	MH614810*	KT824039	KT824006	Raspé et al. 2016; *This study
Boletus botryoides	HKAS53403	China	–	–	KT990738	KT990375	Wu et al. 2016
Boletus edulis	HMJAU4637	Russia	–	–	KF112202	KF112704	Wu et al. 2014
Boletus edulis	VDKO0869	Belgium	MG212531	MH614811*	MG212576	MG212618	Vadthanarat et al. 2018; *This study
Boletus p.p. sp	JD0693	Burundi	MH645583	–	MH645591	MH645599	This study
Boletus p.p. sp.	OR0832	Thailand	MH645584	MH645605	MH645592	MH645600	This study

Species	Voucher	Origin	*atp6*	*cox3*	*tef1*	*rpb2*	Reference(s)
Boletus p.p. sp.	OR1002	Thailand	MH645585	MH645606	MH645593	MH645601	This study
Boletus pallidus	BOTH4356	USA	MH614659	MH614812	MH614708	–	This study
Boletus pallidus	TDB-1231-Bruns	–	AF002142	AF002154	–	–	Kretzer and Bruns 1999
Boletus reticuloceps	HKAS57671	China	–	–	KF112201	KF112703	Wu et al. 2014
Boletus s.s. sp.	OR0446	China	MG212532	MH614813*	MG212577	KF112703	Vadthanarat et al. 2018; *This study
Boletus sp.	HKAS59660	China	–	–	KF112153	KF112664	Wu et al. 2014
Boletus sp.	HKAS63598	China	–	–	KF112152	KF112663	Wu et al. 2014
Boletus violaceofuscus	HKAS62900	China	–	–	KF112219	KF112762	Wu et al. 2014
Borofutus dhakanus	HKAS73789	Bangladesh	–	–	JQ928576	JQ928597	Hosen et al. 2013
Borofutus dhakanus	OR0345	Thailand	MH614660	MH614814	MH614709	MH614755	This study
Buchwaldoboletus lignicola	HKAS76674	China	–	–	KF112277	KF112819	Wu et al. 2014
Buchwaldoboletus lignicola	VDKO1140	Belgium	MH614661	MH614815	MH614710	MH614756	This study
Butyriboletus appendiculatus	VDKO0193b	Belgium	MG212537	MH614816*	MG212582	MG212624	Vadthanarat et al. 2018; *This study
Butyriboletus cf. *roseoflavus*	OR0230	China	KT823974	MH614819*	KT824040	KT824007	Raspé et al. 2016; *This study
Butyriboletus frostii	NY815462	USA	–	–	KF112164	KF112675	Wu et al. 2014
Butyriboletus pseudoregius	VDKO0925	Belgium	MG212538	MH614817*	MG212583	MG212625	Vadthanarat et al. 2018; *This study
Butyriboletus pseudospeciosus	HKAS63513	China	–	–	KT990743	KT990380	Wu et al. 2016
Butyriboletus roseoflavus	HKAS54099	China	–	–	KF739779	KF739703	Wu et al. 2014
Butyriboletus roseopurpureus	BOTH4497	USA	MG897418	MH614818*	MG897428	MG897438	Phookamsak et al., 2019; *This study
Butyriboletus sp.	HKAS52661	China	–	–	KF112169	KF112676	Wu et al. 2014
Butyriboletus sp.	HKAS52525	China	–	–	KF112163	KF112671	Wu et al. 2014
Butyriboletus sp.	HKAS57774	China	–	–	KF112155	KF112670	Wu et al. 2014
Butyriboletus sp.	HKAS59814	China	–	–	KF112199	KF112699	Wu et al. 2014
Butyriboletus sp.	HKAS63528	China	–	–	KF112156	KF112673	Wu et al. 2014
Butyriboletus sp.	MHHNU7456	China	–	–	KT990741	KT990378	Wu et al. 2016
Butyriboletus subsplendidus	HKAS50444	China	–	–	KT990742	KT990379	Wu et al. 2016
Butyriboletus yicibus	HKAS55413	China	–	–	KF112157	KF112674	Wu et al. 2014
Cacaoporus pallidicarneus	OR0681	Thailand	MK372259	MK372296	–	MK372283	This study
Cacaoporus pallidicarneus	OR0683	Thailand	MK372260	MK372297	–	MK372284	This study
Cacaoporus pallidicarneus	OR1306	Thailand	MK372261	MK372298	MK372272	MK372285	This study
Cacaoporus pallidicarneus	SV0221	Thailand	MK372262	MK372299	MK372273	MK372286	This study
Cacaoporus pallidicarneus	SV0451	Thailand	MK372263	MK372300	MK372274	MK372287	This study
Cacaoporus sp.	SV0402	Thailand	MK372270	–	MK372281	MK372293	This study
Cacaoporus tenebrosus	OR0654	Thailand	MK372264	MK372301	MK372275	MK372288	This study
Cacaoporus tenebrosus	OR1435	Thailand	MK372265	MK372302	MK372276	MK372289	This study
Cacaoporus tenebrosus	SV0223	Thailand	MK372266	MK372303	MK372277	MK372290	This study
Cacaoporus tenebrosus	SV0224	Thailand	MK372267	MK372304	MK372278	MK372291	This study
Cacaoporus tenebrosus	SV0422	Thailand	MK372268	MK372305	MK372279	–	This study
Cacaoporus tenebrosus	SV0452	Thailand	MK372269	MK372306	MK372280	MK372292	This study
Caloboletus aff. *calopus*	HKAS74739	China	–	–	KF112166	KF112667	Wu et al. 2014
Caloboletus calopus	ADK4087	Belgium	MG212539	MH614820	KJ184566	KP055030	Vadthanarat et al. 2018; Zhao et al. 2014a, b; This study
Caloboletus inedulis	BOTH3963	USA	MG897414	MH614821*	MG897424	MG897434	Phookamsak et al. 2019; *This study
Caloboletus panniformis	HKAS55444	China	–	–	KF112165	KF112666	Wu et al. 2014
Caloboletus radicans	VDKO1187	Belgium	MG212540	MH614822*	MG212584	MG212626	Vadthanarat et al. 2018; *This study
Caloboletus sp.	HKAS53353	China	–	–	KF112188	KF112668	Wu et al. 2014
Caloboletus sp.	OR0068	Thailand	MH614662	MH614823	MH614711	MH614757	This study
Caloboletus yunnanensis	HKAS69214	China	–	–	KJ184568	KT990396	Zhao et al. 2014a; Wu et al. 2016
Chalciporus aff. *piperatus*	OR0586	Thailand	KT823976	MH614824*	KT824042	KT824009	Raspé et al. 2016; *This study
Chalciporus aff. *rubinus*	OR0139	China	MH614663	–	MH614712	MH614758	This study

Species	Voucher	Origin	*atp6*	*cox3*	*tef1*	*rpb2*	Reference(s)
Chalciporus africanus	JD517	Cameroon	KT823963	MH614825*	KT824029	KT823996	Raspé et al. 2016; *This study
Chalciporus piperatus	VDKO1063	Belgium	MH614664	MH614826	MH614713	MH614759	This study
Chalciporus rubinus	AF2835	Belgium	KT823962	–	KT824028	KT823995	Raspé et al. 2016
Chalciporus sp.	HKAS53400	China	–	–	KF112279	KF112821	Wu et al. 2014
Chalciporus sp.	HKAS74779	China	–	–	KF112278	KF112820	Wu et al. 2014
Chalciporus sp.	OR0363	Thailand	MH645586	MH645607	MH645594	MH645602	This study
Chalciporus sp.	OR0373	Thailand	MH645587	MH645608	MH645595	MH645603	This study
Chiua sp.	OR0141	China	MH614665	MH614827	MH614714	MH614760	This study
Chiua virens	OR0266	China	MG212541	MH614828*	MG212585	MG212627	Vadthanarat et al. 2018; *This study
Chiua viridula	HKAS74928	China	–	–	KF112273	KF112794	Wu et al. 2014
Crocinoboletus cf. *laetissimus*	OR0576	Thailand	KT823975	MH614833*	KT824041	KT824008	Raspé et al. 2016; *This study
Crocinoboletus rufoaureus	HKAS53424	China	–	–	KF112206	KF112710	Wu et al. 2014
Cupreoboletus poikilochromus	GS10070	Italy	–	–	KT157072	KT157068	Gelardi et al. 2015
Cupreoboletus poikilochromus	GS11008	Italy	–	–	KT157071	KT157067	Gelardi et al. 2015
Cyanoboletus brunneoruber	HKAS80579_1	China	–	–	KT990763	KT990401	Wu et al. 2016
Cyanoboletus brunneoruber	OR0233	China	MG212542	MH614834*	MG212586	MG212628	Vadthanarat et al. 2018; *This study
Cyanoboletus instabilis	HKAS59554	China	–	–	KF112186	KF112698	Wu et al. 2014
Cyanoboletus pulverulentus	RW109	Belgium	KT823980	MH614835*	KT824046	KT824013	Raspé et al. 2016; *This study
Cyanoboletus sinopulverulentus	HKAS59609	China	–	–	KF112193	KF112700	Wu et al. 2014
Cyanoboletus sp.	HKAS52639	China	–	–	KF112195	KF112701	Wu et al. 2014
Cyanoboletus sp.	HKAS76850	China	–	–	KF112187	KF112697	Wu et al. 2014
Cyanoboletus sp.	OR0257	China	MG212543	MH614836*	MG212587	MG212629	Vadthanarat et al. 2018; *This study
Cyanoboletus sp.	HKAS90208_1	China	–	–	KT990766	KT990404	Wu et al. 2016
Cyanoboletus sp.	OR0322	Thailand	MH614673	MH614837	MH614722	MH614768	This study
Cyanoboletus sp.	OR0491	China	MH614674	MH614838	MH614723	MH614769	This study
Cyanoboletus sp.	OR0961	Thailand	MH614675	MH614839	MH614724	MH614770	This study
Fistulinella prunicolor	REH9880	Australia	MH614676	MH614840	MH614725	MH614771	This study
Gymnogaster boletoides	NY01194009	Australia	–	–	KT990768	KT990406	Wu et al. 2016
Harrya atriceps	REH7403	Costa Rica	–	–	JX889702	–	Halling et al. 2012b
Harrya chromapes	HKAS50527	China	–	–	KF112270	KF112792	Wu et al. 2014
Harrya moniliformis	HKAS49627	China	–	–	KT990881	KT990500	Wu et al. 2016
Heimioporus cf. *mandarinus*	OR0661	Thailand	MG212545	MH614841*	MG212589	MG212631	Vadthanarat et al. 2018; *This study
Heimioporus japonicus	OR0114	Thailand	KT823971	MH614842*	KT824037	KT824004	Raspé et al. 2016; *This study
Heimioporus retisporus	HKAS52237	China	–	–	KF112228	KF112806	Wu et al. 2014
Heimioporus sp.	OR0218	Thailand	MG212546	–	MG212590	MG212632	Vadthanarat et al. 2018
Hemileccinum depilatum	AF2845	Belgium	MG212547	MH614843*	MG212591	MG212633	Vadthanarat et al. 2018; *This study
Hemileccinum impolitum	ADK4078	Belgium	MG212548	MH614844*	MG212592	MG212634	Vadthanarat et al. 2018; *This study
Hemileccinum indecorum	OR0863	Thailand	MH614677	MH614845	MH614726	MH614772	This study
Hemileccinum rugosum	HKAS84970	China	–	–	KT990773	KT990412	Wu et al. 2016
Hortiboletus amygdalinus	HKAS54166	China	–	–	KT990777	KT990416	Wu et al. 2016
Hortiboletus rubellus	VDKO0403	Belgium	MH614679	MH614847	–	MH614774	This study
Hortiboletus sp.	HKAS50466	China	–	–	KF112183	KF112694	Wu et al. 2014
Hortiboletus sp.	HKAS51239	China	–	–	KF112184	KF112695	Wu et al. 2014
Hortiboletus sp.	HKAS51292	China	–	–	KF112181	KF112692	Wu et al. 2014
Hortiboletus sp.	HKAS76673	China	–	–	KF112182	KF112693	Wu et al. 2014
Hortiboletus subpaludosus	HKAS59608	China	–	–	KF112185	KF112696	Wu et al. 2014
Hourangia cf. *pumila*	OR0762	Thailand	MH614680	MH614848	MH614728	MH614775	This study
Hourangia cheoi	HKAS74744	China	–	–	KF112285	KF112772	Wu et al. 2014

Species	Voucher	Origin	*atp6*	*cox3*	*tef1*	*rpb2*	Reference(s)
Hourangia cheoi	Zhu108	China	–	–	KP136979	KP136928	Zhu et al. 2015
Hourangia nigropunctata	HKAS 57427	China	–	–	KP136927	KP136978	Zhu et al. 2015
Hymenoboletus luteopurpureus	HKAS46334	China	–	–	KF112271	KF112795	Wu et al. 2014
Imleria badia	VDKO0709	Belgium	KT823983	MH614849*	KT824049	KT824016	Raspé et al. 2016; *This study
Imleria obscurebrunnea	OR0263	China	MH614681	MH614850	MH614729	MH614776	This study
Imleria subalpina	HKAS74712	China	–	–	KF112189	KF112706	Wu et al. 2014
Lanmaoa angustispora	HKAS74759	China	–	–	KM605155	KM605178	Wu et al. 2015
Lanmaoa angustispora	HKAS74765	China	–	–	KF112159	KF112680	Wu et al. 2014
Lanmaoa angustispora	HKAS74752	China	–	–	KM605154	KM605177	Wu et al. 2015
Lanmaoa asiatica	HKAS54094	China	–	–	KF112161	KF112682	Wu et al. 2014
Lanmaoa asiatica	HKAS63516	China	–	–	KT990780	KT990419	Wu et al. 2016
Lanmaoa asiatica	OR0228	China	MH614682	MH614851	MH614730	MH614777	This study
Lanmaoa carminipes	BOTH4591	USA	MG897419	MH614852*	MG897429	MG897439	Phookamsak et al. 2019, *This study
Lanmaoa flavorubra	NY775777	Costa Rica	–	–	KF112160	KF112681	Wu et al. 2014
Lanmaoa pallidorosea	BOTH4432	USA	MG897417	MH614853*	MG897427	MG897437	Phookamsak et al. 2019, *This study
Lanmaoa sp.	HKAS52518	China	–	–	KF112162	KF112683	Wu et al. 2014
Lanmaoa sp.	OR0130	Thailand	MH614683	MH614854	MH614731	MH614778	This study
Lanmaoa sp.	OR0370	Thailand	MH614684	MH614855	MH614732	MH614779	This study
Leccinellum aff. *crocipodium*	HKAS76658	China	–	–	KF112252	KF112728	Wu et al. 2014
Leccinellum aff. *griseum*	KPM-NC-0017832	Japan	KC552164	–	JN378450*	–	unpublished, *Orihara et al. 2012
Leccinellum corsicum	Buf4507	USA	–	–	KF030435	–	Nuhn et al. 2013
Leccinellum cremeum	HKAS90639	China	–	–	KT990781	KT990420	Wu et al. 2016
Leccinellum crocipodium	VDKO1006	Belgium	KT823988	MH614856*	KT824054	KT824021	Raspé et al. 2016; *This study
Leccinellum sp.	KPM-NC-0018041	Japan	KC552165	–	KC552094	–	Orihara et al. 2016
Leccinellum sp.	OR0711	Thailand	MH614685	–	MH614733	MH614780	This study
Leccinum monticola	HKAS76669	China	–	–	KF112249	KF112723	Wu et al. 2014
Leccinum quercinum	HKAS63502	China	–	–	KF112250	KF112724	Wu et al. 2014
Leccinum scabrum	RW105a	Belgium	KT823979	MH614857*	KT824045	KT824012	Raspé et al. 2016; *This study
Leccinum scabrum	VDKO0938	Belgium	MG212549	MH614858*	MG212593	MG212635	Vadthanarat et al. 2018; *This study
Leccinum scabrum	KPM-NC-0017840	Scotland	KC552170	–	JN378455	–	Orihara et al. 2016, 2012
Leccinum schistophilum	VDKO1128	Belgium	KT823989	MH614859*	KT824055	KT824022	Raspé et al. 2016; *This study
Leccinum variicolor	VDKO0844	Belgium	MG212550	MH614860*	MG212594	MG212636	Vadthanarat et al. 2018; *This study
Mucilopilus castaneiceps	HKAS75045	China	–	–	KF112211	KF112735	Wu et al. 2014
Neoboletus brunneissimus	HKAS50538	China	–	–	KM605150	KM605173	Wu et al. 2015
Neoboletus brunneissimus	HKAS52660	China	–	–	KF112143	KF112650	Wu et al. 2014
Neoboletus brunneissimus	HKAS57451	China	–	–	KM605149	KM605172	Wu et al. 2015
Neoboletus brunneissimus	OR0249	China	MG212551	MH614861*	MG212595	MG212637	Vadthanarat et al. 2018; *This study
Neoboletus erythropus	VDKO0690	Belgium	KT823982	MH614864*	KT824048	KT824015	Raspé et al. 2016; *This study
Neoboletus ferrugineus	HKAS77718	China	–	–	KT990789	KT990431	Wu et al. 2016
Neoboletus ferrugineus	HKAS77617	China	–	–	KT990788	KT990430	Wu et al. 2016
Neoboletus flavidus	HKAS59443	China	–	–	KU974136	KU974144	Wu et al. 2016
Neoboletus flavidus	HKAS58724	China	–	–	KU974137	KU974145	Wu et al. 2016
Neoboletus hainanensis	HKAS63515	China	–	–	KT990808	KT990449	Wu et al. 2016
Neoboletus hainanensis	HKAS74880	China	–	–	KT990790	KT990432	Wu et al. 2016
Neoboletus hainanensis	HKAS90209	China	–	–	KT990809	KT990450	Wu et al. 2016
Neoboletus hainanensis	HKAS59469	China	–	–	KF112175	KF112669	Wu et al. 2014
Neoboletus junquilleus	AF2922	France	MG212552	MH614862*	MG212596	MG212638	Vadthanarat et al. 2018; *This study

Species	Voucher	Origin	*atp6*	*cox3*	*tef1*	*rpb2*	Reference(s)
Neoboletus magnificus	HKAS54096	China	–	–	KF112149	KF112654	Wu et al. 2014
Neoboletus magnificus	HKAS74939	China	–	–	KF112148	KF112653	Wu et al. 2014
Neoboletus multipunctatus	HKAS76851	China	–	–	KF112144	KF112651	Wu et al. 2014
Neoboletus multipunctatus	OR0128	Thailand	MH614686	MH614863	MH614734	MH614781	This study
Neoboletus obscureumbrinus	OR0553	Thailand	MK372271	–	MK372282	MK372294	This study
Neoboletus obscureumbrinus	HKAS63498	China	–	–	KT990791	KT990433	Wu et al. 2016
Neoboletus obscureumbrinus	HKAS77774	China	–	–	KT990792	KT990434	Wu et al. 2016
Neoboletus obscureumbrinus	HKAS89014	China	–	–	KT990793	KT990435	Wu et al. 2016
Neoboletus obscureumbrinus	HKAS89027	China	–	–	KT990794	KT990436	Wu et al. 2016
Neoboletus rubriporus	HKAS57512	China	–	–	KF112151	KF112656	Wu et al. 2014
Neoboletus rubriporus	HKAS83026	China	–	–	KT990795	KT990437	Wu et al. 2016
Neoboletus sanguineoides	HKAS57766	China	–	–	KT990799	KT990440	Wu et al. 2016
Neoboletus sanguineoides	HKAS74733	China	–	–	KT990800	KT990441	Wu et al. 2016
Neoboletus sanguineoides	HKAS55440	China	–	–	KF112145	KF112652	Wu et al. 2014
Neoboletus sanguineus	HKAS80823	China	–	–	KT990802	KT990442	Wu et al. 2016
Neoboletus tomentulosus	HKAS77656	China	–	–	KT990806	KT990446	Wu et al. 2016
Neoboletus tomentulosus	HKAS53369	China	–	–	KF112154	KF112659	Wu et al. 2014
Neoboletus venenatus	HKAS57489	China	–	–	KF112158	KF112665	Wu et al. 2014
Neoboletus venenatus	HKAS63535	China	–	–	KT990807	KT990448	Wu et al. 2016
Neoboletus sp.	HKAS76660	China	–	–	KF112180	KF112731	Wu et al. 2014
Octaviania asahimontana	KPM-NC-17824	Japan	KC552154	–	JN378430	–	Orihara et al. 2016, 2012
Octaviania asterosperma	AQUI3899	Italy	KC552159	–	KC552093	–	Orihara et al. 2016
Octaviania celatifilia	KPM-NC-17776	Japan	KC552147	–	JN378416	–	Orihara et al. 2016, 2012
Octaviania cyanescens	PNW-FUNGI-5603	USA	KC552160	–	JN378438	–	Orihara et al. 2016, 2012
Octaviania decimae	KPM-NC17763	Japan	KC552145	–	JN378409	–	Orihara et al. 2016, 2012
Octaviania tasmanica	MEL2128484	Australia	KC552157	–	JN378437	–	Orihara et al. 2016, 2012
Octaviania tasmanica	MEL2341996	Australia	KC552156	–	JN378436	–	Orihara et al. 2016, 2012
Octaviania zelleri	MES270	USA	KC552161	–	JN378440	–	Orihara et al. 2016, 2012
Parvixerocomus pseudoaokii	OR0155	China	MG212553	MH614865	MG212597	MG212639	This study
Phylloporus bellus	OR0473	China	MH580778	MH614866*	MH580798	MH580818	Chuankid et al. 2019; *This study
Phylloporus brunneiceps	OR0050	Thailand	KT823968	MH614867*	KT824034	KT824001	Raspé et al. 2016; *This study
Phylloporus castanopsidis	OR0052	Thailand	KT823969	MH614868*	KT824035	KT824002	Raspé et al. 2016; *This study
Phylloporus imbricatus	HKAS68642	China	–	–	KF112299	KF112786	Wu et al. 2014
Phylloporus luxiensis	HKAS75077	China	–	–	KF112298	KF112785	Wu et al. 2014
Phylloporus maculatus	OR0285	China	MH580780	–	MH580800	MH580820	Chuankid et al. 2019
Phylloporus pelletieri	WU18746	Austria	MH580781	MH614869*	MH580801	MH580821	Chuankid et al. 2019; *This study
Phylloporus pusillus	OR1158	Thailand	MH580783	MH614870*	MH580803	MH580823	Chuankid et al. 2019; *This study
Phylloporus rhodoxanthus	WU17978	USA	MH580785	MH614871*	MH580805	MH580824	Chuankid et al. 2019; *This study
Phylloporus rubeolus	OR0251	China	MH580786	MH614872*	MH580806	MH580825	Chuankid et al. 2019; *This study
Phylloporus rubiginosus	OR0169	China	MH580788	MH614873*	MH580808	MH580827	Chuankid et al. 2019; *This study
Phylloporus sp.	OR0896	Thailand	MH580790	MH614874*	MH580810	MH580829	Chuankid et al. 2019; *This study
Phylloporus subbacillisporus	OR0436	China	MH580792	MH614875*	MH580812	MH580831	Chuankid et al. 2019; *This study
Phylloporus subrubeolus	BC022	Thailand	MH580793	MH614876*	MH580813	MH580832	Chuankid et al. 2019; *This study

Species	Voucher	Origin	*atp6*	*cox3*	*tef1*	*rpb2*	Reference(s)
Phylloporus yunnanensis	OR0448	China	MG212554	MH614877*	MG212598	MG212640	Vadthanarat et al. 2018; *This study
Porphyrellus castaneus	OR0241	China	MG212555	MH614878*	MG212599	MG212641	Vadthanarat et al. 2018; *This study
Porphyrellus cf. *nigropurpureus*	ADK3733	Benin	MH614687	MH614879	MH614735	MH614782	This study
Porphyrellus nigropurpureus	HKAS74938	China	–	–	KF112246	KF112763	Wu et al. 2014
Porphyrellus porphyrosporus	MB97 023	Germany	DQ534609	–	GU187734	GU187800	Binder and Hibbett 2006; Binder et al. 2010
Porphyrellus sp.	HKAS53366	China	–	–	KF112241	KF112716	Wu et al. 2014
Porphyrellus sp.	JD659	Burundi	MH614688	MH614880	MH614736	MH614783	This study
Porphyrellus sp.	OR0222	Thailand	MH614689	MH614881	MH614737	MH614784	This study
Pulveroboletus aff. *ravenelii*	HKAS50203	China	–	–	KT990810	KT990451	Wu et al. 2016
Pulveroboletus aff. *ravenelii*	ADK4360	Togo	KT823957	MH614882*	KT824023	KT823990	Raspé et al. 2016; *This study
Pulveroboletus aff. *ravenelii*	ADK4650	Togo	KT823959	MH614883*	KT824025	KT823992	Raspé et al. 2016; *This study
Pulveroboletus aff. *ravenelii*	HKAS53351	China	–	–	KF112261	KF112712	Wu et al. 2014
Pulveroboletus brunneopunctatus	HKAS52615	China	–	–	KT990813	KT990454	Wu et al. 2016
Pulveroboletus brunneopunctatus	HKAS55369	China	–	–	KT990814	KT990455	Wu et al. 2016
Pulveroboletus brunneopunctatus	HKAS74926	China	–	–	KT990815	KT990456	Wu et al. 2016
Pulveroboletus fragrans	OR0673	Thailand	KT823977	MH614884*	KT824043	KT824010	Raspé et al. 2016; *This study
Pulveroboletus macrosporus	HKAS57628	China	–	–	KT990812	KT990453	Wu et al. 2016
Pulveroboletus ravenelii	REH2565	USA	KU665635	MH614885*	KU665636	KU665637	Raspé et al. 2016; *This study
Pulveroboletus sp.	HKAS74933	China	–	–	KF112262	KF112713	Wu et al. 2014
Pulveroboletus sp.	HKAS57665	China	–	–	KF112264	KF112715	Wu et al. 2014
Retiboletus aff. *nigerrimus*	OR0049	Thailand	KT823967	MH614886*	KT824033	KT824000	Raspé et al. 2016; *This study
Retiboletus brunneolus	HKAS52680	China	–	–	KF112179	KF112690	Wu et al. 2014
Retiboletus fuscus	HKAS59460	China	–	–	JQ928580	JQ928601	Hosen et al. 2013
Retiboletus fuscus	OR0231	China	MG212556	MH614887*	MG212600	MG212642	Vadthanarat et al. 2018; *This study
Retiboletus fuscus	HKAS63624	China	–	–	KT990829	KT990466	Wu et al. 2016
Retiboletus fuscus	HKAS74756	China	–	–	KT990830	KT990467	Wu et al. 2016
Retiboletus griseus	MB03 079	USA	KT823964	MH614888*	KT824030	KT823997	Raspé et al. 2016; *This study
Retiboletus griseus	HKAS63590	China	–	–	KF112178	KF112691	Wu et al. 2014
Retiboletus kauffmanii	OR0278	China	MG212557	MH614889*	MG212601	MG212643	Vadthanarat et al. 2018; *This study
Retiboletus nigerrimus	HKAS53418	China	–	–	KT990824	KT990462	Wu et al. 2016
Retiboletus sinensis	HKAS59832	China	–	–	KT990827	KT990464	Wu et al. 2016
Retiboletus zhangfeii	HKAS59699	China	–	–	JQ928582	JQ928603	Hosen et al. 2013
Rhodactina himalayensis	CMU25117	Thailand	MG212558	–	MG212602, MG212603	–	Vadthanarat et al. 2018
Rhodactina rostratispora	SV170	Thailand	MG212560	–	MG212605	MG212645	Vadthanarat et al. 2018
Rossbeevera cryptocyanea	KPM-NC17843	Japan	KT581441	–	KC552072	–	Orihara et al. 2016
Rossbeevera eucyanea	TNS-F-36986	Japan	KC552115	–	KC552068	–	Orihara et al. 2016
Rossbeevera griseovelutina	TNS-F-36989	Japan	KC552124	–	KC552076	–	Orihara et al. 2016
Rossbeevera pachydermis	KPM-NC23336	New Zealand	KJ001064	–	KP222912	–	Orihara et al. 2016
Rossbeevera vittatispora	OSC61484	Australia	KC552109	–	JN378446	–	Orihara et al. 2016, 2012
Royoungia reticulata	HKAS52253	China	–	–	KT990786	KT990427	Wu et al. 2016
Royoungia rubina	HKAS53379	China	–	–	KF112274	KF112796	Wu et al. 2014
Rubroboletus latisporus	HKAS80358	China	–	–	KP055020	KP055029	Zhao et al. 2014b

Species	Voucher	Origin	*atp6*	*cox3*	*tef1*	*rpb2*	Reference(s)
Rubroboletus legaliae	VDKO0936	Belgium	KT823985	MH614890*	KT824051	KT824018	Raspé et al. 2016; *This study
Rubroboletus rhodosanguineus	BOTH4263	USA	MG897416	MH614891*	MG897426	MG897436	Phookamsak et al. 2019, *This study
Rubroboletus rhodoxanthus	HKAS84879	Germany	–	–	KT990831	KT990468	Wu et al. 2016
Rubroboletus satanas	VDKO0968	Belgium	KT823986	MH614892*	KT824052	KT824019	Raspé et al. 2016; *This study
Rubroboletus sinicus	HKAS68620	China	–	–	KF112146	KF112661	Wu et al. 2014
Rubroboletus sinicus	HKAS56304	China	–	–	KJ619483	KP055031	Zhao et al. 2014a; Zhao et al. 2014b
Rubroboletus sp.	HKAS68679	China	–	–	KF112147	KF112662	Wu et al. 2014
Rugiboletus brunneiporus	HKAS68586	China	–	–	KF112197	KF112719	Wu et al. 2014
Rugiboletus brunneiporus	HKAS83009	China	–	–	KM605146	KM605169	Wu et al. 2015
Rugiboletus brunneiporus	HKAS83209	China	–	–	KM605144	KM605168	Wu et al. 2015
Rugiboletus extremiorientalis	HKAS76663	China	–	–	KM605147	KM605170	Wu et al. 2015
Rugiboletus extremiorientalis	OR0406	Thailand	MG212562	MH614893*	MG212607	MG212647	Vadthanarat et al. 2018; *This study
Rugiboletus sp.	HKAS55373	China	–	–	KF112303	KF112804	Wu et al. 2014
Singerocomus inundabilis	TWH9199	Guyana	MH645588	MH645609	MH645596	LC043089*	*Henkel et al. 2016; This study
Singerocomus rubriflavus	TWH9585	Guyana	MH645589	MH645610	MH645597	–	This study
Spongiforma thailandica	DED7873	Thailand	MG212563	MH614894**	KF030436*	MG212648	*Nuhn et al. 2013; Vadthanarat et al. 2018; **This study
Strobilomyces atrosquamosus	HKAS55368	China	–	–	KT990839	KT990476	Wu et al. 2016
Strobilomyces echinocephalus	OR0243	China	MG212564	–	MG212608	MG212649	Vadthanarat et al. 2018
Strobilomyces mirandus	OR0115	Thailand	KT823972	MH614896*	KT824038	KT824005	Raspé et al. 2016; *This study
Strobilomyces strobilaceus	MB03 102	USA	DQ534607*	–	AY883428	AY786065	*Binder and Hibbett 2006, Unpublished
Strobilomyces strobilaceus	RW103	Belgium	KT823978	MH614895*	KT824044	KT824011	Raspé et al. 2016; *This study
Strobilomyces verruculosus	HKAS55389	China	–	–	KF112259	KF112813	Wu et al. 2014
Strobilomyces sp.	OR0259	China	MG212565	MH614897*	MG212609	MG212650	Vadthanarat et al. 2018; *This study
Strobilomyces sp.	OR0319	Thailand	MH614690	MH614898	MH614738	MH614785	This study
Strobilomyces sp.	OR0778	Thailand	MG212566	MH614899*	MG212610	MG212651	Vadthanarat et al. 2018; *This study
Strobilomyces sp.	OR1092	Thailand	MH614691	MH614900	MH614739	MH614786	This study
Suillellus amygdalinus	112605ba	USA	–	–	JQ327024	–	Halling et al. 2012a
Suillellus luridus	VDKO0241b	Belgium	KT823981	MH614901*	KT824047	KT824014	Raspé et al. 2016; *This study
Suillellus queletii	VDKO1185	Belgium	MH645590	MH645611	MH645598	MH645604	This study
Suillellus subamygdalinus	HKAS57262	China	–	–	KF112174	KF112660	Wu et al. 2014
Suillellus subamygdalinus	HKAS53641	China	–	–	KT990841	KT990478	Wu et al. 2016
Suillellus subamygdalinus	HKAS74745	China	–	–	KT990843	KT990479	Wu et al. 2016
Sutorius aff. *eximius*	HKAS52672	China	–	–	KF112207	KF112802	Wu et al. 2014
Sutorius aff. *eximius*	HKAS56291	China	–	–	KF112208	KF112803	Wu et al. 2014
Sutorius australiensis	REH9441	Australia	MG212567	MK386576**	JQ327032*	MG212652	*Halling et al. 2012a; Vadthanarat et al. 2018; **This study
Sutorius eximius	HKAS59657	China	–	–	KT990887	KT990505	Wu et al. 2016
Sutorius eximius	REH9400	USA	MG212568	MH614902**	JQ327029*	MG212653	*Halling et al. 2012a; Vadthanarat et al. 2018; **This study
Sutorius eximius	HKAS50420	China	–	–	KT990750	KT990387	Wu et al. 2016
Sutorius sp.	OR0378B	Thailand	MH614692	MH614903	MH614740	MH614787	This study
Sutorius sp.	OR0379	Thailand	MH614693	MH614904	MH614741	MH614788	This study

Species	Voucher	Origin	*atp6*	*cox3*	*tef1*	*rpb2*	Reference(s)
Tengioboletus glutinosus	HKAS53425	China	–	–	KF112204	KF112800	Wu et al. 2014
Tengioboletus reticulatus	HKAS53426	China	–	–	KF112313	KF112828	Wu et al. 2014
Tengioboletus sp.	HKAS76661	China	–	–	KF112205	KF112801	Wu et al. 2014
Turmalinea persicina	KPM-NC18001	Japan	KC552130	–	KC552082	–	Orihara et al. 2016
Turmalinea yuwanensis	KPM-NC18011	Japan	KC552138	–	KC552089	–	Orihara et al. 2016
Tylocinum griseolum	HKAS50281	China	–	–	KF112284	KF112730	Wu et al. 2014
Tylopilus alpinus	HKAS55438	China	–	–	KF112191	KF112687	Wu et al. 2014
Tylopilus atripurpureus	HKAS50208	China	–	–	KF112283	KF112799	Wu et al. 2014
Tylopilus balloui s.l.	OR0039	Thailand	KT823965	MH614905*	KT824031	KT823998	Raspé et al. 2016; *This study
Tylopilus brunneirubens	HKAS53388	China	–	–	KF112192	KF112688	Wu et al. 2014
Tylopilus felleus	VDKO0992	Belgium	KT823987	MH614906*	KT824053	KT824020	Raspé et al. 2016; *This study
Tylopilus ferrugineus	BOTH3639	USA	MH614694	MH614907	MH614742	MH614789	This study
Tylopilus otsuensis	HKAS53401	China	–	–	KF112224	KF112797	Wu et al. 2014
Tylopilus sp.	HKAS74925	China	–	–	KF112222	KF112739	Wu et al. 2014
Tylopilus sp.	HKAS50229	China	–	–	KF112216	KF112769	Wu et al. 2014
Tylopilus sp.	JD598	Gabon	MH614695	MH614908	MH614743	MH614790	This study
Tylopilus sp.	OR0252	China	MG212569	MH614909*	MG212611	MG212654	Vadthanarat et al. 2018; *This study
Tylopilus sp.	OR0542	Thailand	MG212570	MH614910*	MG212612	MG212655	Vadthanarat et al. 2018; *This study
Tylopilus sp.	OR0583	Thailand	MH614696	–	MH614744	–	This study
Tylopilus sp.	OR1009	Thailand	MH614697	MH614911	–	MH614791	This study
Tylopilus vinaceipallidus	HKAS50210	China	–	–	KF112221	KF112738	Wu et al. 2014
Tylopilus vinaceipallidus	OR0137	China	MG212571	MH614912*	MG212613	MG212656	Vadthanarat et al. 2018; *This study
Tylopilus violaceobrunneus	HKAS89443	China	–	–	KT990886	KT990504	Wu et al. 2016
Tylopilus virens	KPM-NC-0018054	Japan	KC552174	–	KC552103	–	Unpublished
Veloporphyrellus alpinus	HKAS68301	China	JX984515	–	JX984550	–	Li et al. 2014b
Veloporphyrellus conicus	REH8510	Belize	MH614698	MH614913	MH614745	MH614792	This study
Veloporphyrellus gracilioides	HKAS53590	China	–	–	KF112210	KF112734	Wu et al. 2014
Veloporphyrellus pseudovelatus	HKAS59444	China	JX984519	–	JX984553	–	Li et al. 2014b
Veloporphyrellus velatus	HKAS63668	China	JX984523	–	JX984554	–	Li et al. 2014b
Xanthoconium affine	NY00815399	USA	–	–	KT990850	KT990486	Wu et al. 2016
Xanthoconium porophyllum	HKAS90217	China	–	–	KT990851	KT990487	Wu et al. 2016
Xanthoconium sinense	HKAS77651	China	–	–	KT990853	KT990488	Wu et al. 2016
Xerocomellus chrysenteron	VDKO0821	Belgium	KT823984	MH614914*	KT824050	KT824017	Raspé et al. 2016; *This study
Xerocomellus cisalpinus	ADK4864	Belgium	KT823960	MH614915*	KT824026	KT823993	Raspé et al. 2016; *This study
Xerocomellus communis	HKAS50467	China	–	–	KT990858	KT990494	Wu et al. 2016
Xerocomellus corneri	HKAS90206	Philippines	–	–	KT990857	KT990493	Wu et al. 2016
Xerocomellus porosporus	VDKO0311	Belgium	MH614678	MH614846	MH614727	MH614773	This study
Xerocomellus riparielus	VDKO0404	Belgium	MH614699	MH614916	MH614746	MH614793	This study
Xerocomellus sp.	HKAS56311	China	–	–	KF112170	KF112684	Wu et al. 2014
Xerocomus aff. *macrobbii*	HKAS56280	China	–	–	KF112265	KF112708	Wu et al. 2014
Xerocomus fulvipes	HKAS76666	China	–	–	KF112292	KF112789	Wu et al. 2014
Xerocomus magniporus	HKAS58000	China	–	–	KF112293	KF112781	Wu et al. 2014
Xerocomus s.s. sp.	OR0237	China	MH580796	–	MH580816	MH580835	Chuankid et al. 2019
Xerocomus s.s. sp.	OR0443	China	MH580797	MH614917*	MH580817	MH580836	Chuankid et al. 2019; *This study
Xerocomus sp.	OR0053	Thailand	MH580795	MH614918*	MH580815	MH580834	Chuankid et al. 2019; *This study
Xerocomus subtomentosus	VDKO0987	Belgium	MG212572	MH614919*	MG212614	MG212657	Vadthanarat et al. 2018; *This study
Zangia citrina	HKAS52684	China	HQ326850	–	HQ326872	–	Li et al. 2011
Zangia olivacea	HKAS45445	China	HQ326854	–	HQ326873	–	Li et al. 2011

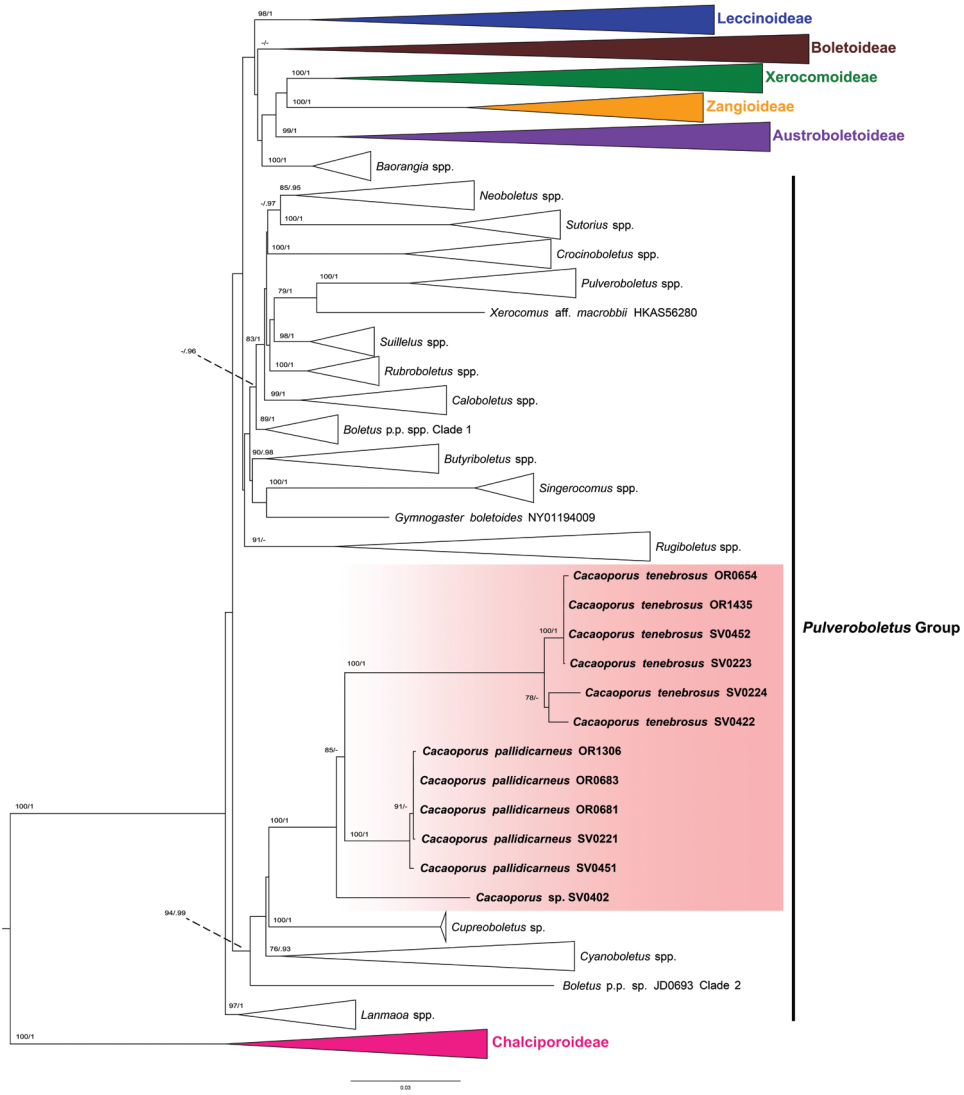

Figure 1. Phylogenetic tree inferred from the four-gene dataset (*atp*6, *cox*3, *rpb*2 and *tef*1), including *Cacaoporus* species and selected Boletaceae using Maximum Likelihood and Bayesian Inference methods (ML tree is presented). The two *Buchwaldoboletus* and nine *Chalciporus* species in subfamily Chalciporoideae were used as outgroup. Most of the taxa not belonging to the *Pulveroboletus* group were collapsed into subfamilies. All genera clades in *Pulveroboletus* group that were highly supported were also collapsed. Bootstrap support values (BS ≥ 70%) and posterior probabilities (PP ≥ 0.90) are shown above the supported branches.

Zhu L. Yang, *S. obscureumbrinus* (Hongo) G. Wu & Zhu L. Yang, *S. rubriporus* G. Wu & Zhu L. Yang, *S. sanguineoides* G. Wu & Zhu L. Yang, *S. sanguineus* G. Wu & Zhu L. Yang, *S. tomentulosus* (M. Zang, W.P. Liu & M.R. Hu) G. Wu & Zhu L. Yang and

S. venenatus (Nagas.) G. Wu & Zhu L. Yang clustered in the *Neoboletus* clade with high support (85% BS and 0.95 PP), while the true *Sutorius*, including the typus generis *S. eximius* (Peck) Halling, Nuhn & Osmundson, formed a different well-supported clade (BS=100% and PP=1).

Taxonomy

Cacaoporus **Raspé & Vadthanarat, gen. nov.**
MycoBank: MB829655

Etymology. Refers to the dark, chocolate brown hymenophore and overall colour of basidiomata.

Diagnosis. Similar to the genus *Sutorius* in having brown basidiomata with brown encrustations in the flesh but differs from *Sutorius* in having the following combination of characters: brown to chocolate brown or greyish-brown to dark brown or blackish-brown basidiomata, without violet tinge, chocolate brown to dark brown hymenophore, tubes not separable from the pileus context, white to off-white basal mycelium which turns reddish-white to pale red when bruised, amygdaliform to ovoid with subacute apex in side view to ovoid basidiospores and dark brown spore deposit.

Description. ***Basidiomata*** stipitate-pileate with poroid hymenophore, small to medium-sized, dull, brown to greyish-brown to dark brown or blackish-brown. ***Pileus*** convex when young becoming plano-convex to slightly depressed with age, with deflexed to inflexed margin; ***surface*** even to subrugulose, minutely tomentose or slightly cracked at the centre; ***context*** soft, yellowish to greyish off-white then slightly greyish-orange to dull orange to greyish-brown when exposed to the air, patchy or marmorated with greyish-brown to dark brown, sometimes with scattered small dark brown to brownish-black encrustations, not or inconsistently reddening when cut. ***Hymenophore*** tubulate, adnate, subventricose to ventricose, slightly depressed around the stipe; ***tubes*** brown to greyish-brown to dark brown, not separable from the pileus context; ***pores*** regularly arranged, mostly roundish at first becoming slightly angular with age, sometimes irregular, elongated around the stipe, dark brown to greyish-brown at first, becoming brown to chocolate brown with age. ***Stipe*** central, terete to sometimes slightly compressed, cylindrical to sometimes slightly wider at the base; surface even, minutely tomentose, dull, dark brown to greyish-brown, basal mycelium white to off-white becoming reddish-white to pale red when touched; ***context*** solid, yellowish to orange white to yellowish-grey to pale orange to dull orange to reddish-grey, marmorated or virgated with brownish-grey to greyish-brown to dark brown, sometimes scattered with small reddish-brown to brownish-black fine encrustations, unchanged or inconsistently reddening when cut. ***Spore print*** dark brown.

Basidiospores amygdaliform to ovoid or ovoid with subacute apex in side view, thin-walled, smooth, slightly reddish to brownish hyaline in water, slightly yellowish to greenish hyaline in KOH or NH_4OH, inamyloid. ***Basidia*** 4-spored, clavate to nar-

rowly clavate without basal clamp connection. ***Cheilocystidia*** fusiform or cylindrical with obtuse apex, sometimes bent or sinuate, thin-walled, often scattered with small brownish-yellow to yellowish-brown crystals on the walls in KOH or NH_4OH. ***Pleurocystidia*** narrowly fusiform with obtuse apex or cylindrical to narrowly subclavate, sometimes bent or sinuate, thin-walled, densely covered with small reddish-brown to brownish dark encrustations on the walls when observed in H_2O, which are discoloured then dissolved in KOH or NH_4OH. ***Pileipellis*** a trichoderm becoming tangled trichoderm to tomentum, composed of thin-walled hyphae; terminal cells mostly slightly sinuate cylindrical to irregular with rounded apex or clavate to elongated clavate. ***Stipitipellis*** a trichoderm to tangled trichoderm or disrupted hymeniderm, composed of loosely to moderately interwoven cylindrical hyphae anastomosing at places. ***Clamp connections*** not seen in any tissue.

Typus generis. *Cacaoporus tenebrosus*

Distribution. Currently known from Thailand.

Notes. *Sutorius* most closely resembles the new genus. In the field, *Cacaoporus* is easily distinguished from the *Sutorius* by the following combination of characters: chocolate brown to dark brown to blackish-brown basidiomata, which are darker than in *Sutorius* and never purplish-brown like in *Sutorius* species; chocolate brown to dark brown hymenophore, which is much darker than in *Sutorius* and never reddish- to purplish-brown like in *Sutorius*; tubes that are not separable from the pileus context but can be separated in *Sutorius*; off-white basal mycelium that more or less turns red when bruised, which is never the case in *Sutorius*.

Cacaoporus pallidicarneus **Vadthanarat, Raspé & Lumyong, sp. nov.**
MycoBank: MB829657
Figs. 2a, 3a, 4a and 5

Etymology. Refers to the context, which is paler than in the other species, especially at the stipe base and in the pileus.

Type. THAILAND, Chiang Mai Province, Mae On District, 18°52'37"N, 99°18'23"E, elev. 860 m, 15 August 2015, *Santhiti Vadthanarat*, SV0221 (CMUB!, isotype BR!).

Diagnosis. *Cacaoporus pallidicarneus* is characterised by having a paler context than the other species and basidiospores that are amygdaliform or elongated amygdaliform to ovoid in side view, sometimes with subacute apex, shorter basidia and fusiform to narrowly bent fusiform to narrowly fusiform hymenophoral cystidia.

Description. ***Basidiomata*** small to medium-sized. ***Pileus*** (1.6)2.4–5.5 cm in diameter, convex when young becoming plano-convex with age; margin deflexed to inflexed, slightly exceeding (1–2 mm), surface even to subrugulose, minutely tomentose, dull, at first brown to greyish-brown to blackish-brown (8F3–4) sometimes paler (8C2) at places, becoming paler to greyish-brown (8E3–5) with age; ***context*** 4–9 mm thick half-way to the margin, soft, yellowish to greyish off-white then slightly

Figure 2. Habit of *Cacaoporus* species. **a** *C. pallidicarneus* (SV0221) **b–d** *C. tenebrosus* (b - SV0223, c - SV0224, d - SV0422). Scale bars: 1 cm (**a–d**).

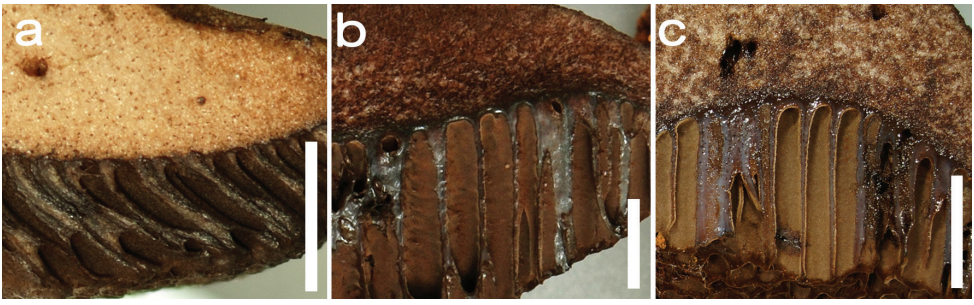

Figure 3. Close-ups of hymenium/pileus context transition zone in *Cacaoporus* species, illustrating the non-separability of both tissues **a** *C. pallidicarneus* (OR0681) **b** *C. tenebrosus* (OR0654) **c** *C. tenebrosus* (SV0452). The transition between both tissues is particularly unmarked in *C. pallidicarneus* (**a**) Scale bars: 3 mm (**a**); 5 mm (**b–c**).

pale orange to greyish-orange (6A3 to 6B3) when exposed to the air, with patchy or marmorated with greyish-brown (8E3) especially when young, scattered with reddish-brown to brownish-black of fine encrustations at places, slightly reddening when cut. ***Stipe*** central, terete or sometimes slightly compressed, cylindrical with slightly wider base, (2.0)2.8–3.7 × 0.4–0.7 cm, surface even, minutely tomentose, dull, greyish-brown to dark brown (8 E/F 3–4 to 8F2), basal mycelium white to off-white becoming pale red (7A3) when bruised; ***context*** solid, yellowish to greyish off-

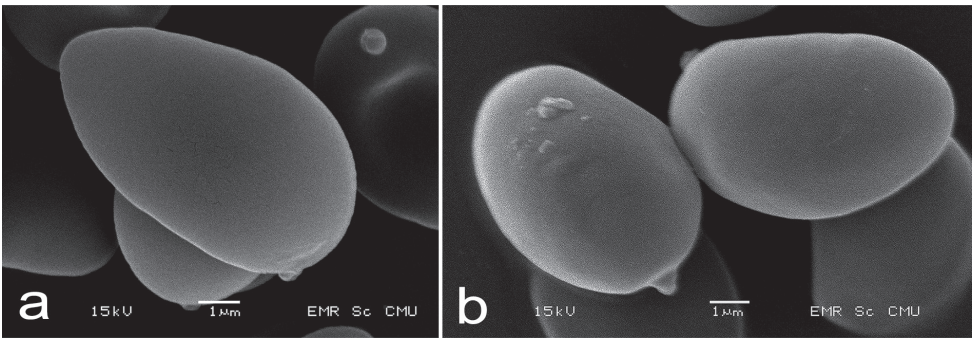

Figure 4. Scanning electron micrographs of *Cacaoporus* basidiospores **a** *C. pallidicarneus* (SV0221) **b** *C. tenebrosus* (SV0223). Scale bars: 1 µm (**a–b**).

white then orange white to pale orange (5A2–3) when exposed to the air, virgate to marmorate with brownish-grey (8F2), less so at the stipe base, at places scattered with brownish-black fine encrustations, unchanged to slowly slightly reddening when cut. ***Hymenophore*** tubulate, adnate, subventricose, slightly depressed around the stipe. ***Tubes*** (2)4–6 mm long half-way to the margin, brown to greyish-brown (8F3), not separable from the pileus context. ***Pores*** 0.4–1.5 mm wide at mid-radius, regularly arranged, mostly roundish to elliptical at first, becoming slightly angular with age, slightly elongated around the stipe, colour distribution even, dark brown to chocolate brown (9F4 to 10F3) at first, becoming chocolate brown to brown (10F4 to 7–8F4–5) with age. ***Odour*** rubbery. ***Taste*** slightly bitter at first, then mild. ***Spore print*** dark brown (8F4/5) in mass.

Macrochemical reactions. KOH, orange brown on cap, yellowish-black on stipe, yellowish-black on the pileus context and stipe context, brownish-black on hymenium; NH_4OH, yellowish-brown on cap, yellowish-orange on stipe, orangey yellow to yellowish-orange on the pileus context, stipe context and hymenium.

Basidiospores [437/7/5] (6.5–)6.7–7.7–8.6(–11.5) × (3.8–)4–4.6–5.1(–5.5) µm Q = (1.4–)1.48–1.68–1.9(–2.44). From the type (3 basidiomata, N = 177) (6.8–)7–7.8–8.5(–9.1) × (4–)4.2–4.6–5(–5) µm, Q = (1.49–)1.5–1.69–1.9(–2.21), amygdaliform or elongated amygdaliform sometimes to ovoid with subacute apex in side view, ovoid in front view, thin-walled, smooth, slightly reddish to brownish hyaline in water, slightly yellowish to greenish hyaline in KOH or NH_4OH, inamyloid. ***Basidia*** 4-spored, (25.3–)25.4–29.7–33.8(–33.8) × (7.3–)7.3–8.4–9.8(–10) µm, clavate without basal clamp connection, slightly yellowish to brownish hyaline in KOH or NH_4OH; sterigmata up to 5 µm long. ***Cheilocystidia*** (16–)16.3–23.4–32.8(–34) × (5.5–)5.8–7.3–9(–9) µm, frequent, fusiform, thin-walled, yellowish to brownish hyaline to brown in KOH or NH_4OH. ***Pleurocystidia*** (44–)44.2–54.7–67.6(–68) × (5–)5–6–7(–7) µm, frequent, usually narrowly bent fusiform to narrowly fusiform with obtuse apex, thin-walled, yellowish to brownish hyaline in KOH or NH_4OH. ***Hymenophoral trama*** subdivergent to divergent, 62–175 µm wide, with 25–100 µm wide, regular to subregular mediostratum, composed of cylindrical, 4–7(11) µm wide

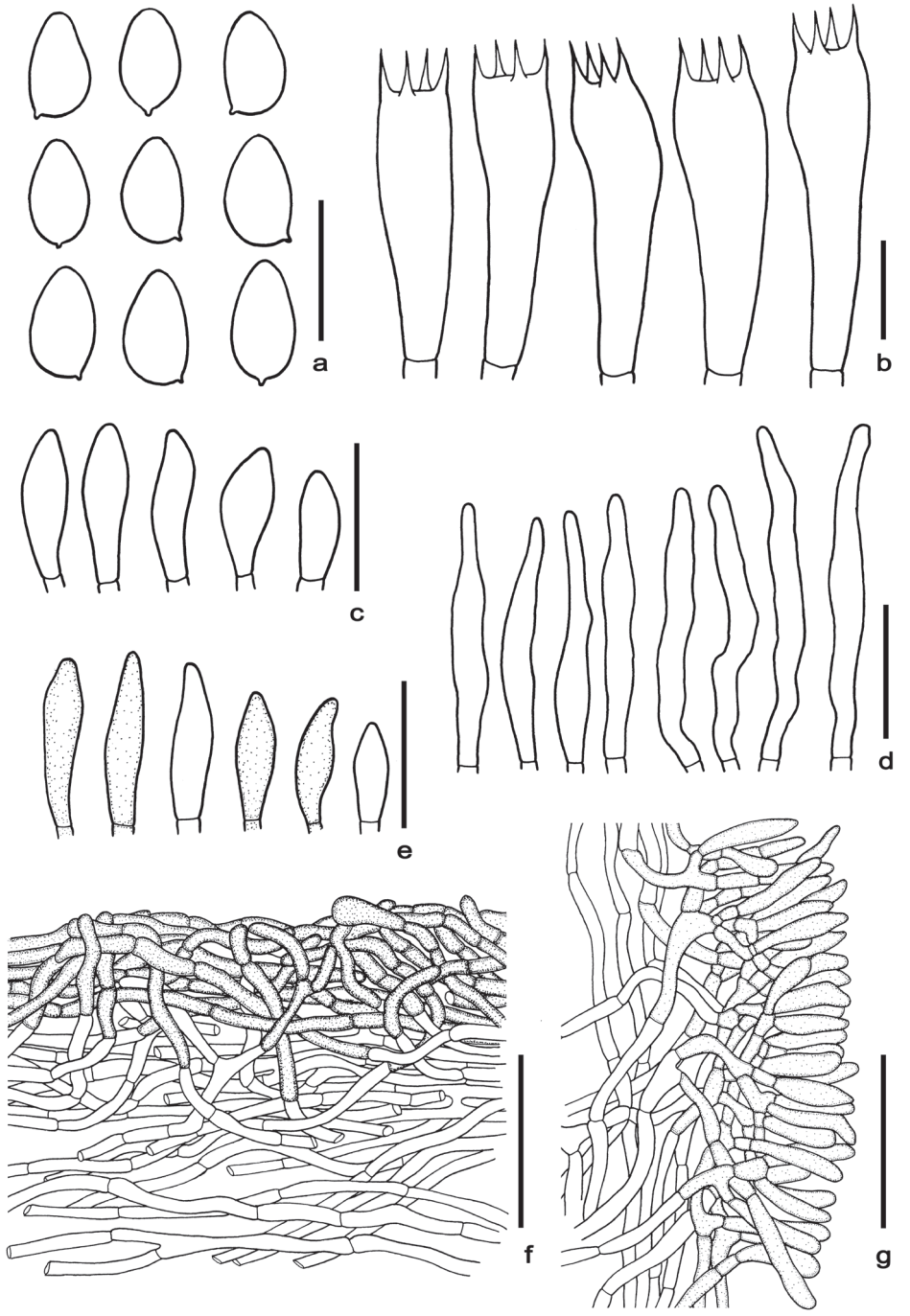

Figure 5. Microscopic features of *Cacaoporus pallidicarneus* **a** basidiospores **b** basidia **c** cheilocystidia **d** pleurocystidia **e** caulocystidia **f** pileipellis **g** stipitipellis. Scale bars: 10 μm (**a–b**); 25 μm (**c–e**); 50 μm (**f–g**). All drawings were made from the type (SV0221).

hyphae, yellowish to brownish hyaline in KOH or NH_4OH. ***Pileipellis*** a trichoderm to tangled trichoderm at first, becoming a tomentum to tangled trichoderm with age, 65–110 µm thick, composed of firmly to moderately interwoven thin-walled hyphae; terminal cells 12–55 × 4–6 µm, slightly bent cylindrical with rounded apex, at places clavate to sub-clavate to elongated clavate, 16–34 × 8–10 µm, slightly dark to reddish to brownish dark in water, yellowish to brownish hyaline to yellowish-brown to slightly dark at places in KOH or NH_4OH. ***Pileus context*** made of moderately interwoven, thin-walled, hyaline hyphae, 6–12 µm wide. ***Stipitipellis*** a disrupted hymeniderm, 55–95 µm thick, composed clavate cells, 11–37 × 5–8 µm, yellowish-brown to slightly dark in KOH or NH_4OH mixed with caulocystidia. ***Caulocystidia*** (17–)17–23.6–31(–31) × (5–)5–6.3–7(–7) µm, frequent, thin-walled, mostly yellowish-brown to slightly dark at places in KOH or NH_4OH. ***Stipe context*** composed of parallel, 3–7 µm wide hyphae, brownish hyaline to yellowish pale brown in KOH or NH_4OH. ***Clamp connections*** not seen in any tissue.

Habitat and Distribution. solitary to gregarious up to 4 basidiomata, on soil in hill evergreen forest dominated by Fagaceae trees, with a few *Dipterocarpus* spp. and *Shorea* spp. or in Dipterocarp forest dominated by *Dipterocarpus* spp. and *Shorea* spp. with a few *Lithocarpus* sp., *Castanopsis* sp. and *Quercus* sp. Currently known only from Chiang Mai Province, Northern Thailand.

Additional specimens examined. THAILAND, Chiang Mai Province, Mae Taeng District, 23 km marker (Ban Tapa), 19°08'50"N, 98°46'50"E, elev. 930 m, 2 August 2013, *Olivier Raspé* & *Anan Thawthong*, OR0681; Ban Mae Sae, 19°14'70"N, 98°38'70"E, elev. 960 m, 3 August 2013, *Olivier Raspé* & *Anan Thawthong*, OR0683; Muang District, Doi Suthep-Pui National Park, 18°48'37"N, 98°53'33"E, elev. 1460 m, 14 July 2016, *Olivier Raspé*, OR1306; Mae On District, 18°52'35"N, 99°18'16"E, elev. 860 m, 6 June 2018, *Santhiti Vadthanarat*, SV0451.

Remarks. We observed some small yellowish to reddish to brownish dark particles or crystals covering the cell walls in pileipellis, stipitipellis and on the hymenium, especially the cystidia and basidia when observed in water. The small particles or crystals were mostly dissolved in KOH.

Cacaoporus pallidicarneus differs from *C. tenebrosus* by its basidiomata context colour which is paler, especially at the stipe base. A combination of the following characters are also distinctive: spore shape which is amygdaliform or elongated amygdaliform or sometimes ovoid with subacute apex in side view and ovoid in front view, while *C. tenebrosus* has ovoid spores, shorter basidia and differently shaped hymenophoral cystidia (see note under *C. tenebrosus*). *Cacaoporus pallidicarneus* has a stipitipellis which is a disrupted hymeniderm composed of caulocystidia and clavate cells, while the other species has a loose trichoderm or tangled trichoderm. Interestingly, one collection (SV0402) had a slightly paler context than *C. tenebrosus* but not as pale as *C. pallidicarneus*. The phylogenetic analyses indicated that this collection might be a species different from *C. pallidicarneus* and *C. tenebrosus*. However, the specimen was immature and, therefore, more collections are needed before the species can be formally recognised.

Cacaoporus tenebrosus **Vadthanarat, Raspé & Lumyong, sp. nov.**
MycoBank: MB829656
Figs. 2b–d, 3b–c, 4b and 6

Etymology. Refers to the overall darkness of basidiomata, including the context.

Type. THAILAND, Chiang Mai Province, Mae On District, 18°52'37"N, 99°18'32"E, elev. 940 m, 15 August 2015, *Santhiti Vadthanarat*, SV0223 (holotype CMUB!, isotype BR!).

Diagnosis. *Cacaoporus tenebrosus* is characterised by having a darker context than the other species, longer basidia and cylindrical to narrowly subclavate hymenophoral cystidia.

Description. ***Basidiomata*** medium-sized. ***Pileus*** (2.3)3.1–5(9) cm in diameter, convex when young becoming plano-convex to slightly depressed with age; margin inflexed to deflexed, slightly exceeding (1–2 mm); surface even to subrugulose, minutely tomentose, slightly cracked at the centre, dull, greyish-brown (10F3) to dark brown to blackish-brown (8F4–5) to the margin; ***context*** 5–10 mm thick half-way to the margin, soft, marmorated, greyish-brown to dark brown (10F3–5) with greyish-brown (9B/D3), scattered with reddish-brown to brownish-black, fine encrustations at places, slightly reddening in paler spots when cut. ***Stipe*** central, terete, cylindrical to sometimes with slightly wider base, 4.3–7.0 × 0.7–1.4 cm, surface even, minutely tomentose, dull, dark brown to greyish-brown (9F4 to 10F3), basal mycelium white to off-white becoming reddish-white to pale red (7A3–4) when bruised; ***context*** solid, greyish-brown to dark brown (9–10F3–5) marmorated with reddish-grey (7/10B2), usually scattered with small reddish-brown to brownish-black fine encrustations, slightly reddening when cut. ***Hymenophore*** tubulate, adnate, subventricose to ventricose, slightly depressed around the stipe. ***Tubes*** (4)7–13 mm long half-way to the margin, brown to dark brown (8F3 to 9F4), not separable from the pileus context. ***Pores*** 0.8–2 mm wide at mid-radius, regularly arranged, mostly roundish at first, becoming slightly angular with age, sometime irregular, elongated around the stipe; colour distribution even, greyish-brown to dark brown (9F4) at first, becoming chocolate brown to brown (10F3 to 7–8F4–5) with age. ***Odour*** mild fungoid. ***Taste*** slightly bitter at first, then mild. ***Spore print*** dark brown (8/9F4) in mass.

Macrochemical reactions. KOH, yellowish then brown to black on cap, stipe, pileus context, stipe context and hymenium; NH_4OH, yellowish then orange to brown on cap, stipe, pileus context, stipe context and hymenium.

Basidiospores [290/8/6] (7.4–)7.7–8.4–9.2(–10) × (4.5–)5–5.3–5.7(–6.1) µm *Q* = (1.25–)1.44–1.57–1.77(–2). From the type (2 basidiomata, *N* = 134) (7.5–)7.7–8.2–9(–9.9) × (4.9–)5–5.4–5.7(–5.9) µm, *Q* = (1.41–)1.43–1.54–1.71(–1.9), ovoid, thin-walled, smooth, slightly reddish to brownish hyaline in water, slightly yellowish to greenish hyaline in KOH or NH_4OH, inamyloid. ***Basidia*** 4-spored, (33.6–)34.3–38.8–45.8(–47) × (7.7–)7.8–9.5–10.8(–10.9) µm, clavate to narrowly clavate without basal clamp connection, yellowish to brownish hyaline to slightly dark in KOH or NH_4OH; sterigmata up to 5 µm long. ***Cheilocystidia*** (22–)22.1–28.7–37(–37) × (3–

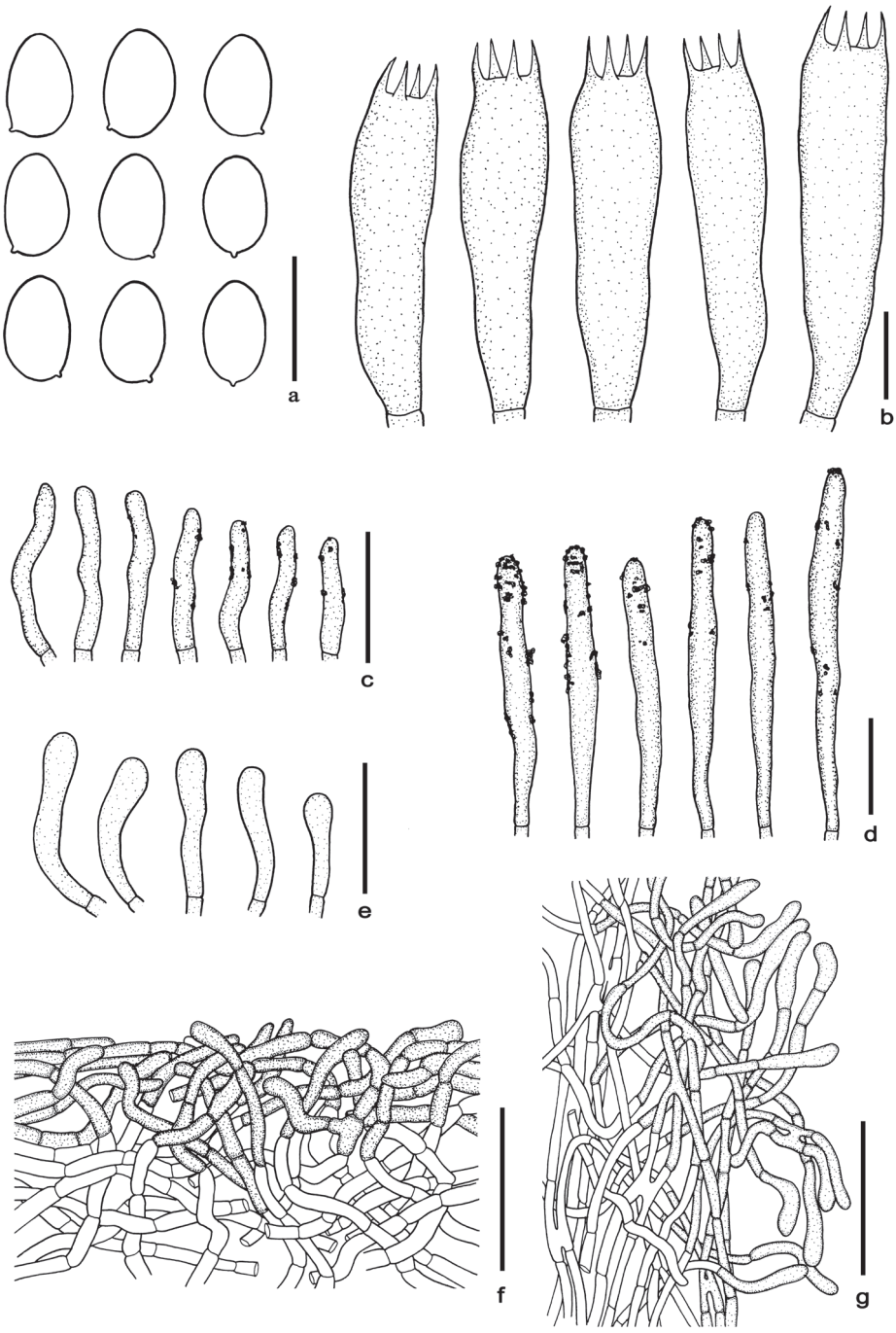

Figure 6. Microscopic features of *Cacaoporus tenebrosus* **a** basidiospores **b** basidia **c** cheilocystidia **d** pleurocystidia **e** caulocystidia **f** pileipellis **g** stipitipellis. Scale bars: 10 μm (**a–b**); 25 μm (**c–e**); 50 μm (**f–g**). All drawings were made from the type (SV0223).

)3.1–4.4–5(–5) µm, frequent, cylindrical with obtuse apex, sometimes bent or sinuate, thin-walled, yellowish-brown to dark brown in KOH or NH_4OH, often scattered with small brownish-yellow to yellowish-brown crystals on the walls in KOH or NH_4OH. ***Pleurocystidia*** (62–)62.5–81.5–99(–99) × (7–)7–8–9(–9) µm, frequent, cylindrical to narrowly subclavate, sometimes bent or sinuate, thin-walled, with yellowish-brown to slightly dark content in KOH or NH_4OH, densely covered with small reddish-brown to brownish dark encrustations on the walls when observed in H_2O, with some scattered small brownish-yellow to yellowish-brown crystals on the walls in KOH or NH_4OH. ***Hymenophoral trama*** subdivergent to divergent, 80–170 µm wide, with 60–80 µm wide of subregular mediostratum, composed of cylindrical, 4–8(11) µm wide hyphae, slightly yellowish to brownish hyaline in KOH or NH_4OH. ***Pileipellis*** a tangled trichoderm to tomentum at places, 70–110 µm thick, composed of moderately interwoven thin-walled hyphae; terminal cells 12–48 × 4–7 µm mostly slightly sinuate, cylindrical to irregular with rounded apex, at places clavate to elongated clavate terminal cells 18–33 × 7–9 µm, slightly dark to reddish to brownish dark in water, yellowish-brown to slightly dark in KOH or NH_4OH, scattered with small brownish-yellow to yellowish-brown crystals on the walls in KOH or NH_4OH. ***Pileus context*** made of moderately interwoven, thin-walled, hyaline hyphae, 7–12 µm wide. ***Stipitipellis*** a trichoderm to tangled trichoderm, 70–120 µm thick, composed of loosely to moderately interwoven cylindrical hyphae anastomosing at places, brownish dark to dark in KOH or NH_4OH. ***Caulocystidia*** (17–)17.6–29.4–46.3(–47) × (4–)4.1–5.5–6.9(–7) µm, clavate to cylindrical with obtuse apex, thin-walled, yellowish to brownish dark in KOH or NH_4OH. ***Stipe context*** composed of parallel, 4–6(12) µm wide hyphae, brownish hyaline to yellowish pale brown in KOH or NH_4OH. ***Clamp connections*** not seen in any tissue.

Habitat and distribution. Gregarious (up to 9 basidiomata) to fasciculate or solitary, on soil in hill evergreen forest dominated by Fagaceae trees, with a few *Dipterocarpus* spp. and *Shorea* spp. or in Dipterocarp forest dominated by *Dipterocarpus* spp., *Shorea* spp. with a few *Lithocarpus* sp., *Castanopsis* sp. and *Quercus* sp. Currently known only from Chiang Mai Province, Northern Thailand.

Additional specimens examined. THAILAND, Chiang Mai Province, Mae Taeng District, 19°07'15"N, 98°43'55"E, elev. 910 m, 29 July 2013, *Olivier Raspé* & *Benjarong Thongbai*, OR0654; ibid. 19°7'29"N, 98°40'59"E, elev. 1010 m, 24 May 2018, *Santhiti Vadthanarat*, SV0422; Mae On District, 18°52'37"N, 99°18'19"E, elev. 850 m, 15 August 2015, *Santhiti Vadthanarat*, SV0224; ibid., 18°52'35"N, 99°18'16"E, elev. 860 m, 15 July 2017, *Olivier Raspé* , OR1435; ibid., 6 June 2018, *Santhiti Vadthanarat*, SV0452.

Remarks. There were many small yellowish to reddish to dark brownish particles or crystals on the walls of pileipellis, stipitipellis and hymenium cells, especially on the cystidia and basidia when observed in water. The small particles or crystals are somewhat dissolved and discoloured in KOH.

Microscopically, *Cacaoporus tenebrosus* differs from *C. pallidicarneus* by having a darker context, longer basidia (33.6–47 µm vs. 25.3–33.8 µm, respectively), longer and larger

hymenophoral cystidia, which also differ in shape (cylindrical to narrowly subclavate in *C. tenebrosus* but fusiform to narrowly fusiform in *C. pallidicarneus*). Phylogenetically, all *Cacaoporus* collections with a dark context formed a clade sister to *C. pallidicarneus* (BS = 85% and PP = 0.88), but some (SV0224 and SV0422) were genetically somewhat distant from the other collections. However, we could not find any difference in morphology. Consequently, we consider them as the same species (*C. tenebrosus*). Study of more collections is needed to confirm or infirm that they belong to the same species.

Discussion

Morphologically, *Cacaoporus* is most similar to *Sutorius*, with which it shares the overall brown colour of basidiomata and encrustations in the flesh. However, the genus *Cacaoporus* has darker basidiomata, especially the hymenophore and pore surface and is more chocolate brown, not reddish-brown or purplish-brown like *Sutorius*, tubes that are not separable from the pileus context whereas they are easily separable in *Sutorius*, white to off-white basal mycelium which becomes reddish when bruised, whereas in *Sutorius*, the basal mycelium is more or less white and unchanging. *Cacaoporus* also produces dark brown spore deposits whereas in *Sutorius*, spore deposits are reddish-brown (Halling et al. 2012). Microscopically, the two genera differ in the shape of basidiospores, which is amygdaliform to ovoid or ovoid with subacute apex in side view in *Cacaoporus*, whereas *Sutorius* produces narrowly ellipsoid to ellipsoid or subfusoid to fusoid basidiospores. Phylogenetically, *Cacaoporus* and *Sutorius* are not closely related - the two genera belong in two different clades of the *Pulveroboletus* group.

Some species in *Porphyrellus* E.-J. Gilbert also have brown to dark brown to umber basidiomata similar to *Cacaoporus*. However, *Porphyrellus* differs from the new genus in having white to greyish-white hymenophore when young, becoming greyish-pink to blackish-pink with age, white to pallid context in pileus and stipe variably staining blue and/or reddish when cut and white basal mycelium that does not turn red when bruised (Wolfe 1979; Wu et al. 2016). Some species in *Strobilomyces* Berk also share some characters with *Cacaoporus*, including dark brown basidiomata, white to off-white basal mycelium that turns red when bruised and the context turning red when cut. However, *Strobilomyces* species clearly differ from *Cacaoporus*, especially in the pileus surface, which is coarsely fibrillose or shows conical to patch-like scales, in the hymenophore, which is whitish-cream or greyish-brown or vinaceous drab and stains reddish then blackish when bruised and also basidiospores, which are subglobose to obtusely ellipsoid with reticulation or longitudinally striate (Gelardi et al. 2012; Antonín et al. 2015; Wu et al. 2016). Moreover, *Porphyrellus* and *Strobilomyces* were phylogenetically inferred to belong in subfamily Boletoideae (Wu et al. 2014, 2016; Vadthanarat et al. 2018) distinct from *Cacaoporus*.

Phylogenetically, *Cacaoporus* was monophyletic and clustered in a well-supported clade with the genera *Cyanoboletus* and *Cupreoboletus* and one undescribed taxon, *Boletus* p.p. sp. (specimen voucher JD0693), belonging to the *Pulveroboletus* group

of Wu et al. (2014, 2016). *Cyanoboletus* and *Cupreoboletus*, however, differ from *Cacaoporus* in important morphological characters. The former two genera have a yellow hymenophore and yellowish context and tissues instantly discolouring dark blue when injured, and olive-brown spore deposits (Gelardi et al. 2014, 2015; Wu et al. 2016). The undescribed taxon represented by the voucher specimen JD0693, which clustered within the same clade as *Cacaoporus*, *Cyanoboletus* and *Cupreoboletus*, is also morphologically very different from *Cacaoporus*, in having yellow tubes, reddish pores, pale yellow to off-white context and reddish-brown pileus and stipe.

Our survey on the diversity of Boletes in the north of Thailand has been conducted since 2012 and no *Cacaoporus* has been found in the forests at elevations lower than 850 m. *Cacaoporus* was found only between 850 m and 1460 m elevation. However, more collections are needed to confirm that the distribution of the genus is restricted to mid- to high-elevation forests and does not occur in the lower elevation, drier forests. Most collections were made from Fagaceae-dominated, evergreen hill forests. The dominant trees in these forests belong to the Fagaceae, including *Lithocarpus*, *Castanopsis* and *Quercus*, but some Dipterocarpaceae may also occur. At the lower end of its elevation range, however, *Cacaoporus* was also found in Dipterocarpaceae-dominated forests (in which Fagaceae, especially *Quercus* spp., also occurs). The Dipterocarpaceae trees include *Dipterocarpus*, namely *D. tuberculatus*, *D. obtusifolius* and *Shorea*, namely *S. obtusa* and *S. siamensis*. The listed trees have previously been reported as ectomycorrhizal hosts of Boletaceae (Moser et al. 2009; Desjardin et al. 2009, 2011; Hosen et al. 2013; Arora and Frank 2014; Halling et al. 2014; Wu et al. 2018) and presumably are also the hosts for *Cacaoporus*.

Interestingly, our phylogeny indicated that the genera *Neoboletus* and *Sutorius* formed two different clades, both with high support (BS = 85% and PP = 0.95 for *Neoboletus*; BS = 100% and PP = 1 for *Sutorius*). Recently, Wu et al. (2016) synonymised *Neoboletus* with *Sutorius* because, in their phylogeny based on a four-gene dataset (28S+*tef*1+*rpb*1+*rpb*2), *Boletus obscureumbrinus*, a species morphologically more similar to *Neoboletus* than to *Sutorius*, seemed to cluster with *Sutorius* rather than with the *Neoboletus* species, although with neither ML nor BI support. Moreover, the *Neoboletus* clade was not supported either. Later, Chai et al. (2019) treated the two genera as different genetic lineages based on morphology and phylogeny (28S+ITS+*tef*1+*rpb*2), in which *B. obscureumbrinus* clustered with the other *Neoboletus* species in a well-supported clade. Our phylogenetic analyses, based on a different set of genes (*atp*6+*tef*1+*rpb*2+*cox*3), confirm the separation of the two genera *Neoboletus* and *Sutorius*. The differences in gene trees obtained could be explained by a long-branch attraction artefact in datasets with different taxon and gene samplings and/or problems in the dataset (e.g. suboptimal alignment). *Neoboletus obscureumbrinus* is quite atypical amongst *Neoboletus* species and its phylogenetic affinities within this genus remain unclear (Fig. 7).

Cacaoporus is the second novel bolete genus described from Thailand, the first one being *Spongiforma* Desjardin, Manfr. Binder, Roekring & Flegel, described in 2009 (Desjardin et al.). However, fungal diversity in Thailand is high and still poorly known (Hyde et al. 2018), with a large number of species and possibly genera that remain to be described.

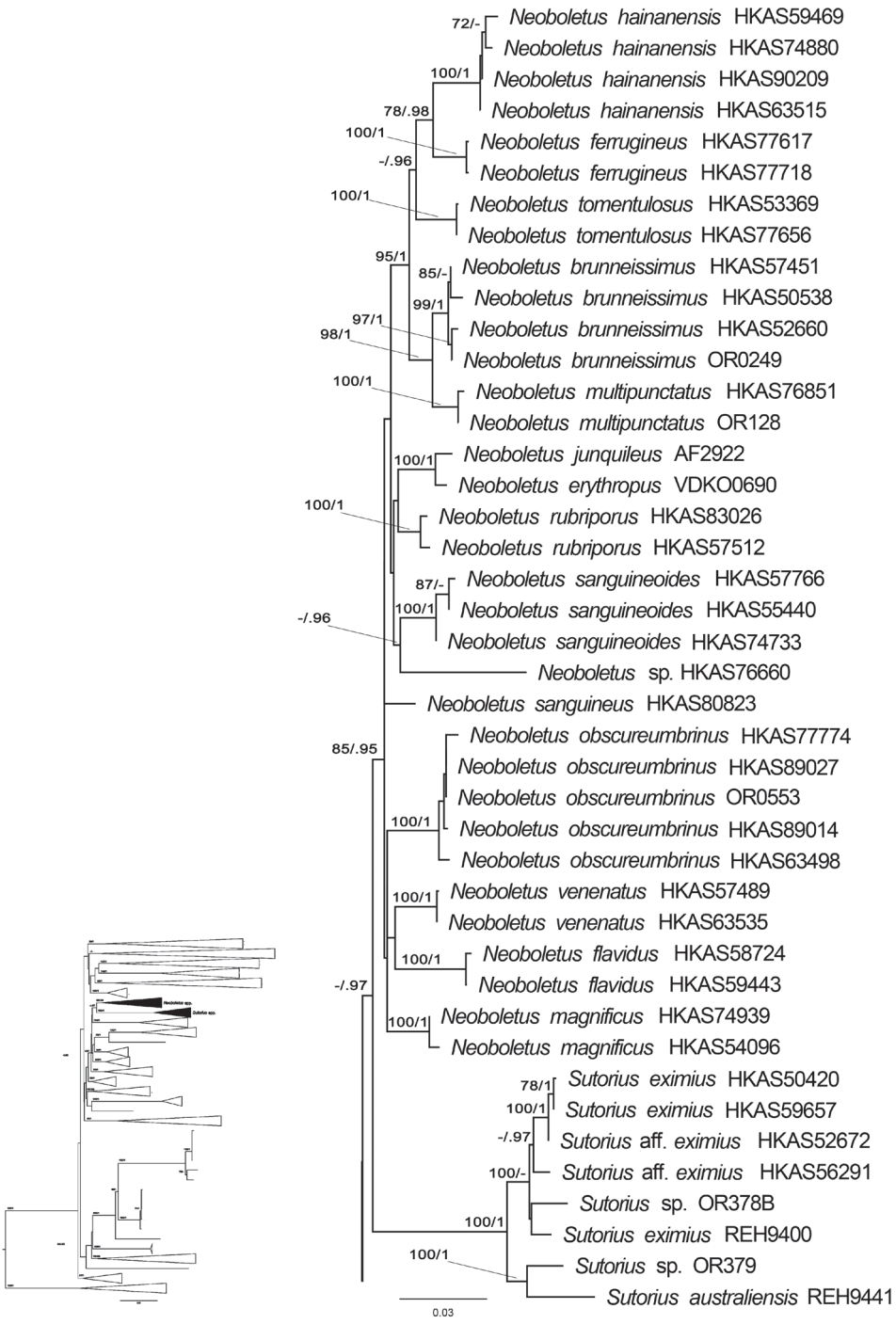

Figure 7. Sub-tree of the phylogram in Fig. 1, showing the well-supported *Sutorius* and *Neoboletus* clades and the unsupported sister relationship of *Neoboletus obscureumbrinus*.

Acknowledgements

Financial support from the Graduate School, Chiang Mai University, is appreciated. The work was partly supported by a TRF Research Team Association Grant (RTA5880006) to SL and OR. OR is grateful to the Fonds National de la Recherche Scientifique (Belgium) for travel grants. The authors are grateful for the permit number 0907.4/4769 granted by the Department of National Parks, Wildlife and Plant Conservation, Ministry of Natural Resources and Environment for collecting in Doi Suthep-Pui National Park. Beatriz Ortiz-Santana (CFMR), Roy E. Halling (NY), and Terry W. Henkel are gratefully acknowledged for the loan of specimens.

References

Antonín V, Vizzini A, Ercole E, Leonardi M (2015) *Strobilomyces pteroreticulosporus* (Boletales), a new species of the *S. strobilaceus* complex from the Republic of Korea and remarks on the variability of *S. confusus*. Phytotaxa 219(1): 78–86. https://doi.org/10.11646/phytotaxa.219.1.6

Arora D, Frank JL (2014) Clarifying the butter Boletes: a new genus, *Butyriboletus*, is established to accommodate *Boletus* sect. *Appendiculati*, and six new species are described. Mycologia 106(3): 464–480. https://doi.org/10.3852/13-052

Binder M, Hibbett DS (2006) Molecular systematics and biological diversification of Boletales. Mycologia 98: 971–981. https://doi.org/10.1080/15572536.2006.11832626

Binder M, Larsson KH, Matheny PB, Hibbett DS (2010) Amylocorticiales ord. nov. and Jaapiales ord. nov.: early diverging clades of agaricomycetidae dominated by corticioid forms. Mycologia 102: 865–880. https://doi.org/10.3852/09-288

Chai H, Xue R, Jiang S, Luo SH, Wang Y, Wu LL, Tang LP, Chen Y, Hong D, Liang ZQ, Zeng NK (2019) New and noteworthy boletes from subtropical and tropical China. MycoKeys 46: 55–96. https://doi.org/10.3897/mycokeys.46.31470

Chuankid B, Vadthanarat S, Hyde KD, Thongklang N, Zhao R, Lumyong S, Raspé O (2019) Three new *Phylloporus* species from tropical China and Thailand. Mycological Progress 18: 603–614. https://doi.org/10.1007/s11557-019-01474-6

Darriba D, Taboada GL, Doallo R, Posada D (2012) jModelTest 2: more models, new heuristics and parallel computing. Nature Methods 9: 772. https://doi.org/10.1038/nmeth.2109

Desjardin DE, Binder M, Roekring S, Flegel T (2009) *Spongiforma*, a new genus of gastroid boletes from Thailand. Fungal Diversity 37: 1–8.

Desjardin DE, Peay KG, Bruns TD (2011) *Spongiforma squarepantsii*, a new species of gasteroid bolete from Borneo. Mycologia 103(5): 1119–1123. https://doi.org/10.3852/10-433

Doyle JJ, Doyle JL (1990) Isolation of plant DNA from fresh tissue. Focus, 12: 13–15. https://doi.org/10.2307/2419362

Gelardi M, Vizzini A, Ercole E, Voyron S, Wu G, Liu XZ (2012) *Strobilomyces echinocephalus* sp. nov. (Boletales) from southwestern China, and a key to the genus *Strobilomyces* worldwide. Mycological Progress 12: 575–588. https://doi.org/10.1007/s11557-012-0865-3

Gelardi M, Simonini G, Ercole E, Vizzini A (2014) *Alessioporus* and *Pulchroboletus* gen. nov. (Boletaceae, Boletineae), two novel genera to accommodate *Xerocomus ichnusanus* and *X. roseoalbidus* from European Mediterranean basin: molecular and morphological evidence. Mycologia 106(6): 1168–1187. https://doi.org/10.3852/14-042

Gelardi M, Simonini G, Ercole E, Davoli P, Vizzini A (2015) *Cupreoboletus* (Boletaceae, Boletineae), a new monotypic genus segregated from *Boletus* sect. *Luridi* to reassign the Mediterranean species *B. poikilochromus*. Mycologia 107(6): 1254–1269. https://doi.org/10.3852/15-070

Halling RE, Desjardin DE, Fechner N, Arora D, Soytong K, Dentinger BTM (2014) New porcini (*Boletus* sect. *Boletus*) from Australia and Thailand. Mycologia 106: 830–834. https://doi.org/10.3852/13-340

Halling RE, Nuhn M, Fechner NA, Osmundson TW, Soytong K, Arora D, Hibbett DS, Binder M (2012a) *Sutorius*: a new genus for *Boletus eximius*. Mycologia 104(4): 951–961. https://doi.org/10.3852/11-376

Halling RE, Nuhn M, Osmundson T, Fechner N, Trappe JM, Soytong K, Arora D, Hibbett DS, Binder M (2012b) Affinities of the *Boletus chromapes* group to *Royoungia* and the description of two new genera, *Harrya* and *Australopilus*. Australian Systematic Botany 25: 418–431. https://doi.org/10.1071/SB12028

Henkel TW, Obase K, Husbands D, Uehling JK, Bonito G, Aime MC, Smith ME (2016) New Boletaceae taxa from Guyana: *Binderoboletus segoi* gen. and sp. nov., *Guyanaporus albipodus* gen. and sp. nov., *Singerocomus rubriflavus* gen. and sp. nov., and a new combination for *Xerocomus inundabilis*. Mycologia 108(1): 157–173. https://doi.org/10.3852/15-075

Hosen MI, Feng B, Wu G, Zhu XT, Li YC, Yang ZL (2013) *Borofutus*, a new genus of Boletaceae from tropical Asia: phylogeny, morphology and taxonomy. Fungal Diversity 58: 215–226. https://doi.org/10.1007/s13225-012-0211-8

Hyde KD, Norphanphoun C, Chen J, Dissanayake AJ, Doilom M, Hongsanan S, Jayawardena RS, Jeewon R, Perera RH, Thongbai B, Wanasinghe DN, Wisitrassameewong K, Tibpromma S, Stadler M (2018) Thailand's amazing diversity: up to 96% of fungi in northern Thailand may be novel. Fungal Diversity 93: 215–239. https://doi.org/10.1007/s13225-018-0415-7 https://doi.org/10.1007/s13225-018-0415-7

Katoh K, Standley DM (2013) MAFFT Multiple sequence alignment software version 7: improvements in performance and usability. Molecular Biology and Evolution 30: 772–780. https://doi.org/10.1093/molbev/mst010

Kornerup A, Wanscher JH (1978) Methuen Handbook of Colour (3rd edn). Eyre Methuen Ltd, London, 252 pp.

Kretzer AM, Bruns TD (1999) Use of *atp*6 in fungal phylogenetics: an example from the Boletales. Molecular Phylogenetics and Evolution 13: 483–492. https://doi.org/10.1006/mpev.1999.0680

Li YC, Feng B, Yang ZL (2011) *Zangia*, a new genus of Boletaceae supported by molecular and morphological evidence. Fungal Diversity 49: 125–143. https://doi.org/10.1007/s13225-011-0096-y

Li YC, Li F, Zeng NK, Cui YY, Yang ZL (2014a) A new genus *Pseudoaustroboletus* (Boletaceae, Boletales) from Asia as inferred from molecular and morphological data. Mycological Progress 13: 1207–1216. https://doi.org/10.1007/s11557-014-1011-1

Li YC, Ortiz-Santana B, Zeng NK, Feng B (2014b) Molecular phylogeny and taxonomy of the genus *Veloporphyrellus*. Mycologia 106(2): 291–306. https://doi.org/10.3852/106.2.291

Matheny PB (2005) Improving phylogenetic inference of mushrooms with RPB1 and RPB2 nucleotide sequences (*Inocybe*; Agaricales). Molecular Phylogenetics and Evolution 35: 1–20. https://doi.org/10.1016/j.ympev.2004.11.014

Miller MA, Holder MT, Vos R, Midford PE, Liebowitz T, Chan L, Hoover P, Warnow T (2009) The CIPRES portals. CIPRES. http://www.phylo.org/portal2/home.

Moser AM, Frank JL, D' Allura JA, Southworth D (2009) Ectomycorrhizal communities of *Quercus garryana* are similar on serpentine and nonserpentine soils. Plant Soil 315: 185–194. https://doi.org/10.1007/s11104-008-9743-9

Neves MA, Binder M, Halling R, Hibbett D, Soytong K (2012) The phylogeny of selected *Phylloporus* species inferred from NUC-LSU and ITS sequences, and descriptions of new species from the Old World. Fungal Diversity 55(1): 109–123. https://doi.org/10.1007/s13225-012-0154-0

Nuhn ME, Binder M, Taylor AFS, Halling RE, Hibbett DS (2013) Phylogenetic overview of the Boletineae. Fungal Biology 117: 479–511. https://doi.org/10.1016/j.funbio.2013.04.008

Orihara T, Lebel T, Ge Z-W, Smith ME, Maekawa N (2016) Evolutionary history of the sequestrate genus *Rossbeevera* (Boletaceae) reveals a new genus *Turmalinea* and highlights the utility of ITS minisatellite-like insertions for molecular identification. Persoonia 37: 173–198. https://doi.org/10.3767/003158516X691212

Orihara T, Smith ME, Shimomura N, Iwase K, Maekawa N (2012) Diversity and systematics of the sequestrate genus *Octaviania* in Japan: two new subgenera and eleven new species. Persoonia 28: 85–112. https://doi.org/10.3767/003158512X650121

Phookamsak R, Hyde KD, Jeewon R, Bhat DJ, Jones EBG, Maharachchikumbura SSN et al. (2019) Fungal diversity notes 929–1035: taxonomic and phylogenetic contributions on genera and species of fungi. Fungal Diversity. https://doi.org/10.1007/s13225-019-00421-w

Raspé O, Vadthanarat S, De Kesel A, Degreef J, Hyde KD, Lumyong S (2016) *Pulveroboletus fragrans*, a new Boletaceae species from Northern Thailand, with a remarkable aromatic odor. Mycological Progress 15: 38. https://doi.org/10.1007/s11557-016-1179-7

Rehner SA, Buckley E (2005) A *Beauveria* phylogeny inferred from nuclear ITS and EF1-α sequences: evidence for cryptic diversification and links to *Cordyceps* teleomorphs. Mycologia 97: 84–98. https://doi.org/10.3852/mycologia.97.1.84

Ronquist F, Teslenko M, van der Mark P, Ayres D, Darling A, Höhna S, et al (2012) MrBayes 3.2: Efficient Bayesian phylogenetic inference and model choice across a large model space. Systematic Biology 61: 539–542. https://doi.org/10.1093/sysbio/sys029

Stamatakis A (2006) RAxML-vi-hpc: maximum likelihood-based phylogenetic analyses with thousands of taxa and mixed models. Bioinformatics 22: 2688–2690. https://doi.org/10.1093/bioinformatics/btl446

Vadthanarat S, Raspé O, Lumyong S (2018) Phylogenetic affinities of the sequestrate genus *Rhodactina* (Boletaceae), with a new species, *R. rostratispora* from Thailand. MycoKeys 29: 63–80. https://doi.org/10.3897/mycokeys.29.22572

Wolfe CB (1979) *Austroboletus* and *Tylopilus* subg. *Porphyrellus*, with emphasis on North American taxa. Bibliotheca Mycologica 69: 1–148.

Wu G, Feng B, Xu J, Zhu XT, Li YC, Zeng NK, Hosen MI, Yang ZL (2014) Molecular phylogenetic analyses redefine seven major clades and reveal 22 new generic clades in the fungal family Boletaceae. Fungal Diversity 69: 93–115. https://doi.org/10.1007/s13225-014-0283-8

Wu G, Lee S ML, Horak E, Yang ZL (2018) *Spongispora temakensis*, a new boletoid genus and species from Singapore. Mycologia 110(5): 919–929. https://doi.org/10.1080/00275514.2018.1496387

Wu G, Li YC, Zhu XT, Zhao K, Han LH, Cui YY, Li F, Xu JP, Yang ZL (2016) One hundred noteworthy boletes from China. Fungal Diversity 81: 25–188. https://doi.org/10.1007/s13225-016-0375-8

Wu G, Zhao K, Li YC, Zeng NK, Feng B, Halling RE, Yang ZL (2015) Four new genera of the fungal family Boletaceae. Fungal Diversity 81: 1–24. https://doi.org/10.1007/s13225-015-0322-0

Zeng NK, Cai Q, Yang ZL (2012) *Corneroboletus*, a new genus to accommodate the southeastern Asian *Boletus indecorus*. Mycologia 104(6): 1420–1432. https://doi.org/10.3852/11-326

Zeng NK, Wu G, Li YC, Liang ZQ, Yang ZL (2014) *Crocinoboletus*, a new genus of Boletaceae (Boletales) with unusual polyene pigments boletocrocins. Phytotaxa 175: 133–140. https://doi.org/10.11646/phytotaxa.175.3.2

Zhao K, Wu G, Feng B, Yang ZL (2014a) Molecular phylogeny of *Caloboletus* (Boletaceae) and a new species in East Asia. Mycological Progress 13: 1127–1136. https://doi.org/10.1007/s11557-014-1001-3

Zhao K, Wu G, Yang ZL (2014b) A new genus, *Rubroboletus*, to accommodate *Boletus sinicus* and its allies. Phytotaxa 188: 61–77. https://doi.org/10.11646/phytotaxa.188.2.1

Zhu XT, Wu G, Zhao K, Halling RE, Yang ZL (2015) *Hourangia*, a new genus of Boletaceae to accommodate *Xerocomus cheoi* and its allied species. Mycological Progress 14: 37. https://doi.org/10.1007/s11557-015-1060-0

MycoKeys 54: 31–47 (2019)
doi: 10.3897/mycokeys.54.35386
http://mycokeys.pensoft.net

RESEARCH ARTICLE

A peer-reviewed open-access journal
MycoKeys
Launched to accelerate biodiversity research

Reassessment of the generic limits for *Hydnellum* and *Sarcodon* (Thelephorales, Basidiomycota)

Karl-Henrik Larsson[1,2], Sten Svantesson[2,3,4], Diana Miscevic[5], Urmas Kõljalg[6], Ellen Larsson[2,3]

1 *Natural History Museum, University of Oslo, P.O. Box 1172 Blindern, NO 0318 Oslo, Norway* **2** *Gothenburg Global Biodiversity Centre, P.O. Box 461, SE 405 30 Göteborg, Sweden* **3** *Department of Biological and Environmental Sciences, University of Gothenburg, P.O. Box 461, SE 405 30 Göteborg, Sweden* **4** *Royal Botanic Gardens Victoria, Birdwood Ave, Melbourne, Victoria 3004, Australia* **5** *Västkuststiftelsen, Sandöhamnsvägen 71, SE 434 94 Vallda, Sweden* **6** *Institute of Ecology and Earth Sciences, 40 Lai Street, 51005 Tartu, Estonia*

Corresponding author: *Karl-Henrik Larsson* (k.h.larsson@nhm.uio.no)

Academic editor: *María P. Martín* | Received 11 April 2019 | Accepted 21 May 2019 | Published 10 June 2019

Citation: Larsson K-H, Svantesson S, Miscevic D, Kõljalg U, Larsson E (2019) Reassessment of the generic limits for *Hydnellum* and *Sarcodon* (Thelephorales, Basidiomycota) MycoKeys 54: 31–47. https://doi.org/10.3897/mycokeys.54.35386

Abstract

DNA sequences from the nuclear LSU and ITS regions were used for phylogenetic analyses of Thelephorales with a focus on the stipitate hydnoid genera *Hydnellum* and *Sarcodon*. Analyses showed that *Hydnellum* and *Sarcodon* are distinct genera but that the current division, based on basidioma texture, makes *Sarcodon* paraphyletic with respect to *Hydnellum*. In order to make genera monophyletic several species are moved from *Sarcodon* to *Hydnellum* and the following new combinations are made: *Hydnellum amygdaliolens*, *H. fennicum*, *H. fuligineoviolaceum*, *H. fuscoindicum*, *H. glaucopus*, *H. joeides*, *H. lepidum*, *H. lundellii*, *H. martioflavum*, *H. scabrosum*, *H. underwoodii*, and *H. versipelle*. Basidiospore size seems to separate the genera in most cases. *Hydnellum* species have basidiospore lengths in the range 4.45–6.95 µm while the corresponding range for *Sarcodon* is 7.4–9 µm. *S. quercinofibulatus* deviates from this pattern with an average spore length around 6 µm. Neotropical *Sarcodon* species represent a separate evolutionary lineage.

Keywords

Phylogeny, stipitate hydnoid, taxonomy, *Thelephorales*, tooth fungi

Introduction

The order Thelephorales is a distinctive lineage of Agaricomycetes, well-known for its almost ubiquitous ectomycorrhizal life style (Tedersoo et al. 2010). Several species have stipitate hydnoid basidiomata (Fig. 1). They have traditionally been divided into four genera, *Phellodon* and *Bankera* with hyaline basidiospores, and *Hydnellum* and *Sarcodon* with yellow to brown tinted basidiospores (Maas Geesteranus 1975). In both cases the genera within each pair differ in basidioma structure, with *Phellodon* and *Hydnellum* being hard and dry, and *Bankera* and *Sarcodon* forming softer, fleshier basidiomata. This difference in texture is, however, difficult to assess and a series of recent molecular phylogenetic analyses, as outlined below, have indicated that the traditional, morphology-based generic limits are equivocal.

In a recent comprehensive study of stipitate hydnoid species from south-eastern North America, Baird et al. (2013) found that *Bankera* could not be separated from *Phellodon* and the genera were hence combined into a more comprehensive *Phellodon*. The same study suggested that the generic limits of *Sarcodon* and *Hydnellum* need reassessment.

Nitare and Högberg (2012) examined the Nordic species of *Sarcodon* and included a preliminary molecular phylogeny for the species accepted in *Sarcodon*. *Hydnellum* species were also included in non-published test runs and found to be nested among *Sarcodon* species. They concluded that revisions of limits of both genera were probably necessary. Miscevic (2013) expanded on the results in Nitare and Högberg (2012) by including more sequences for each species and by including a selection of *Hydnellum* species in published phylogenies. The results were in congruence with Baird et al. (2013) with regard to overall tree topology and again the conclusion was that the limits of *Sarcodon* and *Hydnellum* need further study. A recent phylogenetic overview of Thelephorales (Vizzini et al. 2016) and a study of *Hydnellum* from the Mediterranean region (Loizides et al. 2016) came to similar conclusions, although Vizzini et al. (2016) did not include sequences from several Neotropical *Sarcodon* species described by Grupe et al. (2015, 2016).

In this paper we analyse ITS and nuclear LSU sequences from a wide selection of Thelephorales species with a focus on *Hydnellum* and *Sarcodon* in order to resolve the relationship between these two genera. We also make some nomenclatural changes that follow from the revision of genus circumscriptions. We demonstrate that Neotropical *Sarcodon* species do not cluster with temperate and boreal species and may be warranted as one or more new genera with more data.

Methods

For the phylogenetic analyses we compiled two datasets. The first dataset consists of nuclear LSU sequences from most genera in Thelephorales and from a majority of the *Hydnellum* and *Sarcodon* species occurring in Europe. For our two target genera we chose only sequences generated for this study from recently collected basidiomata.

Figure 1. Fruiting bodies of *Hydnellum* and *Sarcodon* **A** *Hydnellum suaveolens* **B** *H. aurantiacum* **C** *H. ferrugineum* **D** *Sarcodon imbricatus*.

We deliberately excluded sequences from specimens identified as *H. concrescens* or *H. scrobiculatum* since these names seem to cover more than just two species and it is currently unclear how the names should be applied (Ainsworth et al. 2010). Since this study is positioned as a revision of the genus limits we were more interested in sequence quality control than a complete coverage of all species reported from Europe.

For our second dataset we chose a different strategy. Here we included ITS sequences from all *Hydnellum* and *Sarcodon* species represented among our own sequences and in GenBank as of December 1, 2018. The reason is that many species, and especially the recently described species from tropical regions, are only available as ITS sequences. However, we made no attempt to verify the identifications given in GenBank and do not endorse them as correct.

DNA was extracted from recent dried collections of basidiomata from North Europe. Voucher numbers, herbarium location, and GenBank numbers are given in Table 1. DNA extraction and PCR protocols follow Larsson et al (2018). Sequencing was either done in-house at University of Oslo, or as a commercial service by Macrogen Inc., South Korea. Assembly of chromatograms was done with Sequencher 5.2.4 (Gene Codes Co., Ann Arbor). Aligning was performed either manually using the editor in PAUP* 4.0a (Swofford 2002) or the software ALIVIEW 1.18 (Larsson 2014), or automatically utilising the L-INS-i strategy as implemented in MAFFT v. 7.017 (Katoh and Standley 2013), followed by manual adjustment.

Table 1. Specimens sequenced or downloaded from GenBank. Herbarium acronyms follow Thiers. Sequences generated for this study are marked in bold.

Species	Voucher	Herb.	GenBank number	
			ITS	LSU
Amaurodon aquicoeruleus Agerer	Agerer & Bougher	M	AM490944	AM490944
Amaurodon viridis (Alb. & Schwein.:Fr.) J.Schröt	KH Larsson 14947b	O	**MK602707**	**MK602707**
Bankera fuligineoalba (J.C.Schmidt:Fr.) Pouzar	E Larsson 400-13	GB	**MK602708**	**MK602708**
Bankera violascens (Alb. & Schwein.:Fr.) Pouzar	MV 130902	GB	**MK602709**	**MK602709**
Boletopsis leucomelaena (Pers.:Fr.) Fayod	M Krikorev 140912	GB	**MK602710**	**MK602710**
Hydnellum aurantiacum (Batsch:Fr.) P.Karst.	RG Carlsson 08-105	GB	**MK602711**	**MK602711**
Hydnellum aurantiacum	E Bendiksen 177-07	O	**MK602712**	**MK602712**
Hydnellum aurantiacum	O-F-295029	O	**MK602713**	**MK602713**
Hydnellum auratile (Britzelm.) Maas Geest.	O-F-294095	O	**MK602714**	**MK602714**
Hydnellum auratile	O-F-242763	O	**MK602715**	**MK602715**
Hydnellum auratile	J Nitare 110926	GB	**MK602716**	**MK602716**
Hydnellum caeruleum (Hornem.:Fr.) P.Karst.	O-F-291490	O	**MK602717**	**MK602717**
Hydnellum caeruleum	E Bendiksen 575-11	O	**MK602718**	**MK602718**
Hydnellum caeruleum	E Bendiksen 584-11	O	**MK602719**	**MK602719**
Hydnellum complicatum Banker	REB 71		KC571711	
Hydnellum concrescens (Pers.) Banker	K(M)134463	K	EU784267	
Hydnellum cristatum (G.F.Atk.) Stalpers	REB 169	TENN	JN135174	
Hydnellum cumulatum K.A.Harrison	SE Westmoreland 69		AY569026	
Hydnellum cyanopodium K.A.Harrison	SE Westmoreland 85		AY569027	
Hydnellum diabolus Banker	KAH 13873	MICH	AF351863	
Hydnellum dianthifolium Loizides, Arnolds & P.-A.Moreau	ML61211HY		KX619419	
Hydnellum earlianum Banker	REB 375	TENN	JN135179	
Hydnellum ferrugineum (Fr.:Fr.) P.Karst.	O-F-297319	O	**MK602720**	**MK602720**
Hydnellum ferrugineum	E Larsson 356-16	GB	**MK602721**	**MK602721**
Hydnellum ferrugineum	E Larsson 197-14	GB	**MK602722**	**MK602722**
Hydnellum ferrugipes Coker	REB 176		KC571727	
Hydnellum geogenium (Fr.) Banker	O-F-66379	O	**MK602723**	**MK602723**
Hydnellum geogenium	O-F-296213	O	**MK602724**	**MK602724**
Hydnellum geogenium	E Bendiksen 526-11	O	**MK602725**	**MK602725**
Hydnellum gracilipes (P.Karst.) P.Karst.	E Larsson 219-11	GB	**MK602726**	**MK602726**
Hydnellum gracilipes	GB-0113779	GB	**MK602727**	**MK602727**
Hydnellum mirabile (Fr.) P.Karst.	RG Carlsson 11-119	GB	**MK602728**	**MK602728**
Hydnellum mirabile	E Larsson 170-14	GB	**MK602729**	**MK602729**
Hydnellum mirabile	S Lund 140912	GB	**MK602730**	**MK602730**
Hydnellum peckii Banker	S Svantesson 328	GB	**MK602731**	**MK602731**
Hydnellum peckii	E Larsson 174-14	GB	**MK602732**	**MK602732**
Hydnellum peckii	E Bendiksen 567-11	O	**MK602733**	**MK602733**
Hydnellum pineticola K.A.Harrison	RB 94		KC571734	
Hydnellum piperatum Maas Geest.	REB 322	TENN	JN135173	
Hydnellum regium K.A.Harrison	SE Westmoreland 93		AY569031	
Hydnellum scleropodium K.A.Harrison	REB 3	TENN	JN135186	
Hydnellum scrobiculatum (Fr.) P.Karst.	REB 78	TENN	JN135181	
Hydnellum spongiosipes (Peck) Pouzar	REB 52	TENN	JN135184	
Hydnellum suaveolens (Scop.:Fr.) P.Karst.	E Larsson 139-09	GB	**MK602734**	**MK602734**
Hydnellum suaveolens	E Larsson 8-14	GB	**MK602735**	**MK602735**
Hydnellum suaveolens	S Svantesson 877	GB	**MK602736**	**MK602736**
Hydnellum subsuccosum K.A.Harrison	REB 10	TENN	JN135178	
Lenzitopsis daii L.W.Zhou & Kõljalg	Yuan 2959	IFP	JN169799	JN169793
Lenzitopsis oxycedri Malençon & Bertault	KH Larsson 15304	GB	**MK602774**	**MK602774**
Odontia fibrosa (Berk. & M.A.Curtis) Kõljalg	TU115028	TU	**MK602775**	**MK602775**
Phellodon cf niger	E Larsson 35-14	GB	**MK602782**	**MK602782**
Phellodon tomentosus (L.:Fr.) Banker	E Bendiksen 118-10	O	**MK602781**	**MK602781**
Pseudotomentella flavovirens (Höhn. & Litsch.) Svrček	KH Larsson 16190	O	**MK602780**	**MK602780**
Sarcodon amygdaliolens Rubio Casas, Rubio Roldán & Català	SC 2011		JN376763	
Sarcodon aspratus (Berk.) S.Ito			DQ448877	

Species	Voucher	Herb.	GenBank number	
			ITS	LSU
Sarcodon atroviridis (Morgan) Banker	REB 104	TENN	JN135190	
Sarcodon atroviridis	REB 61		KC571768	
Sarcodon bairdii A.C.Grupe & Vasco-Pal.	Vasco 990	HUA	KR698938	
Sarcodon colombiensis A.C.Grupe & Vasco-Pal.	Vasco 2084	HUA	KP972654	
Sarcodon fennicus (P.Karst.) P.Karst.	S Westerberg 110909	GB	**MK602739**	**MK602739**
Sarcodon fennicus	O-F-242833	O	**MK602738**	**MK602738**
Sarcodon fennicus	O-F-204087	O	**MK602737**	**MK602737**
Sarcodon fuligineoviolaceus (Kalchbr.) Pat.	LA 120818	GB	**MK602740**	**MK602740**
Sarcodon fuligineoviolaceus	B Nylén 130918	GB	**MK602741**	**MK602741**
Sarcodon fuligineoviolaceus	A Molia 160-2011	O	**MK602742**	**MK602742**
Sarcodon fuscoindicus (K.A.Harrison) Maas Geest.	OSC 113622	OSC	EU669228	
Sarcodon glaucopus Maas Geest. & Nannf.	RG Carlsson 13-060	GB	**MK602743**	**MK602743**
Sarcodon glaucopus	J Nitare 060916	GB	**MK602744**	**MK602744**
Sarcodon glaucopus	Å Edvinson 110926	GB	**MK602745**	**MK602745**
Sarcodon imbricatus (L.:Fr.) P.Karst.	S Svantesson 355	GB	**MK602748**	**MK602748**
Sarcodon imbricatus	J Rova 140829-2	GB	**MK602746**	**MK602746**
Sarcodon imbricatus	E Larsson 384-10	GB	**MK602747**	**MK602747**
Sarcodon joeides (Pass.) Bataille	RG Carlsson 11-090	GB	**MK602749**	**MK602749**
Sarcodon joeides	K Hjortstam 17589	GB	**MK602750**	**MK602750**
Sarcodon joeides	J Nitare 110829	GB	**MK602751**	**MK602751**
Sarcodon joeides	REB 270		KC571772	
Sarcodon lepidus Maas Geest.	E Grundel 110916	GB	**MK602753**	**MK602753**
Sarcodon lepidus	RG Carlsson 10-065	GB	**MK602752**	**MK602752**
Sarcodon lepidus	J Nitare 110829	GB	**MK602754**	**MK602754**
Sarcodon leucopus (Pers.) Maas Geest. & Nannf.	O-F-296944	O	**MK602756**	**MK602756**
Sarcodon leucopus	O-F-296099	O	**MK602755**	**MK602755**
Sarcodon leucopus	P Hedberg 080811	GB	**MK602757**	**MK602757**
Sarcodon lundellii Maas Geest. & Nannf.	L&A Stridvall 06-049	GB	**MK602758**	**MK602758**
Sarcodon lundellii	O-F-242639	O	**MK602759**	**MK602759**
Sarcodon lundellii	O-F-295814	O	**MK602760**	**MK602760**
Sarcodon martioflavus (Snell, K.A.Harrison & H.A.C.Jacks.) Maas Geest.	A Delin 110804	GB	**MK602763**	**MK602763**
Sarcodon martioflavus	O-F-242435	O	**MK602762**	**MK602762**
Sarcodon martioflavus	O-F-242872	O	**MK602761**	**MK602761**
Sarcodon pakaraimensis A.C.Grupe & T.W.Henkel	T Henkel 9554	BRG	KM668103	
Sarcodon pallidogriseus A.C.Grupe & Vasco-Pal.	Vasco 989	HUA	KR698939	
Sarcodon portoricensis A.C.Grupe & T.J.Baroni	TG Baroni 8776	NY	KM668100	
Sarcodon quercophilus A.C.Grupe & Lodge	CFMR-BZ-3833	NY	KM668101	
Sarcodon quercinofibulatus Pérez-De-Greg., Macau & J.Carbó	JC 20090718-2		JX271818	**MK602773**
Sarcodon rufobrunneus A.C.Grupe & Vasco-Pal.	Vasco 1989	HUA	KR698937	
Sarcodon scabripes (Peck.) Banker	REB 351	TENN	JN135191	
Sarcodon scabrosus (Fr.) P.Karst.	O-F-295824	O	**MK602764**	**MK602764**
Sarcodon scabrosus	O-F-292320	O	**MK602766**	**MK602766**
Sarcodon scabrosus	O-F-360777	O	**MK602765**	**MK602765**
Sarcodon squamosus (Schaeff.) Quél.	O-F-177452	O	**MK602768**	**MK602768**
Sarcodon squamosus	E Larsson 248-12	GB	**MK602767**	**MK602767**
Sarcodon squamosus	O-F-295554	O	**MK602769**	**MK602769**
Sarcodon umbilicatus A.C.Grupe, T.J.Baroni & Lodge	TJ Baroni 10201	NY	KM668102	
Sarcodon underwoodii Banker	REB 50		KC571781	
Sarcodon versipellis (Fr.) Nikol.	RG Carlsson 13-057	GB	**MK602771**	**MK602771**
Sarcodon versipellis	RG Carlsson 11-085	GB	**MK602772**	**MK602772**
Sarcodon versipellis	E Bendiksen 164-07	O	**MK602770**	**MK602770**
Sistotrema brinkmannii (Bres.) J.Erikss.	KH Larsson 14078	GB	KF218967	KF218967
Steccherinum ochraceum (J.F.Gmel.:Fr.) Gray	KH Larsson 11902	GB	JQ031130	JQ031130
Thelephora caryophyllea (Schaeff.:Fr.) Pers.	E Larsson 89-09S	GB	**MK602776**	**MK602776**
Thelephora terrestris Ehrh.:Fr.	E Larsson 295-13	GB	**MK602777**	**MK602777**
Tomentella stuposa (Link) Stalpers	Th-0764	O	**MK602778**	**MK602778**
Tomentellopsis pulchella Kõljalg & Bernicchia	KH Larsson 16366	O	**MK602779**	**MK602779**

In the phylogenetic analyses we assumed the following minimal partitions for the nrDNA region: ITS1, 5.8S, ITS2 and LSU (approximately 1200 bases of the 5' end). Two datasets were analysed separately: an LSU dataset only including the LSU region, and an ITS dataset including ITS1, 5.8S and ITS2. We used the automated best-fit tests implemented in PAUP* 4.0a (Swofford 2002) to select optimal substitution models for each complete, non-partitioned dataset (PHYML) and optimal substitution model partitions for each minimal partition (BEAST). Models and partitions were chosen based on BIC score for the BEAST analysis and AICc score for the PHYML analysis. All tests were conducted using three substitution schemes and evaluated substitution models with equal and gamma-distributed among-site rate variation. The tests for the PHYML analysis also evaluated substitution models with invariant sites. The following partitions and models had the highest ranking, according to BIC: ITS1+ITS2 (GTR+G), 5.8S (K80+G), LSU (GTR+G). According to AICc the GTR+I+G model provided the best fit for both the ITS and the LSU datasets.

To generate Bayesian phylogenetic trees (BI) from the alignments we used BEAST 2.4.7 (Bouckaert et al. 2014). We prepared the xml-files for the BEAST 2 runs in BEAUTI 2.4.7 (Bouckaert et al. 2014). We set the substitution model to GTR+G for the LSU run. In the ITS run we set it to HKY+G for 5.8S, since it is the most similar model to K80+G available in the program. Test runs revealed convergence problems due to insufficient data for some substitution rates in the GTR+G model initially used for the ITS1+ITS2 partition, and it was hence changed to HKY+G. In the ITS run the substitution rate of both partitions were estimated independently. We set the trees of the minimal nrDNA partitions as linked in this analysis and the clock models as unlinked. A lognormal, relaxed clock model was assumed for each partition, as test runs had shown that all partitions had a coefficient of variation well above 0.1 (i.e. implying a relatively high rate variation among branches). The clock rate of each partition was estimated in the runs, using a lognormal prior with a mean set to one in real space. We set the growth rate prior to lognormal, with a mean of 5 and a standard deviation of 2. We ran the Markov Chain Monte Carlo (MCMC) chains of both datasets for 20 million generations with tree and parameter files sampled every 1,000 generations. The analyses all converged well in advance of the 10 % burn-in threshold, had ESS values well above 200 for all parameters, and chain mixing was found to be satisfactory as assessed in TRACER 1.6.0 (Rambaut et al. 2014). After discarding the burn-in trees, maximum clade credibility trees were identified by TREEANNOTATOR 2.4.7 (Bouckaert et al. 2014).

To generate Maximum Likelihood (ML) gene trees we used PHYML 3.1 (Guindon et al. 2010). We set the substitution model to GTR+I+G for both the ITS and LSU datasets. Tree topology search was conducted using NNI+SPR, with ten random starting trees. Non-parametric bootstrap analyses with 1000 replicates were performed on the resulting trees.

Results

Seventy-five Thelephorales specimens from the genera *Amaurodon*, *Bankera*, *Boletopsis*, *Hydnellum*, *Lenzitopsis*, *Phellodon*, *Pseudotomentella*, *Sarcodon*, *Thelephora*, *Tomentella*, and *Tomentellopsis*, were sequenced for this study. In addition, 39 sequences were downloaded from public databases (GenBank, UNITE) including outgroup sequences of *Steccherinum ochraceum* (Polyporales) and *Sistotrema brinkmannii* (Cantharellales) included in the LSU dataset. The ITS analyses were rooted by the default method (BEAST) or left unrooted (PHYML).

The aligned LSU dataset consisted of 1443 nucleotide positions. After exclusion of ambiguous regions 1377 positions remained for the analyses. BI returned a tree where the focus genera *Hydnellum* and *Sarcodon* are distributed over two strongly supported clades. The larger of these clades includes the type of *Hydnellum*, *H. suaveolens*, and an additional 17 species, all except one forming strongly supported terminal clades. Nine of these taxa are currently placed in *Sarcodon*. With a few exceptions the relationships within *Hydnellum* are not resolved. *H. aurantiacum* and *H. auratile* are recovered as a strongly supported group; *Sarcodon scabrosus* and *S. fennicus* are grouped with 0.97 posterior probability support; *S. fuligineoviolaceus*, *S. glaucopus*, and *S. joeides* form a subclade with 0.97 posterior probability support; and finally *H. suaveolens* and *S. versipellis* form a strongly supported clade. The type of *Sarcodon*, *S. imbricatus*, and three other species form the second main clade. The three sequences of *S. imbricatus* cluster together but the clade is unsupported. *Hydnellum* and *Sarcodon* are recovered as sister clades but the support for this arrangement is weak.

For target taxa the ML tree is essentially similar to the BI tree with strong support for the similarly composed *Hydnellum* and *Sarcodon* clades (Fig. 2). As for the BI analysis the relationships among species within *Hydnellum* and *Sarcodon* are not resolved except for a weak to moderate support for grouping *H. aurantiacum* with *H. auratile* and *H. suaveolens* with *S. versipellis*. *S. fuligineoviolaceus*, *S. glaucopus*, and *S. joeides* also group together in the ML tree but without support. Again *S. imbricatus* does not get support and is not separated from *S. quercinofibulatus*.

The aligned ITS dataset consisted of 1068 nucleotide positions of which 505 remained for the analyses after removal of ambiguous regions. Bayesian inference produced a tree with two strongly supported clades (Fig. 3). The smaller one, which we here informally call "Neosarcodon", contains nine *Sarcodon* species, all with a distribution in the tropical and subtropical Americas. Remaining *Hydnellum* and *Sarcodon* taxa, including both type species, formed the other clade. Within the latter clade two subclades are visible, corresponding to the genera *Hydnellum* and *Sarcodon*, and with the same delimitation as in the LSU trees. Only the *Sarcodon* subclade has strong support. Within each larger clade several groups of taxa received moderate to strong support. The reader is referred to Fig. 2 for further details.

The ML tree recovered the same two main clades with strong support but could not resolve the relationships within the larger *Hydnellum*/*Sarcodon* clade. In the ML

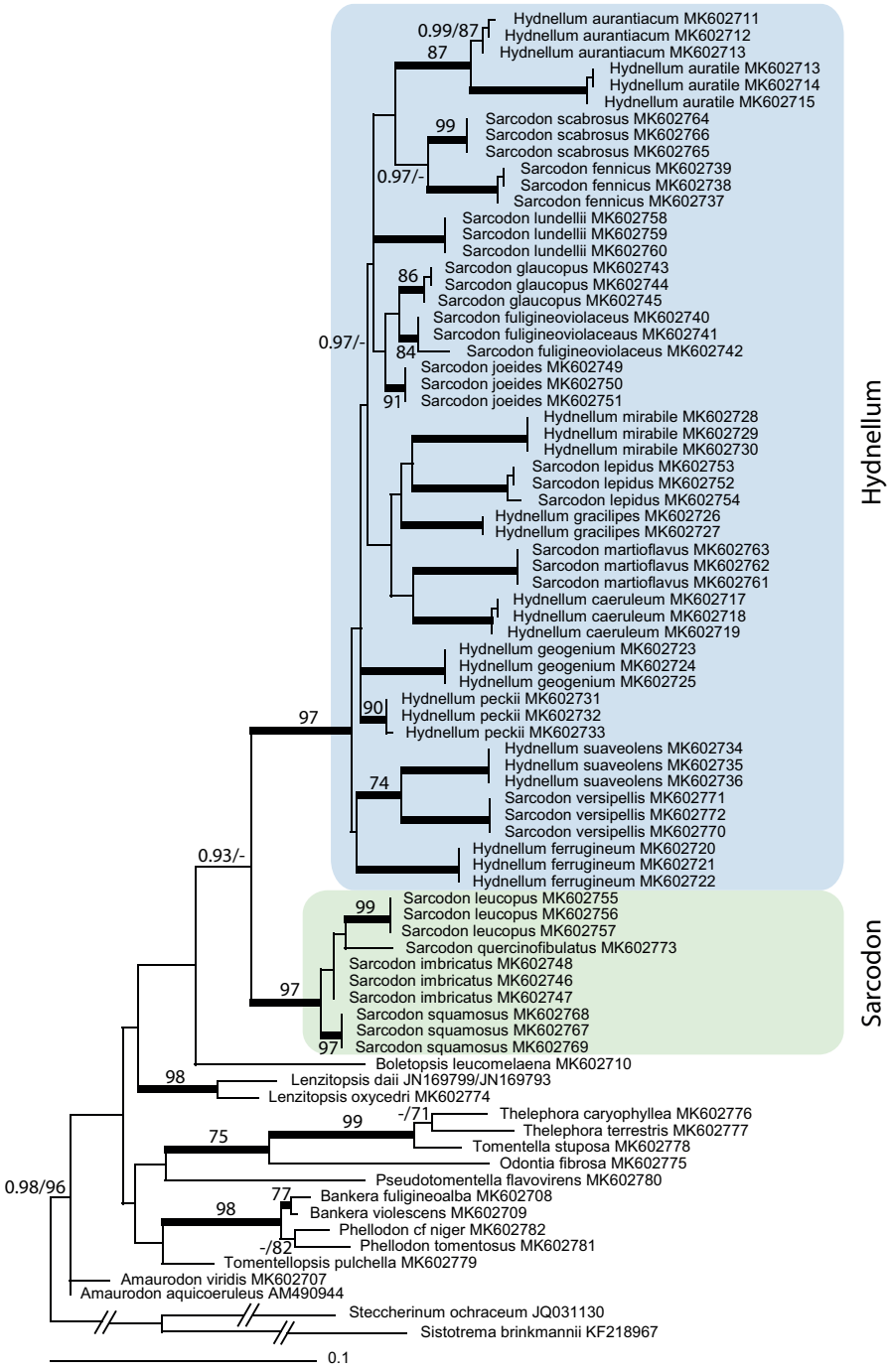

Figure 2. Maximum likelihood analyses of LSU dataset for Thelephorales. Branches in bold have a posterior probability value of 1 in Bayesian inference and 100% bootstrap support in ML analysis, if not otherwise indicated by a figure. Lower support values on other branches are indicated by figures. *Steccherinum ochraceum* and *Sistotrema brinkmannii* are used as outgroup (branch lengths shortened).

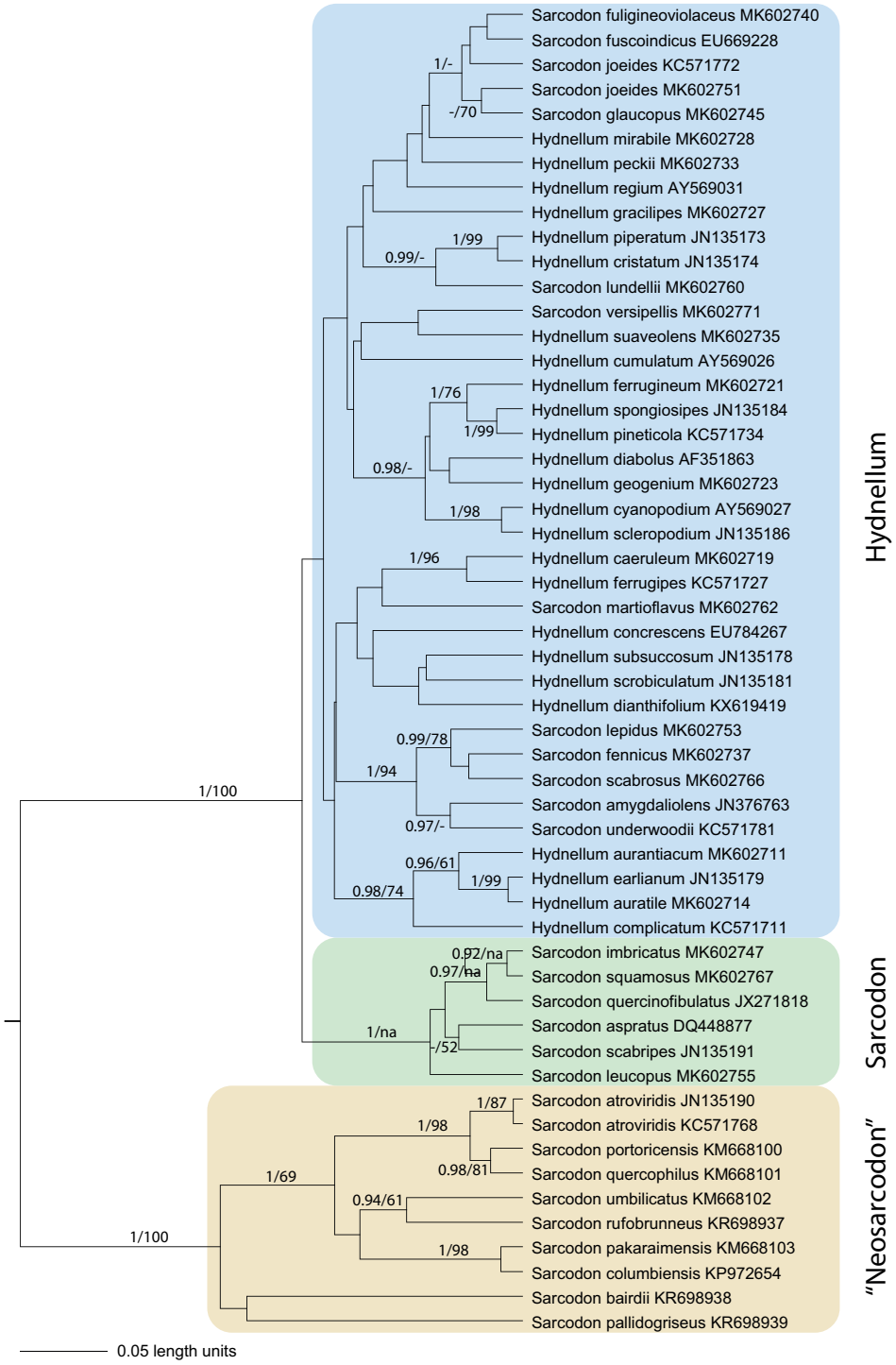

Figure 3. Ultrametric default rooted BEAST tree of ITS dataset for *Hydnellum* and *Sarcodon*. Posterior probability values and bootstrap percent support from ML analysis are indicated by figures; na = not applicable.

tree the clade corresponding to *Hydnellum* in the LSU tree is correctly identified but not supported while the clade corresponding to *Sarcodon* appears polyphyletic.

Based on these results we hereby revise the limits of the two genera by moving a number of species from *Sarcodon* to *Hydnellum*. Consequently the genus description for *Hydnellum* must be emended while the genus description for *Sarcodon* can remain unaltered.

Taxonomy

Hydnellum **P.Karst., Meddn Soc. Fauna Flora fenn. 5: 41 (1879).**

Type species. *Hydnellum suaveolens* (Scop.:Fr.) P.Karst. (1879)

Basionym. *Hydnum suaveolens* Scop.:Fr. (1772)

Basidiomata with pileus and stipe, single or concrescent; pileus thin to thick, at first smooth and velutinous, when mature felted, fibrillose, scaly, ridged, or irregularly pitted and scrupose, mostly brownish but also with white, olive yellowish, orange, purplish or bluish colours, often concentrically zonate; stipe narrow to thick, solid, mostly short; hymenophore hydnoid, usually strongly decurrent; context from soft and brittle to corky or woody; hyphal system monomitic, septa with or without clamps, context hyphae inflated or not; cystidia lacking; basidia narrowly clavate, producing four sterigmata; basidiospores with irregular outline, more or less lobed, verrucose, brownish. Terrestrial, forming ectomycorrhiza with forest trees.

Hydnellum amygdaliolens **(Rubio Casas, Rubio Roldán & Català) E.Larss., K.H.Larss. & Kõljalg, comb. nov.**
MycoBank No.: MB830570

Basionym. *Sarcodon amygdaliolens* Rubio Casas, Rubio Roldán & Català, Boln Soc. Micol. Madrid 35: 44–45. 2011. Holotype: Spain, Tamajón, Barranco la Jara. L. Rubio-Casas & L. Rubio-Roldán, AH 42113.

Hydnellum fennicum **(P.Karst.) E.Larss., K.H.Larss. & Kõljalg, comb. nov.**
MycoBank No.: MB830571

Basionym. *Sarcodon scabrosus* var. *fennicus* P.Karst., Bidr. Känn. Finl. Nat. Folk 37: 104. 1882. Type: not indicated (neotype: H, designated by Maas Geesteranus & Nannfeldt 1969: 406)

***Hydnellum fuligineoviolaceum* (Kalchbr.) E.Larss., K.H.Larss. & Kõljalg, comb. nov.**
MycoBank No.: MB830572

Basionym. *Hydnum fuligineoviolaceum* Kalchbr., in Fries, Hymenomyc. eur. (Upsaliae): 602. 1874. Holotype: Slovakia, Presovsky kraj, Olaszi. C. Kalchbrenner, UPS F-173546.

***Hydnellum fuscoindicum* (K.A.Harrison) E.Larss., K.H.Larss. & Kõljalg, comb. nov.**
MycoBank No.: MB830573

Basionym. *Hydnum fuscoindicum* K.A.Harrison, Can. J. Bot. 42: 1213. 1964. Holotype: USA, Washington, Olympic Nat. Park, A.H. Smith. MICH 10847.

***Hydnellum glaucopus* (Maas Geest. & Nannf.) E.Larss., K.H.Larss. & Kõljalg, comb. nov.**
MycoBank No.: MB830574

Basionym. *Sarcodon glaucopus* Maas Geest. & Nannf., Svensk bot. Tidskr. 63: 407. 1969. Holotype: Sweden, Uppland, Börje par., J. Eriksson. UPS F-013955.

***Hydnellum joeides* (Pass.) E.Larss., K.H.Larss. & Kõljalg, comb. nov.**
MycoBank No.: MB830575

Basionym. *Hydnum joeides* Pass., Nuovo G. bot. ital. 4: 157. 1872. Holotype: Italy, Emilia-Romagna, Collecchio, G. Passerini. PAD.

***Hydnellum lepidum* (Maas Geest.) E. Larss., K.H.Larss. & Kõljalg, comb. nov.**
MycoBank No.: MB830576

Basionym. *Sarcodon lepidus* Maas Geest., Verh. K. ned. Akad. Wet., tweede sect. 65: 105. 1975. Holotype: The Netherlands, Lochem, Ampsen, G. & H. Piepenbroek. L.

***Hydnellum lundellii* (Maas Geest. & Nannf.) E.Larss., K.H.Larss. & Kõljalg, comb. nov.**
MycoBank No.: MB830577

Basionym. *Sarcodon lundellii* Maas Geest. & Nannf., Svensk bot. Tidskr. 63: 421. 1969. Type: Sweden, Uppland, Storvreta, S. Lundell & J.A. Nannfeldt, distributed

in S. Lundell & J.A. Nannfeldt Fungi exs. suec. as number 252 (lectotype, designated here, UPS F-010975; MycoBank No.: MBT387081). The UPS herbarium has two copies of the exsiccate and the specimens of *H. lundellii* are registered as F-010975 and F-013956, respectively. From F-010975 an ITS2 sequence has been generated [GenBank MK753037] and this specimen is here selected as lectotype).

Hydnellum martioflavum **(Snell, K.A.Harrison & H.A.C.Jacks.) E.Larss., K.H.Larss. & Kõljalg, comb. nov.**
MycoBank No.: MB830578

Basionym. *Hydnum martioflavum* Snell, K.A.Harrison & H.A.C.Jacks., Lloydia 25: 161. 1962. Holotype: Canada, Quebec, Ste Anne de la Pocatière, H.A.C. Jackson & W.H. Snell 13 Sep. 1954, BPI 259438.

Hydnellum scabrosum **(Fr.) E.Larss., K.H.Larss. & Kõljalg, comb. nov.**
MycoBank No.: MB830579

Basionym. *Hydnum scabrosum* Fr., Anteckn. Sver. Ätl. Svamp.: 62. 1836. Type: not indicated (neotype: Sweden, Småland, Femsjö, S. Lundell, UPS F-013954, designated by Maas Geesteranus & Nannfeldt 1969: 426)

Hydnellum underwoodii **(Banker) E.Larss., K.H.Larss. & Kõljalg, comb. nov.**
MycoBank No.: MB830580

Basionym. *Sarcodon underwoodii* Banker, Mem. Torrey bot. Club 12: 147. 1906. Holotype: USA, Connecticut, NY 776131.

Hydnellum versipelle **(Fr.) E.Larss., K.H.Larss. & Kõljalg, comb. nov.**
MycoBank No.: MB830581

Basionym. *Hydnum versipelle* Fr., Öfvers. K. Svensk. Vetensk.-Akad. Förhandl. 18(1): 31. 1861. Type: not indicated (neotype: Sweden, Uppland, Danmark par., J. Eriksson & H. Nilsson, UPS F-013958, designated by Maas Geesteranus & Nannfeldt 1969: 430)

Sarcodon **Quél. ex P.Karst., Revue mycol., Toulouse 3 (no. 9): 20 (1881).**

Type species. *Sarcodon imbricatus* (L.:Fr.) P.Karst. (1881)
Basionym. *Hydnum imbricatum* L.:Fr. (1753).

Basidiomata with pileus and stipe, single or concrescent; pileus thin to thick, at first smooth and velutinous, when mature smooth or scaly, brownish; stipe thick, solid, mostly short; hymenophore hydnoid, usually strongly decurrent; context soft and brittle; hyphal system monomitic, septa with clamps, context hyphae inflated; cystidia lacking; basidia narrowly clavate, producing four sterigmata; basidiospores with irregular outline, more or less lobed, verrucose, brownish. Terrestrial, forming ectomycorrhiza with forest trees.

Discussion

In this paper we show that the current morphology-based concepts of *Sarcodon* and *Hydnellum* do not correspond to monophyletic subgroups within the Thelephorales. The characters traditionally used to separate the two genera do not reflect true relationships. These characters, however, are vague and open to subjectivity; hence it is not surprising that they have now been shown to be unreliable. Maas Geesteranus (1975) pointed to the context structure and consistency as the main differentiating character. For *Hydnellum* he describes the context as "... fibrillose, soft or tough, corky to woody, more or less duplex, zoned, ..." and hyphae are said to be "...usually not inflating ...". In *Sarcodon* the same structures are described as "... fleshy, brittle, soft or firm (never corky or woody), not duplex, not zoned ..." and "...hyphae inflating ...". While these morphological characteristics remain true for *Sarcodon*, the corresponding descriptions for *Hydnellum* had to be emended.

Instead of context structure it seems that average basidiospore size may in most cases offer a possibility to separate a *Sarcodon* species from one belonging to *Hydnellum*. Table 2 summarizes basidiospore measurements from the literature. Average basidiospore lengths in *Hydnellum* fall between 4.45 and 6.95 µm while the same figures for *Sarcodon* are 7.4 and 9 µm, ornamentation excluded. However, *S. quercinofibulatus* clearly deviates from this pattern. According to measurements in the protologue (Pérez-de-Gregorio et al. 2011) and in Vizzini et al. (2013) average basidiospore length was measured to 6.95 and 7.0, respectively, but then included the ornamentation. Measurements excluding ornamentation would be approximately 1 µm less. Clearly, for *S. quercinofibulatus* basidiospore length alone will not be decisive for genus placement.

Not all sequences from species described as *Sarcodon* spp. were recovered within either *Sarcodon* or *Hydnellum*. In our ITS-only analyses nine species formed a well-supported clade of their own, separated from *Sarcodon* sensu stricto and *Hydnellum* (Fig. 3). This clade, here informally called "Neosarcodon", contains species collected in tropical and subtropical regions of the Western Hemisphere and may represent one or several distinct genera. However, further analyses based on an expanded dataset using more conservative molecular markers would be required to definitely identify any new higher taxa in the group.

The failure to generate support for *Sarcodon* and *Hydnellum* in the ITS-only analyses reflects the large genetical distances present among the species within this

Table 2. Basidiospore measurements for *Hydnellum* and *Sarcodon* from the literature. Sources: B = Baird et al. (2013), M = Maas Geesteranus (1975), J = Johannesson et al. (1999). All measurements exclude ornamentation. For species treated in this paper names follow our new classification. For other species names are according to cited authors.

Species	Measurements	Mean length
Hydnellum aurantiacum (M)	(5.8–)6–6.7 × (4–)4.3–4.9	6.35
Hydnellum auratile (M)	4.9–5.8 × 3.6–4.5	5.35
Hydnellum caeruleum (M)	5.4–6(–6.3) × 3.4–4.3	5.70
Hydnellum compactum (Pers.:Fr.) P.Karst. (M)	5.4–6.3 × 3.6–4.5	5.85
Hydnellum complicatum (B)	4–5 × 3–5	4.50
Hydnellum concrescens (M)	5.4–6.1 × (3.6–)4–4.5	5.75
Hydnellum cristatum (B)	5–6 × 4–5	5.50
Hydnellum cruentum K.A.Harrison (B)	4–5 × 3–4	4.50
Hydnellum cumulatum (M)	4.3–5.6 × 3.6–4.3	4,95
Hydnellum diabolus (B)	6–7 × 5–6	6.50
Hydnellum earlianum (B)	5–6 × 4–5	5.50
Hydnellum fennicum (M)	6.3–7.6 × 4.5–5.2	6.95
Hydnellum ferrugineum (M)	(5.4–)5.8–6.3 × 3.6–4.5	6.05
Hydnellum ferrugipes (B)	5–7 × 5–6	6.00
Hydnellum fuligineoviolaceum (M)	5.4–6.5 × 4–4.7(–5.4)	5.95
Hydnellum geogenium (M)	4.5–5.2 × 3.1–3.6	4.85
Hydnellum glaucopus (M)	(5–)5.4–5.8(–6.3) × (3.6–)4–4.5	5.60
Hydnellum gracilipes (M)	4.3–4.6 × 2.7–3.6	4.45
Hydnellum joeides (M)	5.4–5.8 × 3.6–4.2	5.60
Hydnellum lepidum (M)	5.8–6.3 × 3.6–4.3	6.05
Hydnellum lundellii (M)	4.9–5.8 × 3.6–4.2	5.35
Hydnellum martioflavum (M)	5–6.3 × 3.6–4.5	5.65
Hydnellum peckii (M)	4.9–5.4 × 3.8–4	5.15
Hydnellum pineticola (B)	5–7 × 4–6	6.00
Hydnellum piperatum (B)	4–6 × 4–5	5.00
Hydnellum scabrosum (M)	(5.4–)6.3–7.3 × (3.6–)4–5	6.80
Hydnellum scleropodium (B)	4–6 × 3–4	5.00
Hydnellum spongiosipes (B)	6–7 × 5–6	6.50
Hydnellum suaveolens (M)	4–5 × 3–3.6	4.50
Hydnellum subsuccosum (B)	5–6 × 4–6	5.50
Hydnellum versipelle (M)	4.5–5.5 × 3.5–4.5	5.00
Hydnellum underwoodii (B)	5–7 × 5–6	6.00
Sarcodon atroviridis (B)	8–9 × 7–8	8.50
Sarcodon excentricus R.E.Baird (B)	8–9 × 6–8	8.50
Sarcodon harrisonii R.E.Baird (B)	7–9 × 6–8	8.00
Sarcodon leucopus (M)	(6.7–)7.2–7.6(–9) × 4.5–5.6	7.40
Sarcodon imbricatus (M)	7.2–8.2 × 4.9–5.4	7.70
Sarcodon scabripes (B)	8–10 × 7–9	9.00
Sarcodon squamosus (J)	7.2–8.2 × 4.9–5.4	7.70

marker. Our general experience with the ITS region for thelephoralean target genera is that species are extremely well separated and the internal variation surprisingly low, even when a large number of specimens from both Europe and America are considered. On the other hand, the genetical difference among species is moderate to high, making alignments difficult and prone to ambiguities. In our ITS analyses we chose to remove ambiguous regions, thus halving the number of nucleotide positions suggested by

automatic alignment through MAFFT. This seems to have affected the ML analyses most. However, the ITS analyses only served to position neotropical *Sarcodon* species and the results clearly show that they belong to a separate lineage.

Otto (1997) suggested that *Hydnum auratile* is a later synonym of *Hydnum aurantiacum* and that the species we now call *Hydnellum aurantiacum* should be named *Hydnellum floriforme* (Schaeff.) Banker. The name change is based on a reinterpretation of Batsch's original illustration, which, according to Otto, clearly shows the same species as *Hydnum auratile*. In phylogenetic analyses *H. aurantiacum* and *H. auratile* are sister taxa and during our study we have sequenced several specimens identified as *H. auratile* that turned out to be *H. aurantiacum*. Thus separating these species can be hazardous and to interpret illustrations must be even harder. We currently do not accept this unfortunate name change.

The present study will serve as the basis for further exploration of species limits within *Hydnellum* and *Sarcodon*. As has been demonstrated for the genera, many species interpretations are in need of revision. Over the years we have found numerous specimen misidentifications as well as specimens that could not be assigned to pre-existing names. A closer inspection of the ITS tree in Fig. 3, where we let the terminals retain the identifications given in GenBank, shows some examples. The American sequence of *Sarcodon joeides* (KC571772) does not cluster with the European representative of the same species (MK602751) and the American sequence named *Hydnellum earlianum* seems to be identical to what is in Europe called *H. auratile*. Considering that many stipitate hydnoid species are red-listed and used as indicators of forests in need of conservation (Ainsworth 2005, Nitare 2019), it is of utmost importance to sort out the taxonomy of these species.

Acknowledgements

This study was supported by grants from ArtsDatabanken, Norway, to KH Larsson (ADB54-09), from Artdatabanken, Sweden, to E Larsson (2014-152 4.3), and from Estonian Research Council to U Kõljalg (IUT20-30). We also acknowledge support to S Svantesson from Kungliga Vetenskaps- och Vitterhetssamhället i Göteborg and from Kapten Carl Stenholms donatationsfond. We are grateful to many dedicated mycologists in Norway, Sweden and Finland for sending valuable collections. We are especially grateful to Johan Nitare for sharing with us his outstanding knowledge of stipitate hydnoid fungi and for duplicates from his herbarium. We also thank Martyn Ainsworth and Terry Henkel whose thorough reviews improved this paper considerably.

References

Ainsworth AM (2005) BAP Fungi Handbook. English Nature Research Reports 600, English Nature, Peterborough, 115 pp.

Ainsworth AM, Parfitt D, Rogers HJ, Boddy L (2010) Cryptic taxa within European species of Hydnellum and Phellodon revealed by combined molecular and morphological analysis. Fungal Ecology 3: 65–80. https://doi.org/10.1016/j.funeco.2009.07.001

Baird R, Wallace LE, Baker G, Scruggs M (2013) Stipitate hydnoid fungi of the temperate southeastern United States. Fungal Diversity 62: 41–114. https://doi.org/10.1007/s13225-013-0261-6

Bouckaert R, Heled J, Kühnert D, Vaughan T, Wu C-H, Xie D, Suchard MA, Rambaut A, Drummond AJ (2014) BEAST 2: A software platform for Bayesian evolutionary analysis. PLOS Computational Biology 10(4). https://doi.org/10.1371/journal.pcbi.1003537

Grupe A, Baker A, Uehling JK, Smith ME, Baroni TJ, Lodge DJ, Henkel TW (2015) *Sarcodon* in the Neotropics I: new species from Guyana, Puerto Rico and Belize. Mycologia 107: 591–606, https://doi.org/10.3852/14-185

Grupe A, Vasco-Palacios AM, Smith ME, Boekhout T, Henkel TW (2016) *Sarcodon* in the Neotropics II: four new species from Colombia and a key to the regional species. Mycologia 108: 791–805. https://doi.org/10.3852/15-254

Guindon S, Dufayard JF, Lefort V, Anisimova M, Hordijk W, Gascuel O (2010) New algorithms and methods to estimate maximum-likelihood phylogenies: assessing the performance of PhyML 3.0. Systematic Biology 59: 307–321. https://doi.org/10.1093/sysbio/syq010

Johannesson H, Ryman S, Lundmark H, Danell E (1999) *Sarcodon imbricatus* and *S. squamosus* - two confused species. Mycological Research 103: 1447–1452. https://doi.org/10.1017/S0953756299008709

Katoh K, Standley DM (2013) MAFFT multiple sequence alignment software version 7, improvements in performance and usability. Molecular Biology and Evolution 30: 772–780. https://doi.org/10.1093/molbev/mst010

Larsson, A (2014) AliView: a fast and lightweight alignment viewer and editor for large data sets. Bioinformatics 30: 3276–3278. https://doi.org/10.1093/bioinformatics/btu531

Larsson E, Vauras J, Cripps CL (2018) *Inocybe praetervisa* group - a clade of four closely related species with partly different geographical distribution ranges in Europe. Mycoscience 59: 277–287. https://doi.org/10.1016/j.myc.2017.11.002

Loizides M, Alvarado P, Assoyov B, Arnolds E, Moreau P-A (2016) *Hydnellum dianthifolium* sp. nov. (Basidiomycota, Thelephorales, a new tooth-fungus from southern Europe with notes on *H. concrescens* and *H. scrobiculatum*. Phytotaxa 280: 23–35. https://doi.org/10.11646/phytotaxa.280.1.2

Maas Geesteranus RA (1975) Die Terrestrischen Stachelpilze Europas (The Terrestrial Hydnums of Europe). North-Holland Publishing, 1–127.

Maas Geesteranus RA, Nannfeldt JA (1969) The genus *Sarcodon* in Sweden in the light of recent investigations. Svensk Botanisk Tidskrift 63: 401–440.

Miscevic, D (2013) A phylogenetic study of the genus *Sarcodon*. MSc degree project, Department of Biological and Environmental Sciences, University of Gothenburg, Sweden.

Nitare J (2019) Skyddsvärd skog. Naturvårdsarter och andra kriterier för naturvärdesbedömning. Skogsstyrelsens förlag, Jönköping.

Nitare J, Högberg N (2012) Svenska arter av fjälltaggsvampar (*Sarcodon*) – en preliminär rapport. Svensk Mykologisk Tidskrift 33(3): 2–49.

Otto P (1997) Kommentierter Bestimmungsschlüssel der terrestrischen Stachelpilze Deutschlands mit taxonomischen and nomenklatorischen Anmerkungen. Boletus 21(1): 1–21.

Pérez-de-Gregorio MÁ, Macau N, Carbó J (2011) *Sarcodon quercinofibulatum*, una nueva especie del género con hifas fibulíferas. Revista Catalana de Micologia 33: 25–30.

Rambaut A, Suchard MA, Xie D, Drummond AJ (2014) Tracer v1.6. http://tree.bio.ed.ac.uk/software/tracer

Swofford DL (2002) PAUP*. Phylogenetic Analysis Using Parsimony (*and Other Methods). Version 4.0a, build 159. Sinauer Associates, Sunderland, MA.

Tedersoo L, May TW, Smith ME (2010) Ectomycorrhizal lifestyle in fungi: global diversity, distribution, and evolution of phylogenetic lineages. Mycorrhiza 20: 217–263. https://doi.org/10.1007/s00572-009-0274-x

Thiers B (continuously updated) Index Herbariorum: A global directory of public herbaria and associated staff. New York Botanical Garden's Virtual Herbarium. http://sweetgum.nybg.org/science/ih [accessed 1 December 2018]

Vizzini A, Carbone M, Boccardo F, Ercole E (2013) Molecular validation of *Sarcodon quercinofibulatus*, a species of the *S. imbricatus* complex associated with Fagaceae, and notes on *Sarcodon*. Mycological Progress 12: 465–474. https://doi.org/10.1007/s11557-012-0851-9

Vizzini A, Angelini C, Los C, Ercole E (2016) *Thelephora dominicana* (Basidiomycota, Thelephorales), a new species from the Dominican Republic, and preliminary notes on thelephoroid genera. Phytotaxa 265: 27–38. https://doi.org/10.11646/phytotaxa.265.1.2

MycoKeys 54: 49–76 (2019)
doi: 10.3897/mycokeys.54.34571
http://mycokeys.pensoft.net

RESEARCH ARTICLE

A peer-reviewed open-access journal
MycoKeys
Launched to accelerate biodiversity research

Octospora conidiophora (Pyronemataceae) – a new species from South Africa and the first report of anamorph in bryophilous Pezizales

Zuzana Sochorová[1,3], Peter Döbbeler[2], Michal Sochor[3], Jacques van Rooy[4,5]

1 *Department of Botany, Faculty of Science, Palacký University Olomouc, Šlechtitelů 27, Olomouc, CZ-78371, Czech Republic* **2** *Ludwig-Maximilians-Universität München, Systematische Botanik und Mykologie, Menzinger Straße 67, München, D-80638, Germany* **3** *Department of Genetic Resources for Vegetables, Medicinal and Special Plants, Crop Research Institute, Centre of the Region Haná for Biotechnological and Agricultural Research, Šlechtitelů 29, Olomouc, CZ-78371, Czech Republic* **4** *National Herbarium, South African National Biodiversity Institute (SANBI), Private Bag X101, Pretoria 0001, South Africa* **5** *School of Animal, Plant and Environmental Sciences, University of the Witwatersrand, Johannesburg, PO WITS 2050, South Africa*

Corresponding author: *Zuzana Sochorová* (asco.sochorova@gmail.com)

Academic editor: *D. Haelewaters* | Received 15 March 2019 | Accepted 26 April 2019 | Published 10 June 2019

Citation: Sochorová Z, Döbbeler P, Sochor M, van Rooy J (2019) *Octospora conidiophora* (Pyronemataceae) – a new species from South Africa and the first report of anamorph in bryophilous Pezizales. MycoKeys 54: 49–76. https://doi.org/10.3897/mycokeys.54.34571

Abstract

Octospora conidiophora is described as a new species, based on collections from South Africa. It is characterised by apothecia with a distinct margin, smooth or finely warted ellipsoid ascospores, stiff, thick-walled hyaline hairs, warted mycelial hyphae and growth on pleurocarpous mosses *Trichosteleum perchlorosum* and *Sematophyllum brachycarpum* (Hypnales) on decaying wood in afromontane forests. It is the first species of bryophilous Pezizales in which an anamorph has been observed; it produces long, claviform, curved, hyaline and transversely septate conidia. Three other cryptic species of *Octospora* were detected using three molecular markers (LSU and SSU nrDNA and EF1α), but these could not be distinguished phenotypically. These are not described formally here and an informal species aggregate *O. conidiophora* agg. is established for them. The new species and finds of *Lamprospora campylopodis* growing on *Campylopus pyriformis* and *Neottiella albocincta* on *Atrichum androgynum* represent the first records of bryophilous Pezizales in South Africa.

Keywords

Afromontane forests, bryosymbionts, conidia, cryptic biodiversity, muscicolous parasites, *Sematophyllum*, *Trichosteleum*, South Africa

Introduction

The family Pyronemataceae is not only highly diverse in terms of morphology but also ecologically (Perry et al. 2007, Hansen et al. 2013). It includes six related genera that obligately grow on bryophytes – *Octospora* Hedw., *Lamprospora* De Not., *Neottiella* (Cooke) Sacc., *Octosporopsis* U.Lindem. & M.Vega, *Octosporella* Döbbeler and *Filicupula* Y.J.Yao & Spooner. These ascomycetes, known as bryoparasitic, bryophilous or bryosymbiotic Pezizales, form ca. 0.2–15 mm broad apothecia or perithecia-like apothecia (in *Octosporella*), coloured in shades of orange or red. They infect their hosts by elaborate infection structures consisting of superficial appressoria and intracellular haustoria (Döbbeler 1980). Together with their hosts, they can be found on various substrates like soil, burnt ground, rocks or bark and wood, both in natural and anthropogenic habitats in arctic to tropical regions (e.g. Benkert 1987; Schumacher 1993; Döbbeler 1997; Egertová et al. 2018).

Only rare reports of bryophilous Pezizales from the African continent are known: *Lamprospora maireana* Seaver, described on the basis of material from Algeria (Seaver 1914); *Octospora tetraspora* (Fuckel) Korf var. *aegyptiaca* J.Moravec from Egypt (Moravec 1972), later revised by D. Benkert as *O. leucoloma* Hedw. var. *tetraspora* Benkert, as indicated by his revision label; and *O. kilimanjarensis* J.Moravec, described from Tanzania (Moravec 1997) and later reported from Ethiopia together with a probably undescribed *Octospora* species (Lindemann 2013).

From southern Africa, thus far, no finds of these fungi have been reported and no vouchers are deposited in the South African National Collection of Fungi (PREM; Riana Jacobs-Venter pers. comm.). Surprisingly, during three weeks of our field excursions in KwaZulu-Natal and Mpumalanga, eastern South Africa, in February and March 2018, 39 populations of bryophilous Pezizales (*Octospora*, *Lamprospora* and *Neottiella*) were recorded. Only three of them could be assigned to described species, based on morphological characters, host association and DNA sequencing: *Lamprospora campylopodis* W.D.Buckley growing on *Campylopus pyriformis* (Schultz) Brid. (two collections) and *Neottiella albocincta* (Berk. & M.A.Curtis) Sacc. on *Atrichum androgynum* (Müll. Hal.) A.Jaeger (one collection). The remaining specimens were separated into six morphospecies. One of them, an undescribed *Octospora* species, growing on pleurocarpous mosses from the family Sematophyllaceae (Hypnales), turned out to be very common and remarkable in several aspects after detailed analysis. The aim of this contribution is to provide a description of this species, clarify its phylogenetic relationships and discuss associated taxonomical problems.

Methods

Sample collection and observation

Fungi were collected in February and March 2018 in South African Provinces KwaZulu-Natal and Mpumalanga. The description of *Octospora conidiophora* is based on 11 collections belonging to the most frequent genotype. Observations of apothecial fea-

tures were made on vital (marked by *) or rehydrated (†) material mostly in tap water, cresyl blue (CRB), lactophenol cotton blue (LPCB) or lactic acid cotton blue (LACB). Absence of amyloidity of asci was confirmed in Lugol´s solution. Infection structures were observed on rehydrated material. Parts of the host plants (leaves and rhizoids) close to an apothecium were separated, pulled apart, treated with LPCB and studied by light microscopy. The preparations were screened at 100× to 200× magnification for the presence of conidia. Infection structures and conidia usually occurred in the same mounts. Illustrations and measurements of hyphae, appressoria and haustoria, as well as conidia, were done in LPCB. The mosses were identified as hosts, based on the presence of appressoria on leaves or rhizoids. The host species were determined using standard techniques for bryophytes (Magill 1981). Collections are deposited in the Mycological department of the National Museum in Prague (PRM) and the herbarium of the Botanische Staatssammlung München (M).

DNA extraction, PCR amplification and sequencing

DNA was extracted from dried apothecia by the CTAB method as outlined by Doyle and Doyle (1987). Up to three apothecia were homogenised by a pestle and incubated in 300 µl extraction buffer at 65 °C for one hour; the extract was subsequently purified in chloroform-isoamyl alcohol mixture, precipitated by isopropanol and finally dissolved in water and incubated with RNase for 30 min at 37 °C. DNA quality was checked on agarose gel. Molecular sequence data were generated for three loci: the 28S subunit of ribosomal DNA (LSU) was amplified with primers LR0R and LR6 (Vilgalys and Hester 1990), the 18S subunit of rDNA (SSU) with primers NS1 and NS6 (White et al. 1990) and translation elongation factor-1alpha (EF1α) with primers EF1-983F and EF1–1567R (Rehner and Buckley 2005). PCR was performed with Kapa polymerase (Kapa Biosystems, Wilmington, USA) following a standard protocol with 37 cycles and annealing temperature of 54 °C. The PCR products were purified by precipitation with polyethylene glycol (10% PEG 6000 and 1.25 M NaCl in the precipitation mixture) and sequenced from both directions using the same primers by the Sanger method at Macrogen Europe, Amsterdam, The Netherlands.

Phylogenetic analysis

Newly generated sequences were assembled, edited and aligned in GENEIOUS 7.1.7. (Biomatters, New Zealand) using the MAFFT plugin, manually corrected and deposited in NCBI GenBank under accession numbers MK569288–MK569376. Datasets were compiled from these and previously published sequences (Table 1), aligned, trimmed in order not to contain too many missing data at the ends and concatenated in GENEIOUS 7.1.7. Bayesian Inference for concatenated data was computed in MRBAYES (ver. 3.2.4; Ronquist et al. 2012) with 2×10^7 generations, sampling every 1000th tree, in two independent runs, each with 4 chains, the first 50% (10^7) generations being ex-

Table 1. Specimens used for the phylogeny inference and their GenBank accession numbers. Newly generated sequences are MK569288–MK569376.

Taxon	Collection code	LSU	SSU	EF1α
Lamprospora campylopodis W.D.Buckley	48633	MF066054	MK569364	MK569289
Lamprospora dictydiola Boud.	ldic	MF754056	MK569365	MF754054
Lamprospora miniata De Not. var. *parvispora* Benkert	LMSk	MF066065	MK569366	MF754055
Lamprospora sylvatica Egertová & Eckstein	UA1	MG947604	MK569367	MK569290
Neottiella rutilans (Fr.) Dennis	46853	MK569313	MK569336	MK569288
Neottiella vivida (Nyl.) Dennis	NVZla	MF066068	MK569337	MF754051
Octospora affinis Benkert & L.G.Krieglst.	OAFZla	MF754075	MK569347	MF754045
Octospora conidiophora Sochorová & Döbbeler	ZE11/18	MK569315	MK569348	MK569291
Octospora conidiophora	ZE23/18	MK569324	MK569349	MK569294
Octospora conidiophora	ZE45/18	MK569316		MK569296
Octospora conidiophora	ZE46/18	MK569317	MK569350	MK569298
Octospora conidiophora	ZE48/18	MK569321	MK569351	MK569297
Octospora conidiophora	ZE57/18	MK569318	MK569352	MK569295
Octospora conidiophora	ZE62/18	MK569323	MK569354	MK569299
Octospora conidiophora	ZE63/18	MK569319	MK569355	MK569292
Octospora conidiophora	ZE71/18	MK569322	MK569356	MK569293
Octospora conidiophora	ZE75/18	MK569320	MK569357	MK569300
Octospora conidiophora	ZE77/18	MK569331	MK569353	MK569301
Octospora conidiophora agg. – lineage B	ZE37/18	MK569325	MK569358	MK569302
Octospora conidiophora agg. – lineage B	ZE38/18	MK569329	MK569359	MK569303
Octospora conidiophora agg. – lineage B	ZE51/18	MK569327	MK569362	MK569306
Octospora conidiophora agg. – lineage B	ZE52/18	MK569326	MK569360	MK569304
Octospora conidiophora agg. – lineage B	ZE53/18	MK569328	MK569361	MK569307
Octospora conidiophora agg. – lineage B	ZE65/18	MK569330	MK569363	MK569305
Octospora conidiophora agg. – lineage C	ZE44/18	MK569332	MK569373	MK569308
Octospora conidiophora agg. – lineage C	ZE56/18	MK569333	MK569374	MK569309
Octospora conidiophora agg. – lineage D	ZE69/18	MK569334	MK569375	MK569310
Octospora erzbergeri Benkert	ERZ	MF754068	MK569340	MF754042
Octospora excipulata (Clem.) Benkert	OExc	MF754062	MK569369	MF754047
Octospora fissidentis Benkert & Brouwer	Fis	MF754073	MK569341	MF754044
Octospora humosa (Fr.) Dennis	OHZla	MF754074	MK569343	MF754043
Octospora ithacaensis (Rehm) K.B.Khare	OLOi	MF754071	MK569346	MF754053
Octospora kelabitiana Egertová & Döbbeler	Oct-Jat	MF754065	MK569372	MF754048
Octospora kelabitiana	ZE61/16	MF754064	MK569376	MF754049
Octospora leucoloma Hedw.	Oleu	MF066067	MK569370	
Octospora orthotrichi (Cooke & Ellis) K.B.Khare & V.P.Tewari	HR8	MK569314	MK569342	MK569311
Octospora phagospora (Flageolet & Lorton) Dennis & Itzerott	PHG44	MF754072	MK569344	MF754046
Octospora pseudoampezzana (Svrček) Caillet & Moyne	OP1	MF754069	MK569339	MF754050
Octospora wrightii (Berk. & M.A.Curtis) J.Moravec	WRIG	MF754070	MK569345	
Octosporella perforata (Döbbeler) Döbbeler	PERF	MF754060	MK569368	MF754052
Octosporopsis erinacea Egertová & Döbbeler	DUM20/1	MF754057	MK569338	MF754041
Otidea leporina (Batsch) Fuckel	KGOL	MK569335	MK569371	MK569312

cluded as burn-in. The most suitable substitution model for each locus was determined in PARTITIONFINDER 2.1.1 (Lanfear et al. 2017) using the AIC corrected for small samples (AICc) and a greedy search. Single-locus phylogenies were computed with similar settings, but with 6×10^6 MCMC generations and the parameter temp. = 0.01.

Divergence times were estimated with BEAST 2.5.1 (Bouckaert et al. 2014) using the LSU and SSU data from our sample set (one sample per species or phylogenetic lineage) and six additional species: *Caloscypha fulgens* (Pers.) Boud., *Scutellinia scutellata* (L.) Lambotte, *Cheilymenia stercorea* (Pers.) Boud., *Aleuria aurantia* (Pers.) Fuckel, *Pyronema domesticum* (Sowerby) Sacc. and *Sarcoscypha coccinea* (Gray) Boud. (all sequences obtained from Beimforde et al. 2014; EF1α was not analysed by these authors and, therefore, not included in our molecular dating). Four calibration points were used for the analysis and the divergence times, together with their confidence intervals, were also taken from Beimforde et al. (2014), namely divergence *Cheilymenia-Scutellinia*, divergence *Aleuria-*(*Cheilymenia*+*Scutellinia*), split-off of *Sarcoscypha* and split-off of *Caloscypha*. Monophyly was forced for all of the points except the second one due to an unclear position of the *Octospora* clade. Analysis was run under GTR+I+G substitution model (as for MRBAYES), with relaxed clock log normal model and 10^8 MCMC generations, but the first 50% were excluded as burn-in. Priors included the Yule model with uniform birth rate and exponential gamma shape. Convergence and stationarity were analysed using TRACER v1.7.1 (Rambaut et al. 2018) and results were considered when effective sample size (ESS) ≥ 1000. Statistical uncertainty of divergence time estimates was assessed through the calculation of highest probability density (HPD) values.

Results

Phylogenetic and phenotypic analysis

After trimming, the total length of the concatenated alignment was 2702 bp (539 bp from EF1α, 1102 bp from LSU and 1061 bp from SSU, including gaps). Every studied locus provided sufficient polymorphism both amongst and within previously phenotypically delimited groups (Suppl. material 1: Table S1). Four distinct phylogenetic lineages were detected in the concatenated data, as well as in single-locus data within the group of specimens that were hosted by Sematophyllaceae (Fig. 1, Suppl. material 2: Fig. S1). Divergence between them was between 4 and 59 nucleotide differences at every locus (Suppl. material 1: Table S1). The four South African lineages formed a highly supported and distinct clade together with *O. kelabitiana* (Fig. 1). Molecular dating analysis estimated the basal split of bryophilous Pezizales to be 87–172 Ma old (95% confidence interval; mean = 149 Ma), the basal split of the South African accessions was estimated at 23–73 Ma (mean = 47 Ma; Fig. 2).

No significant differences in phenotypic traits were detected amongst the South African lineages using standard characters and methods. They shared the structure of excipulum, stiff, thick-walled hyaline hairs, ellipsoid hyaline ascospores which can be either smooth or ornamented with fine warts and which contain 1 or 2 guttules, warted mycelial hyphae, appressoria, haustoria and presence of anamorph. Although differences amongst individual collections were observed, phenotypic characters did not correspond to the molecular markers and many characters exhibited variability both amongst and within the four phylogenetic lineages (Table 2).

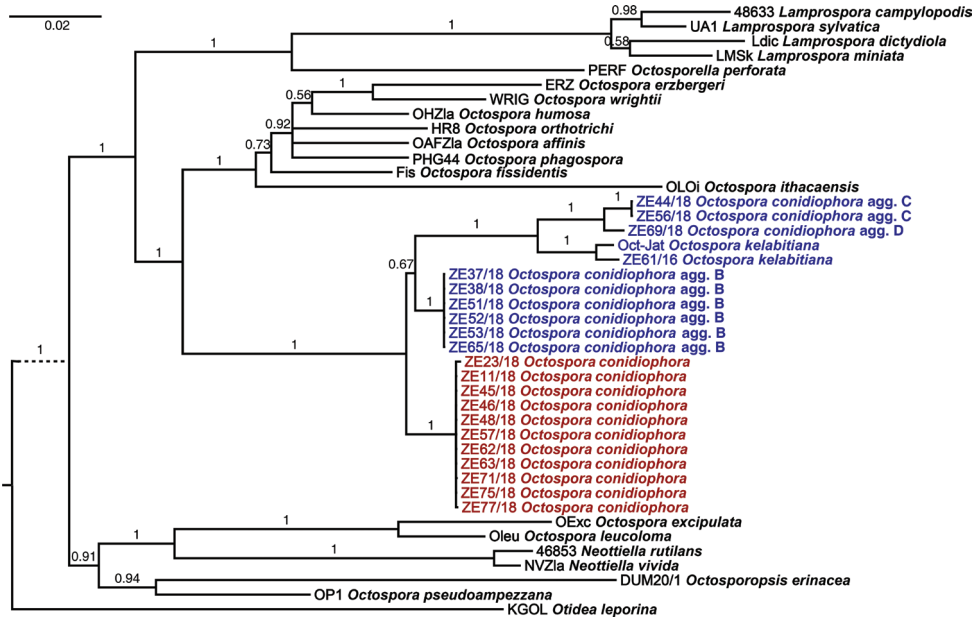

Figure 1. Bayesian phylogeny inference, based on concatenated alignment of EF1α, LSU and SSU sequences. Bayesian posterior probabilities are shown above branches; *Otidea leporina* serves as outgroup; trees based on analysis of each locus are shown in Suppl. material 2: Fig. S1.

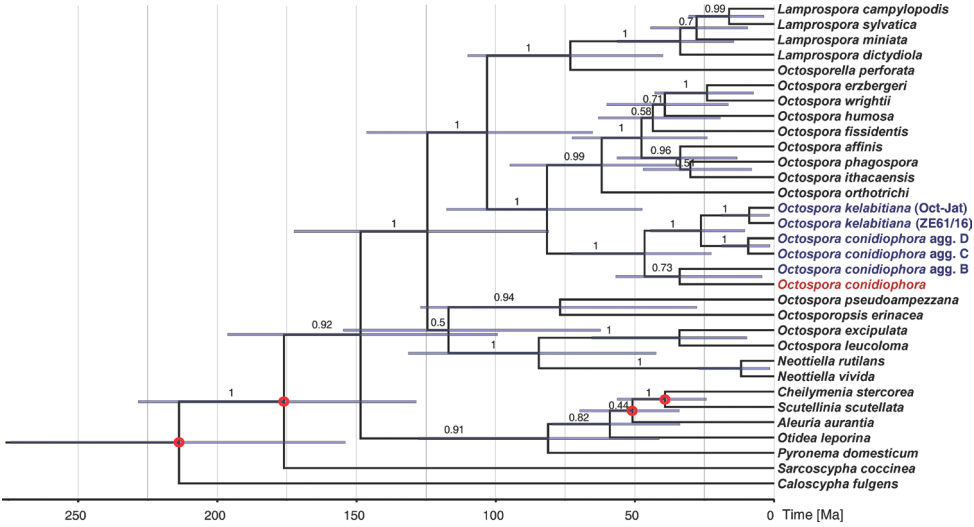

Figure 2. Maximum clade credibility tree with estimated divergence times, based on SSU and LSU data; calibration points are marked by red circles, posterior probabilities shown above branches, bars indicate the 95% highest posterior density (HPD) intervals.

Table 2. Variability of selected characters in *O. conidiophora* agg.

Voucher	Ornament of ascospores	(†) Size of ascospores [µm]	(†) Mean size of ascospores [µm]	(†) Q of ascospores	(†) Qm	Observation of conidia	Host
Lineage A - *Octospora conidiophora* s. str.							
ZE11/18	smooth	14.4–16.0 × 8.0–9.1	15.1 × 8.4	1.65–1.91	1.79	yes	*S. brachycarpum*
ZE23/18	smooth	14.0–16.3 × 7.5–9.0	14.9 × 8.0	1.66–2.03	1.84	yes	*T. perchlorosum*
ZE45/18	smooth	13.6–16.2 × 7.5–8.3	15.2 × 7.9	1.74–2.08	1.92	yes	*T. perchlorosum*
ZE46/18	smooth	15.0–17.0 × 8.0–9.9	15.9 × 8.7	1.63–2.06	1.82	yes	*T. perchlorosum*
ZE48/18	smooth	14.5–17.0 × 8.3–9.9	16.1 × 9.0	1.64–1.99	1.79	yes	*T. perchlorosum*
ZE57/18	smooth	14.9–16.2 × 7.9–9.0	15.5 × 8.2	1.69–1.99	1.87	yes	*T. perchlorosum*
ZE62/18	smooth	14.0–16.7 × 8.0–8.9	15.2 × 8.2	1.72–1.99	1.85	yes	*T. perchlorosum*
ZE63/18	smooth	14.0–17.0 × 8.0–9.2	15.4 × 8.7	1.67–1.89	1.77	yes	*T. perchlorosum*
ZE71/18	warted	13.0–15.0 × 8.0–9.9	14.1 × 8.9	1.39–1.73	1.59	no	*T. perchlorosum*
ZE75/18	smooth	14.0–16.1 × 7.8–9.1	15.1 × 8.4	1.65–1.94	1.79	yes	*T. perchlorosum*
ZE77/18	warted	13.5–15.4 × 8.7–10.5	14.4 × 9.4	1.40–1.67	1.53	yes	*T. perchlorosum*
all specimens		13.0–17.0 × 7.5–10.5	15.2 × 8.5	1.39–2.08	1.79		
Lineage B							
ZE37/18	warted	13.3–15.5 × 8.3–9.9	14.6 × 9.1	1.47–1.82	1.60	yes	*S. brachycarpum*
ZE38/18	warted	12.5–15.1 × 8.0–9.7	13.8 × 8.8	1.46–1.78	1.57	no	*T. perchlorosum*
ZE51/18	warted	13.5–15.7 × 8.4–10.2	14.5 × 9.4	1.45–1.65	1.54	yes	*T. perchlorosum*
ZE52/18	warted	13.5–16.0 × 8.0–9.5	14.7 × 8.8	1.47–1.83	1.66	yes	*T. perchlorosum*
ZE53/18	warted	14.0–15.3 × 8.0–10.1	14.7 × 9.3	1.47–1.85	1.56	no	*T. perchlorosum*
ZE65/18	warted	13.5–16.2 × 7.7–9.9	14.4 × 8.8	1.47–1.75	1.60	yes	*T. perchlorosum*
all specimens		12.5–16.2 × 7.7–10.2	14.5 × 9.1	1.45–1.85	1.59		
Lineage C							
ZE44/18	warted	13.5–15.9 × 7.2–8.1	14.6 × 7.8	1.71–2.01	1.87	yes	*S. brachycarpum*
ZE56/18	warted	13.1–15.4 × 7.0–8.2	14.1 × 7.6	1.66–2.11	1.84	yes	*S. brachycarpum*
both specimens		13.1–15.9 × 7.0–8.2	14.3 × 7.7	1.66–2.11	1.86		
Lineage D							
ZE69/18	smooth or lightly warted	13.5–18.0 × 7.9–9.9	15.5 × 8.6	1.61–2.02	1.80	yes	*S. brachycarpum*

Taxonomy

***Octospora conidiophora* Sochorová & Döbbeler, sp. nov.**
MycoBank no.: MB829095
Figs 3–9

Etymology. *Conidiophorus* (Gr./Lat.) refers to production of conidia.

Diagnosis. Differs from *Octospora kelabitiana* by larger apothecia with a distinct margin, infection of pleurocarpous mosses of the family Sematophyllaceae and frequent formation of a *Spermospora*-like anamorph.

TYPE: SOUTH AFRICA. KwaZulu-Natal Province: Uthukela District Municipality, uKhahlamba Drakensberg Park, Injasuti, 29°7.72'S, 29°25.27'E, 1750 m alt., on *Trichosteleum perchlorosum* on decaying wood, 2 Mar. 2018, Z. Egertová (So-

Figure 3. *Octospora conidiophora*. **A–E** Apothecia in situ **F** Habitat **A, E** ZE63/18 **B** ZE57/18 **C, F** ZE11/18 **D** holotype ZE48/18.

chorová) and M. Sochor ZE48/18, holotype: PRM 951743, isotype: M; LSU GenBank accession number: MK569321, SSU GenBank accession number: MK569351, EF1α GenBank accession number: MK569297.

Description. *Apothecial features*: Apothecia in groups on plants of *Trichosteleum perchlorosum* or *Sematophyllum brachycarpum* or between them, 0.2–1.5 mm broad, up to 0.65 mm high, first subglobose with a small apical opening, later hemispherical, turbinate to disc-shaped, pinkish-orange, sessile, mostly with a well-developed margin, outer surface of excipulum with adpressed to shortly protruding hairs or hyphae.

Hairs *55–205 × 4–10.5 µm, scattered at flanks, hyaline, scarcely septate, obtuse, thick-walled, wall *0.5–3.5 µm thick. Excipulum at the base *230–330 µm thick,

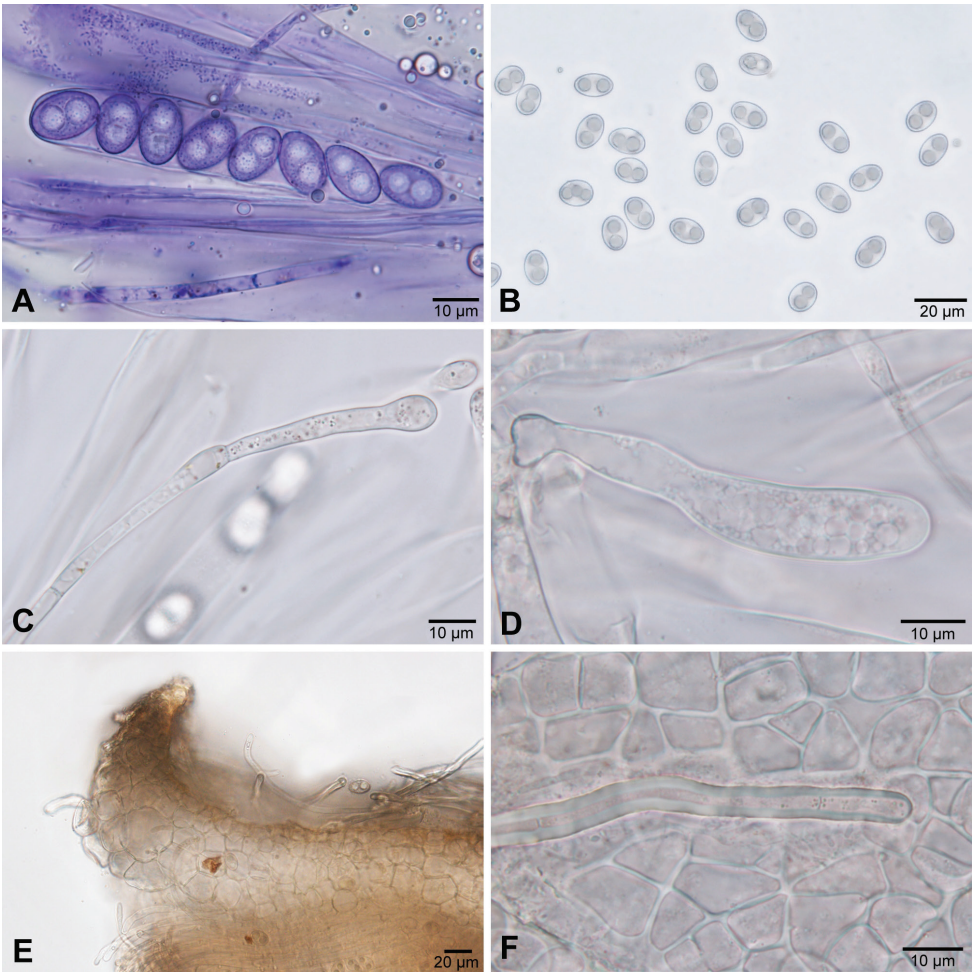

Figure 4. Microscopic characters of *Octospora conidiophora*. **A** Ascospores inside ascus stained with CRB **B** Free ascospores in tap water **C** Paraphyse in tap water **D** Young ascus in tap water **E** Margin of apothecium in tap water **F** Hair and excipular cells in tap water **A–F** ZE77/18.

laterally about 50 µm thick, composed of angular to subangular (triangular, trapezoid, rectangular), globose, subglobose or irregularly shaped cells, *6–43 × 5–42 µm, outermost cells thick-walled (neighbouring cells divided by up to *6 µm broad wall). Margin *60–280 µm broad, consisting of globose, subglobose, pyriform or trapezoid cells, *10–38 × 7–30 µm.

Subhymenium *40–75 µm wide, consisting of densely packed cylindrical cells *3–7 µm wide mixed with angular or irregularly shaped cells, *4.5–8 × 4.5–6 µm. Paraphyses filiform, straight or bent, unbranched, septate, uppermost one or two cells containing little very pale droplets (*0.5–2 µm in diameter), *2.1–3.5 µm broad (†1.5–2.3 µm), terminal cell *19–83 × 3–7 µm (†18–57 × 3–5.5 µm). Asci *146–197 × 12–15.5 µm (†135–192 × 9.5–12.5 µm), cylindrical, unitunicate, operculate, inamyloid, aris-

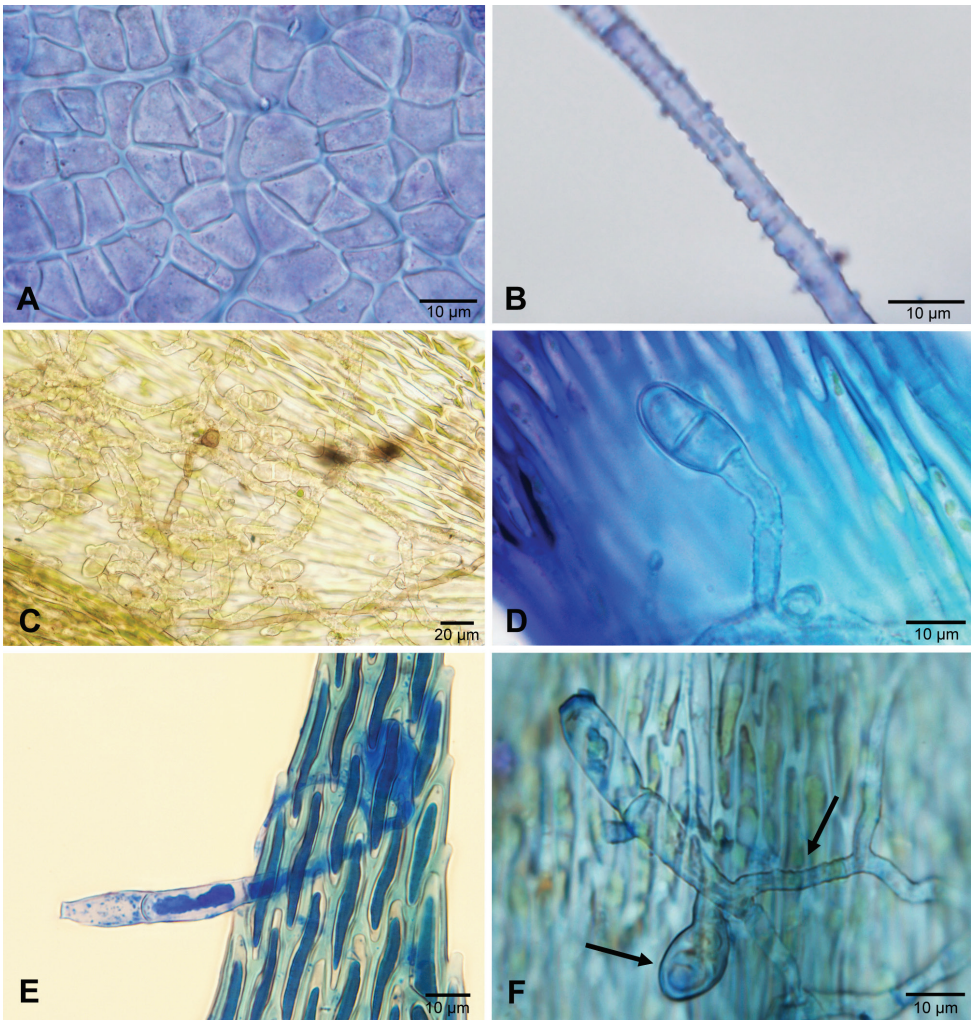

Figure 5. Microscopic characters of *Octospora conidiophora*. **A** Cells of the outermost layer of excipulum from an outside view stained with CRB **B** Mycelial hypha stained with CRB **C** Appressoria and hyphae on a leaf of *Sematophyllum brachycarpum* in tap water **D** Appressorium stained with LACB **E** Germinating conidium stained with LPCB **F** Germinated conidium produced a bifurcate warted hypha (right arrow), appressorium (left arrow) probably not connected to the conidium, in LACB **A, B, F** ZE77/18 **C, E** ZE11/18 **D** holotype ZE48/18.

ing from croziers, with 8 uniseriate ascospores. Ascospores *13–17.2 × 7–10.5 µm, mean 15.2 × 9 µm, Q = 1.34–1.99, Qm = 1.69 (†13–17 × 7.5–10.5 µm, mean 15.2 × 8.5 µm, Q = 1.39–2.08, Qm = 1.79), ellipsoid to narrowly ellipsoid, hyaline, containing one or two lipid guttules (up to *8 µm in diameter if one, *4–5.5 µm if two), smooth or ornamented with cyanophilous, very small, obtuse warts 0.1–0.3 µm broad; germinating with a single germ tube.

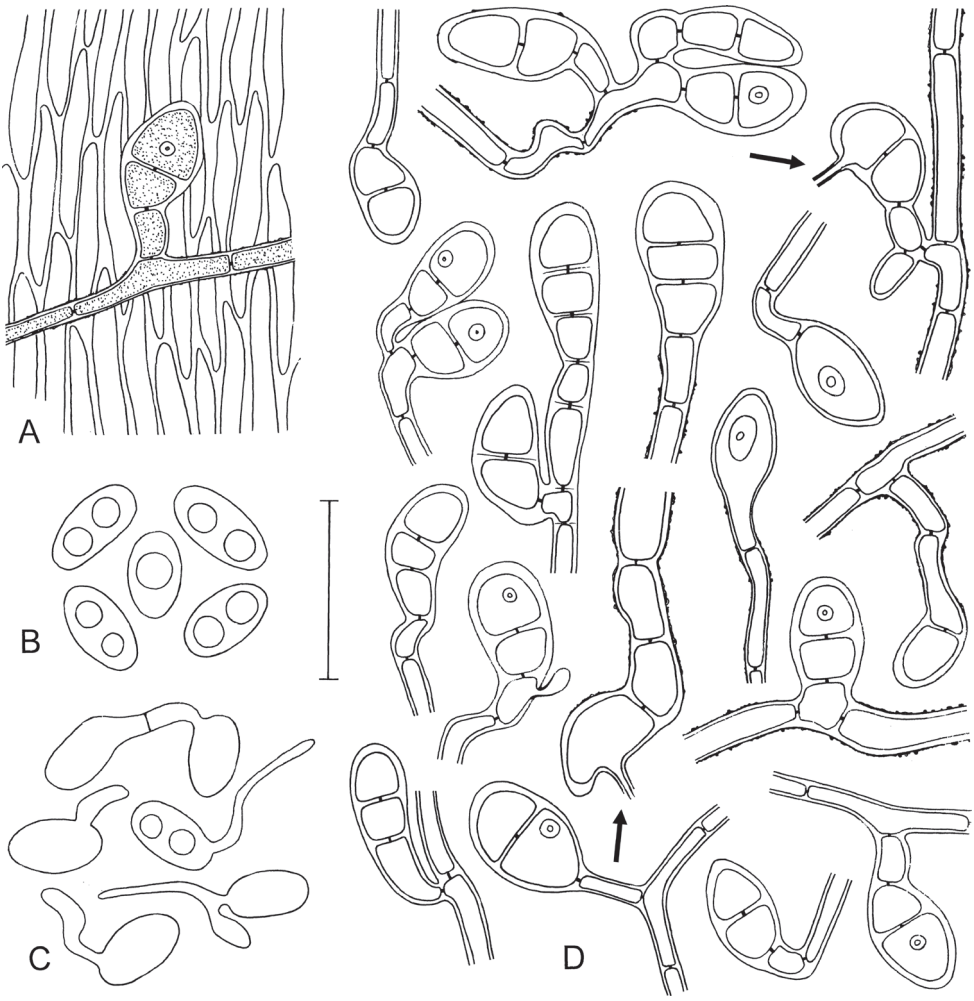

Figure 6. Microscopic characters of *Octospora conidiophora*. **A** Hypha with two-celled appresorium closely attached to the cells of the host leaf **B** Ascospores **C** Germinating ascospores found on leaves **D** Variation of appressoria mostly seen from above, infection pegs not always observed, appressoria seen in lateral view with infection pegs (indicated by arrows) **A, B, D** holotype ZE48/18 **C** ZE11/18. Scale bar: 30 µm. Illustrated by P.D.

Mycelial features (†): Hyphae restricted to the lowermost plant parts, irregularly growing on and between the leaf bases, stems and especially the rhizoids, hyaline, with ramifications and anastomoses, often thick-walled, (2–)3–6(–7) µm in diameter (excluding ornamentation); hyphal surface with minute to large protuberances, in optical section with numerous minute or larger, semi- or subglobose warts or spines, in surface view, these structures sometimes looking like ridges extended perpendicularly to the hyphal axis; largest warts up to 1.5(–2) µm high; hyphae growing within hyphae present; whole hyphal wall slightly cyanophilous, outermost rough part strongly cyanophilous.

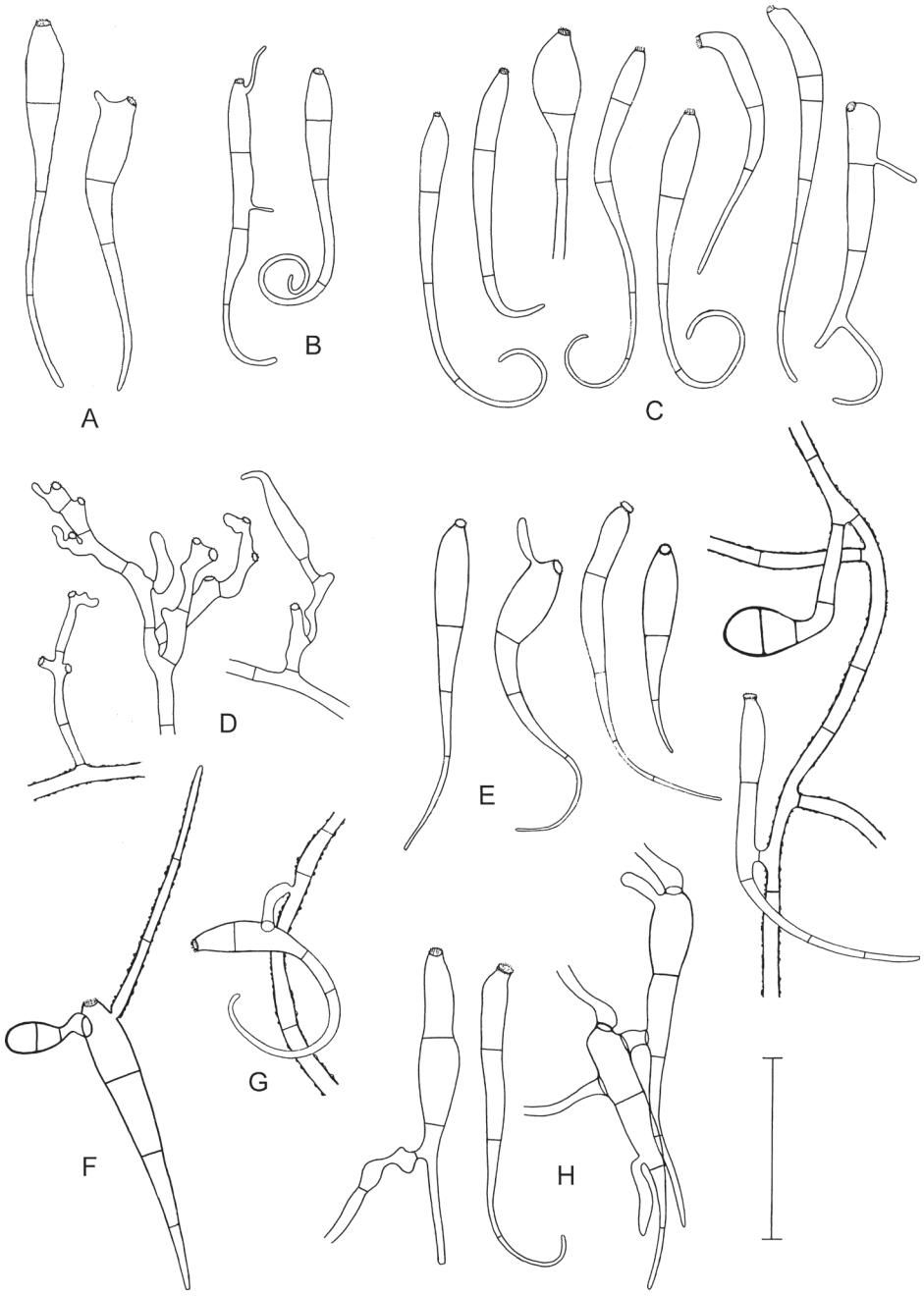

Figure 7. Microscopic characters of *Octospora conidiophora*. **A–C, E–H** Conidia, distal curved part apparently sometimes broken off, some conidia germinating **D** Conidogenous cells, on the right with a developing conidium **E** (on the right) Conidium anastomosing to mycelial hypha with two-celled appressorium **F** Conidium germinating by a hypha with a warty surface and a two-celled appressorium **G** Conidium with anastomosis to mycelial hypha **H** (on the right) Two germinating conidia with an anastomosis between them **A, F** ZE63/18 **B** ZE46/18 **C** ZE77/18 **D, E** holotype ZE48/18 **G** ZE57/18 **H** ZE11/18. Scale bar: 50 µm. Illustrated by P.D.

Appressoria variable, frequent (even more than 30 per leaf observed) and easy to detect, closely attached to both leaf sides or to rhizoids, colourless, 1-, 2- or 3-celled, from above elliptical, (14–)16–23(–26) µm long, (8–)11–16 µm wide, laterally seen slightly kidney-shaped, (7–)9–13(–16) µm high, with walls up to 2.5(–4) µm thick; surface rough but not warty, cyanophilous; appressorial cytoplasma strongly cyanophilous; appressoria mostly laterally formed on short stalks; stalks often gradually expanding toward the appressorium; perforation of the host cell wall by means of a delicate peg; peg often surrounded by a brown, straight or curved lignituber-like swelling measuring up to 10(–15) × 2–4(–6) µm; rhizoid wall at the perforation point slightly uplifted towards the appressorium; perforation point not always visible from above.

Haustoria within living leaf cells or rhizoidal cells, at first as a thick short filament, later becoming up to 55 µm long, orientated longitudinally in the rhizoid and developing ramifications (in wider rhizoids), rarely filling out the whole host cell; haustorial cytoplasm strongly cyanophilous.

Anamorph (†): Conidia variable in shape and size, claviform, hyaline, transversely septate, ca. (50–)70–115(–154) µm long (including the tail); proximal cell usually distinctly wider than the subproximal cell, rarely cells almost cylindrical, both cells measuring together (30–)35–48(–55) × (6–)7.5–12(–15) µm, subproximal cell continuously attenuating into a tail; tail typically curved to curled, 1- or 2-(3-) celled, (15–)30–60(–100) µm long and (1.5–)2(–2.5) µm in diameter at the distal end; proximal cell of the conidia with a conspicuous, circular, slightly protruding, delicately fringed scar, (3–)4(–4.5) µm in diameter, resulting from detachment from the conidiogenous cell; scar sometimes slightly laterally positioned; walls of conidia cyanophilous; the two proximal cells smooth, the tail sometimes warty (like the hyphae); germ tube one (to three) per conidium, arising from the scar or laterally from different regions of the conidia, including the tail cells.

Conidiogenous cells irregularly shaped, shorter and wider than sterile hyphal cells, rich in cytoplasmic content, usually with 1(–2) scars; shape and size of the scars like those at the conidia, also with a delicately fringed margin.

Hosts. *Trichosteleum perchlorosum*, *Sematophyllum brachycarpum* (Sematophyllaceae, Hypnales)

Distribution. South Africa, Mpumalanga and KwaZulu-Natal Provinces (Fig. 8).

Conservation status. *Octospora conidiophora* seems to be a common representative of the genus in South Africa, widespread and forming abundant populations. Its hosts are also common and widespread in the region (see below). Although the main habitat (afromontane forest) is naturally fragmented, it is often protected against human activities by nature reserves or national parks. Therefore, *O. conidiophora* does not fulfil the criteria for categories CR (critically endangered) to NT (near threatened) and we propose its evaluation as LC (least concern) for the present moment.

Additional specimens examined. South Africa. Mpumalanga Province: Ehlanzeni District Municipality, Graskop Gorge, 24°56.74'S, 30°50.8'E, 1355 m alt., on *Trichosteleum perchlorosum* on decaying wood, 6 Mar. 2018, Z. Egertová and M. Sochor ZE62/18 (PRM 951745); Ehlanzeni District Municipality, Graskop Gorge, 24°56.88'S, 30°50.75'E, 1435 m alt., on *Trichosteleum perchlorosum* on decaying wood,

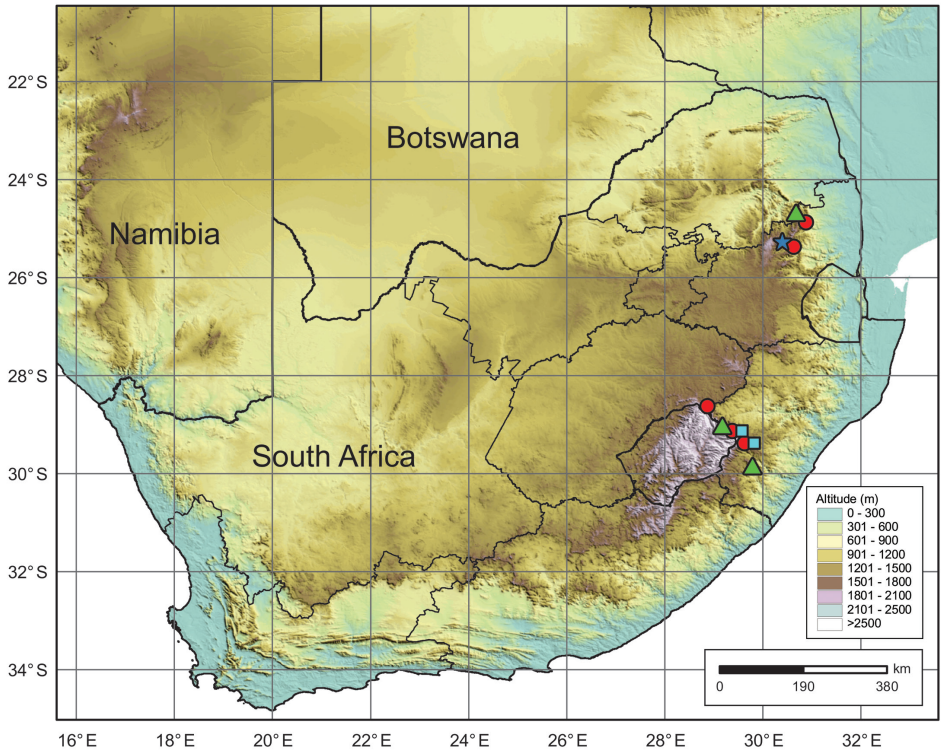

Figure 8. Geographical distribution of the four lineages of *Octospora conidiophora* agg. in South Africa. Red circle: lineage A (O. con*idiophora* s.str.); green triangle: lineage B; light blue square: lineage C, dark blue star: lineage D.

6 Mar. 2018, Z. Egertová and M. Sochor ZE63/18 (PRM 951746); Ehlanzeni District Municipality, Buffelskloof Nature Reserve, 25°15.98'S, 30°31.08'E, 1725 m alt., on *Trichosteleum perchlorosum* on decaying wood, 10 Mar. 2018, Z. Egertová and M. Sochor ZE75/18 (PRM 951748); Ehlanzeni District Municipality, Buffelskloof Nature Reserve, 25°16.37'S, 30°30.62'E, 1605 m alt., on *Trichosteleum perchlorosum* on decaying wood, 9 Mar. 2018, Z. Egertová and M. Sochor ZE71/18 (PRM 951747); Ehlanzeni District Municipality, Buffelskloof Nature Reserve, 25°16.53'S, 30°30.25'E, 1625 m alt., on *Trichosteleum perchlorosum* on decaying wood, 10 Mar. 2018, Z. Egertová and M. Sochor ZE77/18 (PRM 951749). KwaZulu-Natal Province: Uthukela District Municipality, Royal Natal National Park, 28°40.88'S, 28°55.73'E, 1760 m alt., on *Sematophyllum brachycarpum* on decaying stem, 19 Feb. 2018, Z. Egertová and M. Sochor ZE11/18 (PRM 951739); Uthukela District Municipality, Royal Natal National Park, 28°44.05'S, 28°54.85'E, 1800 m alt., on *Trichosteleum perchlorosum* on decaying stem, 20 Feb. 2018, Z. Egertová and M. Sochor ZE23/18 (PRM 951740). Uthukela District Municipality, uKhahlamba Drakensberg Park, Injasuti, 29°8.95'S, 29°25.35'E, 1665 m alt., on *Trichosteleum perchlorosum* on decaying wood, 3 Mar. 2018, Z. Egertová and M. Sochor ZE57/18 (PRM 951744); Uthukela District Mu-

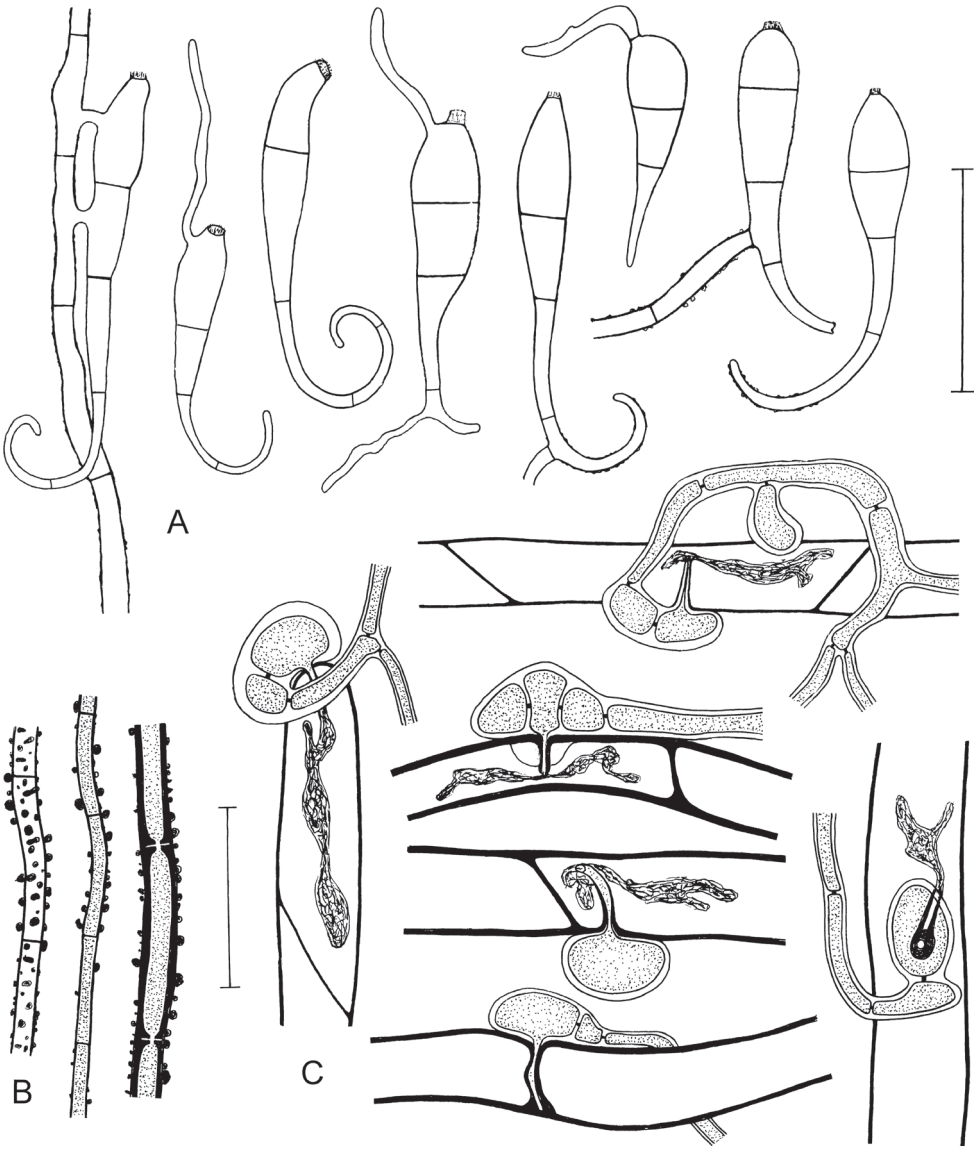

Figure 9. Microscopic characters of *Octospora conidiophora* agg. (lineage B). **A** Conidia, distal curved part apparently sometimes broken off, five conidia germinating by formation of usually a single hypha, conidium on the left connected to a hypha by two anastomoses **B** Strongly warted hyphae, the left one seen from above, the two others in optical section **C** Appresssoria infecting rhizoids in lateral view, the right one seen from above, infection pegs surrounded by lignituber-like tubes formed by the host cell wall, intracellular haustoria present apart from the lowermost infection where the peg is completely encapsulated by the host cell wall **A, B, C** ZE37/18. Scale bars: 50 μm (**A**); 30 μm (**B, C**). Illustrated by P.D.

nicipality, uKhahlamba Drakensberg Park, Giants Castle Nature Reserve, 29°16.93'S, 29°30.93'E, 1765 m alt., on *Trichosteleum perchlorosum* on decaying wood, 1 Mar. 2018, Z. Egertová and M. Sochor ZE46/18 (PRM 951742); Uthukela District Mu-

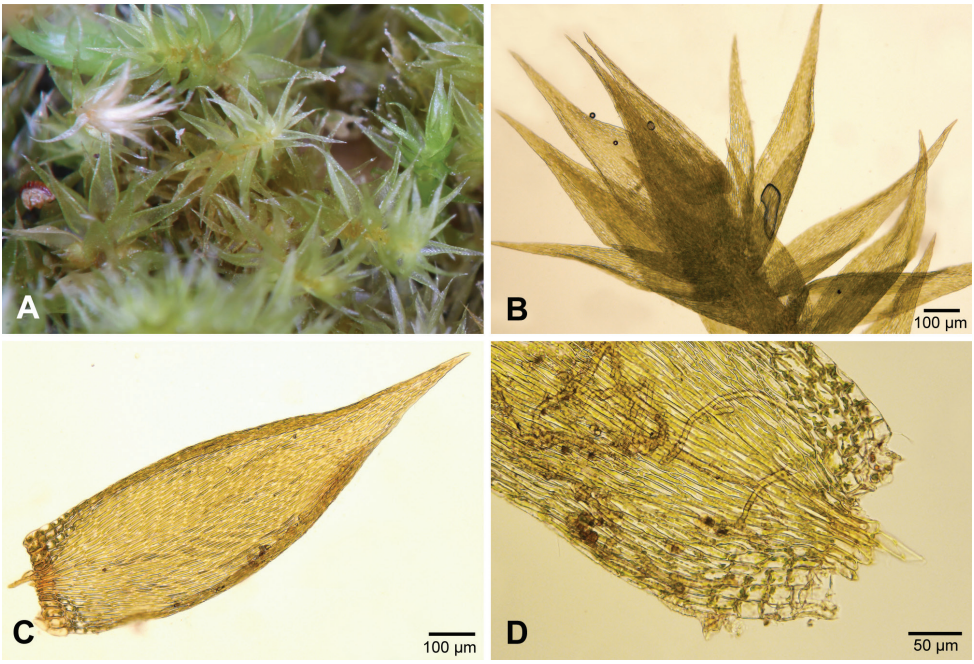

Figure 10. *Sematophyllum brachycarpum.* **A** Plants **B** Typical shoot with leaves **C** Leaf **D** Leaf base with alar cells.

nicipality, uKhahlamba Drakensberg Park, Giants Castle Nature Reserve, 29°16.98'S, 29°30.87'E, 1775 m alt., on *Trichosteleum perchlorosum* on decaying wood, 1 Mar. 2018, Z. Egertová and M. Sochor ZE45/18 (PRM 951741).

Data to other lineages. Lineage B: Mpumalanga Province: Ehlanzeni District Municipality, 3040 m WSW from the Graskop railway station, 24°56.28'S, 30°48.65'E, 1495 m alt., on *Trichosteleum perchlorosum* on decaying wood, 7 Mar. 2018, Z. Egertová and M. Sochor ZE65/18 (PRM 951735). KwaZulu-Natal Province: Uthukela District Municipality, uKhahlamba Drakensberg Park, Injasuti, 29°7.62'S, 29°25.33'E, 1725 m alt., on *Trichosteleum perchlorosum* on decaying wood, 2 Mar. 2018, Z. Egertová and M. Sochor ZE51/18 (PRM 951732); Uthukela District Municipality, uKhahlamba Drakensberg Park, Injasuti, 29°7.57'S, 29°25.38'E, 1715 m alt., on *Trichosteleum perchlorosum* on decaying wood, 2 Mar. 2018, Z. Egertová and M. Sochor ZE52/18 (PRM 951733); Uthukela District Municipality, uKhahlamba Drakensberg Park, Injasuti, 29°7.98'S, 29°26.25'E, 1500 m alt., on *Trichosteleum perchlorosum* on decaying wood, 2 Mar. 2018, Z. Egertová and M. Sochor ZE53/18 (PRM 951734); Sisonke District Municipality, Marutswa Forest, 29°48.55'S, 29°47.28'E, 1465 m alt., on *Sematophyllum brachycarpum* on decaying stem, 24 Feb. 2018, Z. Egertová and M. Sochor ZE37/18 (PRM 951730); Sisonke District Municipality, Marutswa Forest, 29°48.6'S, 29°47.37'E, 1480 m alt., on *Trichosteleum perchlorosum* on decaying stem, 24 Feb. 2018, Z. Egertová and M. Sochor ZE38/18 (PRM 951731).

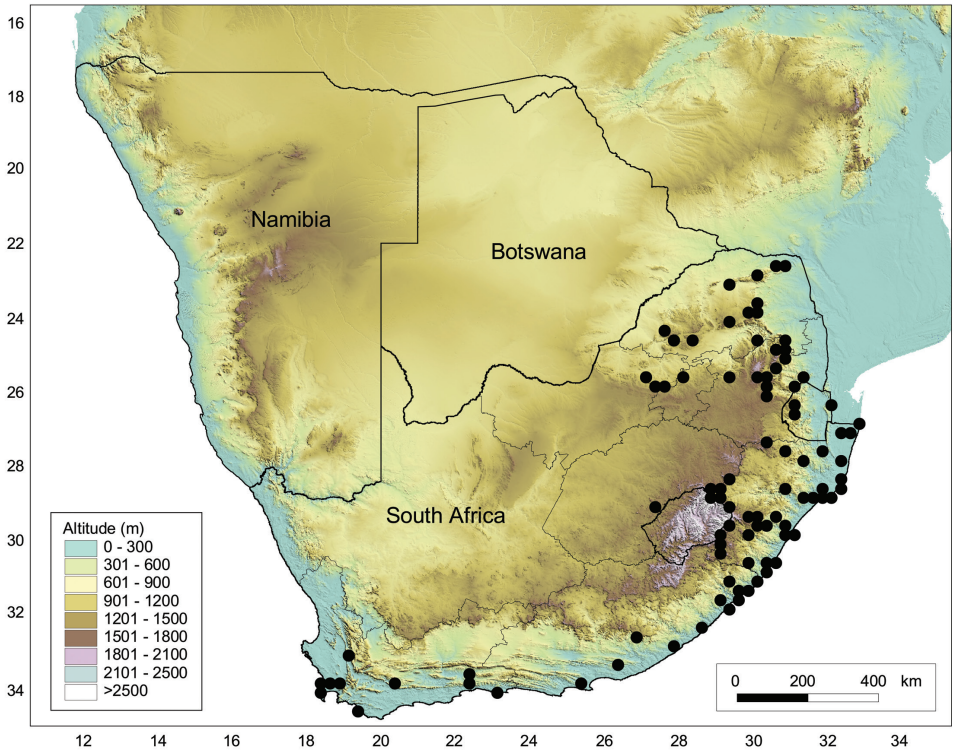

Figure 11. Geographical distribution of *Sematophyllum brachycarpum* in southern Africa based on records in BM, L, MO and PRE.

Lineage C: KwaZulu-Natal Province: Uthukela District Municipality, uKhahlamba Drakensberg Park, Giants Castle Nature Reserve, 29°17.02'S, 29°30.87'E, 1780 m alt., on *Sematophyllum brachycarpum* on decaying wood, 28 Feb. 2018, Z. Egertová and M. Sochor ZE44/18 (PRM 951736); Uthukela District Municipality, uKhahlamba Drakensberg Park, Injasuti, 29°8.33'S, 29°25.68'E, 1565 m alt., on *Sematophyllum brachycarpum* on decaying wood, 3 Mar. 2018, Z. Egertová and M. Sochor ZE56/18 (PRM 951737).

Lineage D: Mpumalanga Province: Ehlanzeni District Municipality, Buffelskloof Nature Reserve, 25°16.93'S, 30°30.45'E, 1470 m alt., on *Sematophyllum brachycarpum* on decaying wood, 9 Mar. 2018, Z. Egertová and M. Sochor ZE69/18 (PRM 951738).

Taxonomic affinities. The phylogenetically closest and phenotypically most similar species is *Octospora kelabitiana* described from Borneo, which shares most characters with the African species. It also has apothecia with stiff, thick-walled hyaline hairs, ellipsoid, hyaline ascospores of similar size like *O. conidiophora* († in H_2O (13.5)14.5–17(18) × 7–8(9) µm, in LPCB (12.5)13–16(17) × (6.5)7–8(8.5) µm), filiform, unbranched paraphyses, smooth appressoria of similar size and even the warted mycelial hyphae, which is a character unknown in any other species of bryophilous Pezizales (Egertová et

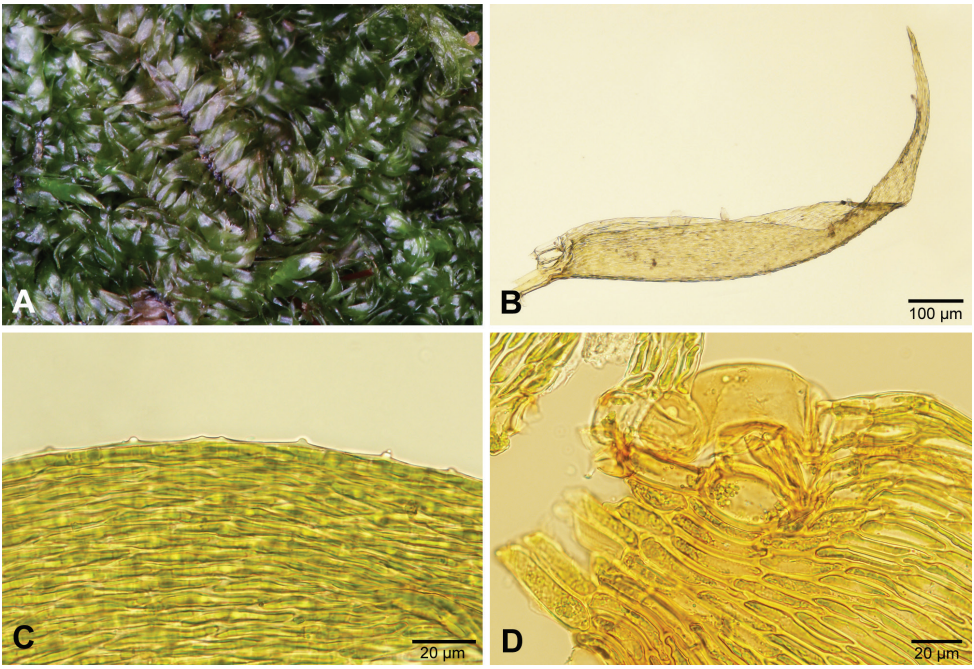

Figure 12. *Trichosteleum perchlorosum.* A. Plants. B. Leaf. C. Leaf papillae. D. Alar cells.

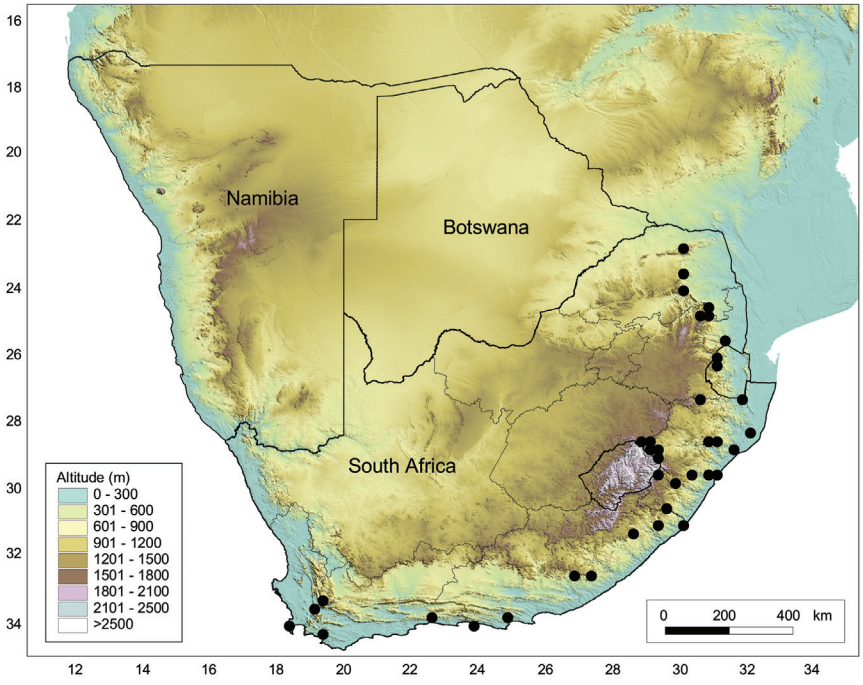

Figure 13. Geographical distribution of *Trichosteleum perchlorosum* in southern Africa based on records in BM, L, MO and PRE.

al. 2018). Nevertheless, it can be distinguished easily by growth on a completely different host – thallose liverworts from the genus *Riccardia* Gray. Furthermore, its apothecia are smaller, often taller than wide and lack a distinct margin. Its appressoria are usually one-celled, less often two-celled, while in *O. conidiophora*, two-celled appressoria are very common and even three-celled ones were found. Anamorph has not been detected in *O. kelabitiana*.

Discussion

According to the available literature and data from the main South African public fungarium (PREM), bryophilous Pezizales are completely unknown from southern Africa, despite the fact that this is a large and species-rich region, which hosts a very diverse bryoflora (Van Rooy and Phephu 2016). Our initial work revealed that this group of fungi is relatively common and probably also very diverse in southern Africa, despite the fact that the work was carried out in extraordinarily dry (and thus unsuitable) summer. Amongst others, four phenotypically similar, yet molecularly distinct lineages were discovered on two host species (lineages A and B on *Trichosteleum perchlorosum* and *Sematophyllum brachycarpum*, lineages C and D only on *S. brachycarpum*). This research brings novel insights into evolution and systematics of bryophilous ascomycetes and also raises important questions on taxonomic evaluation of these lineages. Therefore, we briefly discuss the taxonomy of cryptic taxa and suggest a suitable taxonomic solution for our collections. As *O. conidiophora* is the first species of bryophilous Pezizales with a detected anamorph, we also discuss this finding. Finally, diagnostic characters and data on distribution of the host mosses are provided as they may help expand the known distribution area of *O. conidiophora* in the future.

Taxonomic approach

The four lineages could not be distinguished phenotypically on the basis of characters that are normally studied in bryophilous Pezizales, although genetic differentiation was very high at all of the three studied loci (Suppl. material 1: Table S1). Such great genetic distances are usually observed amongst different species or even genera. The observed genetic distances, together with molecular dating, imply that the phenotypically more or less homogeneous morphotype actually represents a group of several cryptic species that have already become reproductively isolated in the Tertiary (Fig. 2). Similar cryptic diversity is probably quite common in fungi, including many genera of Pezizales, e.g. *Genea* Vittad. (Smith et al. 2006, Alvarado et al. 2016), *Geopyxis* (Pers.) Sacc. (Wang et al. 2016), *Helvella* L. (Nguyen et al. 2013, Skrede et al. 2017), *Terfezia* (Tul. & C.Tul.) Tul. & C.Tul. (Ferdman et al. 2009), *Trichophaea* Boud. (Van Vooren 2016) and *Tuber* P.Micheli ex F.H.Wigg. (Bonuso et al. 2010). In bryophilous Pezizales, intraspecific sequence variability was observed, e.g. in *Octosporopsis nicolai* (Maire) U.Lindem., M.Vega & T.Richt. (Lindemann et al. 2014) and *Octospora kela-*

bitiana (Egertová et al. 2018). Each of the species comprised two genetic lineages that, nevertheless, were relatively weakly diverged and were therefore not treated taxonomically. Besides the significant genetic distances amongst the South African populations, another fact speaks against the possibility that the four lineages could be treated as a single species; the whole clade includes *Octospora kelabitiana* (Fig. 1), a distinct species from Borneo infecting liverwort *Riccardia*. A widely defined species (i.e. including the four lineages but excluding *O. kelabitiana*) would therefore be paraphyletic.

The current approach of many authors to delimitation of species is based primarily or solely on DNA sequence data and sequence-based diagnoses have become almost a common practice in macromycetes (e.g. Buyck et al. 2016, Leacock et al. 2016, Taşkın et al. 2016, Wang et al. 2016, Korhonen et al. 2018). Some authors even aim to base descriptions of new species on environmental sequence data only (e.g. Hibbett et al. 2011). Although molecular phylogenetics is an excellent tool for evaluation of biodiversity, assignment of scientific binominal to molecularly defined species leads to several practical problems, mainly those related to limited accessibility of the methods for many field mycologists. Especially in developing countries, in which even standard optical microscopy can be barely affordable at the leading institutes, determination of species via DNA sequencing is still a matter for the distant future. This methodological obstacle may soon result (or has already resulted in some groups) in the split of traditional phenotype-based taxonomy and molecular taxonomy. Until recently, molecular taxonomy mostly worked with groups, such as molecular operational taxonomic unit (MOTU; Hibbett et al. 2011), phylogenetic species (O'Donnell et al. 2011), virtual taxon (Öpik et al. 2010) etc. and designated an alphanumeric code to them. Nevertheless, many of the molecular taxa are currently given traditional scientific names, often without studying related, validly described species that cannot be sequenced for various reasons. This process, although justified by the aim of cataloguing of global biodiversity, makes the resulting taxonomy impractical or even unusable for field mycologists (and sometimes also for molecular biologists). Another problem with descriptions of species, based on molecular data, is the fact that the borderline between intraspecific and interspecific molecular variation is often unclear (Thines et al. 2018), dependent on many evolutionary factors (e.g. Leliaert et al. 2014) and may become fuzzy after a more intensive and/or extensive sampling is performed, particularly if only one or few molecular markers are used. Nevertheless, this problem also exists with traditional taxonomy (e.g. Flynn and Miller 1990, Paal et al. 1998, Benkert 2001). One solution to the problems mentioned above is an integrative approach. This takes advantage of both multiple characters (morphology, DNA, ecology etc.) and results in robust, phylogeny-based taxonomy that is accessible to various users (e.g. Araújo et al. 2015, Skrede et al. 2017, Haelewaters et al. 2018).

After thorough consideration of the above-mentioned facts, we decided not to formally describe all of the four discovered cryptic species at the present moment. Instead, we prefer to establish two taxa: *O. conidiophora* (s.str.), which refers to the most common phylogenetic lineage A and the informal taxon *O. conidiophora* agg., which applies to all of the four South African cryptic species, but also to the morphologically distinct and host-specific Bornean *O. kelabitiana*. Although the name *O. kelabitiana* is older and should therefore be selected for the aggregate, we believe that the name *O. conidiophora* agg. better suits the pragmatic

purposes of this informal taxon. Our approach enables field mycologists to determine their specimens at least on the aggregate level and, at the same time, preserves a monophyletic taxonomical system. Detailed studies may reveal phenotypic differences between the South African lineages of *O. conidiophora* agg., which can then be formally described as species. Until then, we prefer to leave lineages B, C and D without a Latin binominal.

Anamorph

Conidia have been reported in several genera of Pezizales. The most frequent type of conidia are amerospores which are produced, e.g. in *Caloscypha* Boud. (Paden et al. 1978), *Desmazierella* Lib. (Hughes 1951), *Iodophanus* Korf (Korf 1958, sub *Ascophanus* Boud.), *Pachyphlodes* Zobel (Healy et al. 2015), *Peziza* Fr. (Berthet 1964a, Paden 1967, 1972), *Ruhlandiella* Henn. (Warcup and Talbot 1989, sub *Muciturbo* P.H.B.Talbot), *Thecotheus* Boud. (Conway 1975), *Urnula* Fr. (Davidson 1950), *Cookeina* Kuntze, *Phillipsia* Berk. (Paden 1975), *Pithya* Fuckel (Paden 1972), *Nanoscypha* Denison (Pfister 1973), *Sarcoscypha* (Fr.) Boud. (Harrington 1990), *Geopyxis* (Paden 1972), *Pyropyxis* Egger (Egger 1984, Filippova et al. 2016) and *Trichophaea* (Hennebert 1973). Staurospores can be found in *Miladina lecithina* (Cooke) Svrček (Descals and Webster 1978). The conidia of *O. conidiophora* can be classified as scolecospores or phragmospores and are therefore unique amongst Pezizales with known teleomorph. In their shape, they resemble the conidia of the anamorphic genus *Spermospora* R. Sprague (Ascomycota, Pezizomycotina), a parasite of grasses (Sprague 1948, Seifert et al. 2011).

Detached conidia were regularly found between the rhizoids and leaves in almost all collections of *Octospora conidiophora* agg. (with the exception of specimens ZE38/18, ZE53/18 and ZE71/18, probably due to limited material). The distal part of the conidia is sometimes short and straight. It is not clear whether this is an artefact caused by breaking off during preparation, although tail fragments have not been found. Germinating conidia are not rare. Longer germination tubes look like normal hyphae with the characteristic warty surface structure (Figs. 5F, 7F). Conidia germinating by a two-celled appressorium (Fig. 7F) or connected to a mycelial hypha by an anastomosis (Figs. 7E, G, 9A) have been repeatedly observed. Conidiogenous cells (Fig. 7D) are much more difficult to detect than conidia and have only been found in a few collections. The scars formed by detachment of conidia must not be confused with the ends of torn-off hyphae, which inevitably result during preparation. Fully developed conidia still connected to the conidiogeneous cells have not been found. Apparently, mature conidia easily detach from their conidiogenous cells. A developing, still attached conidium was observed once (Fig. 7D).

Octospora conidiophora agg. is the first case amongst bryophilous Pezizales in which an anamorph has been detected. The absence of records of anamorphic states in other species can be caused either by their real rarity or only by their difficulty in detection. The latter can have many reasons. First, bryophilous ascomycetes, in general, stand rather on the periphery of researchers´ interest (see Döbbeler 1997). Second, anamorphs are usually inconspicuous and therefore not easy to encounter. Even if an

anamorph is found, it can be difficult to link it with the corresponding teleomorph, because many fungal species commonly occur together. Moreover, anamorphs and teleomorphs are often formed in different environmental conditions (Kendrick 1979) and often at different times. And third, anamorphs are often studied in aseptic cultures and subsequently cultures are used for confirmation of their identity by molecular methods; unfortunately, cultivation of bryophilous Pezizales seems to be problematic (Berthet 1964b) and is not commonly attempted. Although an anamorph has not been confirmed by cultivation methods in *O. conidiophora* agg., the connection of anamorph and teleomorph is based on the evidence discussed above: conidia were repeatedly found amongst the moss plants near the teleomorph; germinating conidia have hyphae with the same ornamentation as observed in the mycelium bearing apothecia; conidiogenous cells occur on the mycelial hyphae; conidia anastomose with mycelial hyphae; the germlings form appressoria.

Hosts

Sematophyllum brachycarpum (Hampe) Broth.

Syn: *Hypnum brachycarpum* Hampe

Sematophyllum brachycarpum can be distinguished from other species of *Sematophyllum* in southern Africa by the complanate, straight leaves with relatively large groups of alar cells (in 3–4 rows) that are not much inflated or coloured (Fig. 10, see also Câmara et al. 2019).

The species is by far the most common and widespread species of *Sematophyllum* in South Africa; *S. brachycarpum* is found in forests and wooded areas of the Limpopo, Mpumalanga, North West, Gauteng, Free State, KwaZulu-Natal, Eastern Cape and Western Cape Provinces (Fig. 11, see also Câmara et al. 2019). It occurs as an epiphyte or occasionally on soil or rocks, from sea level up to 1900 m alt. The species is widely distributed throughout the Afromontane Region, as defined by Van Rooy and Van Wyk (2010) and was found to belong to the Widespread Afromontane Subelement, a subdivision of the Afromontane Forest Element (Van Rooy and Van Wyk 2011). The Widespread Afromontane Subelement is centred in the Midlands of KwaZulu-Natal and the Drakensberg escarpment of Mpumalanga as well as in forests in the south-western Cape. The species has also been recorded from Lesotho, Swaziland, Mozambique, Zimbabwe, Zambia, Uganda and Kenya (O'Shea 2006).

Trichosteleum perchlorosum Broth. & Bryhn

Trichosteleum perchlorosum is the only southern African species of Sematophyllaceae (sensu stricto) with papillose leaf cells. However, the papillae are sometimes difficult to see or may be absent on some leaves. The falcate leaves with enlarged, inflated

and coloured alar cells will also help to identify the species (Fig. 12, see also Câmara et al. 2019).

The species is endemic to the southern part of Africa and occurs as an epiphyte and also on decaying logs or rocks from sea level up to 3090 m high (Drakensberg of KwaZulu-Natal). It is most frequently collected in the KwaZulu-Natal Province of South Africa, but it is also known from Limpopo, Mpumalanga, Eastern Cape and Western Cape Provinces, as well as Swaziland (Fig. 13, see also Câmara et al. 2019). *Trichosteleum perchlorosum* is widespread throughout the Afromontane Region sensu Van Rooy and Van Wyk (2010), but unknown from Afromontane outliers in the Magaliesberg of Gauteng and the North West, the eastern Free State and the Waterberg of Limpopo. It was therefore included in the Tropical Afromontane Subelement (Van Rooy and Van Wyk 2011), which is centred in the Drakensberg escarpment of Mpumalanga and the Midlands of KwaZulu-Natal. This species was also reported from Zimbabwe (O'Shea 2006).

Acknowledgements

ZS and MS thank John Manning for financial support of the travel to South Africa. Riana Jacobs-Venter is acknowledged for providing information on the absence of bryophilous Pezizales in the South African National Collection of Fungi and Markéta Šandová and Miriam Brožíková (PRM) for information about *Octospora tetraspora* var. *aegyptiaca*. We are grateful to Hester Steyn and Elizma Fouche for editing the maps and the editor Danny Haelewaters and the reviewers, Nicolas Van Vooren and Donald H. Pfister, for comments to the manuscript. The work was partly supported by the Ministry of Agriculture of the Czech Republic, institutional support MZE-RO0418. ZS was supported by an internal grant from Palacký University (IGA_PrF_2019_004). Research was conducted under permit no. OP 1264/2018.

References

Alvarado P, Cabero J, Moreno G, Bratek Z, Van Vooren N, Kaounas V, Konstantinidis G, Agnello C, Merényi Z, Smith ME, Vizzini A, Trappe JM (2016) Phylogenetic overview of the genus *Genea* (Pezizales, Ascomycota) with an emphasis on European taxa. Mycologia 108(2): 441–456. https://doi.org/10.3852/15-199

Araújo JPM, Evans HC, Geiser DM, Mackay WP, Hughes DP (2015) Unravelling the diversity behind the *Ophiocordyceps unilateralis* (Ophiocordycipitaceae) complex: Three new species of zombie-ant fungi from the Brazilian Amazon. Phytotaxa 220(3): 224–238. https://doi.org/10.11646/phytotaxa.220.3.2

Beimforde C, Feldberg K, Nylinder S, Rikkinen J, Tuovila H, Dörfelt H, Gube M, Jackson DJ, Reitner J, Seyfullah LJ, Schmidt AR (2014) Estimating the Phanerozoic history of the Ascomycota lineages: Combining fossil and molecular data. Molecular Phylogenetics and Evolution 78(1): 307–319. https://doi.org/10.1016/j.ympev.2014.04.024

Benkert D (1987) Beiträge zur Taxonomie der Gattung *Lamprospora* (Pezizales). Zeitschrift für Mykologie 53(2): 195–271.

Benkert D (2001) Neotypisierung von *Lamprospora miniata* De Not. (Ascomycetes, Pezizales) und die Problematik des '*Lamprospora miniata*-Komplexes'. Micologia 2000: 47–61.

Berthet P (1964a) Formes conidiennes de divers Discomycètes. Bulletin de la Société mycologique de France 80: 125–149.

Berthet P (1964b) Essai biotaxinomique sur les Discomycètes. Thesis. University of Lyon, 158 pp.

Bonuso E, Zambonelli A, Bergemann SE, Iotti M, Garbelotto M (2010) Multilocus phylogenetic and coalescent analyses identify two cryptic species in the Italian bianchetto truffle, *Tuber borchii* Vittad. Conservation Genetics 11(4): 1453–1466. https://doi.org/10.1007/s10592-009-9972-3

Bouckaert R, Heled J, Kühnert D, Vaughan T, Wu CH, Xie D, Suchard MA, Rambaut A, Drummond AJ (2014) BEAST 2: A software platform for Bayesian evolutionary analysis. PLoS Computational Biology 10(4): 1–6. https://doi.org/10.1371/journal.pcbi.1003537

Buyck B, Olariaga I, Justice J, Lewis D, Roody W, Hofstetter V (2016) The dilemma of species recognition in the field when sequence data are not in phase with phenotypic variability. Cryptogamie, Mycologie 37(3): 367–389. https://doi.org/10.7872/crym/v37.iss3.2016.367

Câmara PEAS, Van Rooy J, Carvalho Silva M, Magill RE (2019) A revision of the family Sematophyllaceae (Bryophyta) in southern Africa. Acta Musei Silesiae, Scientiae Naturales 68: 147–164 (in press). https://doi.org/10.2478/cszma-2019-0015

Conway KE (1975) Ascocarp ontogeny and imperfect state of *Thecotheus* (Pezizales, Ascomycetes). Mycologia 67(2): 241–252. https://doi.org/10.1080/00275514.1975.12019746

Davidson RW (1950) *Urnula craterium* is possibly the perfect stage of *Strumella coryneoidea*. Mycologia 42(6): 735–742. https://doi.org/10.1080/00275514.1950.12017876

Descals E, Webster J (1978) *Miladina lechithina* (Pezizales), the ascigerous state of *Actinospora megalospora*. Transactions of the British Mycological Society 70(3): 466–472. https://doi.org/10.1016/S0007-1536(78)80150-8

Döbbeler P (1980) Untersuchungen an moosparasitischen Pezizales aus der Verwandtschaft von *Octospora*. Nova Hedwigia 31(4): 817–864.

Döbbeler P (1997) Biodiversity of bryophilous ascomycetes. Biodiversity and Conservation 6(5): 721–738. https://doi.org/10.1023/A:1018370304090

Doyle JJ, Doyle JL (1987) A rapid DNA isolation procedure for small quantities of fresh leaf tissue. Phytochemical Bulletin 19: 11–15.

Egertová Z, Döbbeler P, Sochor M (2018) *Octosporopsis erinacea* and *Octospora kelabitiana* (Pezizales) – two new hepaticolous ascomycetes from Borneo. Mycological Progress 17(1–2): 103–113. https://doi.org/10.1007/s11557-017-1354-5

Egger KN (1984) *Pyropyxis*, a new pyrophilous operculate discomycete with a *Dichobotrys* anamorph. Canadian Journal of Botany 62(4): 705–708. https://doi.org/10.1139/b84-103

Ferdman Y, Sitrit Y, Li Y-F, Roth-Bejerano N, Kagan-Zur V (2009) Cryptic species in the *Terfezia boudieri* complex. Antonie van Leeuwenhoek International Journal 95(4): 351–362. https://doi.org/10.1007/s10482-009-9321-z

Filippova N, Bulyonkova T, Lindemann U (2016) New records of two pyrophilous ascomycetes from Siberia: *Pyropyxis rubra* and *Rhodotarzetta rosea.* Ascomycete.org 8(4): 119–126. https://doi.org/10.25664/art-0181

Flynn T, Miller OK (1990) Biosystematics of *Agrocybe molesta* and sibling species allied to *Agrocybe praecox* in North America and Europe. Mycological Research 94(8): 1103–1110. https://doi.org/10.1016/s0953-7562(09)81341-5

Haelewaters D, De Kesel A, Pfister DH (2018) Integrative taxonomy reveals hidden species within a common fungal parasite of ladybirds. Scientific Reports 8(1): 15966. https://doi.org/10.1038/s41598-018-34319-5

Hansen K, Perry BA, Dranginis AW, Pfister DH (2013) A phylogeny of the highly diverse cup-fungus family Pyronemataceae (Pezizomycetes, Ascomycota) clarifies relationships and evolution of selected life history traits. Molecular Phylogenetics and Evolution 67(2): 311–335. https://doi.org/10.1016/j.ympev.2013.01.014

Harrington FA (1990) *Sarcoscypha* in North America (Pezizales, Sarcoscyphaceae). Mycotaxon 38: 417–458.

Healy R, Hobart C, Tocci GE, Bóna L, Merényi Z, Paz Conde A, Smith ME (2015) Fun with the discomycetes: revisiting collections of Korf's anamorphic Pezizales and Thaxter's New England truffles leads to a connection between forms and the description of two new truffle species: *Pachyphlodes pfisteri* and *P. nemoralis*. Ascomycete.org 7(6): 357–366. https://doi.org/10.25664/art-0160

Hennebert G (1973) *Botrytis* and *Botrytis*-like genera. Persoonia 7(2): 183–204.

Hibbett DS, Ohman A, Glotzer D, Nuhn M, Kirk P, Nilsson RH (2011) Progress in molecular and morphological taxon discovery in Fungi and options for formal classification of environmental sequences. Fungal Biology Reviews 25(1): 38–47. https://doi.org/10.1016/j.fbr.2011.01.001

Hughes SJ (1951) Studies on microfungi IX. *Calcarisporium*, *Verticicladium* and *Hansfordia* (gen. nov.). Mycological Papers 43: 3–25.

Kendrick WB (1979) The whole fungus. The sexual-asexual synthesis. National Museum of Natural Sciences and National Museums of Canada, Ottawa.

Korf PR (1958) Japanese discomycetes notes I–VIII. Science reports of the Yokohama National University. Section II, 7: 7–35.

Korhonen A, Seelan JSS, Miettinen O (2018) Cryptic species diversity in polypores: the *Skeletocutis nivea* species complex. MycoKeys 36: 45–82. https://doi.org/10.3897/mycokeys.36.27002

Lanfear R, Frandsen PB, Wright AM, Senfeld T, Calcott B (2017) PartitionFinder 2: New methods for selecting partitioned models of evolution for molecular and morphological phylogenetic analyses. Molecular Biology and Evolution 34(3): 772–773. https://doi.org/10.1093/molbev/msw260

Leacock PR, Riddell J, Wilson AW, Zhang R, Ning C, Mueller GM (2016) *Cantharellus chicagoensis* sp. nov. is supported by molecular and morphological analysis as a new yellow chanterelle in midwestern United States. Mycologia 108(4): 765–772. https://doi.org/10.3852/15-230.

Leliaert F, Verbruggen H, Vanormelingen P, Steen F, López-Bautista JM, Zuccarello GC, De Clerck O (2014) DNA-based species delimitation in algae. European Journal of Phycology 49(2): 179–196. https://doi.org/10.1080/09670262.2014.904524

Lindemann U, Vega M, Richter T, Alvarado P (2014) *Octosporopsis nicolai* – a mysterious member of the Pyronemataceae. Zeitschrift für Mykologie 80(2): 565–592.

Lindemann U (2013) Beiträge zur Erforschung der Pilzflora Äthiopiens. Operculate Discomyceten, Teil 1. Ascomycete.org 5(3): 97–103. https://doi.org/10.25664/art-0084

Magill RE (1981) Flora of Southern Africa: Bryophyta. Part 1 Mosses. Fascicle 1 Sphagnaceae-Grimmiaceae. Botanical Research Institute, South Africa.

Moravec J (1972) One interesting collection of operculate discomycete from Cairo (Egypt). Česká Mykologie 26(3): 138–140.

Moravec J (1997) [1996]. Fungi of the Kilimanjaro. II. *Octospora kilimanjarensis* sp. nov., a new species of the section *Neottiellae* (Discomycetes, Pezizales). Czech Mycology 49(3–4): 149–161.

Nguyen NH, Landeros F, Garibay-Orijel R, Hansen L, Vellinga EC (2013) The *Helvella lacunosa* species complex in western North America: cryptic species, misapplied names and parasites. Mycologia 105(5): 1275–1286. https://doi.org/10.3852/12-391

O'Donnell K, Rooney AP, Mills GL, Kuo M, Weber NS, Rehner SA (2011) Phylogeny and historical biogeography of true morels (*Morchella*) reveals an early Cretaceous origin and high continental endemism and provincialism in the Holarctic. Fungal Genetics and Biology 48(3): 252–265. https://doi.org/10.1016/j.fgb.2010.09.006

O'Shea BJ (2006) Checklist of the mosses of sub-Saharan Africa (version 5, 12/06). Tropical Bryology Research Reports 6: 1–252.

Öpik M, Vanatoa A, Vanatoa E, Moora M, Davison J, Kalwij JM, Reier U, Zobel M (2010) The online database Maarj AM reveals global and ecosystemic distribution patterns in arbuscular mycorrhizal fungi (Glomeromycota). New Phytologist 188(1): 223–241. https://doi.org/10.1111/j.1469-8137.2010.03334.x

Paal J, Kullman B, Huijser HA (1998) Multivariate analysis of the *Scutellinia umbrorum* complex (Pezizales, Ascomycetes) from five ecotopes in the Netherlands. Persoonia 16(4): 491–512.

Paden JW (1967) The conidial state of *Peziza brunneoatra*. Mycologia 59(5): 932–934. https://doi.org/10.2307/3757207

Paden JW (1972) Imperfect states and the taxonomy of the Pezizales. Persoonia 6(4): 405–414.

Paden JW (1975) Ascospore germination, growth in culture, and imperfect spore formation in *Cookeina sulcipes* and *Phillipsia crispata*. Canadian Journal of Botany 53(1): 56–61. https://doi.org/10.1139/b75-008

Paden JW, Sutherland JR, Woods TAD (1978) *Caloscypha fulgens* (Ascomycetidae, Pezizales): the perfect state of the conifer seed pathogen *Geniculodendron pyriforme* (Deuteromycotina, Hyphomycetes). Canadian Journal of Botany 56(19): 2375–2379. https://doi.org/10.1139/b78-289

Perry BA, Hansen K, Pfister DH (2007) A phylogenetic overview of the family Pyronemataceae (Ascomycota, Pezizales). Mycological Research 111(5): 549–571. https://doi.org/10.1016/j.mycres.2007.03.014

Pfister DH (1973) Caribbean Discomycetes 3. Ascospore germination and growth in culture of *Nanoscypha tetraspora* (Pezizales, Sarcoscyphineae). Mycologia 65(4): 952–956. https://doi.org/10.2307/3758534

Rambaut A, Drummond AJ, Xie D, Baele G, Suchard MA (2018) Posterior summarization in Bayesian phylogenetics using Tracer 1.7. Systematic Biology 67(5): 901–904. https://doi.org/10.1093/sysbio/syy032

Rehner SA, Buckley E (2005) A *Beauveria* phylogeny inferred from nuclear ITS and EF1-α sequences: evidence for cryptic diversification and links to *Cordyceps* teleomorphs. Mycologia 97(1): 84–98. https://doi.org/10.1080/15572536.2006.11832842

Ronquist F, Teslenko M, van der Mark P, Ayres DL, Darling A, Höhna S, Larget B, Liu L, Suchard MA, Huelsenbeck JP (2012) MrBayes 3.2: efficient Bayesian phylogenetic inference and model choice across a large model space. Systematic Biology 61(3): 539–542. https://doi.org/10.1093/sysbio/sys029

Seaver FJ (1914) A preliminary study of the genus *Lamprospora*. Mycologia 6(1): 5–24. https://doi.org/10.1080/00275514.1914.12020943

Seifert KA, Morgan-Jones G, Gams W, Kendrick B (2011) The genera of Hyphomycetes. CBS Biodiversity Series 9. Utrecht, CBS-KNAW Fungal Biodiversity Centre.

Schumacher TK (1993) Studies in arctic and alpine *Lamprospora* species. Sydowia 45(2): 307–337.

Skrede I, Carlsen T, Schumacher T (2017) A synopsis of the saddle fungi (*Helvella*: Ascomycota) in Europe – species delimitation, taxonomy and typification. Persoonia 39: 201–253. https://doi.org/10.3767/persoonia.2017.39.09

Smith ME, Trappe JM, Rizzo DM (2006) *Genea*, *Genabea* and *Gilkeya* gen. nov.: ascomata and ectomycorrhiza formation in a *Quercus* woodland. Mycologia 98(5): 699–716. https://doi.org/10.1080/15572536.2006.11832642

Sprague R (1948) Some leafspot fungi on western Gramineae – II. Mycologia. 40(2): 177–193. https://doi.org/10.1080/00275514.1948.12017698

Taşkın H, Doğan HH, Büyükalaca S, Clowez P, Moreau PA, O'Donnell K (2016) Four new morel (*Morchella*) species in the elata subclade (*M.* sect. *Distantes*) from Turkey. Mycotaxon 131(2): 467–482. https://doi.org/10.5248/131.467

Thines M, Crous PW, Aime MC, Aoki T, Cai L, Hyde KD, Miller AN, Zhang N, Stadler M (2018) Ten reasons why a sequence-based nomenclature is not useful for fungi anytime soon. IMA Fungus 9(1): 177–183. https://doi.org/10.5598/imafungus.2018.09.01.11

Van Rooy J, Phephu N (2016) Centres of moss diversity in southern Africa. Bryophyte Diversity and Evolution 38(1): 27–39. https://doi.org/10.11646/bde.38.1.3

Van Rooy J, Van Wyk AE (2010) The bryofloristic regions of southern Africa. Journal of Bryology 32(2): 80–91. https://doi.org/10.1179/037366810X12578498136039

Van Rooy J, Van Wyk AE (2011) The bryofloristic elements of southern Africa. Journal of Bryology 33(1): 17–29. https://doi.org/10.1179/1743282010Y.0000000007

Van Vooren N (2016) *Trichophaea dougoudii* sp. nov. (Pezizales), un nouveau discomycète de l'étage alpin. Ascomycete.org 8(5): 227–234. https://doi.org/10.25664/art-0190

Vilgalys R, Hester M (1990) Rapid genetic identification and mapping of enzymatically amplified ribosomal DNA from several *Cryptococcus* species. Journal of Bacteriology 172(8): 4238–4246. https://doi.org/10.1128/jb.172.8.4238-4246.1990

Wang XH, Huhtinen S, Hansen K (2016) Multilocus phylogenetic and coalescent-based methods reveal dilemma in generic limits, cryptic species, and a prevalent intercontinental dis-

junct distribution in *Geopyxis* (Pyronemataceae s. l., Pezizomycetes). Mycologia 108(6): 1189–1215. https://doi.org/10.3852/16-100

Warcup JH, Talbot PHB (1989) *Muciturbo*: A new genus of hypogeous ectomycorrhizal Ascomycetes. Mycological Research 92(1): 95–100. https://doi.org/10.1016/S0953-7562(89)80101-7

White TJ, Bruns T, Lee S, Taylor JW (1990) Amplification and direct sequencing of fungal ribosomal RNA genes for phylogenetics. In: Innis MA, Gelfand DH, Sninsky JJ, White TJ (Eds) PCR Protocols: A Guide to Methods and Applications. Academic Press, New York, 315–322. https://doi.org/10.1016/B978-0-12-372180-8.50042-1

Supplementary material 1

Table S1. Distance matrices (nucleotide difference) for each locus of *Octospora conidiophora* agg. and several randomly selected taxa

Authors: Zuzana Sochorová, Peter Döbbeler, Michal Sochor, Jacques van Rooy

Data type: molecular data

Link: https://doi.org/10.3897/mycokeys.54.34571.suppl1

Supplementary material 2

Figure S1. Bayesian phylogeny inference based on single-locus analyses

Authors: Zuzana Sochorová, Peter Döbbeler, Michal Sochor, Jacques van Rooy

Data type: phylogenetic tree

Explanation note: Bayesian posterior probability are shown above branches.

Link: https://doi.org/10.3897/mycokeys.54.34571.suppl2

MycoKeys 54: 77–98 (2019)
doi: 10.3897/mycokeys.54.34362
http://mycokeys.pensoft.net

RESEARCH ARTICLE

A peer-reviewed open-access journal
MycoKeys
Launched to accelerate biodiversity research

Phylogeny and diversity of *Haploporus* (Polyporaceae, Basidiomycota)

Meng Zhou[1], Li Wang[2], Tom W. May[3], Josef Vlasák[4], Jia-Jia Chen[5], Yu-Cheng Dai[6]

1 *Beijing advanced innovation centre for tree breeding by molecular design, Institute of Microbiology, PO Box 61, Beijing Forestry University, Beijing 100083, China* **2** *School of Economics and Management, Beijing Forestry University, Beijing 100083, China* **3** *Royal Botanic Gardens Victoria, Melbourne, Victoria 3004, Australia* **4** *Biology Centre of the Academy of Sciences of the Czech Republic, Branišovská 31, CZ-370 05 České Budějovice, Czech Republic* **5** *College of Plant Protection, Nanjing Agricultural University, Nanjing, Jiangsu 210095, China* **6** *Beijing Advanced Innovation Center for Tree Breeding by Molecular Design, Beijing Forestry University, Beijing 100083, China*

Corresponding author: *Yu-Cheng Dai* (yuchengd@yahoo.com)

Academic editor: *A. Vizzini* | Received 8 March 2019 | Accepted 7 May 2019 | Published 12 June 2019

Citation: Zhou M, Wang L, May TW, Vlasák J, Chen J-J, Dai Y-C (2019) Phylogeny and diversity of *Haploporus* (Polyporaceae, Basidiomycota). MycoKeys 54: 77–98. https://doi.org/10.3897/mycokeys.54.34362

Abstract

Four species of *Haploporus*, *H. angustisporus*, *H. crassus*, *H. gilbertsonii* and *H. microsporus* are described as new and *H. pirongia* is proposed as a new combination, based on morphological characteristics and molecular phylogenetic analyses inferred from internal transcribed spacer (ITS) and large subunit nuclear ribosomal RNA gene (nLSU) sequences. *Haploporus angustisporus*, *H. crassus* and *H. microsporus* occur in China, *H. gilbertsonii* occurs in the USA, and the distribution of *H. pirongia* is extended from New Zealand to Australia. *Haploporus angustisporus* is characterized by the distinct narrow oblong basidiospores measuring 10.5–13.5 × 3.9–5 µm. *Haploporus crassus* is characterized by the presence of ventricose cystidioles occasionally with a simple septum, dissepimental hyphae usually with a simple septum, unique thick-walled basidia and distinctly wide oblong basidiospores measuring 13.5–16.5 × 7.5–9.5 µm. *Haploporus gilbertsonii* is characterized by its large pores (2–3 per mm), a dimitic hyphal structure with non-dextrinoid skeletal hyphae and wide oblong basidiospores measuring 12–15 × 6–8 µm. *Haploporus microsporus* is characterized by distinctly small pores (7–9 per mm), the presence of dendrohyphidia, and distinctly small ellipsoid basidiospores measuring 5.3–6.7 × 3–4.1 µm. *Haploporus pirongia* is proposed as a new combination. *Haploporus amarus* is shown to be a synonym of *H. odorus* and *Pachykytospora wasseri* is considered a synonym of *H. subtrameteus*.

Keywords

Polyporales, taxonomy, wood-inhabiting fungi

Introduction

Haploporus Bondartsev & Singer (Polyporales, Basidiomycota) is characterized by annual to perennial, resupinate to pileate basidiocarps, a di- to trimitic hyphal system with clamped connections on the generative hyphae, cyanophilous skeletal hyphae, cylindrical to subglobose, hyaline, thick-walled, cyanophilous and ornamented basidiospores, and formation of a white rot (Singer 1944, Dai et al. 2002, Piątek 2005, Li et al. 2007, Shen et al. 2016). *Pachykytospora* was shown to be, micro-morphologically, similar to Haploporus, differing only in having resupinate basidiocarps; both names were treated as synonyms (Dai et al. 2002) and consequently, all Pachykytospora species have been transferred to Haploporus (Dai et al. 2002, Piątek 2005, Shen et al. 2016), but *P. major* G.Y.Zheng&Z.S.Bi (add lit.), which belong to Megasporia because of its thin-walled and smooth basidiospores (Dai and Li 2002). The monophyly of Pachykytospora was confirmed later on by molecular analysis (Shen et al. 2016). So far 13 species have been accepted in *Haploporus* (Dai et al. 2002, Hattori et al. 2002, Piątek 2005, Li et al. 2007, Dai and Kashiwadani 2009, Shen et al. 2016).

During a study on taxonomy of Polyporaceae, several specimens of *Haploporus* from USA, Australia and China were studied. After morphological examinations and phylogenetic analysis of ITS and nLSU sequences, four new species were confirmed to be members of the *Haploporus* lineage. In this paper, we describe and illustrate these new species. In addition, *Poria pirongia* G. Cunn. was originally described from New Zealand (Cunningham 1947), and treated as a synonym of *Poria papyracea* (Schwein.) Cooke (= *Haploporus papyraceus* (Schwein.) Y.C.Dai&Niemelä (Cunningham 1965, Lowe 1966 and Buchanan and Ryvarden 1988) is shown to represent an independent species, based on new specimens and both morphology and phylogenetic evidences. Therefore, a new combination (*H. pirongia*) is proposed.

Materials and methods

Morphological studies

Sections were studied microscopically according to Dai (2010) at magnifications ≤1000× using a Nikon Eclipse 80i microscope with phase contrast illumination. Drawings were made with the aid of a drawing tube. Microscopic features, measurements, and drawings were made from sections stained with Cotton Blue and Melzer's reagent. Spores were measured from sections cut from the tubes. To present spore size variation, the 5% of measurements excluded from each end of the range are given in parentheses. Basidiospore spine lengths were not included in the measurements. Abbreviations include: IKI = Melzer's reagent, IKI– = negative in Melzer's reagent, KOH = 5% potassium hydroxide, CB = Cotton Blue, CB+ = cyanophilous, L = mean spore length (arithmetic average of all spores), W = mean spore width (arithmetic average

of all spores), Q = the L/W ratio, and n = number of spores measured / from given number of specimens. Color terms follow Petersen (1996). Herbarium abbreviations follow Thiers (2018).

Molecular study and phylogenetic analysis

A CTAB rapid plant genome extraction kit (Aidlab Biotechnologies, Beijing) was used to obtain PCR products from dried specimens, according to the manufacturer's instructions with some modifications (Cao et al. 2012, Zhao et al. 2013). The DNA was amplified with the primers: ITS5 and ITS4 for ITS (White et al. 1990), and LR0R and LR7 (http://www.biology.duke.edu/fungi/mycolab/primers.htm) for nLSU (Vilgalys and Hester 1990). The PCR procedure for ITS was as follows: initial denaturation at 95 °C for 3 min, followed by 34 cycles at 94 °C for 40 s, 54 °C for 45 s and 72 °C for 1 min, and a final extension of 72 °C for 10 min. The PCR procedure for nLSU was as follows: initial denaturation at 94 °C for 1 min, followed by 34 cycles at 94 °C for 30 s, 50 °C for 1 min and 72 °C for 1.5 min, and a final extension of 72 °C for 10 min. The PCR products were purified and sequenced at the Beijing Genomics Institute, China with the same primers.

Phylogenetic analyses. New sequences, deposited in GenBank (http://www.ncbi.nlm.nih.gov/genbank/) (Table 1), were aligned with additional sequences retrieved from GenBank (Table 1) using BioEdit 7.0.5.3 (Hall 1999) and ClustalX 1.83 (Thompson et al. 1997). The sequence quality were checked followed Nilsson et al. (2012). *Perenniporia hainaniana* B.K.Cui&C.L.Zhao and *P. medulla-panis* (Jacq.) Donk were used as outgroups, following Shen et al. (2016). Prior to phylogenetic analysis, ambiguous regions at the start and the end of the alignment were trimmed and gaps were manually adjusted to optimize the alignment were trimmed. The edited alignment was deposited at TreeBase (http://purl.org/phylo/treebase; submission ID 24089).

Maximum parsimony (MP) and Bayesian inference (BI) were employed to perform phylogenetic analysis of the two aligned datasets. The two phylogenetic analysis algorithms generated nearly identical topologies for each dataset, and, thus only the topology from the MP analysis is presented along with statistical values from the MP and BI algorithms. Most parsimonious phylogenies were inferred from the ITS + nLSU, and their combinability was evaluated with the incongruence length difference (ILD) test (Farris et al. 1994) implemented in PAUP* 4.0b10 (Swofford 2002), under a heuristic search and 1000 homogeneity replicates giving a P value of 1.000, much greater than 0.01, which means there is no discrepancy among the two loci in reconstructing phylogenetic trees. Phylogenetic analysis approaches followed Zhao et al. (2015). The tree construction procedure was performed in PAUP* version 4.0b10 (Swofford 2002). All characters were equally weighted, and gaps were treated as missing data. Trees were inferred using the heuristic search option with TBR branch swapping and 1000 random sequence additions. Max-trees were set to 5000, branches of zero length were collapsed and all parsimonious trees were saved. Clade robustness was assessed using a

Table 1. Information on the sequences used in this study.

Species	Sample no.	Location	GenBank accession no.	
			ITS	nLSU
Haploporus alabamae	JV_0610_K16-Kout	Belize	KY264039	
	Dollinger 895	USA	KY264038	**MK433606**
	JV 1704/75	Costa Rica	MK429754	**MK433607**
H. angustisporus	**Cui 9046**	**China**	**KU941862**	**KU941887**
	Dai 10951	**China**	**KX900634**	**KX900681**
H. crassus	**Dai 13580**	**China**	**FJ627252**	**KU941886**
H. cylindrosporus	Dai 15643	China	KU941853	KU941877
	Dai 15664	China	KU941854	KU941878
H. gilbertsonii	**JV 1209/63-J**	**USA**	**MK429755**	**MK433608**
	JV 1611/5-J	**USA**	**MK429756**	**MK433609**
H. latisporus	Dai 11873	China	KU941847	KU941871
	Dai 10562	China	KU941848	KU941872
H. microsporus	**Dai 12147**	**China**	**KU941861**	**KU941885**
H. nanosporus	LYAD 2044a	Gabon	KU941859	KU941883
	LYAD 2044b	Gabon	KU941860	KU941884
H. nepalensis	Dai 12937	China	KU941855	KU941879
	Cui 10729	China	KU941856	KU941880
H. odorus	Dai 11296	China	KU941845	KU941869
	Yuan 2365	China	KU941846	KU941870
H. cf. *odorus*	KUC20121123-29	Republic of Korea	KJ668537	KJ668390
H. papyraceus	Dai 10778	China	KU941839	KU941863
	Cui 8706	China	KU941840	KU941864
	KUC20130719-04	Republic of Korea	KJ668535	KJ668388
H. pirongia	**Dai 18659**	**Australia**	**MH631017**	**MH631021**
	Dai 18660	**Australia**	**MH631018**	**MH631022**
	Dai 18661	**Australia**	**MH631019**	**MH631023**
	Dai 18662	**Australia**	**MH631020**	**MH631024**
	PDD 95714	**New Zealand**	**MK429757**	
H. septatus	Dai 13581	China	KU941843	KU941867
	Cui 4100	China	KU941844	KU941868
H. sp.	KUC20080606-35	Republic of Korea	KJ668534	KJ668387
H. subpapyraceus	Dai 9324	China	KU941841	KU941865
	Cui 2651	China	KU941842	KU941866
H. subtrameteus	Dai 4222	China	KU941849	KU941873
	Cui 10656	China	KU941850	KU941874
	Dai11270	China	KY264042	
H. cf. *subtrameteus*	KUC20121102-36	Republic of Korea	KJ668536	KJ668389
H. thindii	Cui 9373	China	KU941851	KU941875
	Cui 9682	China	KU941852	KU941876
H. tuberculosus	15559	Sweden	KU941857	KU941881
	15560	Austria	KU941858	KU941882
H. tuberculosus (as *Pachykytospora*)	KA11 (GB)	Sweden	JX124705	
	JV 9610/20	Slovakia	KY264040	**MK433610**
	JV 0509/19	Czech Republic	KY264041	**MK433611**
Pachykytospora wasseri	LE814872 (T)	Russia	KM411456	KM411472
Perenniporia hainaniana	Cui 6364	China	JQ861743	JQ861759
P. medulla-panis	Cui 3274	China	JN112792	JN112793

bootstrap (BT) analysis with 1000 replicates (Felsenstein 1985). Descriptive tree statistics tree length (TL), consistency index (CI), retention index (RI), rescaled consistency index (RC), and homoplasy index (HI) were calculated for each maximum parsimonious tree (MPT) generated. jModeltest v.2.17 (Darriba et al. 2012) was used to determine the best-fit evolution model of the combined dataset for Bayesian inference (BI). The Bayesian inference (BI) was conducted with MrBayes 3.2.6 (Ronquist et al. 2012) in two independent runs, each of which had four chains for 10 million generations and started from random trees. Trees were sampled every 1000th generation. The first 25% of sampled trees were discarded as burn-in, whereas other trees were used to construct a 50 % majority consensus tree and for calculating Bayesian posterior probabilities (BPPs).

Phylogenetic trees were visualized using Treeview (Page 1996). Nodes that received Bootstrap support ≥50% and Bayesian posterior probabilities (BPP) ≥0.90 are considered as significantly supported.

Results

Molecular phylogeny

The combined ITS and 28S dataset included sequences from 46 fungal collections representing 21 species. The dataset had an aligned length of 2054 characters, of which 1399 characters are constant, 98 are variable and parsimony-uninformative, and 557 are parsimony-informative. MP analysis yielded 4 equally parsimonious trees (TL = 1370, CI = 0. 639, RI = 0.870, RC = 0.556, HI = 0.361). The best model for the combined ITS and 28S sequences dataset estimated and applied in the BI was GTR+I+G. BI resulted in a similar topology with an average standard deviation of split frequencies = 0.004515 to MP analysis, and thus only the MP tree is provided. Both BT values (≥50%) and BPPs (≥0.90) are shown at the nodes (Fig. 1). The ITS-based phylogenies included ITS sequences from 47 fungal collections representing 21 species. The dataset had an aligned length of 711 characters, of which 317 characters are constant, 54 are variable and parsimony-uninformative, and 340 are parsimony-informative. MP analysis yielded 4 equally parsimonious trees (TL = 927, CI = 0. 653, RI = 0.888, RC = 0.580, HI = 0.347). The best model for the ITS sequences dataset estimated and applied in the BI was GTR+I+G. BI resulted in a similar topology with an average standard deviation of split frequencies = 0.005040 to MP analysis, and thus only the MP tree is provided. Both BT values (≥50%) and BPPs (≥0.90) are shown at the nodes (Fig. 2).

In both 28S+ITS- and ITS-based phylogenies (Figs. 1–2), five new well-supported lineages were identified. Among them three well-supported terminal clades and two isolated branches (100% MP and 1.00 BI). *Haploporus angustisporus* is sister to *H. alabamae* (Berk. & Cooke) Y.C.Dai&Niemelä and this two species clade is related to *H. nanosporus* (A.David&Rajchenb.) Piątek, whereas *H. gilbertsonii* clustered with *H. cylindrosporus* L.L. Shen, Y.C.Dai&B.K.Cui, *H. thindii* (Natarajan & Koland.) Y.C.Dai, *H. nepalensis* (T. Hatt.) Piątek and *H. tuberculosus* (Fr.) Niemelä&Y.C.Dai. Four Australian specimens and a specimen of *Poria pirongia* from New Zealand formed

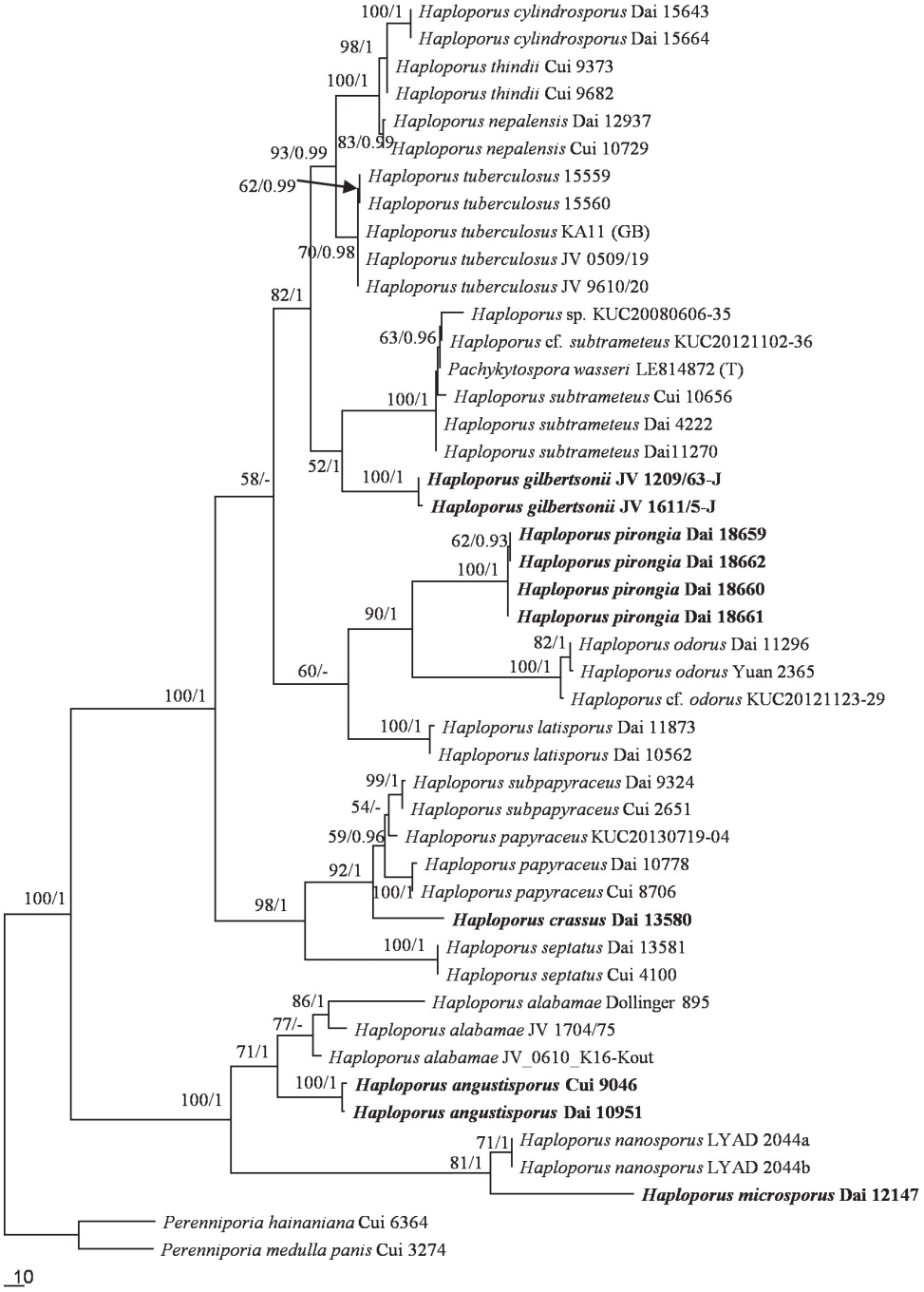

Figure 1. Maximum parsimony strict consensus tree illustrating the phylogeny of *Haploporus* based on ITS+nLSU sequences. Branches are labeled with parsimony bootstrap proportions (before slanting line) greater than 50% and bayesian posterior probabilities (after slanting line) greater than 0.90.

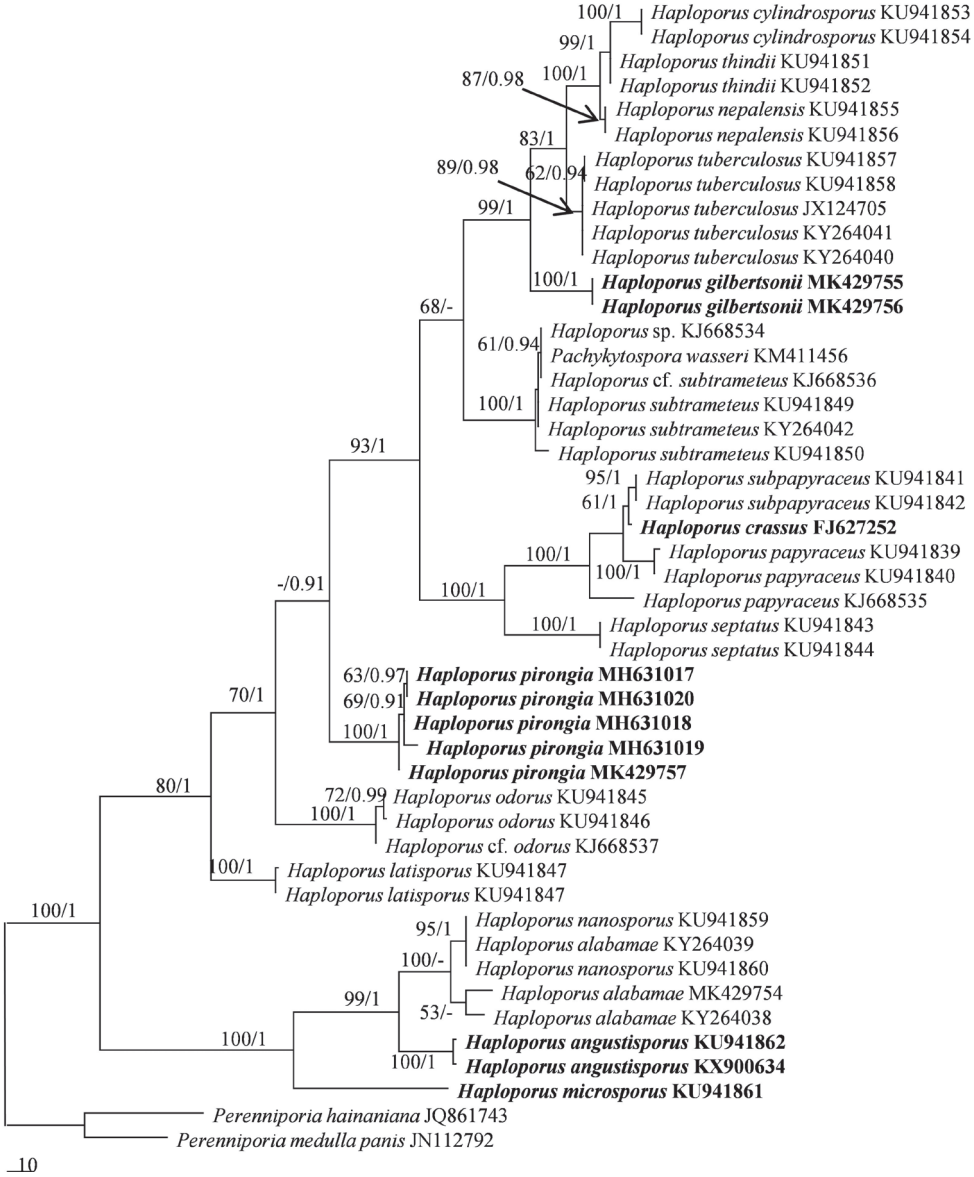

Figure 2. Maximum parsimony strict consensus tree illustrating the phylogeny of *Haploporus* based on ITS sequences. Branches are labeled with parsimony bootstrap proportions (before slanting line) greater than 50% and bayesian posterior probabilities (after slanting line) greater than 0.90.

a well-supported clade (100% MP and 1.00 BI), sister to the *H. odorus* clade. In addition, the other two lineages formed two distinct sublineages; *Haploporus crassus* is closely related to *H. papyraceus* and *H. subpapyraceus* L.L.Shen, Y.C.Dai&B.K.Cui; whereas The *H. nanosporus* and *H. microsporus* clades are sister clades.

Figure 3. A basidiocarp of *Haploporus angustisporus* (Holotype). Scale bar: 1.0 cm.

Taxonomy

Haploporus angustisporus **Meng Zhou&Y.C.Dai, sp. nov.**
MycoBank: MB829583
Figs 3–4

Diagnosis. Differs from other *Haploporus* species by the combination of its resupinate habit, a dimitic hyphal structure with dextrinoid skeletal hyphae, the absence of dendrohyphidia, and distinct narrow oblong basidiospores measuring 10–13.5 × 4–5 µm.

Holotype. CHINA. Guangdong Prov., Lianzhou County, Nanling Nat. Res., on fallen angiosperm branch, 15 May 2009, *Dai 10951* (Holotype in BJFC).

Etymology. *Angustisporus* (Lat.): referring to the species having narrow basidiospores.

Fruitbody. Basidiocarps annual, resupinate, adnate, soft corky when fresh, become corky upon drying, without odor or tasteless when fresh, up to 3 cm long, 2.5 cm wide, 2 mm thick at center. Pore surface cream to pale yellowish brown when fresh, brownish when bruised, olivaceous buff to pale brown upon drying; sterile margin indistinct, very narrow to almost lacking; pores angular, 3–5 per mm; dissepiments thick, entire. Subiculum cream, corky, thin, about 0.1 mm thick. Tubes light buff, corky, about 1.9 mm long.

Hyphal structure. Hyphal system dimitic: generative hyphae bearing clamp connections, hyaline, thin-walled; skeletal hyphae dominant, thick-walled, frequently branched, dextrinoid, CB+, tissues unchanging in KOH.

Subiculum. Generative hyphae infrequent, hyaline, thin-walled, rarely branched, 1.5–2.5 µm in diam; skeletal hyphae dominant, hyaline, thick-walled with a narrow lumen to subsolid, frequently branched, interwoven, 1–2.5 µm in diam.

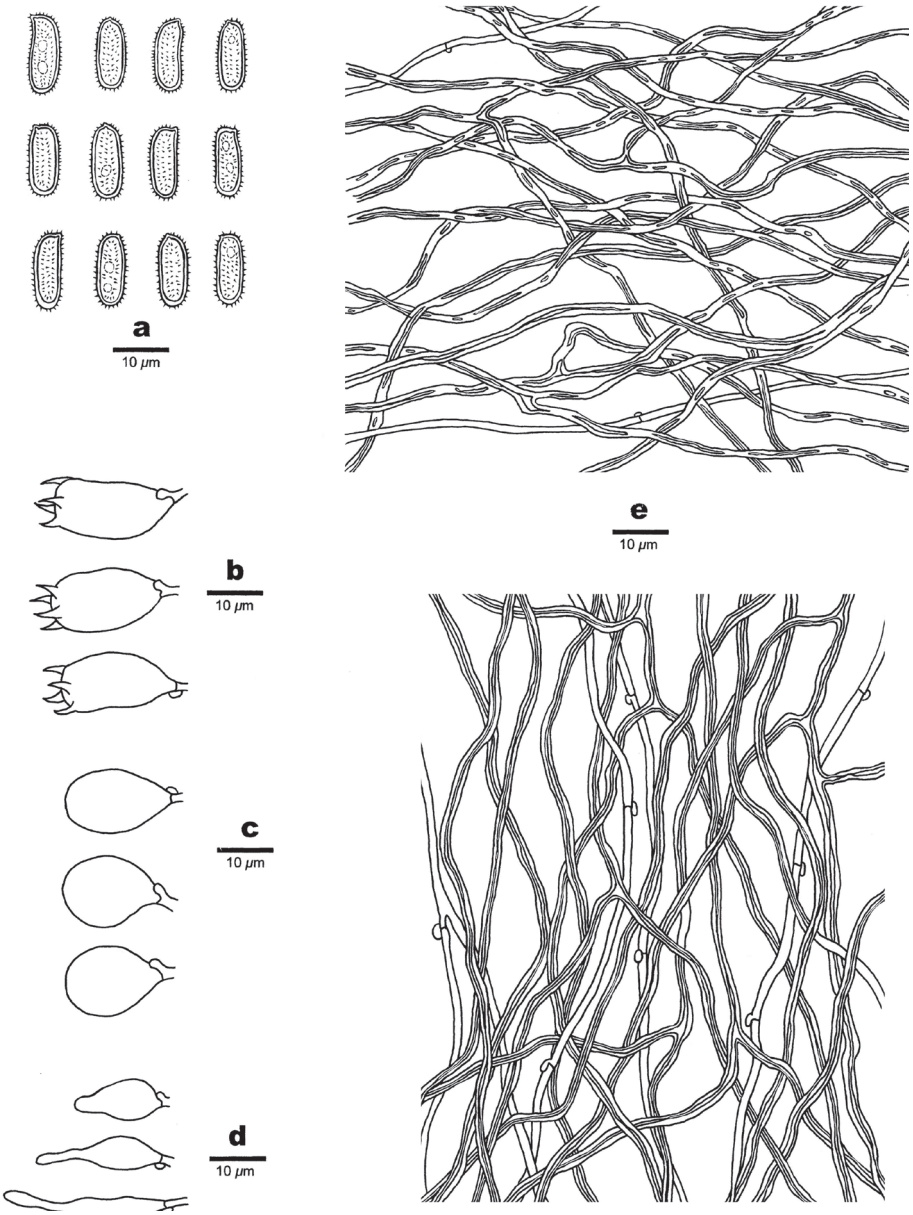

Figure 4. Microscopic structures of *Haploporus angustisporus* (Holotype). **a** Basidiospores **b** Basidia **c** Basidioles **d** Cystidioles **e** Hyphae from subiculum **f** Hyphae from trama.

Tubes. Generative hyphae frequent, hyaline, thin-walled, occasionally branched, 1.5–2.5 µm in diam; skeletal hyphae distinctly thick-walled with a narrow to wide lumen, frequently branched, interwoven, 1.2–2.5 µm in diam. Cystidia absent; cystidioles present, fusiform, 23–35 × 4–7 µm. Basidioles dominant, pear-shaped to subglobose, basidia barrel-shaped with 4-sterigmata and a basal clamp connection, 21–26 × 8–11 µm; . Dendrohyphidia absent. Some irregular-shaped crystals present among tube tramal structures.

Spores. Basidiospores oblong, hyaline, thick-walled, with short tuberculate ornamentation, IKI–, CB+, 10–13.5(–14) × (3.5–)4–5 μm, L = 11.25 μm, W = 4.44 μm, Q = 2.38–2.70 (n = 60/2).

Additional specimen examined (paratype). CHINA. Guangdong Prov., Fengkai County, Heishiding Nat. Res., on fallen angiosperm branch, 1 July 2010, *Cui 9046* (in BJFC).

Haploporus crassus **Meng Zhou&Y.C.Dai, sp. nov.**
MycoBank: MB829584
Fig. 5

Diagnosis. Differs from other *Haploporus* species by the combination of a resupinate habit, a dimitic hyphal structure with non-dextrinoid skeletal hyphae, the presence of ventricose cystidioles occasionally with a simple septum, dissepimental hyphae usually with a simple septum, unique thick-walled basidia and distinct wide oblong basidiospores measuring 13.5–16.5 × 7.5–9.5 μm.

Holotype. CHINA. Yunnan Prov., Xinping County, Ailaoshan Nat. Res., on rotten angiosperm wood, 15 Oct. 2013, *Dai 13580* (Holotype in BJFC).

Etymology. *Crassus* (Lat.): referring to the species having wide basidiospores.

Fruitbody. Basidiocarps annual, resupinate, adnate, soft corky when fresh, become corky and cracked upon drying, without odor or taste when fresh, up to 35 cm long, 3 cm wide and 1 mm thick at center. Pore surface white to cream when fresh, becoming buff-yellow upon drying; sterile margin indistinct, very narrow to almost lacking; pores round, 3–5 per mm; dissepiments thin, mostly entire, sometimes lacerate. Subiculum cream, corky, thin, about 0.1 mm thick. Tubes light buff, corky, about 0.9 mm long.

Hyphal structure. Hyphal system dimitic: generative hyphae bearing clamp connections, hyaline, thin-walled; skeletal hyphae dominant, thick-walled, frequently branched, IKI–, CB+, tissues unchanging in KOH.

Subiculum. Generative hyphae infrequent hyaline, thin-walled, rarely branched, 1.5–2.5 μm in diam; skeletal hyphae dominant, hyaline, thick-walled with a narrow lumen, frequently branched, interwoven, 1–2 μm in diam.

Tubes. Generative hyphae frequent, hyaline, thin-walled, occasionally branched, 1.5–3 μm in diam; skeletal hyphae dominant, distinctly thick-walled with a narrow to wide lumen, frequently branched, interwoven, 1.5–2.5 μm in diam; dissepimental hyphae usually with a simple septum. Cystidia absent; cystidioles present, ventricose, usually with a small umbo having a simple septum, occasionally with a few small guttules, 21–31× 8–10 μm. Basidioles thick-walled, dominant, similar in shape to basidia, but smaller; basidia thick-walled, pear-shaped to barrel-shaped with 4-sterigmata and a basal clamp connection, occasionally with some small guttules, 22–31 × 8–13 μm; dendrohyphidia absent. Some irregular-shaped crystals present among tube tramal stru ctures.

Spores. Basidiospores oblong, hyaline, thick-walled, with tuberculate ornamentation, IKI–, CB+, 13.5–16.5(–17) × (7–)7.5–9.5 μm, L = 15.06 μm, W = 8.15 μm, Q = 1.85 (n = 30/1).

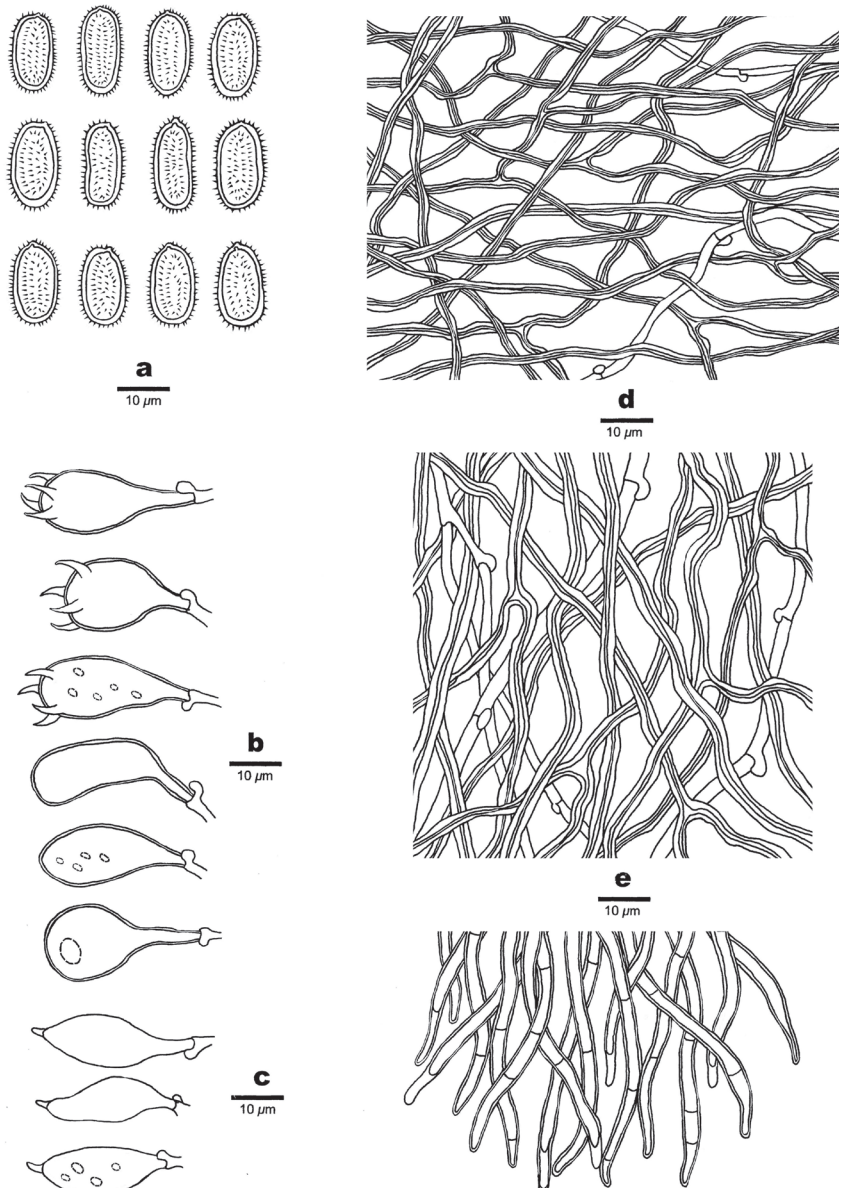

Figure 5. Microscopic structures of *Haploporus crassus* (Holotype). **a** Basidiospores **b** Basidia and Basidioles **c** Cystidioles **d** Hyphae from subiculum **e** Hyphae from trama **f** Hyphae at dissepiment.

Haploporus gilbertsonii **Meng Zhou, Vlasák&Y.C.Dai, sp. nov.**
Figs 6–7
MycoBank: MB829649

Diagnosis. Differs from other *Haploporus* species by its relatively large pores, 2–3 per mm, a dimitic hyphal structure with non-dextrinoid skeletal hyphae,

Figure 6. A basidiocarp of *Haploporus gilbertsonii* (Holotype). Scale bar: 1.0 cm.

the absence of dendrohyphidia, and wide oblong basidiospores measuring 12–15 × 6–8 µm.

Holotype. USA. Arizona, Santa Rita Mt., Madera Canyon, on dead tree of *Quercus*, 20 Nov. 2016, *Vlasák Jr. 1611/5-J* (Holotype in PRM, isotype in JV and BJFC).

Etymology. *Gilbertsonii* (Lat.): in honor of Prof. R.L. Gilbertson, the American mycologist.

Fruitbody. Basidiocarps annual, resupinate, difficult to separate from the substrate, corky when dry, up to 10 cm long, 8 cm wide and 0.8 mm thick at center. Pore surface pale buff to buff when dry; sterile margin indistinct, very narrow to almost lacking; pores round to angular, 2–3 per mm; dissepiments thick, entire. Subiculum cream, corky, thin, about 0.3 mm thick. Tubes light buff, corky, about 0.5 mm long.

Hyphal structure. Hyphal system dimitic: generative hyphae bearing clamp connections, hyaline, thin-walled; skeletal hyphae dominant, thick-walled, frequently branched, IKI–, CB–, tissues unchanging in KOH.

Subiculum. Generative hyphae infrequent, hyaline, thin-walled, occasionally branched, 2–3 µm in diam; skeletal hyphae dominant, hyaline, distinctly thick-walled, frequently branched, interwoven, 1.5–3 µm in diam.

Tubes. Generative hyphae infrequent, hyaline, thin-walled, occasionally branched, 1–3 µm in diam; skeletal hyphae dominant, distinctly thick-walled, frequently branched, interwoven, 2–4 µm in diam. Cystidia absent; cystidioles present, fusiform, hyaline, thin-walled, 13–23 × 4.5–6 µm. Basidia pear-shaped to barrel-shaped with

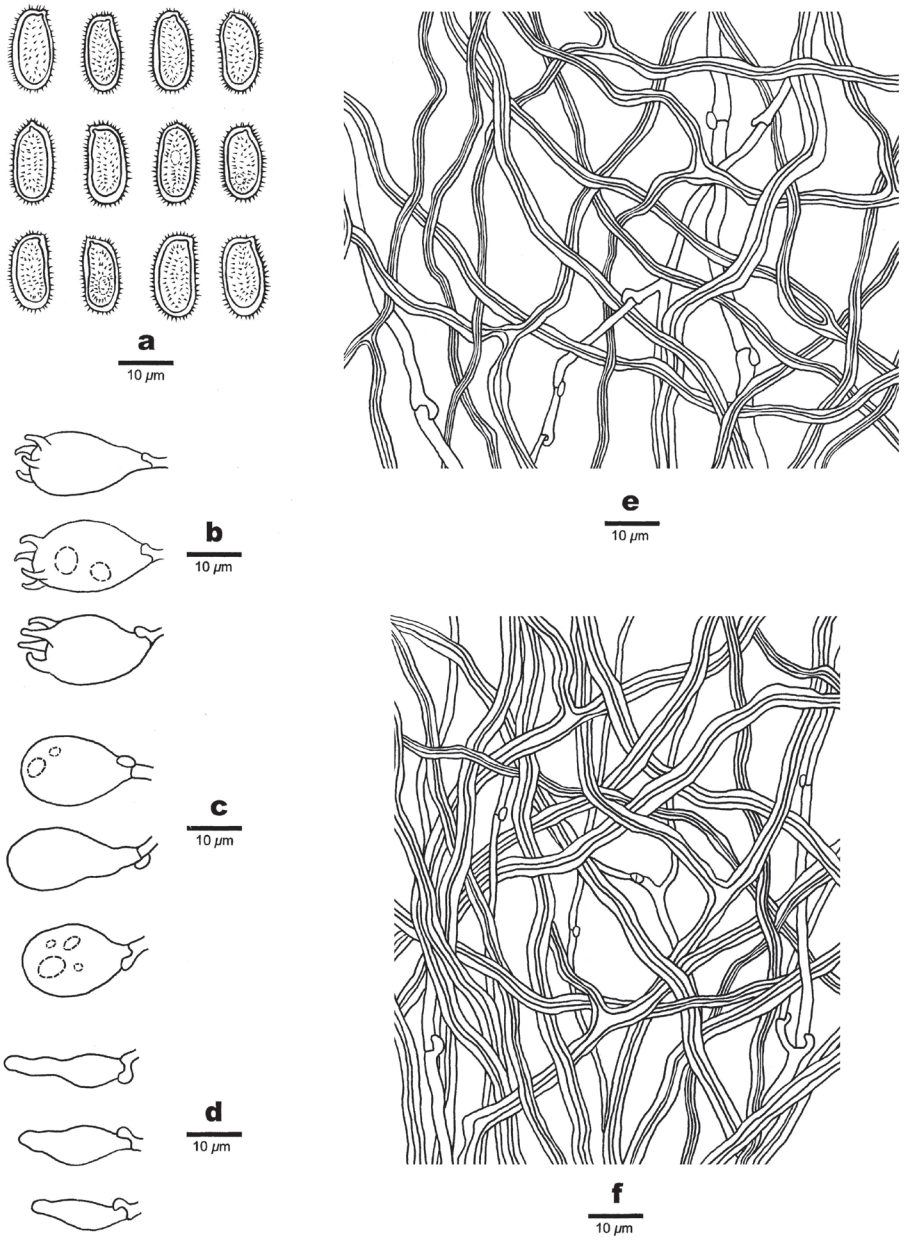

Figure 7. Microscopic structures of *Haploporus gilbertsonii* (Holotype). **a** Basidiospores **b** Basidia **c** Basidioles **d** Cystidioles **e** Hyphae from subiculum **f** Hyphae from trama.

4-sterigmata and a basal clamp connection, occasionally with a few large guttules, 21–25 × 10–14 µm; basidioles dominant, similar in shape to basidia, but slightly smaller. Dendrohyphidia absent. Some irregular-shaped crystals present among tube tramal structures.

Figure 8. A basidiocarp of *Haploporus microsporus* (Holotype). Scale bar: 1.0 cm.

Spores. Basidiospores oblong, hyaline, thick-walled, with tuberculate ornamentation, IKI–, CB+, 12–15(–16) × (5.5–)6–8 μm, L = 14.07 μm, W = 6.9 μm, Q = 1.83–2.15 (n = 60/2).

Additional specimen examined (paratype). USA. Arizona, Chiricahua Mt., Turkey Canyon, on dead tree of *Quercus*, 5 Sep. 2012, *Vlasák Jr. 1209/63-J* (JV, dupl. in BJFC).

Haploporus microsporus **Meng Zhou&Y.C.Dai, sp. nov.**
MycoBank: MB829585
Figs 8–9

Diagnosis. Differs from other *Haploporus* species by the combination of a resupinate habit, a dimitic hyphal structure with dextrinoid skeletal hyphae, distinct small pores, 7–9 per mm, the presence of dendrohyphidia, and distinct small ellipsoid basidiospores measuring 5.3–6.7 × 3–4.1 μm.

Holotype. CHINA. Hainan Prov., Ledong County, Jianfengling Nat. Res., on dead angiosperm tree, 23 March 2011, *Dai 12147* (Holotype in BJFC).

Etymology. *Microsporus* (Lat.): referring to the small basidiospores of this species.

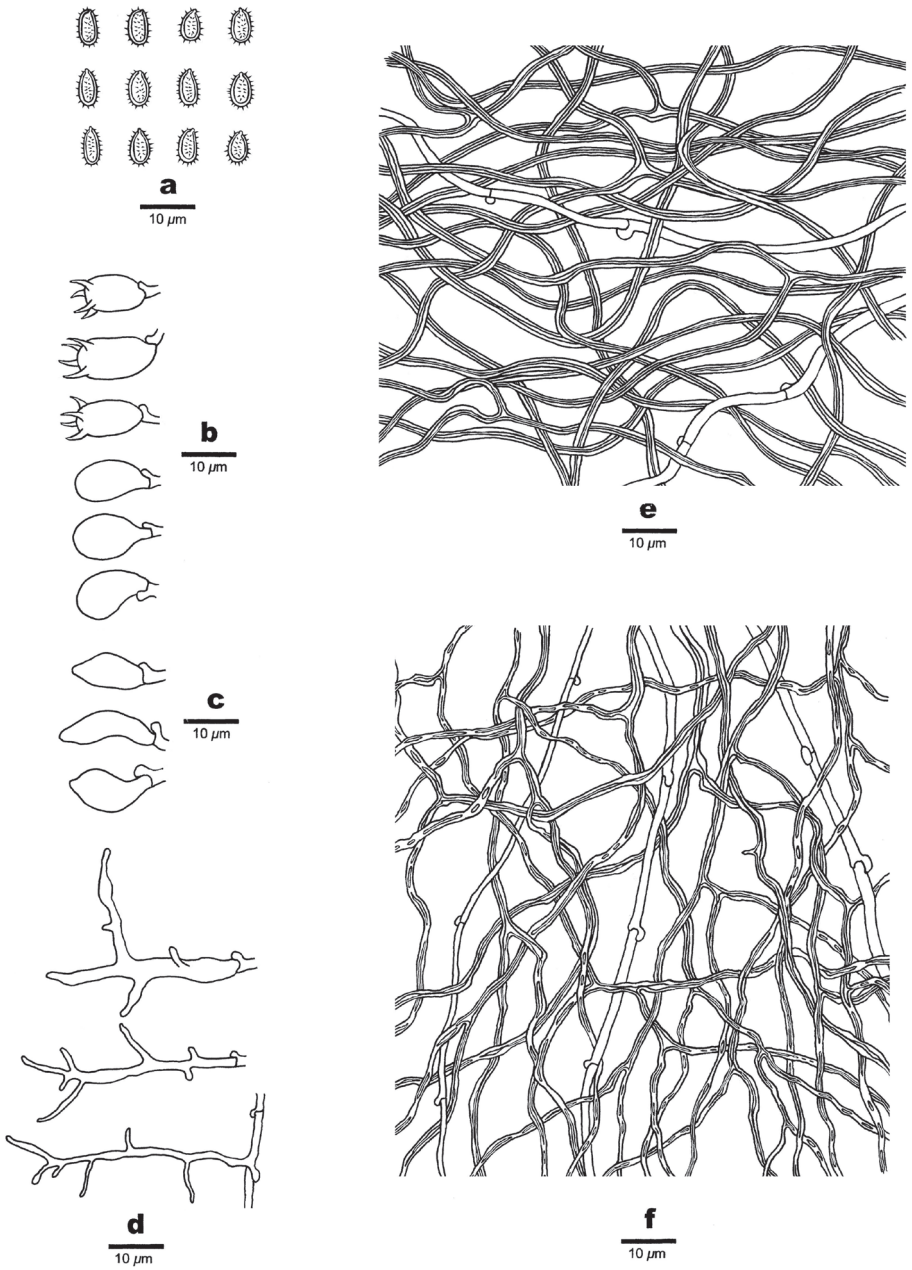

Figure 9. Microscopic structures of *Haploporus microsporus* (Holotype). **a** Basidiospores **b** Basidia and Basidioles **c** Cystidioles **d** Dendrohyphidia **e** Hyphae from subiculum **f** Hyphae from trama.

Fruitbody. Basidiocarps annual, resupinate, adnate, soft corky when fresh, become corky upon drying, odor- or tasteless when fresh, up to 20 cm long, 4.5 cm wide and 2 mm thick at center. Pore surface pinkish buff to clay-buff when dry; sterile margin

indistinct, very narrow to almost lacking; pores angular, 7–9 per mm; dissepiments thick, entire. Subiculum cream, corky, thin, about 0.2 mm thick. Tubes light buff, corky, about 1.8 mm long.

Hyphal structure. Hyphal system dimitic: generative hyphae bearing clamp connections, hyaline, thin-walled; skeletal hyphae dominant, thick-walled, frequently branched, dextrinoid, CB–, skeletal hyphae swollen in KOH.

Subiculum. Generative hyphae infrequent, hyaline, thin-walled, rarely branched, 1.5–2.5 μm in diam; skeletal hyphae dominant, hyaline, thick-walled with a narrow to wide lumen, frequently branched, interwoven, 1.5–3 μm in diam.

Tubes. Generative hyphae infrequent, hyaline, thin-walled, rarely branched, 1.5–3 μm in diam; skeletal hyphae distinctly thick-walled with a narrow lumen to subsolid, frequently branched, interwoven, 1–2 μm in diam. Cystidioles present, fusiform, 10–20 × 3.5–6 μm. Basidia barrel-shaped with 4-sterigmata and a basal clamp connection, 11–16 × 5.5–6.5 μm; basidioles dominant, similar in shape to basidia, but slightly smaller. Dendrohyphidia abundant, frequently branched. Some irregular-shaped crystals present among tube tramal structures

Spores. Basidiospores ellipsoid, hyaline, thick-walled, with tuberculate ornamentation, dextrinoid, CB+, 5.3–6.7(–7) × (2.9–)3–4.1 μm, L = 5.98 μm, W = 3.90 μm, Q = 1.78 (n = 30/1).

Haploporus pirongia **(G. Cunn.) Meng Zhou, Y.C.Dai&T.W. May, comb. nov.**
MycoBank: MB829650
Figs 10–11

Poria pirongia G. Cunn., Bull. N.Z. Dept. Sci. Industr. Res., Pl. Dis. Div. 72: 39 (1947) (Basionym)

Etymology. the epithet *pirongia*, derived from the type locality, Mount Pirongia, is a noun in apposition, and therefore remains spelt the same when transferred from *Poria* to *Haploporus*, despite the latter genus being masculine in gender.

Fruitbody. Basidiocarps annual, resupinate, difficult to separate from the substrate, soft corky when fresh, corky upon drying, odor- or tasteless when fresh, up to 8 cm long, 2 cm wide and 1.7 mm thick at center. Pore surface white to cream when fresh, pale brownish when bruised, pinkish buff to clay-buff upon drying; sterile margin very narrow to almost lacking; pores round to angular, 3–4 per mm; dissepiments thick, entire. Subiculum cream, corky, thin, about 0.3 mm thick. Tubes light buff, corky, about 1.4 mm long.

Hyphal structure. Hyphal system trimitic: generative hyphae bearing clamp connections, hyaline, thin-walled, frequently branched; skeletal hyphae dominant, thick-walled to subsolid, hyaline to slightly yellowish, frequently branched; binding hyphae abundant, slightly thick-walled, IKI–, CB+, tissues unchanging in KOH.

Subiculum. Generative hyphae frequent, hyaline, thin-walled, frequently branched, 2.3–3.5 μm in diam; skeletal hyphae dominant, hyaline, distinctly thick-

Figure 10. Basidiocarps of *Haploporus pirongia*. Scale bar: 1.0 cm.

walled with a narrow lumen to subsolid, occasionally branched, interwoven, 2.5–4 μm in diam; binding hyphae abundant, slightly thick-walled,1–2 μm in diam.

Tubes. Generative hyphae frequent, hyaline, thin-walled, frequently branched, 1.7–3.5 μm in diam; skeletal hyphae distinctly thick-walled with a narrow to wide lumen, frequently branched, interwoven, 2.5–4 μm in diam; binding hyphae slightly thick-walled,1–2.5 μm in diam. Cystidia absent; cystidioles present, fusiform, occasionally with an apical simple septum, sometimes with a few small guttules, 21–28 × 5–7 μm. Basidioles dominant, similar in shape to basidia, but slightly smaller, occasionally with a few large guttules; basidia pear-shaped to barrel-shaped with 4-sterigmata and a basal clamp connection, 21–35 × 8–11 μm. Hyphae at dissepiment usually thick-walled with simple septum. Dendrohyphidia absent. Some irregular-shaped crystals present among tube tramal structures.

Spores. Basidiospores oblong-ellipsoid to cylindrical, hyaline, thick-walled, with tuberculate ornamentations, some with a guttule, IKI–, CB+, 11–14(–15) × (4.8–)5.2–7 μm, L = 12.35 μm, W = 6.11 μm, Q = 1.83–2.15 (n = 90/3).

Specimens examined. AUSTRALIA. Victoria, Melbourne, Dandenong Ranges Botanical Garden, on dead branch of *Rhododendron*, 12 May 2018, *Dai 18659*, *18660* & *18661* (MEL, dupl. in BJFC); on dead branch of *Eucalyptus*, 12 May 2018, *Dai 18662* (MEL, dupl. in BJFC). NEW ZEALAND. Omahu Bush, on *Melicytus*, 15 Feb 2010, Cooper (PDD 95714, dupl. in BJFC).

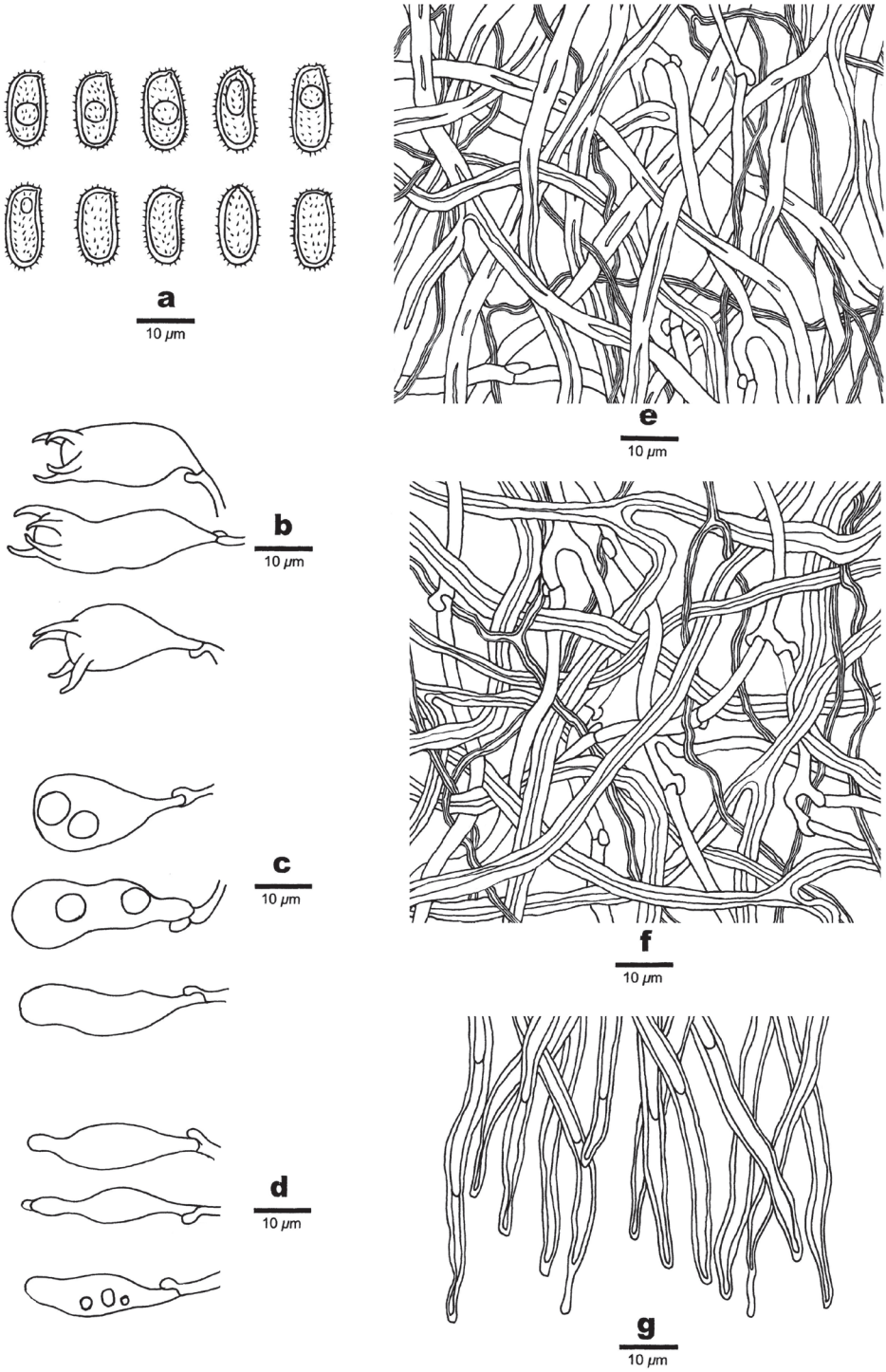

Figure 11. Microscopic structures of *Haploporus pirongia*. **a** Basidiospores **b** Basidia **c** Basidioles **d** Cystidioles **e** Hyphae from subiculum **f** Hyphae from trama **g** Hyphae at dissepiment.

***Haploporus odorus* (Sommerf.) Bondartsev & Singer in Singer, Mycologia 36: 68 (1944)**

=*Haploporus amarus* X.L. Zeng & Y.P. Bai, Acta Mycol. Sin. 12(1): 13 (1993). Holotype: China, Jilin Province, Northeast Normal University, Changchun, NENU, Zeng 1931.

Notes. *Haploporus amarus* was described from NE China (Zeng and Bai 1993). The type was studied, and its morphology is in agreement with that of *H. odorus*.

***Haploporus subtrameteus* (Pilát) Y.C.Dai&Niemelä, in Dai, Niemelä and Kinnunen, *Ann. bot. fenn.* 39(3): 181 (2002)**

=*Pachykytospora wasseri* Zmitr., Malysheva & Spirin, *Ukrainskiy Botanichnyi Zhurnal* 64(1): 42 (2007) Holotypus: Russia, Samara Reg., Stavropol Dist., Zhiguli Nat. Res., Padus avium, 12.09.2006, V.F. Malysheva, E.F. Malysheva, I.V. Zmitrovich, isotypus, LE 214872.

Notes. In our phylogenies (Figs. 1 and 2), *P. wasseri* (Zmitrovich et al. 2007) nested within *H. subtrameteus* clade. In addition, there are not major morphological differences between the two taxa (Zmitrovich et al. 2007).

Discussion

In the ITS-based phylogeny (Fig. 2), *Haploporus angustisporus* is closely related to *H. alabamae and H. nanosporus*. Morphologically, *Haploporus angustisporus* may be confused with *H. alabamae* in having approximately the same basidiospores size (9.5–12.5 × 4–5.5 µm vs. 10–13.5 × 4–5 µm) but *H. alabamae* has a trimitic hyphal system and lacks cystidioles (Gilbertson and Ryvarden 1986–1987). *Haploporus nanosporus* differs from *H. angustisporus* by its smaller pores (9–12 per mm vs. 3–5 per mm), non-dextrinoid skeletal hyphae, and smaller basidiospores (5–6 × 3–4 µm vs. 10–13.5 × 4–5 µm, Piątek 2005).

Haploporus gilbertsonii is closely related to *H. cylindrosporus*, *H. thindii*, *H. nepalensis* and *H. tuberculosus*. However, *Haploporus thindii* differs from *H. gilbertsonii* by its distinctly slimmer basidia (20–37 × 6.5–9.1 µm vs. 21–25 × 10–14 µm) and the absence of cystidioles (Yu et al. 2005). *Haploporus nepalensis* is distinguished by its smaller basidiospores (5.5–11.5 × 4.5–6.5 µm vs. 12–15 × 6–8 µm) and the absence of cystidioles (Piątek 2003). Whereas *Haploporus tuberculosus* is distinguished from *H. gilbertsonii* by its trimitic hyphal system and longer basidia (30–43 × 11–13.5 µm vs. 21–25 × 10–14 µm, Ryvarden and Gilbertson 1994).

The *Haploporus nanosporus* and *H. microsporus* clades are sister clades and *Haploporus nanosporus* is closely related to *H. alabamae* and *H. angustisporus*. *Haploporus* and *H. nanosporus* both have small basidiospores and occurs in tropical ecosystems,and

all other differing in having larger basidiospores. However, *H. nanosporus* differs from *H. microsporus* by the absence of dendrohyphidia at the dissepiments, a trimitic hyphal system and absence of cystidioles (Piątek 2005). In addition, *Haploporus alabamae* differs from *H. microsporus* through a trimitic hyphal system and absence of cystidioles (Gilbertson and Ryvarden 1986–1987). *Haploporus angustisporus* differs from *H. microsporus* by its longer basidiospores (10–13.5 × 4–5 μm vs. 5.3–6.7 × 3–4.1 μm).

In the ITS-LSU based phylogeny (Fig. 1), *Haploporus crassus* is closely related to *H. papyraceus* and *H. subpapyraceus*. However, morphologically *Haploporus papyraceus* differs from *H. crassus* by the presence of dendrohyphidia at the dissepiments, absence of cystidioles and thin-walled basidioles (Ryvarden and Johansen 1980). *Haploporus subpapyraceus* also differs from *H. crassus* in having dextrinoid skeletal hyphae and thin-walled basidioles (Shen et al. 2016).

Haploporus pirongia is related to *H. odorus*, but the latter has a perennial and pileate basidiocarp with strong anise odor, ovoid basidiospores and lacks cystidioles (Niemelä 1971). *Haploporus pirongia* resembles *H. thindii* and *H. subpapyraceus* by sharing resupinate basidiocarps with approximately the same pore size. However, *Haploporus thindii* has a dimitic hyphal structure, lacks cystidioles, and has a distribution in subtropical India and valley of Tibet of China (Natarajan and Kolandavelu 1993, Dai et al. 2007). Moreover, *H. subpapyraceus* has ellipsoid basidiospores (9–12 × 5.5–8 μm, Shen et al. 2016).

Gilbertson and Ryvarden (1987) reported *Haploporus tuberculosus* (as *Pachykytospora tuberculosa*) from the USA, but only in a small region of southern Arizona where it should be "quite common on oaks, especially in Chiricahua Mountains". Locally, we have collected in this region only *H. gilbertsonii* and believe that, in most cases, this species was mistaken for *H. tuberculosus* in Arizona. The presence of *H. tuberculosus* in America is questionable.

Acknowledgements

The research is supported by the National Natural Science Foundation of China (Project No. U1802231). We thank the curator of PDD for making material available on loan, and Shaun Pennycook for advice on the spelling of epithets.

References

Buchanan PK, Ryvarden L (1988) Type studies in the Polyporaceae 18. Species described by GH Cunningham. Mycotaxon 33: 1–38.

Cao Y, Wu SH, Dai YC (2012) Species clarification of the prize medicinal *Ganoderma* mushroom "Lingzhi". Fungal Diversity 56: 49–62. https://doi.org/10.1007/s13225-012-0178-5

Cunningham GH (1947) New Zealand Polyporaceae 1. The genus *Poria*. Bulletin of the New Zealand Department of Industrial Research 72: 1–43.

Cunningham GH (1965) Polyporaceae of New Zealand. Bulletin of the New Zealand Department Scientific and Industrial Research 64: 1–304.

Dai YC (2010) Hymenochaetaceae (Basidiomycota) in China. Fungal Diversity 45: 131–343. https://doi.org/10.1007/s13225-010-0066-9

Dai YC, Cui BK, Liu XY (2010) *Bondarzewia podocarpi*, a new and remarkable polypore from tropical China. Mycologia 102: 881–886. https://doi.org/10.3852/09-050

Dai YC, Kashiwadani H (2009) *Haploporus subtrameteus* (Polyporaceae, Basidiomycota) found in Japan. Mycoscience 50: 452–454. https://doi.org/10.1007/s10267-009-0498-9

Dai YC, Li TH (2002) *Megasporoporia major* (Basidiomycota), a new combination. Mycosystema 21: 519–521.

Dai YC, Niemelä T, Kinnunen J (2002) The polypore genera *Abundisporus* and *Perenniporia* (Basidiomycota) in China, with notes on *Haploporus*. Annales Botanicci Fennici 39: 169–182.

Dai YC, Yu CJ, Wang HC (2007) Polypores from eastern Xizang (Tibet), western China. Annales Botanicci Fennici 44: 135–145.

Darriba D, Taboada GL, Doallo R, Posada D (2012) jModelTest 2: more models, new heuristics and parallel computing. Nature Methods 9: 772. https://doi.org/10.1038/nmeth.2109

Donk MA (1967) Notes on European polypores 2. Persoonia 5: 47–130.

Farris JS, Mari Källersjö, Kluge AG, Bult C (1994) Testing significance of incongruence. Cladistics 10: 315–319. https://doi.org/10.1111/j.1096-0031.1994.tb00181.x

Felsenstein J (1985) Confidence intervals on phylogenetics: An approach using the bootstrap. Evolution 39: 783–791. https://doi.org/10.1111/j.1558-5646.1985.tb00420.x

Gilbertson RL, Ryvarden L (1986–1987) North American polypores 1–2. Fungiflora, Oslo, 1–885.

Hall TA (1999) Bioedit: A user-friendly biological sequence alignment editor and analysis program for Windows 95/98/NT. Nucleic Acids Symposium Series 41: 95–98.

Hattori T, Adhikari MK, Suda T, Doi Y (2002) A list of polypores (Basidiomycotina, Aphyllophorales) collected in Jumla. Nepal. Bulletin of the National Science Museum 28: 27–38.

Li J, Dai YC, Yuan HS (2007) A new species of *Haploporus* (Basidiomycotina) from China. Mycotaxon 99: 181–187.

Lowe JL (1966) Polyporaceae of North America. The genus *Poria*. Technical Bulletin of State University College, Syracuse University Forestry 90: 1–183.

Niemelä T (1971) On Fennoscandian polypores 1. *Haploporus odorus* (Sommerf.) Bond. & Sing. Annales Botanicci Fennici 8: 237–244.

Natarajan K, Kolandavelu K (1993) A new species of *Pachykytospora* Kotl. et Pouz. from india. Cryptogamic Botany 3: 195–196.

Nilsson RH, Tedersoo L, Abarenkov K, Ryberg M, Kristiansson E, Hartmann M, Schoch CL, Nylander JAA, Bergsten J, Porter TM, Jumpponen A, Vaishampayan P, Ovaskainen O, Hallenberg N, Bengtsson-Palme J, Eriksson KM, Larsson KH, Larsson E, Kõljalg U (2012) Five simple guidelines for establishing basic authenticity and reliability of newly generated fungal ITS sequences. MycoKeys 4: 37–63. https://doi.org/10.3897/mycokeys.4.3606

Page RDM (1996) TreeView: Application to display phylogenetic trees on personal computers. Computer Applications in the Biosciences Cabios 12: 357–358.

Petersen JH (1996) Farvekort. The Danish Mycological Society´s colour-chart. Foreningen til Svampekundskabens Fremme, Greve, 1–6.

Piątek M (2003) *Haploporus tuberculosus*, a new polypore genus and species in Belarus, with a new combination in *Haploporus*. Polish Botanical Journal 48: 81–83.

Piątek M (2005) Taxonomic position and world distribution of *Pachykytospora nanospora* (Polyporaceae). Annales Botanicci Fennici 42: 23–25.

Ronquist F, Teslenko M, van der Mark P, Ayres DL, Darling A, Hőhna S, Larget B, Liu L, Suchard MA, Huelsenbeck JP (2012) MrBayes 3.2: Efficient Bayesian phylogenetic inference and model choice across a large model space. Systematic Biology 61: 539–542. https://doi.org/10.1093/sysbio/sys029

Ryvarden L, Gilbertson RL (1994) European polypores. Part 2. Synopsis Fungorum 7: 394–743.

Ryvarden L, Johansen I (1980) A preliminary polypore flora of East Africa. Fungifora. Oslo, 1–636.

Singer R (1944) Notes on taxonomy and nomenclature of the polypores. Mycologia 36: 65–69. https://doi.org/10.2307/3754880

Shen LL, Chen JJ, Wang M, Cui BK (2016) Taxonomy and multi-gene phylogeny of *Haploporus* (Polyporales, Basidiomycota) Mycological Progress 15: 731–742. https://doi.org/10.1007/s11557-016-1203-y

Swofford DL (2002) PAUP*: Phylogenetic analysis using parsimony (*and other methods). Sinauer Associates, Massachusetts.

Thiers B (2018) Index Herbariorum: A global directory of public herbaria and associated staff. New York Botanical Garden's Virtual Herbarium, New York. http://sweetgum.nybg.org/science/ih/

Thompson JD, Gibson TJ, Plewniak F, Jeanmougin F, Higgins DG (1997) The CLUSTAL X windows interface: flexible strategies for multiple sequence alignment aided by quality analysis tools. Nucleic Acids Research 25: 4876–4882. https://doi.org/10.1093/nar/25.24.4876

Vilgalys R, Hester M (1990) Rapid genetic identification and mapping of enzymatically amplified ribosomal DNA from several *Cryptococcus* species. Journal of Bacteriology 172: 4238–4246. https://doi.org/10.1128/jb.172.8.4238-4246.1990

White TJ, Bruns T, Lee S, Taylor J (1990) Amplification and direct sequencing of fungal ribosomal RNA genes for phylogenetics. In: Innis MA, Gefand DH, Sninsky JJ, White JT (Eds) PCR Protocols: A guide to methods and applications (Eds). Academic Press, San Diego, 315–322. https://doi.org/10.1016/B978-0-12-372180-8.50042-1

Yu CJ, Zuo L, Dai YC (2005) Three polypores from Xizang new to China. Fungal Science 20: 61–68.

Zeng XL, Bai YP (1993) The genus *Haploporus* in China. Mycosystema 12: 12–15.

Zhao CL, Chen H, Song J, Cui BK (2015) Phylogeny and taxonomy of the genus *Abundisporus* (Polyporales, Basidiomycota). Mycological Progress 14: 38. https://doi.org/10.1007/s11557-015-1062-y

Zhao CL, Cui BK, Dai YC (2013) New species and phylogeny of *Perenniporia* based on morphological and molecular characters. Fungal Diversity 58: 47–60. https://doi.org/10.1007/s13225-012-0177-6

Zmitrovich IV, Malysheva VF, Spirin WA (2007) A new *Pachykytospora* species (Basidiomycota, Polyporales) from Zhiguli, European Russia. Ukrayins'kyi Botanichnyi Zhurnal 64: 42–46.

MycoKeys 54: 99–133 (2019)
doi: 10.3897/mycokeys.54.35697
http://mycokeys.pensoft.net

RESEARCH ARTICLE

A peer-reviewed open-access journal
MycoKeys
Launched to accelerate biodiversity research

Placement of Triblidiaceae in Rhytismatales and comments on unique ascospore morphologies in Leotiomycetes (Fungi, Ascomycota)

Jason M. Karakehian[1], Luis Quijada[1], Gernot Friebes[2], Joey B. Tanney[3], Donald H. Pfister[1]

1 *Farlow Herbarium of Harvard University, 22 Divinity Avenue, Cambridge, MA, 02138, USA* **2** *Universalmuseum Joanneum, Centre of Natural History, Botany & Mycology, Weinzöttlstraße 16, 8045 Graz, Austria* **3** *Pacific Forestry Centre, Canadian Forest Service, Natural Resources Canada, 506 West Burnside Road, Victoria, BC V8Z 1M5, Canada*

Corresponding author: *Jason M. Karakehian* (jasonkarakehian@gmail.com)

Academic editor: *Thorsten Lumbsch* | Received 23 April 2019 | Accepted 17 May 2019 | Published 18 June 2019

Citation: Karakehian JM, Quijada L, Friebes G, Tanney JB, Pfister DH (2019) Placement of Triblidiaceae in Rhytismatales and comments on unique ascospore morphologies in Leotiomycetes (Fungi, Ascomycota). MycoKeys 54: 99–133. https://doi.org/10.3897/mycokeys.54.35697

Abstract

Triblidiaceae is a family of uncommonly encountered, non-lichenized discomycetes. A recent classification circumscribed the family to include *Triblidium* (4 spp. and 1 subsp.), *Huangshania* (2 spp.) and *Pseudographis* (2 spp. and 1 var.). The apothecia of these fungi are persistent and drought-tolerant; they possess stromatic, highly melanized covering layers that open and close with fluctuations of humidity. Triblidialean fungi occur primarily on the bark of *Quercus*, Pinaceae and Ericaceae, presumably as saprobes. Though the type species of *Huangshania* is from China, these fungi are mostly known from collections originating from Western Hemisphere temperate and boreal forests. The higher-rank classification of triblidialean fungi has been in flux due in part to an overemphasis on ascospore morphology. Muriform ascospores are observed in species of *Triblidium* and in *Pseudographis elatina*. An intense, dark blue/purple ascospore wall reaction in iodine-based reagents is observed in species of *Pseudographis*. These morphologies have led, in part, to these genera being shuffled among unrelated taxa in Hysteriaceae (Dothideomycetes, Hysteriales) and Graphidaceae (Lecanoromycetes, Ostropales). Triblidiaceae has been placed within the monofamilial order Triblidiales (affinity Lecanoromycetes). Here, we demonstrate with a three-gene phylogenetic approach that triblidialean fungi are related to taxa in Rhytismatales (Leotiomycetes). We synonymize Triblidiales under Rhytismatales and emend Triblidiaceae to include *Triblidium* and *Huangshania*, with *Pseudographis* placed within Rhytismataceae. A history of Triblidiaceae is provided along with a description of the emended family. We discuss how the inclusion of triblidialean fungi in Rhytismatales brings some rarely observed or even unique ascospore morphologies to the order and to Leotiomycetes.

Keywords
Convergent evolution, desiccation-tolerant fungi, discomycetes, fungal ecology, systematics, spore morphology, taxonomy

Introduction

In 2015 J.M.K. made a collection of *Triblidium caliciiforme* Rebentisch: Fries during a New Brunswick Museum BiotaNB bioblitz. Our research on this species revealed that it is one of a handful of North American specimens (Magnes 1997; Farr and Rossman 2019; Mushroom Observer 2019; MyCoPortal 2019). Around this time other North American collections were made by J.M.K., J.B.T. and L.Q. of *Pseudographis pinicola* (Nylander) Rehm and *T. caliciiforme.* As we undertook our research G.F. made several collections of various species of *Triblidium* Rebentisch: Fries and one of *Pseudographis elatina* (Acharius) Nylander in Austria. Species in these two genera are more extensively represented in European fungaria (Magnes 1997) than in North America. Our collective morphological observations of these specimens in the living state have provided the impetus to undertake this study of the systematics of Triblidiaceae Rehm as emended by Magnes (1997). For some of these species, the molecular characters that we have generated are the first to be used in research.

Magnes's *Weltmonographie der Triblidiaceae* (1997) is the primary reference for our study. Magnes (1997: 27–28) adopted Eriksson's (1992) circumscription of Triblidiaceae to include three genera: *Triblidium* (4 spp., 1 subsp.), *Pseudographis* Nylander (2 spp., 1 var.) and *Huangshania* O. E. Eriksson (2 spp.). We employ "triblidialean fungi" as a term of convenience to collectively refer to these genera. Magnes's concept of the family is as follows.

Immature apothecia are closed, superficial, pulvinate bodies that open prior to maturity (hemiangiocarpous). In early developmental stages the monolocular centrum consists of paraphysoids that are soon replaced by paraphyses immersed in a gel. The excipulum is stromatic and highly melanized. Asci are elongate-cylindrical, unitunicate, and do not react in iodine-based reagents. Ascus apices are undifferentiated or possess a ± reduced apical ring. The walls of discharged asci are often distinctly transverse-striate or wrinkly. Ascospores are large, elongated and transverse-septate or ellipsoid and muriform, hyaline, and lack a gelatinous sheath. In ascospores of *Pseudographis* species the cell wall reacts opaque dark blue to dark purple in iodine-based reagents (Figs 1, 2). Conidial states are unknown (Magnes 1997: 5, 27).

Eriksson (1992) erected Triblidiales to accommodate Triblidiaceae. Magnes (1997: 5–6) classified the family within Rhytismatales M. E. Barr ex Minter (Leotiomycetes), considering Triblidiales a synonym. Rhytismatales encompasses non-lichenized, saprobic or parasitic to pathogenic fungi. Members of the order typically produce desiccation-tolerant ascomata with heavily melanized stromatic covering layers that close in arid conditions. The "tar-spot" fungus, *Rhytisma acerinum*, a foliar parasite of *Acer* spp., is arguably the most frequently encountered member of the order in Europe and North America; it is the type species of the order.

Triblidialean fungi are associated with plant genera in three families in the Northern Hemisphere: Pinaceae, Ericaceae, and Fagaceae (Magnes 1997: 16). A few collections are known from the Southern Hemisphere on *Nothofagus* (Nothofagaceae) in Chile. They typically inhabit elevated substrates: bark and (more rarely) decorticated wood of living and dead trees. Such substrates represent harsh ecological niches that are exposed to high solar radiation, wind, and extreme fluctuations in humidity and temperature, as well as being nutrient poor (Sherwood 1981: 17, 19). Triblidialean fungi are considered to be saprobes, and Magnes (1997: 28) speculates an endophytic state exists in *Triblidium carestiae* (De Notaris) Rehm and *T. hafellneri* Magnes that grow on dwarf Ericaceae.

Triblidialean fungi are distributed within temperate and boreal forests. They are known primarily from the Northern Hemisphere, from lowland to subalpine elevations, though Magnes (1997: 16–17) cited a paucity of collection data related to actual distribution of these fungi. Many taxa are known from Central and Northern Europe, but the occurrence of these in similar climatic and ecologic regions in North America remains unclear due to limited collections from this continent. Though the centers of distribution of *Rhododendron* and Pinaceae occur in China, triblidialean fungi from this country are only represented by *Huangshania verrucosa* O. E. Eriksson (Magnes 1997: 16–17).

The occurrence of mature, sporulating apothecia of triblidialean fungi are not restricted to a particular season in the Northern Hemisphere. We surveyed collection dates of specimens of *Triblidium* and *Pseudographis* that were studied by Magnes (1997) and observed that collections were made in very nearly every month of the year for both genera. *Huangshania* is known only from type and authentic material of *H. verrucosa* collected in central China in November and from type material only of *H. novae-fundlandiae* (Rehm) Magnes collected in eastern Canada in February. Additionally, our own collections of various *Triblidium* and *Pseudographis* species were made in February to September.

Our primary aim in conducting this research is to evaluate Magnes's (1997) emendation and classification of Triblidiaceae in Rhytismatales using a molecular phylogenetic approach. Our results facilitate a phylogenetically informed interpretation of the unique and distinctive ascomatal morphologies that have led, in part, to such confusion in the classification of these fungi at ordinal and familial ranks. The inclusion of triblidialean fungi in Rhytismatales brings to light instances of ascospore morphologies that are more commonly observed among lichenized and non-lichenized taxa in Lecanoromycetes and Dothideomycetes. We have generated 27 new gene sequences from nine species, some of which represent taxa that have not been previously sampled. This data will enrich future systematic and metagenomic studies.

We conclude our Introduction with a history of Triblidiaceae Rehm sensu Magnes. In Results, we present our three-gene phylogeny, as well as a taxonomic section with an emended taxonomy and a description of Triblidiaceae. We also provide a note including the salient features of *Pseudographis* that is intended to supplement the description of Rhytismataceae Chevallier given by Baral (in Jaklitsch et al. 2016: 192–194). We conclude with a discussion on occurence of triblidialean fungi, their trophic state, and ascospore morphology as related to their ecological significance.

History of Triblidiaceae Rehm

Notes

The following history is adapted and expanded from Magnes (1997: 7–9) who provided a concise table of the various circumscriptions of Triblidiaceae since the origin of the family (p. 9). Throughout, we have adopted the exact spelling of taxa used in the literature under discussion. Regarding Rehm (1887–1896) in particular, it is worth noting that the spelling of the same taxon varies frequently (e.g. "Triblidieae" and "Tryblidieae"). Citations of Rehm (1887–1896) are complicated in that the publication was issued in parts over a number of years; we are using exact publication dates in our citations based on Stafleu and Cowan (1983: 476–478). The current classification of various taxa follows Jaklitsch et al. (2016). We conclude with a summary of Magnes's contribution to the study of the family and some recent findings.

Orthography and etymology

Triblidiaceae is the correct spelling of this family. The name is based on the generic name *Triblidium* and a single species, *T. caliciforme* (Rebentisch 1805: 40). Rehm (1888: 196) provided the following etymologic and orthographic note: "Tryblidium stammt von τρύβλιον, die Schale, und ist demgemäss zu schreiben." The Greek term "τρύβλιον" can be transliterated to *tryblion* (Latin: *tryblium*) (Brown 1956: 244; Stearn 2010: 253–254) and translates to English as *a cup, bowl* (Liddell and Scott 1875: 1664). Fries (1823: 183) used the same Greek word. The Greek suffix *–idium* indicates smallness (Stearn 2010: 296). Article 60.1 and specifically article 60.4 of the current nomenclatural code (Turland et al. 2018) allow for the use of "y" in scientific names though it is foreign to classical Latin. Regardless, Article F.3.2 states that the spelling used in a sanctioning work is treated as conserved. *Triblidium* is used consistently in the sanctioning works by Fries (Article F.3.1) (i.e. Fries 1823: 183, 1828: 130–131, 1832: 193). Rehm (1888: 191) erected Triblidiaceae as "Tryblidiaceae", and it is clear from the etymological note and a correction to replace the suborder name "Triblidieae" with "Tryblideae" on page 99 (Rehm 1896: [1271]) that he intended a consistent orthography that included "y." Regarding the spelling of the epithet, which has been used as *caliciforme* and *caliciiforme*, Rebentisch (1805: 40) stated in the protolog that this *Triblidium* species resembles *Calicium sphaerocephalum*, though it is larger. The correct spelling of the epithet "*caliciiforme*" is thus obtained from the stem of the generic name *Calicium*, to which the connecting vowel *i* is added (Article 60.10 (a and b), ex. 35 in Turland et al. 2018) followed by the neutral suffix *-forme* to indicate similarity in form. Therefore, the correct spelling of this taxon is *Triblidium caliciiforme*.

Rehm's Triblidiaceae and classification

Rehm's higher-rank classification for class Ascomycetes included two orders based on the gross morphology of ascomata: Hysteriaceae and Discomycetes (Rehm 1887–1896). Order Hysteriaceae was characterized by black, membranous to carbonaceous, oblong ascomata that open at maturity by a longitudinal slit (Rehm 1887: 1). These represented

a transition between members of Pyrenomycetes and Discomycetes. The genera included are currently placed in Dothideomycetes, such as *Hysterium*, *Glonium*, and *Acrospermum*, and more disparate fungi currently placed in Leotiomycetes, such as *Hypoderma* and *Lophodermium* (both Rhytismatales). Discomycetes encompassed club-, cup-, dish- and lens-shaped ascomata that support a hymenium that is entirely exposed at maturity (Rehm 1887: 56). Discomycetes was divided into two principal groups: Pezizaceae, with cup-shaped apothecia that initially develop closed but open widely at maturity to reveal a flat hymenium, and Helvellaceae that produces larger, fleshy, stipitate ascomata with a hymenium that is exposed during development (Rehm 1887: 59). Pezizaceae consisted of five suborders: Phacidiaceae, Stictideae, Triblidieae [Tryblidieae], Dermateaceae, and Pezizeae (Rehm 1887: 59–60). According to Rehm, the apothecia of members of suborder Tryblidieae develop within the substrate, becoming erumpent and finally sessile. These are pulvinate and substipitate, with a membranous or horny exterior. At maturity lobes of covering tissue pull away to reveal the disc. Suborder Tryblidieae included Rehm's new families Tryblidiaceae and Heterosphaerieae (containing *Heterosphaeria*, *Odontotrema* and *Scleroderris* [= *Godronia*]), with Tryblidiaceae distinguished by solitary, round to lentiform, black apothecia that open with thick, torn margins. The family included two genera: *Tryblidium* Rebentisch and *Tryblidiopsis* P. Karsten (Rehm 1888: 191).

Regarding *Pseudographis*, Rehm (1888) placed the genus in Discomycetes, suborder Phacidiaceae. This taxon was subdivided into families Pseudophacidieae and Euphacidieae. Species comprising both families produced ascomata that were immersed within the substrate in early development. They differed in that ascomata of Pseudophacidieae species emerged from the surrounding host tissues by splitting them aside and did not remain covered by a thin layer of host cells at maturity. The gross texture of their excipular tissues were membraneous or carbonaceous while those of Euphacidieae were only membranous (e.g. *Phacidium*, *Coccomyces* and *Rhytisma*, among others) (Rehm 1887: 60). Pseudophacidieae included *Pseudographis*, along with *Pseudophacidium*, *Clithris* [= *Colpoma*], *Cryptomyces* (all Leotiomycetes) and *Dothoria* (Dothideomycetes), among others. Rehm treated both *P. elatina* and *P. pinicola*, noting the affinities of these to members of his suborder Tryblidieae, but he retained them in Pseudophacidieae due to differences in development that he perceived (Rehm 1888: 99). However, in his Additions (1896: 1249) Rehm relegated the type species of the genus, *P. elatina*, to synonymy under *Tryblidium melaxanthum*. The complete history of *Pseudographis* is given in Magnes (1997: 62–63).

In a later work Rehm (1904: 522–526) summarized his dealings with certain nomenclatural acts that had confused the circumscription of Triblidiaceae. De Notaris (1847: 15–16) had created a later homonym of *Triblidium* based on *T. hysterinum* Dufour (1828: 321) [= *Rhytidhysteron hysterinum*]. He then created a younger synonym, *Blitridium* (anagram of *Triblidium*), to accommodate *Triblidium caliciiforme* Rebentisch (De Notaris 1864: 374). Saccardo, against the principle of priority, adopted De Notaris's *Triblidium* (Saccardo 1883: 740) and *Blitridium* (Saccardo 1889: 802). Rehm (1888: 196–198), observing the rule of priority, relegated *Blitridium* to synonymy under *Triblidium* Rebentisch. Likewise, he synonymized de Notaris's *Triblidium* under *Tryblidiella* Saccardo (1883) [= *Rhytidhysteron* Spegazzini (1881)] (Rehm 1889: 233).

In his last summarizing work, Rehm (1912: 137–139) treated Triblidiaceae with a revised circumscription to include not just *Tryblidiopsis* and *Tryblidium*, but also *Pseudographis* and *Tryblidiella*. This circumscription followed Höhnel (1909: 73, 1910: 2) who discussed *Tryblidium*, *Tryblidiopsis* and *Pseudographis* and who recognized Tryblidiaceae to contain the former two genera. In Höhnel's opinion, Tryblidiaceae and Pseudophacidiaceae (that contained *Pseudographis*) were sister taxa, as evidenced by their similarities in developing within host tissues and then finally becoming erumpent and sessile at maturity. He perceived that both families were entirely similar in ascomatal structure but that they were not typical Discomycetes due to differences in centrum development and ascomatal dehiscence, thus they formed a transitional link to Dothideaceae (Höhnel 1909: 73). Later, Höhnel (1910: 2) explicitly placed *Pseudographis* within Tryblidiaceae.

Höhnel's widening circumscription of Triblidiaceae

From his observations of the structure of the sterile tissues of apothecia, Höhnel (1918: 145–146, 154) expanded his circumscription of Triblidiaceae beyond *Tryblidium*, *Tryblidiopsis* and *Pseudographis* to include other, unrelated genera: *Crumenula* [= *Crumenulopsis*] (Leotiomycetes, Helotiales), *Melachroia* [= *Podophacidium*] (Leotiomycetes, Helotiales *incertae sedis*) and *Tryblidiella* [containing *Rhytidhysteron* (as *Rhytidhysterium*)]. In a posthumously published paper, Höhnel (1924: 68, 70) elaborated on the structure of the apothecial tissues that he considered to hold taxonomic significance, namely the hypothecium (medullary excipulum) that he described as thick and composed of "thick-walled, cartilaginous, densely plectenchymatic intertwined hyphae." He then expanded Triblidiaceae to encompass yet more unrelated genera including: *Asterocalyx* (Leotiomycetes, Helotiales *incertae sedis*), *Tympanis* (Leotiomycetes, Phacidiales, Tympanidaceae), *Godronia* (Leotiomycetes, Helotiales, Godroniaceae), *Scleroderris* [= *Godronia*] and *Cenangium* (Leotiomycetes, Helotiales, Cenangiaceae).

Nannfeldt's treatment

Nannfeldt (1932: 312, 331) did not conduct an in-depth study of *Tryblidium* due to a lack of sufficient material and treated the genus only briefly. He made no recommendations regarding its classification apart from noting that the apothecial structure indicated a close relationship to Helotiales and their similarities with *Tryblidiopsis* and *Heterosphaeria*. Nannfeldt commented that the muriform ascospores of *Tryblidium* were unique in Helotiales. He considered *Pseudographis* to be a link between Discomycetes and apothecial lichens and placed this genus in Lecanorales due to the epithecium and asci that he interpreted as thick-walled.

Sherwood and Hawksworth's classification

Hawksworth and Sherwood (1982: 264) commented on the relationship between Odontotremataceae and Triblidiaceae. Odontotremataceae are minute saprobic or lichenicolous inoperculate discomycetes, often with melanized excipular tissues and dentate margins, and with iodine-negative asci with thickened apices that are pierced by

a pore. The authors noted that the asci of Triblidiaceae and Graphidaceae (Ostropales) also share this feature. Furthermore, the "reddish-purple" reaction of *Pseudographis* ascospores in iodine reagents suggested affinities between Triblidiaceae and Graphidales [= Ostropales]. They circumscribed Triblidiaceae to include *Pseudographis* and *Triblidium*, but removed *Tryblidiopsis* to Rhytismatales. Thus, Triblidiaceae was placed within Ostropales (Hawksworth et al. 1983: 273–274; Sherwood-Pike 1987: 139, 141).

Hawksworth and Sherwood's (1982: 264) aforementioned observation regarding ascus morphology in Triblidiaceae was discussed by Eriksson (1992: 6–7) who commented that younger asci generally appear to have thicker walls than those that are mature because they are not fully extended and turgid. This is a developmental rather than a taxonomic character, in contrast to the mature asci of true ostropalean fungi wherein the apices are actually thickened. Furthermore, Hawksworth and Sherwood were almost certainly basing their statements on observations made from preserved material, wherein all of the asci are dead and would show thickened walls, a phenomenon comprehensively reviewed by Baral (1992: 351–352, figs 6–10).

Magnes (1997: 8–9) observed that Hawksworth and Sherwood (1982) did not comment on the type of interascal filaments (paraphysoids/paraphyses) in Triblidiaceae. He concluded that as the authors considered the family to be closely related to Odontotremataceae (that have paraphyses only), they must have regarded the interascal filaments of Triblidiaceae as paraphyses.

Eriksson describes *Huangshania* and classification of Triblidiaceae in Triblidiales

Eriksson (1992) addressed the relationships of Triblidiaceae in the course of describing *Huangshania*. His circumscription of the family followed that of Hawksworth and Sherwood (1982) with the addition of *Huangshania* to *Triblidium* and *Pseudographis*. He noted that similarities in ascomatal structure across the three genera indicated a natural group. Eriksson and Hawksworth (1991: 44) maintained Triblidiaceae within Graphidales with uncertainty. However, with his newly circumscribed family, Eriksson revaluated this classification. He considered a number of orders belonging to three classes that possessed apothecioid ascomata and angiocarpous/hemiangiocarpous modes of development in which to place Triblidiaceae. One group of orders consisted of primarily lichenized taxa in Lecanoromycetes: Graphidales [= Ostropales], Gyalectales [= Ostropales] and Peltigerales. Another group consisted of primarily non-lichenized taxa in Leotiomycetes: Lahmiales, Leotiales, and Rhytismatales. The final order, Patellariales, consist of bitunicate, non-lichenized, apothecioid taxa in Dothideomycetes (Eriksson 1992: 8–9; Jaklitsch et al. 2016). Eriksson considered that *Graphis*, the type genus of Graphidales, shared a morphological character with *Pseudographis* in ascospores that turn blue in iodine reagents. However, *Graphis* species differed from those of *Triblidium* in thicker walled asci with thickened apices and well-differentiated pore structures. Eriksson considered Triblidiaceae to have affinities with members of Graphidales, but the family differed in ascus wall structure and centrum morphology. Therefore, it was prudent to erect a separate order: Triblidiales. This would have the added benefit of maintaining a more homogenous circumscription of Graphidales (Eriksson 1992: 8–9).

Triblidiaceae Rehm sensu Magnes

Based on Rehm's (1912) circumscription, Magnes (1997) comprehensively revised Triblidiaceae. We found only four names involving *Triblidium* and *Pseudographis* that he did not treat. He described two new species of *Triblidium* and a variety of *P. elatina*. Species excluded from Triblidiaceae were assigned to 22 genera belonging to seven orders (Magnes 1997: 5–6).

Magnes's circumscription of Triblidiaceae followed Eriksson's (1992). Eriksson had rejected placing Triblidiaceae in Rhytismatales because he considered paraphysoids not to be present in this order, though he noted similarities in ascus structure (Eriksson 1992: 9). Magnes claimed that paraphysoids were in fact present in certain genera of Rhytismataceae. He cited literature and noted his own observations of these structures in *Tryblidiopsis pinastri*. Therefore, based on similarities in ascomatal development and ascus structures, he hypothesized that Triblidiaceae formed an isolated group within Rhytismatales and classified the family within this order, relegating Triblidiales to synonymy. Furthermore, Magnes (1997: 17) suggested a close relationship between Triblidiaceae and Rhytismataceae, particularly with members of *Coccomyces* (citing Sherwood 1980). He rejected a close relationship between Triblidiaceae and Graphidaceae due to differences in spore wall development (citing Sherwood 1977: 12, fig. 2) and different ascus structures.

A molecular phylogeny of Rhytismatales

Important research in the systematics of Rhytismatales was conducted by Lantz et al. (2011). They elucidated a core clade of Rhytismatales sensu stricto, and demonstrated that ascoma and spore shape, characters used in traditional morphology-based delimitation of genera, were generally unreliable. However, the authors noted that these could be useful in some cases, when combined with other characters (p. 57). Notably, two strongly supported clades were observed in their two-gene molecular phylogeny that included 91 species. The clades were informally termed "radiate" and "bilateral." The radiate clade encompassed species that produce circular ascomata opening in a radiate fashion to form tooth-like processes to expose the disk, versus species that produce hysterioid or otherwise elongated ascomata that open in a bilateral fashion along a single, longitudinal slit.

Materials and methods

Specimens

Collection methods and handling of fresh specimens

Triblidialean fungi are best collected in humid weather as the disc is exposed, making apothecia more visible. Alternatively, dry ascomata can be sprayed with tap water. Specimens of triblidialean fungi were placed in paper bags, allowed to air-dry, and stored in a cool, dry location in the laboratory. Specimens may remain alive and capable of sporulation when rehydrated up to a month or possibly more after collection. Although asci may not discharge after this time, ascospores may remain viable within asci for a lengthy period.

Fungarium specimens
Because specimens of triblidialean fungi are often small, only two apothecia were removed from any given specimen: one for morphological analysis and the other for DNA extraction. In particular cases, we used only one apothecium for both of these purposes.

Morphological data collection

Macrophotography of ascomata
Samples of substratum bearing apothecia were hydrated with a spray bottle containing tap water. Macrophotographs were made in the laboratory with a Canon EOS 60d digital SLR camera mounted to a height-adjustable camera support mounted on a table. Macrolenses included either a Canon EF-S 60 mm or a Canon MP-E 65 mm with an attachable ring light. Subjects were photographed against dark-gray or black matboard.

Microphotography and analysis of digital microphotographs
We employed a laboratory-dedicated Olympus SZX9 stereomicroscope or an Olympus BX40 compound light microscope with an Olympus XC50 5.0 megapixel digital camera and Olympus cellSens Standard 1.14 image processing software, calibrated to these optical devices. Austrian specimens collected and studied by G.F. were examined using an Olympus SZX10 stereomicroscope and an Olympus BX51 compound light microscope. Images and data were gathered with an Olympus DP72 digital camera and measurements were made with an eyepiece reticle or with Olympus cellSens Dimension software.

Mounting media, stains and reagents for compound light microscopy
In all cases, tap water was used as a mounting medium. Material for crush-mounts or sectioning was wetted in dilute ammonia or in 70% ethanol and then rehydrated in tap water. Ammoniacal or SDS Congo red were used to stain cell walls. Cresyl blue, phloxine, cotton blue in lactophenol, and Lugol's and Melzer's iodine reagents were used to stain cell contents. Living cells were stained with cresyl blue or dilute Lugol's. Three-percent potassium hydroxide (KOH) was used as a mountant in crush mount or section preparations in order to facilitate separation of cells. This reagent was also used to pretreat asci for subsequent treatment with Lugol's and Melzer's. Analysis of living and dead cells, as well as the use of various mounting media and iodine-based reagents in fungal taxonomy, follows Baral (1987, 1992), Largent et al. (1977) and Leonard (2006).

Observations of living, mature ascospores
These were studied from ascospore deposits and from hand-sections or squash mounts. Ascospores obtained from deposits may show a large variation in size. For this reason, we also measured mature-looking ascospores still inside asci and noted the number of ascospores per ascus. Ascospore deposits were obtained by placing a cover-glass over sufficiently hydrated apothecia in a Petri dish lined with moist filter paper and sealed with Parafilm. The progress of ascospore accumulation was monitored under high magnification with a stereomicroscope by focusing down onto the undersurface of the

cover-glass. Ejected ascospores appear as small, gem-like, shining bodies suspended in small droplets of condensation. After a period of one hour to overnight, the cover-glasses were carefully removed with forceps and gently placed on a small droplet of tap water or other reagent on a microscope slide.

Structure and tissues of apothecia

In addition to crush-mounts of various apothecial tissues, we prepared longitudinal sections of apothecia by hand-sectioning or by using a freezing stage microtome. Hand-sections were prepared from hydrated specimens under magnification with a stereomicroscope. One-half of a double-sided razor was repeatedly drawn across the median area of an apothecium. Use of a freezing stage microtome allowed uniformity in thickness. Material sectioned in this way is dead. Pieces of substratum supporting an apothecium were hydrated, soaked in a solution of dilute gum arabic, and oriented on an electric, water-cooled freezing stage (Physitemp BFS-5MP) mounted to a sliding microtome. Additional dilute gum arabic matrix was then added to completely envelop and support the tissue during sectioning. Sections were cut to approximately 15–25 μm and were removed from the blade with a fine-point paintbrush to water on a microscope slide. Sections of apothecia that were more or less the greatest width were representative of the middle of the apothecium. These were preferred for light microscopy. The remaining sections were air-dried and placed in a microscope slide packet to be kept with the specimen. This technique is outlined in Dring (1971: 103–105), Gray (1954: 157–160) and Sass (1958: 93–94). Sections made in this way greatly facilitate histologic analysis and yield publication-quality microphotographs. Furthermore, this technique follows Sherwood (1977, 1980) for ostropalean and rhytismatalean fungi. Analysis and descriptions of apothecial structure and fungal tissue type designations follow Korf (1973).

Cultures

Culture media

Difco potato dextrose agar (PDA) and Difco malt extract agar (MEA) were used to cultivate mycelium for DNA extraction. These media were prepared according to the manufacturer's instructions with deionized water and autoclaved for 15 m (121 °C, 19 psi), cooled, and poured into 60 × 15 mm polystyrene Petri dishes in a laminar flow hood.

Inoculation of media

Polysporous cultures were established by means of ascospore deposition directly onto PDA or MEA. A piece of substratum bearing 1–3 air-dried apothecia was excised from the sample under a stereomicroscope. It is important to not rehydrate air-dried specimens prior to this step as discharged ascospores may be lost. This is especially important in tribidialean fungi with large ascospores, and where a small number of mature asci are present. Care was taken to cut only around these apothecia and to not include any other sporo-

mata that may be incidentally present. The apothecia were then placed on a small piece of well-dampened filter paper. A Petri dish with PDA or MEA was inverted so that the surface of the media faced down. The bottom of the dish was tilted up slightly and, using forceps, the hydrated paper and apothecia were carefully inserted and placed on the inner surface of the lid. The dish was wrapped in Parafilm. A circle was drawn in alcohol-soluble marker on the bottom of the dish over the apothecia. This served to demarcate where the ascospores should land on the media. The progress of the ascospore print was checked every hour under a stereomicroscope as described above. When sufficient ascospores had accumulated, the paper and apothecia were carefully removed and the plate resealed with Parafilm. The apothecia were dried and placed in a small, appropriately labeled packet so that they might be reexamined if necessary. The surface of the inoculated media was checked daily for 7 days to monitor ascospore germination and growth of any fungal or bacterial contaminants. As PDA and MEA are transparent, this was accomplished by placing the inverted Petri dish on a compound light microscope stage and scanning with the 4× and 10× objectives. Cultures were stored in an incubator at 22 °C in darkness.

Phylogenetic analysis

Sampling

We sampled approximately 100 mg of living mycelium from pure cultures. These samples were stored at −80 °C until DNA extraction was performed. Since apothecia of triblidialean fungi in fungarium specimens are typically sparse, only one or one-half of an apothecium was removed from any given specimen for DNA extraction.

DNA extraction

Samples from pure cultures were processed using Qiagen (Germantown, Maryland) DNeasy Plant Mini Kit according to manufacturer protocols. Fungarium specimens were processed using Qiagen QIAmp DNA Micro Kit according to manufacturer protocols with a 12–24 hour cell-lysis period in an agitating hybridization oven set to 56 °C.

DNA amplification and sequencing

Undiluted DNA extracts, as well as 1/10 and 1/100 dilutions were used as templates. Polymerase chain reaction (PCR) amplification of ribosomal DNA (rDNA) included the nuclear internal transcribed spacer region (ITS) that is composed of the non-coding regions ITS1 and ITS2 that flank the gene encoding the 5.8S subunit, the nuclear large subunit (LSU), and the mitochondrial small subunit (mtSSU). The choice of gene regions for PCR followed Lantz et al. (2011) with the inclusion of the ITS region (Schoch et al. 2012). Primers for ITS included ITS1F (Gardes and Bruns 1993) and ITS4 (White et al. 1990). For recalcitrant isolates or those extracted from old specimens, internal primers ITS2 and ITS3 (White et al. 1990) were employed to target shorter ITS fragments for amplification. Primers for mtSSU

were mrSSU1, mrSSU2, mrSSU2R and mrSSU3R (Zoller et al. 1999). Primers for LSU were LR0R: 5'– ACCCGCTGAACTTAAGC–3' and LR3R: 5'– GTCTTGAAACACGGACC–3' (Vilgalys 2018), LR3 and LR6 (Vilgalys and Hester 1990). For each PCR reaction (25 µL) we used Lucigen (Middleton, Wisconsin) EconoTaq polymerase and EconoTaq 10x buffer. Each reaction mix was composed as follows: 0.125 µL polymerase, 1.25 µL 10 mM of each primer pair, 0.5 µL 10 mM dNTP, 2.5 µL buffer, 1.25 µL dimethyl sulfoxide (DMSO), 1.25 µL 1% bovine serum albumin (BSA), 11.875 µL dH20 and 5 µL DNA template in solution. The addition of BSA and DMSO followed Farell and Alexandre (2012). The optimum annealing temperature (T_a) in °C for each primer pair was determined using IDT (Coralville, Iowa) OligoAnalyzer (IDT 2019). The sequence of one primer is analyzed at a time and the following concentration parameters for the reaction mix listed above are also entered: oligonucleotide: 0.5 µM; Na+: 50 mM; Mg++: 1.5 mM; dNTP: 0.2 mM. The T_a was obtained by subtracting 5 °C from the lowest melting temperature of the two primers. Thermocycler PCR profiles are as follows: for ITS, initial denaturing at 95 °C for 2 min followed by 35 cycles of denaturing at 95 °C for 1 min, annealing at (T_a) for 1 min and extension at 72 °C for 45 sec, with a final extension step of 72 °C for 10 min; for LSU, initial denaturing at 94 °C for 2 min followed by 40 cycles of denaturing at 94 °C for 1 min, annealing at (T_a) for 1 min and extension at 72 °C for 1:30 min with a final extension step of 72 °C for 7 min; for mtSSU, initial denaturing at 94 °C for 3 min followed by 40 cycles of denaturing at 94 °C for 1 min, annealing at (T_a) for 1 min and extension at 72 °C for 1 min with a final extension step of 72 °C for 7 min. PCR products were visualized via gel electrophoresis using 1% gel agarose, stained with Biotium (Fremont, California) GelRed nucleic acid stain and visualized with UV light. PCR product cleanup, sequencing reactions and Sanger sequencing were performed by GENEWIZ sequencing service (Cambridge, Massachusetts) using the same primer pairs as in the PCR reactions. When necessary, PCR products were purified with New England BioLabs (Ipswich, Massachusetts) Monarch PCR & DNA Cleanup Kit (5 µg) or Qiagen QIAquick Gel Extraction Kit using Biotium GelGreen nucleic acid stain.

Handling sequence data

Sequences were edited in Geneious (v. 6.1.7) (Kearse et al. 2012) or Sequencher 5.1 (Sequencher 2012). A BLASTn (Altschul et al. 1990) search was used to verify the sequence as originating from the intended organism and to identify closely related sequences for inclusion into the dataset as a subject. Sequences were accessioned into GenBank (Clark et al. 2015) citing the respective collection numbers from which they originated. These GenBank accession numbers are listed in Table 1 along with additional sequences downloaded from GenBank that were combined into the dataset. A footnote providing information on the origin and other pertinent information is provided for each of these sequences.

Table 1. Specimens used in this study with family, order, voucher/strain number and GenBank accession numbers. New sequences of *Triblidium*, *Huangshania* and *Pseudographis* are indicated in bold.

Order	Family	Species	Voucher or strain	ITS	LSU	mtSSU
Geoglossales	Geoglossaceae	*Trichoglossum hirsutum*	AFTOL-ID 64	DQ491494	AY544653	AY544758
Cyttariales	Cyttariaceae	*Cyttaria darwinii*	Isolate 57	NA	EU107206	EU107235
		Cyattaria hariotii	Isolate 55	NA	EU107218	EU107246
		Cyttaria exigua	Isolate 77	NA	EU107214	EU107240
Erysiphales	Erysiphaceae	*Blumeria graminis*	?	AB000935	AB022362	NA
		Arthrocladiella mougeotii	?	AF073358	AB022379	NA
Helotiales	Helotiaceae	*Cudoniella clavus*	AFTOL-ID 166	DQ491502	DQ470944	FJ713604
	Lachnaceae	*Erioscyphella abnormis*	KUS F52080 (7)	JN033395	JN086698	JN086772
Leotiales	Leotiaceae	*Leotia lubrica*	AFTOL-ID 1253	DQ491484	AY544644	AY544746
		Microglossum olivaceum	FH-DSH97-103	AY789398	AY789397	NA
		Microglossum viride	SAV 10249	KC595263	KC595264	NA
Medeolariales	Medeolariaceae	*Medeolaria farlowii*	DHP # 07-637	GQ406809	GQ406807	NA
Phacidiales	Phacidiaceae	*Phacidium lacerum*	AFTOL-ID 1253	KJ663841	DQ470976	FJ190623
		Pseudophacidium ledi	Lantz 366 (UPS)	NA	HM140563	HM14383
		Potebniamyces pyri	S001	DQ491510	DQ470949	NA
Rhytismatales	Cudoniaceae	*Spathularia flavida* 1	KUS-F52331	JN033405	JN086708	JN086781
		Spathularia flavida 2	CBS 399.52	NA	AY541496	AY575101
		Cudonia confusa	M. Carbone 312	KC833165	KC833216	NA
		Cudonia circinans	Lantz & Widén 402 (UPS)	EU784190	HM140551	HM143791
	Rhytismataceae	*Coccomyces dentatus*	OSC 100021	DQ491499	AY544657	AY544736
		Coccomyces leptideus	Lantz 393 (UPS)	NA	HM140506	HM143783
		Hypoderma cordylines	?	JF683420	HM140521	HM143795
		Hypoderma rubi	ICMP 17339	JF683419	HM140526	HM143801
		Hypohelion scirpinum	Lantz 394 (UPS)	NA	HM140531	HM143806
		Lophodermium eucalypti	ICMP 16796	EF191235	HM140541	HM143817
		Rhytisma acerinum	?	GQ253100	FJ495190	HM143837
	Marthamycetaceae	*Marthamyces quadrifidus*	ICMP: 18329	NA	HM140559	HM143832
		Propolis farinosa	ICMP 17354 (8)	MH682229	HM140562	MH698451
		Cyclaneusma minus	CBS 496.73	NR153910	FJ176868	FJ190629
		Mellitiosporium versicolor	Lantz 357 (UPS)	NA	HM140560	NA
		Naemacyclus culmigenus	TNS: F-41728	AB745435	AB745437	AB745436
Thelebolales	Thelebolaceae	*Thelebolus globosus*	AFTOL-ID 5016	NA	FJ176905	FJ190662
		Thelebolus ellipsoideus	AFTOL-ID 5005	NA	FJ176895	FJ190657
Chaetomellales	Chaetomellaceae	*Chaetomella oblonga*	CBS 110.76	AY487082	AY487083	NA
		Pilidium acerinum	CBS 736.68	NR119500	AY487092	NA
		Xeropilidium dennisii	TU104501	LT158441	KX090824	NA
Rhytismatales	Triblidiaceae	***Huangshania verrucosa***	UME-29336a	MK751793	MK751802	MK751716
		Triblidium caliciiforme	FH-15071105	MK751797	MK751806	MK751720
		Triblidium caliciiforme	CUP-18080101	MK751798	MK751807	MK751721
		Triblidium caliciiforme	E-00012551	MK751799	MK751808	MK751722
		Triblidium caliciiforme	E-00905002	MK751800	MK751809	MK751723
		Triblidium caliciiforme	GJO-0088904	MK751801	MK751810	MK751724
	Rhytismataceae	***Pseudographis elatina***	GJO-0090016	MK751794	MK751803	MK751717
		Pseudographis elatina	NCBI:txid1695903	Genome	Genome	Genome
		Pseudographis pinicola	FH-18061706	MK751795	MK751804	MK751718
		Pseudographis pinicola	FH-NB842	MK751796	MK751805	MK751719

Phylogenetic analysis

We performed the phylogenetic analysis using three different DNA regions (ITS, LSU, mtSSU) from representative species of the Leotiomycete orders Cyttariales, Erysiphales, Helotiales, Leotiales, Marthamycetales, Medeolariales, Phacidiales, Rhytismatales, Thelebolales and Chaetomellales, with Geoglossales as an outgroup. We generated 27 new sequences including three genera: *Triblidium*, *Pseudographis*, and *Huangshania*. For information about the taxa sampling see Table 1. The sequences were aligned using the L-INS-i algorithm for the ITS region, and G-INS-i algorithm for mtSSU and LSU (Katoh and Toh 2008) with MAFFT v. 7.017 (Katoh et al. 2002). The Gblocks program v. 0.91b (Castresana 2000) was used to identify and eliminate ambiguously aligned regions, using the following relaxed settings (Talavera and Castresana 2007): minimum number of sequences for a conserved or flanking position = 24; maximum number of contiguous non-conserved position = 10; minimum length of a block = 5; and gaps in an alignment column allowed in up to half the number of included sequences. The analyses were performed using the optimal model of nucleotide substitution identified with JModeltest (Posada 2008), based on the Akaike information criterion (Akaike 1974). Maximum likelihood (ML) and Bayesian Inference (BI) analyses were performed using Geneious v. 6.1.7. (Kearse et al. 2012). Bayesian inference analyses followed Quijada et al. (2014), only varying in the number of starting trees (10 million generations) and the tree sampling (every 1000th generation) for BI analysis. Branch support in ML was inferred from 1000 rounds of bootstrap (BS) replicates. We only considered supported clades for ML those with bootstraps values ≥75% and with posterior probability (PP) values ≥0.95 (strongly supported) for BI. Phylogenetics trees were drawn with Geneious and artwork was prepared in Adobe Illustrator CS5.

Results

Results from phylogenetic analyses of combined ITS, LSU and mtSSU DNA sequences are presented in Figure 3. Relationships among Leotiomycetes were investigated using three gene regions of 46 taxa that include 39 species in 30 genera, 13 families and 10 orders. The final alignment used for phylogenetic analysis contained 2229 bp (60% of the first alignment length), with 1280 variable and 908 parsimony-informative positions. The analyses identified 13 clades corresponding to 13 families and 10 orders of Leotiomycetes (Fig. 3). Rhytismatales (Fig. 3, clade F) contains eight important clades denoted by letters A–E and G–I. Rhytismataceae is polyphyletic (Fig. 3, clades C and H). Some species of *Coccomyces* and *Hypohelion* form a supported clade (Fig. 3, clade C: 100% MLBS, 0.99 BIPP) that corresponds to the radiate clade in Lantz et al. (2011). Within the radiate clade is a supported clade for Triblidiaceae, with *Huangshania* forming a lineage with *Triblidium* (Fig. 3, clade A: 100% MLBS, 1.00 BIPP). On the other hand, the two species of *Pseudographis* (*P. elatina* and *P. pinicola*) are in one supported clade (Fig. 3, clade H: 100% MLBS, 1.00 BIPP) distantly related

to *Triblidium*. *Pseudographis* groups with other species in the bilateral clade (Lantz et al. 2011). This supported clade is represented here by some species of three different genera (*Hyphoderma*, *Lophodermium*, *Rhytisma*) (Fig. 3, clade G: 100% BIPP, 90.7 MLBS), notably containing the type species of Rhytismataceae, *R. acerinum*. The clade representing Cudoniaceae (Fig. 3, clade E) is sister to the radiate clade (Fig. 3, clade B) containing Triblidiaceae and certain members of Rhytismataceae.

Taxonomy

Triblidiaceae Rehm, Rabenh. Krypt.-Fl. ed. 2 (Leipzig), Band 1, Abth. 3: 191 (1888) emend. Karakehian
Figs 1, 3, clade A

Type genus. *Triblidium* Rebentisch: Fries, Index pl. berol.: 40 (1805); Syst. mycol. [Index]: 193 (1832).

Included genera. *Triblidium* and *Huangshania*.

Position in classification. Triblidiaceae, Rhytismatales, Leotiomycetes, Pezizomycotina, Ascomycota.

Description of Triblidiaceae. Ascomata apothecia, scattered or in small clusters, primarily on bark of living or dead trees but occasionally also on decorticated wood, substratum not visibly degraded, without dark zone lines (Fig. 1a, b, e–g); primordia developing within the substratum, gradually emerging becoming superficial; young apothecia closed, pulvinate; excipulum stromatic and highly melanized (Fig. 1c, m), surface appearing dark brown-black, highly sculptured with coarse, polygonal areolae or ± cracked (Fig. 1a, b, f, g); in early developmental stages the monolocular centrum consists of paraphysoids (cf. Eriksson 1992: 5, fig. 5) that are replaced by paraphyses; apothecia rupturing the covering layer before full maturity (hemiangiocarpous) by several radial cracks, opening in humid conditions and closing when dry (Fig. 1a, b, f, g), persistent; approximately 0.6–1 mm high and 1–3 mm diameter; disk generally pale gray or brown or pale orange in some species (Fig. 1b, g). **Asci** elongate-cylindrical; apices ± hemispherical, undifferentiated, thin-walled, iodine negative (Fig. 1k, l, n, o), dehiscence via apical rupture; dehisced asci often with fine, transverse striations (Fig. 1u); spore number variable, generally 4–8 (Fig. 1c, d, n). **Paraphyses** narrow, filiform, apices flexuous, sparingly branched, hyaline, embedded in gel, lacking pigmented epithecium/exudate. **Ascospores** large, hyaline, ellipsoid to oblong-ellipsoid, muriform, smooth (*Triblidium*) or elongate-fusiform, transversely septate, smooth (in *H. novae-fundlandiae*) or coarsely verrucose (in *H. verrucosa*), iodine negative, appearing thick-walled when dead, lacking a gelatinous sheath (Fig. 1h–j, p–t). **Anamorph** unknown. **Trophic status**: presumed saprobes on woody plant hosts in Fagaceae, Ericaceae and Pinaceae. **Distribution**: mostly known from Northern Hemisphere, boreal and temperate forests (emended from Magnes 1997).

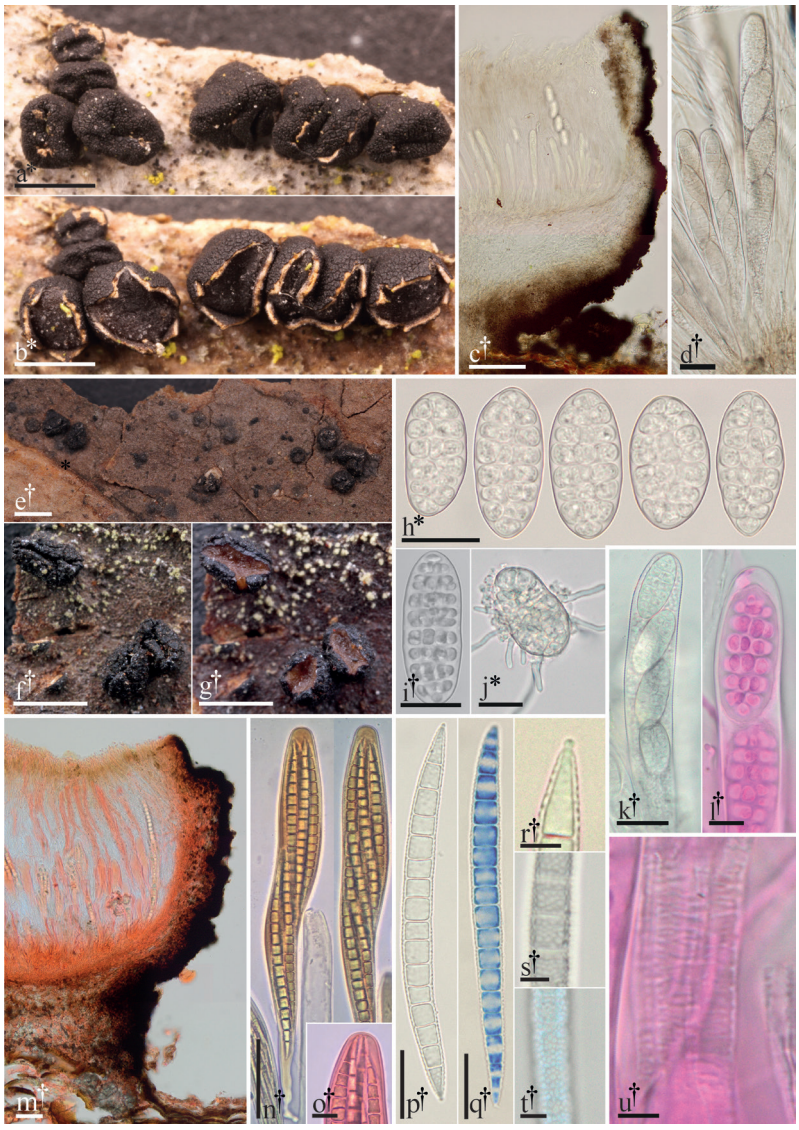

Figure 1. Morphological features of Triblidiaceae. **a–d, h–l, u** *Triblidium caliciiforme* **a** dried apothecia on bark **b** same apothecia hydrated **c** 15 µm thick longitudinal section **d** dead asci containing living ascospores **h–i** ascospores **j** germinating ascospore **k** dead ascus containing living ascospores, detailing the apex **l** ascus detailing the apex (phl) **u** fine transverse striations of dehisced ascus (phl). **e–g, m–t** *Huangshania verrucosa* **e** habit of apothecia on bark (dried) **f** detail of dried apothecia **g** detail of same apothecia hydrated **m** 15 µm thick longitudinal section in (Cr) **n** asci (KOH & Mlz) **o** detail of ascus apex (Cr) **p** ascospore **q** ascospore (cb/l) **r** detail of plug-like structure in a terminal cell of an ascospore **s–t** detail of verrucose ascospore surface (t in cb/l). All microphotographs of cells and tissues mounted in water unless otherwise noted: Congo red (Cr), cotton blue in lactophenol (cb/l), Melzer's reagent (Mlz), phloxine (phl), potassium hydroxide (KOH). † = dead, * = living. Scale bars: 1 mm (**a–b, e–g**); 50 µm (**c, m–n**); 20 µm (**h–k, p–q**); 10 µm (**l, o**); 5 µm (**r–u**). Specimens photographed: *T. caliciiforme*: **a–b, d, j** GJO-0088904; **i** FH-15071105; **c, h, k–l, u** CUP-18080101; *H. verrucosa*: UME-29336a.

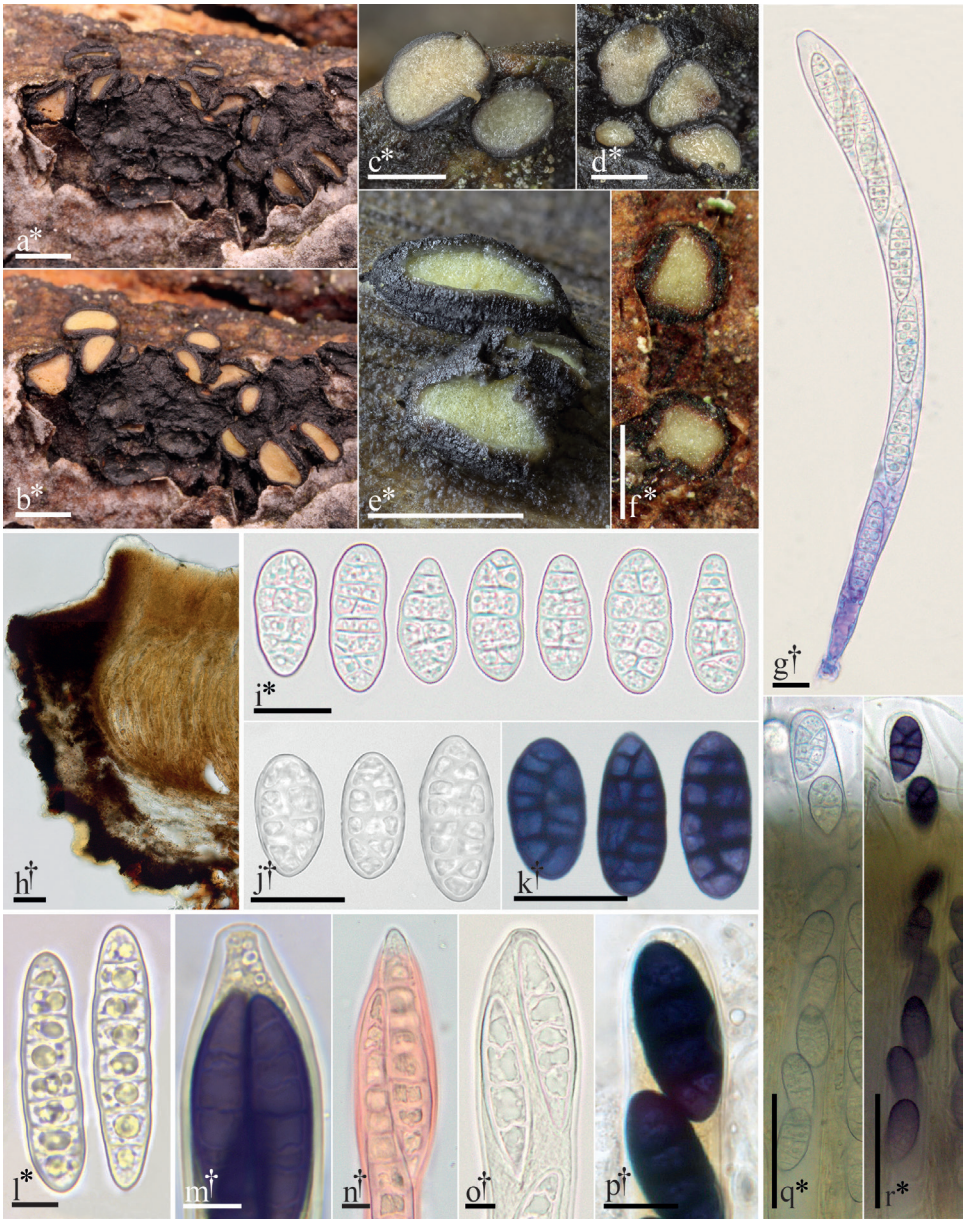

Figure 2. Morphological features of *Pseudographis*. **a–e, g, l–o** *Pseudographis pinicola* **a** dried apothecia on bark **b** same apothecia hydrated **c–e** hydrated apothecia **g** dead ascus containing living ascospores (cb), **l** ascospores **m** ascus containing mature ascospores, detail of apex (in dilute L) **n** ascospore emerging from ascus apex (Cr) **o** ascus apex. **f, h–k, p–r** *Pseudographis elatina* **f** hydrated ascomata **h** 15 µm thick longitudinal section **i–j** ascospores **k** ascospores (in dilute L) **p** detail of ascus apex (L) **q** turgid ascus **r** same ascus (in dilute L). All microphotographs of cells and tissues mounted in water unless otherwise noted: cresyl blue (cb), Congo red (Cr), Lugol's solution (L). † = dead, * = living. Scale bars: 1 mm (**a–f**); 50 µm (**h, q–r**); 20 µm (**i–k**); 10 µm (**g, n–p**); 5 µm (**l–m**). Specimens photographed: *P. pinicola*: **a–b, g, l–o**, FH-18061706; **c–e** courtesy of Adam Polhorský; *P. elatina*: GJO-0090016.

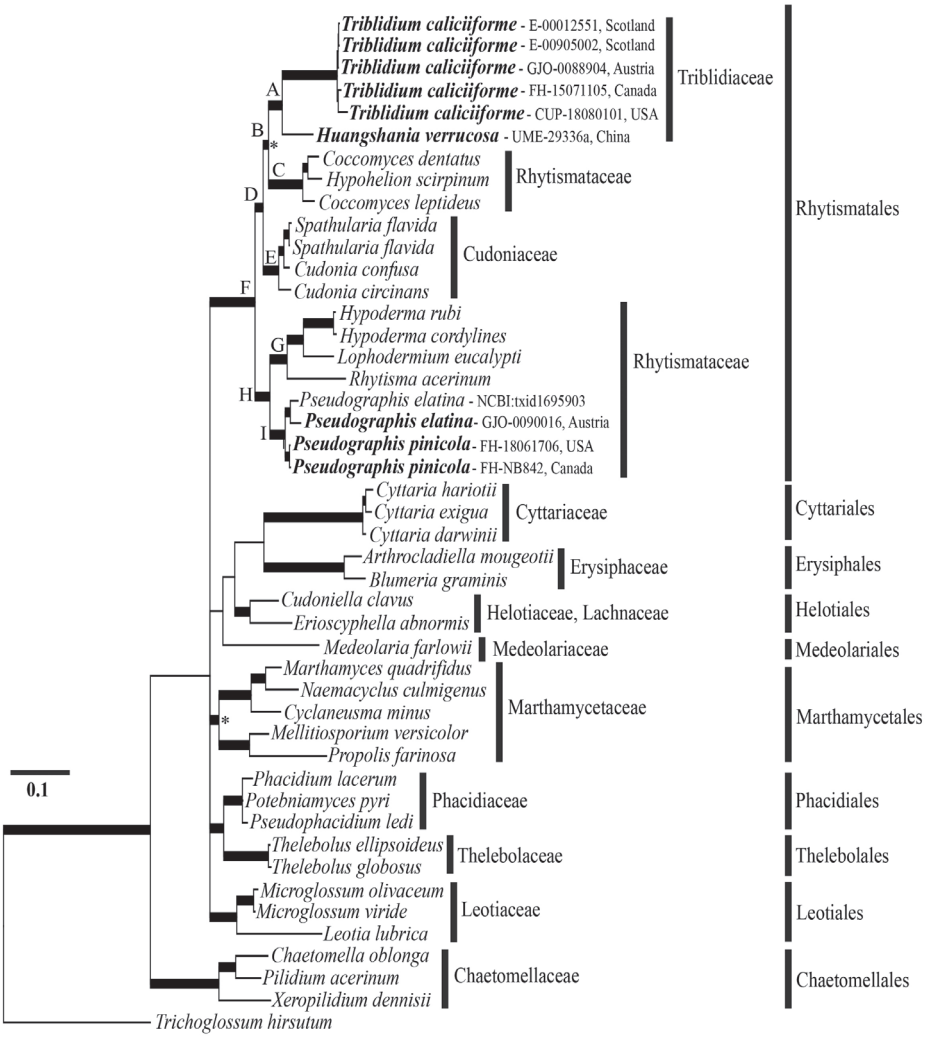

Figure 3. Bayesian majority-rule consensus tree of Leotiomycetes based on the ITS1-5.8S-ITS2 + LSU + mtSSU region. Thickened branches are those that were well supported by ML and BI methods. An asterisk indicates that this branch was supported only by Bayesian inference. Classification, orders and families follows Baral in Jaklitsch et al. (2016) using *Trichoglossum hirsutum* as the outgroup. Species for which molecular sequences have been generated for this study are given in bold followed by fungarium acronym, a dash, then identifying number.

Description of Rhytismataceae including characters of *Pseudographis* species

An expanded morphological description of this family includes characters of muriform ascospores (in *P. elatina*, Fig. 2i–k, p–r) and ascospore surfaces that react intensely dark blue/purple in iodine-based reagents (Fig. 2k, m, p, r) (Magnes 1997: 54; Baral in Jaklitsch et al. 2016: 192–194).

Specimens examined

Specimens also examined by Magnes (1997) are denoted by an asterisk (*).

Triblidiaceae

Triblidium caliciiforme. Austria, Burgenland, Günser Mountains, Oberwart district, Markt Neuhodis, 545 m, 11 Mar 2018, on bark of living *Quercus petraea*, G. Friebes GJO-0088904. Canada, New Brunswick, Protected Natural Area south-east of Cranberry Lake, 94 m, 11 Jul 2015, on decorticated branch still attached to living *Quercus rubra*, J. M. Karakehian FH-15071105 (FH). Scotland, Mid-Perth (VC 88), south side of Loch Earn, Ardvorlich Woods, 26 Aug 1981, on *Quercus* bark, B. J. Coppins 8659, E-00012551 (E)*. VC 96 Easterness, Aviemore, Torr Alvie SSSI: Bogach carr, 220 m, 23 Sept 2008, on *Salix*, B. J. Coppins and C. J. Ellis [Coppins 22725] E-00905002 (E). United States of America, New York, Ringwood Preserve, 448 m, 1 Aug 2018, on bark of living *Quercus alba*, J. M. Karakehian CUP-18080101 (CUP). —*Huangshania verrucosa*. China, Anhwei, Huangshan Mountains, not far from Yun-gu Si, 1 Nov 1980, on bark of *Pinus* sp., O. E. Eriksson 8001101-2a (UME-29336a, isotype)*.

Rhytismataceae, *Pseudographis*

Pseudographis elatina. Austria, Styria, Styrian border mountains, Koralpe, Reinischkogelzug Bezirk Deutschlandsberg, 1080 m, 30 Mar 2018, on bark of living *Abies alba*, G. Friebes GJO-0090016. —*Pseudographis pinicola*. Canada, New Brunswick, Charlotte County, Little Lepreau, 28 Sept 2016, on bark of living *Larix laricina*, J. Tanney FH-NB842 (FH). United States of America, New Hampshire, White Mountain National Forest, Mt. Washington, Tuckerman Ravine Trail, 1058 m, 17 Jun 2018, on bark of fallen log of *Picea* sp., J. M. Karakehian FH-18061706 (FH).

Discussion

Recent molecular phylogenetic studies in *Pseudographis* and our results.

Two molecular phylogenetic studies of Leotiomycetes have included isolates of *Pseudographis elatina*. These are Prieto et al. (2018) and Johnston et al. (2019). In their five-gene phylogeny, Prieto et al. (2018) used two genes derived from a *P. elatina* genome, but did not provide an accession number identifying the source of this data. Their phylogeny demonstrated that this *P. elatina* isolate grouped with three other species of Rhytismatales in a well-supported clade and they claimed that their results "confirmed" inclusion of Triblidiales within Leotiomycetes. This finding was incidental to their primary result of identifying the first lichenized lineage within Leotiomycetes. In their 15-gene phylogeny, Johnston et al. (2019) included data from *P. elatina* genome NCBI:txid1695903. Based

upon the results of their analysis, they placed Triblidiaceae within Rhytismatales. The results reported by Prieto et al. (2018) and Johnston et al. (2019) support the inclusion of *Pseudographis* within Rhytismatales. However, conclusions regarding the placement of Triblidiaceae within Rhytismatales are speculative. Triblidiales is typified by Triblidiaceae that is, in turn, typified by *Triblidium* and not *Pseudographis*.

Regarding the *P. elatina* genome NCBI:txid1695903, we were initially unable to find any information about the material from which this genome was sequenced. However, we learned that the genome was derived from a culture: CBS 651.97 (Joseph Spatafora pers. com.). The CBS database provides information on the specimen from which the culture was established (Oregon, USA; on bark of living *Pseudotsuga menziesii*; Verkley and Sherwood; October 13, 1996; no. 509), but there is no indication of where this specimen is deposited. We were unable to locate it through online searches.

We included three gene sequences from the *P. elatina* genome (NCBI:txid1695903) in our phylogenetic analysis. Our results indicate that this isolate of *P. elatina* is conspecific with our Austrian isolate (GJO-0090016) (Fig. 3, clade I). Furthermore, our study demonstrates that *Pseudographis* does not cluster with *Triblidium* (Fig. 3, clade A), but with other genera circumscribed within Rhytismataceae.

Magnes (1997) proposed classifying Triblidiaceae in Rhytismatales. The results of our phylogenetic analysis partially support his hypothesis. Triblidiaceae is a monophyletic family composed of *Triblidium* and *Huangshania* (Fig. 3, clade A) that groups within the radiate clade of Rhytismatales (Lantz et al. 2011). *Pseudographis* is not part of Triblidiaceae (Fig. 3, clade F) and groups within the bilateral clade of Rhytismatales (Lantz et al. 2011) (Fig. 3, clade H). According to these results, we have emended the concept of Triblidiaceae and expanded the circumscription of Rhytismataceae to include species of *Pseudographis*. These possess a character novel to the family: ascospore cell walls that produce a strong blue/purple reaction in iodine-based reagents.

Triblidialean fungi in taxonomic manuals

Triblidialean fungi are not generally treated in modern taxonomic works. Magnes (1997: 16–17) noted that the last most detailed study of *Triblidium* and *Pseudographis* was Rehm's (1887–1896). Dennis (1981) treated these fungi only superficially. They are not in Korf's (1973) key to discomycetes and Magnes (1997: 8) claimed that this omission is one of the most important reasons that these fungi have been rarely collected, identified, and deposited in herbaria. Though they are not treated in the lichenological literature, lichenologists may encounter and collect triblidialean fungi as they co-occur in the same habitat as some corticolous and lignicolous lichens.

The occurrence of triblidialean fungi

Whether a species is common or rare is a question that often arises. Are they rare or are they rarely collected? Regarding triblidialean fungi in Northeastern United States,

J.M.K. searched approximately 30 *Picea rubens* trees for *P. pinicola* in New Hampshire in June, 2018, and made one collection from an individual tree. In August of that year, in the state of New York, J.M.K. searched approximately 20 *Quercus alba* trees for *T. caliciiforme* and made one collection, as well as one collection of an undescribed *Triblidium* species on a different tree. In May, 2018, J.M.K. visited Newfoundland, Canada to search for a specimen of *Huangshania novae-fundlandiae* in the type locality and, together with a small group of experienced local botanists, searched approximately two dozen *Pinus strobus* trees with no result. Our experiences, at least in Northeastern United States, suggest that these fungi are not abundant.

In contrast, it seems that collecting in Europe may be more productive with various species. There are many collections made by Magnes (1997) in Austria and our co-author, G.F., has supplied many fresh collections for this study from some of Magnes's collecting sites. Observations of other European specimens may be accessed through Baral (2019).

Potential impact of host tree diseases on distribution of triblidialean fungi

Diseases carried by introduced plants or imported forest products may affect the current and future distribution of triblidialean fungi. Triblidialean fungi are host restricted within woody angiosperms and gymnosperms as far as is known. As an example of narrow host preference we can point to *T. caliciiforme* and our undescribed *Triblidium* species, both of which occur primarily on *Quercus*. Fungal diseases that cause bark decay on living oak trees may impact populations of *Triblidium*. These are referred to as "smooth patch" diseases. They cause the decomposition and sloughing of the rough outer bark, forming regions that are slightly sunken, smooth and lighter in color than surrounding regions. As these regions expand and become confluent on the trunk they become extensive. Smooth patch diseases are caused by species of *Aleurodiscus*, *Dendrothele*, and *Hyphoderma* (all Agaricomycetes, Basidiomycota) (Sinclair and Lyon 2005: 520). Additionally, *Bretziella fagacearum*, causal agent of oak wilt disease, and *Lachnellula willkommii*, causal agent of European larch canker, are both examples of alien invasive species introduced to North America that cause disease and mortality on triblidialean host tree species.

On the occurrence of paraphysoids in *Rhytismatales*

The literature is incomplete regarding the occurrence of paraphysoids in Rhytismatales. Nannfeldt (1932: 314) thought that paraphysoids did not occur in *Triblidium* and disagreed with Rehm on the subject. Hawksworth and Sherwood (1982: 264) did not comment on their occurrence in *Triblidium* or *Pseudographis* (Magnes 1997:8). Eriksson (1992: 9) observed paraphysoids in *Huangshania*, and noted them in *Triblidium* and *Pseudographis*. However, he thought they were absent in species of Rhytismatales and therefore declined to place Triblidiaceae within this order, despite similarities in ascus structure.

Magnes (1997: 5, 11–12) noted the occurrence of paraphysoids in Rhytismatales by his own observations of *Triblidiopsis pinastri* and considered them a key taxonomic feature of triblidialean fungi. For further documentation, he cited Arx and Müller (1954: 131) who discussed ascomatal development in Hypodermataceae Rehm [= Rhytismataceae]. More supportive, Magnes also cited Gordon (1966: 319–320, 1968: 49) on centrum development in Hypodermataceae that demonstrate the presence of paraphysoids in species of *Lophodermium*. We note that Bellemère (1967) described paraphysoids in the development of ascomata in *Therrya fuckelii* (pp. 417–427) and *Colpoma juniperi* (pp. 443–451). Clearly, additional work is needed to document the occurrence of paraphysoids in Rhytismatales.

On the trophic status of triblidialean fungi and potential endophytism

Little is clearly understood about the trophic mode of triblidialean fungi. Some species, such as *T. caliciiforme* and *P. pinicola*, grow readily on standard culture media (Karakehian, pers. obs.). We presume that ascospores of triblidialean fungi colonize dead woody tissues, especially bark of both living and dead trees, and that they are saprobes. Sherwood (1981: 19) observed that the ascomata of many lignicolous discomycetes inhabit substrata that do not appear to be degraded or affected in any way. This is certainly the case among triblidialean fungi, where ascomata form just below the surface of apparently non-degraded bark and from which they ultimately erupt (see diagram in Rehm 1888: 193, fig. c). We speculate that these fungi exist as a protected, diffuse mycelium growing within bark or the cork cambium, from where they periodically extend hyphae to the surface of the outer bark to produce ascomata. They may also colonize living woody plant tissues and exist as latent saprobes in an endophytic state.

Life histories characterized by alternating endophyte-saprotroph trophic modes are reported among phylogenetically diverse Ascomycota families, for example Dermateaceae (Chen et al. 2016), Mollisiaceae (Kowalski and Kehr 1995; Tanney et al. 2016), Tympanidaceae (Kowalski and Kehr 1992), and Xylariaceae (Okane et al. 2008). Endophytism is common in foliar Rhytismataceae species and is reported in some Rhytismataceae species that produce apothecia exclusively from woody substrates. For example, *Coccomyces strobi* commonly forms apothecia on dead, self-pruned branches of *Pinus strobus* and is also reported as a foliar endophyte on the same host (McMullin et al. 2019). Tanney et al. (2018) mentioned the isolation of *Coccomyces irretitus* as a foliar endophyte of *Picea rubens*; *C. irretitus* is a bark- and decorticated wood-inhabiting species that is, coincidentally, easily mistaken for *Pseudographis* species in the field. *Tryblidiopsis* species occur on *Picea* and occupy a similar ecological niche as *C. strobi*, occurring as ubiquitous saprotrophs on self-pruned branches but also as endophytes of leaves, cambium, and bark (Kowalski and Kehr 1992; Barklund and Kowalski 1996; Tanney and Seifert 2019). Similarly, *Therrya* species are reported as branch endophytes and implicated in self-pruning of branches in *Pinus* (Kowalski and Kehr 1992; Solheim et al. 2013). *Colpoma quercinum* is one of the most commonly isolated branch endophytes from *Quercus robur* and is associated with branch pruning (Butin and

Kowalski 1983; Kehr and Wulf 1993; Agostinelli et al. 2018). These examples describe a life history strategy that allows the fungus to gain entry into the host (e.g. via foliar infection or branch wounds) and colonize and persist endophytically within cambium and bark until conditions, such as the physiological status of the host substrata, become suitable for more extensive saprotrophic (or weakly parasitic) colonization and subsequent reproduction (Tanney et al. 2016). This latent endophytic colonization likely explains why apothecia of branch-associated Rhytismataceae species are observed soon after branch death, for example caused by shading or physical damage (e.g. lightning; Solheim et al. 2013).

There is currently little evidence of endophytism in triblidialean fungi, although Magnes (1997) conjectured that *Triblidium* species associated with ericaceous shrubs (e.g. *T. carestiae* and *T. hafellneri*) are endophytic based on the rapid formation of apothecia following twig death. That triblidialean life histories are poorly understood is expected given their apparent rarity and the overall paucity of studies investigating branch endophytes and bark fungi associated with triblidialean hosts (e.g. Pinaceae and Ericaceae). The lack of available reference sequences also means that triblidialean species would be unidentifiable in sequence-based studies. Thus, future work should involve ascertaining the extent of host tissue colonization by triblidialean species, for example, isolating from various stem and branch tissues of living hosts exhibiting triblidialean apothecia. Reference sequences generated from this current study will facilitate identification of triblidialean species in future metabarcoding studies and also aid in testing the endophyte hypothesis.

In xeric habitats, wood-inhabiting fungi may not gain the entirety of their nutrition from the degradation of the substrate. It is possible that other sources such as leachates from foliage or epiphytic lichens, insect exudates or bird droppings may come into play. Some of these fungi may also be deriving nutrition from casual associations with algae (Sherwood 1981: 19), as is speculated in *Xerotrema megalospora* (Sherwood and Coppins 1980: 370). From our observations, interaction between algae and triblidialean fungi seems unlikely and it is not known in other Rhytismatales.

Ascospore morphology of triblidialean fungi

The inclusion of *Triblidium*, *Pseudographis* and *Huangshania* in Rhytismatales introduces ascospore morphologies that were not previously found in the order. We discuss these spore characters because they are novel in the context of non-lichenized, inoperculate discomycetes. These morphologies include: muriform ascospores in *Triblidium* and *Pseudographis*, the virtually opaque dark blue/purple reaction in the ascospore wall in iodine-based reagents in *Pseudographis*, and the large, regularly spaced verrucae and polar cell "plugs" in ascospores of *Huangshania verrucosa*.

As outlined in our History, previous classifications have placed *Triblidium* and *Pseudographis* among various groups that now comprise Dothideomycetes, Lecanoromycetes and Leotiomycetes. This has been due in part to an overestimation of the taxonomic significance of their peculiar ascospore characters. Muriform ascospores

are more frequently observed in taxa belonging to Lecanoromycetes and Dothideomycetes, and ascospores that display a bluing reaction in iodine-based reagents are commonly observed in Lecanoromycetes, particularly in Graphidaceae (Ostropales) (Fig. 4a). In light of our phylogenetic approach to the classification of this group, we may claim with a greater degree of confidence that these ascospore morphologies have arisen independently within Leotiomycetes.

In order to gain an overview of ascospore morphology within Rhytismatales, we reviewed each genus using a current classification of the order that contains three families: Cudoniaceae, Marthamycetaceae, and Rhytismataceae (Baral in Jaklitsch et al. 2016: 190–194). We generated a spreadsheet of 74 genera, including *Angelina* (Rhytismataceae) (Karakehian et al. 2014), *Triblidium, Huangshania* (both Triblidiaceae) and *Pseudographis* (Rhytismataceae) that were not listed in the published classification under Rhytismatales. We excluded *Tridens*, which has muriform spores and that clearly belongs in Dothideomycetes based on a review of literature and morphological observations of material in FH (Karakehian pers. obs.).

Excluding triblidialean fungi, ascospores of Rhytismatales are generally characterized as hyaline, smooth, filiform, aseptate, enclosed within a gelatinous sheath and supplied with rounded, gelatinous caps at the poles. Many species of commonly encountered genera such as *Rhytisma*, *Coccomyces* and *Colpoma* share this morphology. However, in many genera ellipsoid, cylindric, clavate, fusiform, or hourglass-shaped (bifusoid) ascospores are found. The presence or absence of a gelatinous sheath also varies widely. Ascospore color such as dusky-grays or browns, as well as gelatinous appendages, are reported in a handful of genera (Baral in Jaklitsch et al. 2016: 190–194).

Muriform ascospores, as observed in *Triblidium* and *Pseudographis elatina*, are known in one other genus currently placed in Rhytismatales, *Mellitiosporium* (Fig. 4b). A sequence from a specimen of *M. versicolor*, the type species of the genus according to Dennis (1981: 37 [Addenda and corrigenda]), was included in a gene phylogeny of Rhytismatales by Lantz et al. (2011). *Mellitiosporium* and a handful of other genera were placed in Marthamycetaceae, erected in 2015. This family will be removed from Rhytismatales to its own order, Marthamycetales, based on the results of a study by Johnston et al. (2019). *Triblidium* (Triblidiaceae) and *Pseudographis* (Rhytismataceae) will remain the only genera within Rhytismatales whose members possess muriform spores.

Across Leotiomycetes, muriform ascospores are rare. Nannfeldt (1932: 314) claimed that muriform ascospores were found only in a few species of Helotiales (sensu Nannfeldt) and Korf (1973) observed that their occurrence was so rare and "…almost unheard of… (p. 294)" in discomycetes that "… one should immediately suspect he has a bitunicate ascomycete in hand if they are found (p. 253)." However, Baral in Jaklitsch et al. (2016: 165–166) noted that, in regards to Dermateaceae (Helotiales), ascospores may become "septate to muriform." We reviewed the work of Baral in Jaklitsch et al. (2016: 157–205), Korf (1973), Sherwood (1981: 20–21) and Dennis (1981) for the presence of muriform ascospores in Leotiomycetes. We found that, in addition to *Mellitiosporium* and Baral's observation regarding Dermateaceae (probably referring to *Pezicula*), that muriform ascospores are also observed in members of *Claussenomyces* (Tympanidaceae) (Fig. 4c–e) and in *Waltonia pinicola* (Helotiales *incertae sedis*).

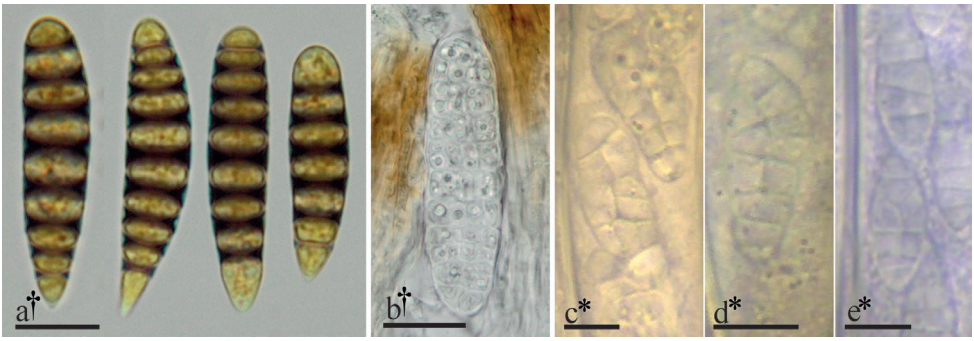

Figure 4. Select examples of ascospore morphologies in Graphidaceae and Leotiomycetes **a** ascospores of *Glyphis cicatricosa* in Lugol's solution **b** muriform ascospore of *Mellitiosporium versicolor* **c–e** muriform ascospores of *Claussenomyces* spp. within living, immature asci. All microphotographs of cells and tissues mounted in water unless otherwise noted. † = dead, * = living. Scale bars: 10 µm (**a**); 20 µm (**b**); 5 µm = (**c–e**). Specimens photographed: a = J.M.K personal collection; b = U.S.A., Oregon, Horse Rock Ridge, M. A. Sherwood, L. H. Pike & D. Wagner, 21 Mar 1979, FH [s.n.], image courtesy of Farlow Herbarium of Harvard University; **c–e** = L.Q. personal collections.

The taxonomic significance of ascospore septation should be considered with caution. Although spore septation has been used as a character in fungal classification it is unreliable as a single trait. Both muriform and transverse-septate ascospores are observed among species of the same genus in Graphidaceae (Staiger et al. 2006: 769–771). This is the case in other groups of lichens (Lumbsch et al. 1997; Nelson et al. 2014; Luangsuphabool et al. 2018) as well as in non-lichenized taxa (Mugambi and Huhndorf 2009). In the triblidialean fungi, among species of *Pseudographis* we observe muriform spores in *P. elatina* and strictly transverse-septate spores in *P. pinicola*.

Muriform ascospores may have adaptive significance in harsh terrestrial ecosystems where suspended, exposed bark and wood are potential substrata for colonization. All non-lichenized muriform-spored discomycetes occur in this habitat (Sherwood 1981: 26). Calhim et al. (2018) analyzed spore morphology in relation to trophic modes and substrate associations. Their results indicated that in regards to evolutionary drivers of spore morphology, deposition of undamaged spores on specific substrates is more strongly selected for than is spore dispersal. Large, muriform ascospores of the type produced by *Triblidium* species represent an evolutionary approach to the mitigation of damage that may occur during spore transport and deposition. Gregory (1961: 82) stated that deposition by wind impaction is more efficient for large spores and Sherwood (1981: 25) noted that longitudinal and transverse septa increase structural stability, eliminating the need for a very thick wall.

Muriform spores may also present advantages in the efficient colonization of substratum. The larger number of cells in muriform ascospores increase the chances of successful colonization even if some cells are damaged in transport or deposition (Sherwood 1981: 26). Furthermore, rapid colonization may be achieved by the simultaneous germination of many cells. The germ tubes form an advancing perimeter of hyphae around the deposited spore (Fig. 1j). Finally, if not every cell germinates at once, and

if the ascospore happens to be dislodged during germination or if conditions turn adverse before the fungus becomes established, then the ungerminated cells may represent additional chances for successful colonization.

The intense blue/purple reaction of the ascospores of *Pseudographis* species in iodine reagents is unique within Leotiomycetes. There are no other species within Rhytismatales that share this character. In Leotiomycetes, a tepid blue or blue-green reaction is reported in spores of *Strossmayeria* and in the related species *Durella connivens* (both Helotiales, *Strossmayeria* lineage) (Baral in Jaklitsch et al. 2016: 176–177).

In the ascospores of *Strossmayeria* species, the reaction appears to be erratic. It is not entirely clear to us if it occurs in the ascospore wall, gel sheath, or both. Iturriaga and Korf (1990: 383) stated that the blue reaction of the ascospores is a "rare phenomenon in Ascomycetes". It occurs in both ascospores and ectal excipulum. It is generally lighter in the ascospores and is highly variable in that it may be fleeting, long-lasting or not occurring for hours. The reaction was reported to be stronger in asci containing mature ascospores (possibly due to agglomeration), and was particularly strong in the ascospore and gel layer of *S. jamaicensis* (p. 433). We attempted to observe the blue reaction in material collected in 2016 from Mozambique. This failed even with KOH pretreatment. We then tried with dried material from FH that was 30 years old and observed an extremely faint reaction in only a few asci that contained mature-appearing ascospores.

Though the ascospore iodine reaction is equally intense in *Pseudographis* species and many species of lichenized Ascomycota in Graphidaceae (Ostropales, Lecanoromycetes), the reaction is localized differently in the spore walls of the two groups. In *Pseudographis*, the reaction is entirely uniform across the ascospore surface. In undiluted iodine reagent mounts the coloring may be so opaque that the septa are obscured even at the highest illumination settings in transmitted light microscopy. The reacting material presumably occurs within the cell wall or in some coating on the very surface of the ascospore (Fig. 2k, m, p, r). In comparison, in ascospores of Graphidaceae species, the spore walls are laminate, with a non-reactive outer spore wall and a reactive inner wall that stains dark blue/purple black. This reactive material surrounds the inner cells, and the lumina and cell walls of these remain clearly observable in light microscopy even in undiluted iodine reagents (Fig. 4a).

The dark-blue/purple reaction in *Pseudographis* ascospores leads to questions regarding the composition and structure of the reacting substance, as well as its biological role. Because the quality of the staining reaction appears to be analogous to what is observed in the cell walls and surface ornamentations of basidiospores in genera such as *Lentinellus*, *Russula* and *Amanita* in Agaricomycetes (Basidiomycota), we began to address these questions by searching for literature on amyloid reactions in Basidiomycota.

Dodd and McCracken (1972) reported on the molecular structure and biological role of polysaccharides in selected Agaricomycetes genera that possess amyloid basidiospores and basidiome tissues. The authors proposed that the starch on the surface of basidiospores may act as a permeability barrier to maintain dormancy. A thin layer of amylose molecules (one of two components of starch) may serve as an oxygen barrier, slowing metabolism and thus conserving nutrients within the spore. As the amylose

molecules are cold-water soluble, when environmental conditions are humid the layer will dissolve to some threshold degree that allows oxygen to diffuse into the spore. Thus, basidiospores remain dormant and viable for a period until environmental conditions are optimal for growth.

Are *Pseudographis* ascospores enveloped in a starch-based, degradable film? Basic research in the chemistry and physical properties of these films as water and oxygen barriers in biodegradable food packaging may offer some insights (Rindlav-Westling et al. 1998; Stading et al. 2001; Forssell et al. 2002). Starch-based films are hydrophilic and their water permeabilities are affected by humidity. Water sorption occurs naturally in these films. A proposed mechanism for increased oxygen and water permeability in starch-based films is that as water is taken up, the network of crystalized strands in the film becomes heterogeneous. The film swells as humidity increases and pores of various sizes form. Oxygen permeability increases dramatically at approximately 60–70% ambient humidity (Stading et al. 2001: 209, 212). This model of starch-film modification and permeability is alternative to the one proposed by Dodd and McCracken (1972), where some component of starch is removed. Ascospores enveloped in a hygroscopic film is a conceivable adaptation to the xeric substrates and habitats characteristic of triblidialean species.

To conclude our Discussion, we will discuss ascospore wall sculpturing and the terminal cell structures observed in *Huangshania verrucosa* (Fig. 1r–t). There are no other species within Rhytismatales with ascospore surface sculpturing. This feature is rare within the related order Helotiales (Leotiomycetes) with ascospores of *Drepanopeziza verrucispora* with acute spines and *Mollisia dextrinospora* ornamented by fine verrucae, for example.

The evolutionary and ecological significance of spore ornamentation is only beginning to be addressed by recent research. However, Pringle et al. (2015: 214) stated that to their knowledge, there is no research on the evolutionary origin of spore ornamentation, or even whether smooth spores represent a loss from an ornamented ancestral state. Both Halbwachs et al. (2015) and Calhim et al. (2018) demonstrated that spore ornamentation occurred more frequently in ectomycorrhizal genera than in saprobic ones. Halbwachs et al. (2015 p. 198), citing Lilleskov and Bruns (2005), speculated that spore ornamentation may facilitate adhesion to invertebrate exoskeletons in the delivery of spores of ectomycorrhizal species deep enough into the soil to germinate near fine root tips of host species.

How then might spore ornamentation be advantageous for saprobic species that colonize above-ground substrates? In light of the system described by Reynolds (2013), wherein passively dispersed organisms travel only so far as to the nearest unoccupied location from the parent in order to escape depleted resources, but not so far away as to leave behind a resource pool that is reliable and predictable, we may consider that ascospores of *H. verrucosa* do not travel far from parent ascomata. This implies that bark is the preferred substratum on which ascospores are to be deposited due to impaction. We may then speculate that the roughened ascospore surface may be an adaptation to facilitate adhesion to bark or other woody tissues. The increased adhesive quality of

the ascospores might prevent them from being dislodged by wash-out or wind during deposition as well as subsequent germination and colonization phases.

In *H. verrucosa* there is an extension of the sporoplast or an otherwise differentiated structure in the terminal cells of ascospores (Eriksson 1992: 4). We also observed this feature (Fig. 1p, r). Magnes (1997: 77) described these as round appendages approximately 2 µm wide. Eriksson (1992: 4, fig. 3, 7) described them as "firm, subspherical to conical, plug-like appendages." They do not differentially stain in Congo red or in cotton blue in lactophenol. Without data from ascospore germination experiments it is unknown if these structures may act as germ pores. Excluding triblidalean fungi, ascospores in Rhytismatales are predominantly thin-walled, and we are not aware of the occurrence of germ pores in any taxon in the order.

Conclusion

The history of Triblidiaceae is one among many cases in systematic mycology of the challenges present in the classification of fungi that result from the use of seemingly distinctive morphological characters, such as ascospore morphology, that are unreliable when tested using molecular phylogenetic methods. Our research supports Magnes's hypothesis of the relationship of *Triblidium*, *Huangshania* and *Pseudographis* within Rhytismatales. However, we have restricted his concept of Triblidiaceae to circumscribe *Triblidium* and *Huangshania* and we have expanded the circumscription of Rhytismataceae to include *Pseudographis*. Our results have allowed us to investigate ecosystem pressures that have selected for these distinctive ascospore morphologies from a phylogenetically informed perspective. Discomycetes inhabiting desiccated standing or suspended dead wood or bark substrata face the same rigors as epiphytic lichens and lichenicolous fungi. These have convergently evolved many ascomatal features that are unique to this habitat and differ from those discomycetes that occur in mesic habitats. These characters include dark, stromatic excipular tissues that close over the hymenium in dry conditions, pigmented epithecia (exudates), and muriform ascospores (Sherwood 1981: 15–16). Molecular phylogenetic methods and more comprehensive taxon sampling may produce more robust hypotheses of evolutionary relationships under a phylogenetic species concept (Taylor et al. 2000). This approach, combined with analysis of morphology in the context of the severe constraints imposed by the habitat, may aid in elucidating testable questions in the biology and ecology of these organisms.

Acknowledgements

Thank you to our reviewers Hans-Otto Baral and David W. Minter. Kanchi N. Gandhi for advising us on nomenclature. Hans-Otto Baral for suggestions on ascospore morphologies. Thank you to Joey Spatafora for permission to use data from the *P. elatina* genome and for providing us with information on its origin, as well as Peter

Johnston for sharing with us sequences extracted from this genome and for his communications. Ove E. Eriksson for his assistance with specimens of *H. verrucosa* and in our search for *H. novae-fundlandiae* as well as Adrus and Maria Voitk and everyone at Foray Newfoundland and Labrador who came out and helped to look for this fungus. Henrik Lantz and Martin Magnes for kindly responding to our various questions. James K. Mitchell and Katherine LoBuglio for helpful input. Stephen Clayden and staff of New Brunswick Museum, Saint John, New Brunswick. David Malloch for permission to collect *P. pinicola* on his property. Dan Sperduto, Erica Roberts and Clare R. Mendelsohn at White Mountain National Forest, New Hampshire, for their assistance in obtaining a research permit to collect on Mt. Washington. Kathie Hodge for introducing us to historic Ringwood Preserve in New York. Judy Warnement, Gretchen Wade, Diane Rielinger and staff at Harvard Botany Libraries. Michaela Schmull, Genevieve Tocci and Hannah Merchant at FH. Curators and collections staff at the following institutions for their professionalism and timely processing our loan requests: B, BPI, CUP, E, F, GJO, GZU, K, L, M, MICH, MPU, NY, NYS, O, PDD, PH, S, UME, UPS and W. Luis Quijada acknowledges Fundación Ramón Areces for his postdoctoral funding.

Funding for this project was provided by New Brunswick Museum Florence M. Christie Research Fellowship in Mycology, and the Friends of the Farlow Reference Library and Herbarium of Cryptogamic Botany of Harvard University Graduate Student Fellowship.

References

Agostinelli M, Cleary M, Martín JA, Albrectsen BR, Witzell J (2018) Pedunculate oaks (*Quercus robur* L.) differing in vitality as reservoirs for fungal biodiversity. Frontiers in Microbiology 9: 1758. https://doi.org/10.3389/fmicb.2018.01758

Akaike H (1974) A new look at the statistical model identification. IEEE transactions on Automatic Control 19: 716–723. https://doi.org/10.1109/TAC.1974.1100705

Altschul SF, Gish W, Miller W, Myers EW, Lipman DJ (1990) Basic local alignment search tool. Journal of Molecular Biology 215: 403–410. https://doi.org/10.1016/S0022-2836(05)80360-2

Arx J, Müller E (1954) Die Gattungen der amerosporen Pyrenomyceten. Beiträge zur Kryptogamenflora der Schweiz 11: 1–434. https://hdl.handle.net/2027/mdp.39015006930849

Baral H-O (1987) Lugol's solution/IKI versus Melzer's reagent: Hemiamyloidity, a universal feature of the ascus wall. Mycotaxon 29: 399–450.

Baral H-O (1992) Vital versus herbarium taxonomy: morphological differences between living and dead cells of ascomycetes, and their taxonomic implications. Mycotaxon 44: 333–390.

Baral H-O (2019) In vivo veritas. Ascomycetes taxonomy website. https://in-vivo-veritas.de [Accessed on: 2019-5-17]

Barklund P, Kowalski T (1996) Endophytic fungi in branches of Norway spruce with particular reference to *Tryblidiopsis pinastri*. Canadian Journal of Botany 74: 673–678. https://doi.org/10.1139/b96-085

Bellemère A (1967) Contribution a l'étude du développement de l'apothécie chez les discomycètes inoperculés. Bulletin Trimestriel de la Société Mycologique de France 83: 393–931.

Brown RW (1956) Composition of Scientific Words: A Manual of Methods and a Lexicon of Materials for the Practice of Logotechnics (Rev. ed.). Privately published, 882 pp. https://archive.org/details/compositionofsci00brow

Butin H, Kowalski T (1983) Die natürliche Astreinigung und ihre biologischen Voraussetzungen: II. Die Pilzflora der Stieleiche (*Quercus robur* L.) 1. European Journal of Forest Pathology 13: 428–439. https://doi.org/10.1111/j.1439-0329.1983.tb00145.x

Calhim S, Halme P, Petersen JH, Læssøe T, Bässler C, Heilmann-Clausen J (2018) Fungal spore diversity reflects substrate-specific deposition challenges. Scientific Reports 8: 5356–5365. https://doi.org/10.1038/s41598-018-23292-8

Castresana J (2000) Selection of conserved blocks from multiple alignments for their use in phylogenetic analysis. Molecular Biology and Evolution 17: 540–552. https://doi.org/10.1093/oxfordjournals.molbev.a026334

Chen C, Verkley GJ, Sun G, Groenewald JZ, Crous PW (2016) Redefining common endophytes and plant pathogens in *Neofabraea*, *Pezicula*, and related genera. Fungal Biology 120: 1291–1322. https://doi.org/10.1016/j.funbio.2015.09.013

Clark K, Karsch-Mizrachi I, Lipman DJ, Ostell J, Sayers EW (2015) GenBank. Nucleic acids research 44 (D1): D67–72. https://doi.org/10.1093/nar/gkv1276

de Notaris G (1847) Prime linee di una nuova disposizione de' Pirenomiceti Isterini. Giornale Botanico Italiano 2: 5–52.

de Notaris G (1864) Proposte di alcune rettificazioni al profilo dei Discomiceti. Commentario della Societa Crittogamologica Italiana 5: 357–388.

Dennis RWG (1981) British Ascomycetes (Rev. ed.). Cramer, Vaduz, 585 pp.

Dodd JL, McCracken DA (1972) Starch in Fungi. Its molecular structure in three genera and an hypothesis concerning its physiological role. Mycologia 64: 1341–1343. https://doi.org/10.1080/00275514.1972.12019387

Dring DM (1971) Techniques for microscopic preparation. In: Booth C (Ed.) Methods in microbiology, Vol. 4. Academic Press, London, 95–111. https://doi.org/10.1016/S0580-9517(09)70008-X

Dufour ML (1828) Notice sur deux cryptogames peu connues et nouvelles pour la flore française. Annales des sciences naturelles; botanique 13: 319–322, pl. 10.

Eriksson OE (1992) *Huangshania verrucosa* gen. et sp. nov. (Triblidiaceae, Triblidiales ordo nov.), a discomycete on *Pinus* from China. Systema Ascomycetum 11: 1–10.

Eriksson OE, Hawksworth DL (1991) Outline of the ascomycetes – 1990. Systema Ascomycetum 9: 39–271.

Farell EM, Alexandre G (2012) Bovine serum albumin further enhances the effects of organic solvents on increased yield of polymerase chain reaction of GC-rich templates. BMC Research Notes 5: 257–265. https://doi.org/10.1186/1756-0500-5-257

Farr DF, Rossman AY (2019) Fungal Databases, U.S. National Fungus Collections, ARS, USDA, Fungus-Host Distributions. https://nt.ars-grin.gov/fungaldatabases/fungushost/FungusHost.cfm [Accessed on: 2019-02-15]

Forssell P, Lahtinen R, Lahelin M, Myllärinen P (2002) Oxygen permeability of amylose and amylopectin films. Carbohydrate Polymers 47: 125–129. https://doi.org/10.1016/S0144-8617(01)00175-8

Fries EM (1823) Systema mycologicum, sistens fungorum ordines, genera et species, hucusque cognitas, quas ad normam methodi naturalis determinavit, disposuit atque descripsit Elias Fries (Vol. II). Sumptibus Ernesti Mauritii, Gryphiswaldiae, 621 pp. http://bibdigital.rjb.csic.es/ing/Libro.php?Libro=958&Pagina=1

Fries EM (1828) Elenchus Fungorum, sistens commentarium in Systema mycologicum (Vol. II). Sumptibus Ernesti Mauritii, Gryphiswaldiae, 154 pp. http://bibdigital.rjb.csic.es/ing/Libro.php?Libro=3066&Pagina=1

Fries EM (1832) Index alphabeticus generum, specierum et synonymorum in Eliae Fries systemate mycologico ejusque supplemento "Elencho fungorum" enumeratum. Sumptibus Ernesti Mauritii, Gryphiswaldiae, 202 pp. [Appended to end of Systema Mycologicum, vol. 3]. http://bibdigital.rjb.csic.es/ing/Libro.php?Libro=959&Pagina=533

Gardes M, Bruns TD (1993) ITS primers with enhanced specificity for Basidiomycetes: application to the identification of mycorrhizae and rusts. Molecular Ecology 2: 113–118. https://doi.org/10.1111/j.1365-294X.1993.tb00005.x

Gray P (1954) The microtomist's formulary and guide. The Blakiston Company, Inc, 1–794. https://archive.org/details/microtomistsform00gray

Gordon CC (1966) Ascocarpic centrum ontogeny of species of Hypodermataceae of conifers. American Journal of Botany 53: 319–327. https://doi.org/10.1002/j.1537-2197.1966.tb07342.x

Gordon CC (1968) Ascocarpic centrum ontogeny of species of Hypodermataceae of conifers. II. American Journal of Botany 55: 45–52. https://doi.org/10.1002/j.1537-2197.1968.tb06943.x

Gregory PH (1961) The microbiology of the atmosphere. Leonard Hill [Books] and Interscience Publishers, London, 251 pp. https://archive.org/details/microbiologyofat00greg

Halbwachs H, Brandl R, Bässler C (2015) Spore wall traits of ectomycorrhizal and saprotrophic agarics may mirror their distinct lifestyles. Fungal Ecology 17: 197–204. https://doi.org/10.1016/j.funeco.2014.10.003

Hawksworth DL, Sherwood MA (1982) Two new families in the Ascomycotina. Mycotaxon 16: 262–264.

Hawksworth DL, Sutton BC, Ainsworth GC (1983) Ainsworth & Bisby's Dictionary of the Fungi (7th edn). Commonwealth Mycological Institute, Kew, 445 pp.

Höhnel F von (1909) Fragmente zur Mykologie (VI. Mitteilung, Nr. 182 bis 288). Sitzungsberichte der Kaiserlichen Akademie der Wissenschaften. Mathematisch-naturwissenschaftliche Classe, Abteilung 1, 118: 1–178 [275–452].

Höhnel F von (1910) Fragmente zur Mykologie (XI. Mitteilung, Nr. 527 bis 573). Sitzungsberichte der Kaiserlichen Akademie der Wissenschaften. Wien. Mathematisch-naturwissenschaftliche Classe, Abteilung 1, 119: 1–63 [617–679].

Höhnel F von (1918) Mycologische Fragmente. Annales Mycologici 16: 35–174.

Höhnel F von (1924) Über die systematische Stellung der Gattungen *Tympanis* Tode, *Scleroderris* Fr., *Godronia* Moug., und *Asterocalyx* Höhn [Postumously published by J. Weese]. Mitteilungen aus dem Botanischen Institut der Technischen Hochschule in Wien 1: 67–70.

IDT [Integrated DNA Technologies] (2019) OligoAnalyzer. https://www.idtdna.com/calc/analyzer

Iturriaga T, Korf RP (1990) A monograph of the discomycete genus *Strossmayeria* (Leotiaceae), with comments on its anamorph, *Pseudospiropes* (Dematiaceae). Mycotaxon 36: 383–454.

Jaklitsch W, Baral H-O, Lücking R, Lumbsch HT (2016) Syllabus of plant families. In: Frey W (Ed.) Adolf Engler's Syllabus der Pflanzenfamilien. Part 1/2 Ascomycota (13th edn). Borntraeger Science Publishers, Stuttgart, 322 pp. https://www.schweizerbart.de/publications/detail/isbn/9783443010898/Syllabus_of_Plant_Families_Part_1_2_A

Johnston PR, Quijada L, Smith CA, Baral H-O, Hosoya T, Baschien C, Pärtel K, Zhuang WY, Haelewaters D, Park D, Carl S, López-Giráldez F, Wang Z, Townsend JP (2019) A multigene phylogeny toward a new phylogenetic classification of Leotiomycetes. IMA Fungus 1: 1–22. https://doi.org/10.1186/s43008-019-0002-x

Karakehian JM, LoBuglio K, Pfister DH (2014) Placement of the genus *Angelina* within Rhytismatales and observations of *Angelina rufescens*. Mycologia 106: 154–162. https://doi.org/10.3852/13-174

Katoh K, Misawa K, Kuma K, Miyata T (2002) MAFFT, a novel method for rapid multiple sequence alignment based on fast Fourier transform. Nucleic Acid Research 30: 3059–3066. https://doi.org/10.1093/nar/gkf436

Katoh K, Toh H (2008) Improved accuracy of multiple ncRNA alignment by incorporating structural information into a MAFFT-based framework. BMC Bioinformatics 9: 212. https://doi.org/10.1186/1471-2105-9-212

Kearse M, Moir R, Wilson A, Stones-Havas S, Cheung M, Sturrock S, Buxton S, Cooper A, Markowitz S, Duran C, Thierer T, Ashton B, Mentjies P, Drummond A (2012) Geneious Basic: an integrated and extendable desktop software platform for the organization and analysis of sequence data. Bioinformatics 28: 1647–1649. https://doi.org/10.1093/bioinformatics/bts199

Kehr RD, Wulf A (1993) Fungi associated with above-ground portions of declining oaks (*Quercus robur*) in Germany. European Journal of Forest Pathology 23: 18–27. https://doi.org/10.1111/j.1439-0329.1993.tb00803.x

Korf RP (1973) Discomycetes and Tuberales. In: Ainsworth GC, Sparrow FK, Sussman AS (Eds) The Fungi: An Advanced Treatise (Vol. 4a). Academic Press, London, 249–319.

Kowalski T, Kehr RD (1992) Endophytic fungal colonization of branch bases in several forest tree species. Sydowia 44: 137–168. https://www.zobodat.at/pdf/Sydowia_44_0137-0168.pdf

Kowalski T, Kehr RD (1995) Two new species of *Phialocephala* occurring on *Picea* and *Alnus*. Canadian Journal of Botany 73: 26–32. https://doi.org/10.1139/b95-004

Lantz H, Johnston PR, Park D, Minter DW (2011) Molecular phylogeny reveals a core clade of Rhytismatales. Mycologia 103: 57–74. https://doi.org/10.3852/10-060

Largent D, Johnson D, Watling R (1977) How to Identify Mushrooms to Genus III: Microscopic Features. Mad River Press, Eureka, 148 pp.

Leonard LM (2006) Melzer's, Lugol's or iodine for identification of white-spored Agaricales? McIlvainea 16: 43–51. https://www.namyco.org/docs/Melzer__Lugo.pdf

Liddell HG, Scott R (1875) Greek-English Lexicon (6th edn). Clarendon Press, Oxford, 1865 pp.

Lilleskov EA, Bruns TD (2005) Spore dispersal of a resupinate ectomycorrhizal fungus, *Tomentella sublilacina*, via soil food webs. Mycologia 97: 762–769. https://doi.org/10.1080/15572536.2006.11832767

Luangsuphabool L, Lumbsch HT, Piapukiew J, Sangvichien E (2018) *Architrypethelium murisporum* (Ascomycota, Trypetheliaceae), a remarkable new lichen species from Thailand challenging ascospore septation as an indicator of phylogenetic relationships. MycoKeys 34: 25–34. https://doi.org/10.3897/mycokeys.34.23836

Lumbsch HT, Guderley R, Feige GB (1997) Ascospore septation in *Diploschistes* (Thelotremataceae, lichenized Ascomycota) and the taxonomic significance of macro- and microcephalic ascospore types. Plant Systematics and Evolution 205: 179–184. https://doi.org/10.1007/BF01464403

Magnes M (1997) Weltmonographie der Triblidiaceae. Bibliotheca Mycologica, 165. J. Cramer, Berlin, 177 pp. https://www.schweizerbart.de/publications/detail/isbn/9783443590673/Bibliotheca_Mycologica_Band_165

McMullin DR, Tanney JB, McDonald KP, Miller JD (2019) Phthalides produced by *Coccomyces strobi* (Rhytismataceae, Rhytismatales) isolated from needles of *Pinus strobus*. Phytochemistry Letters 29: 17–24. https://doi.org/10.1016/j.phytol.2018.10.016

Mushroom Observer (2019) https://mushroomobserver.org [Accessed on: 2019-1-15]

Mugambi GK, Huhndorf SM (2009) Molecular phylogenetics of Pleosporales: Melanommataceae and Lophiostomataceae re-circumscribed (Pleosporomycetidae, Dothideomycetes, Ascomycota). Studies in Mycology 64: 103–121. https://doi.org/10.3114/sim.2009.64.05

MyCoPortal (2019) Mycology Collections data Portal. http://mycoportal.org/portal/index.php [Accessed on: 2019-01-15]

Nannfeldt JA (1932) Studien über die Morphologie und Systematik der nicht-lichenisierten inoperculaten Discomyceten. Nova Acta Regiae Societatis Scientiarum Upsaliensis (Ser. 4) 8: 1–368. [23 tables]

Nelson MP, Lücking R, Aptroot A, Andrew CJ, Cáceres M, Plata ER, Gueidan C, da Silva Canêz L, Knight A, Ludwig, LR, Mercado-Díaz JA, Parnmen S, Lumbsch HT (2014) Elucidating phylogenetic relationships and genus-level classification within the fungal family Trypetheliaceae (Ascomycota: Dothideomycetes). Taxon 63: 974–992. https://doi.org/10.12705/635.9

Okane I, Srikitikulchai P, Toyama K, Læssøe T, Sivichai S, Hywel-Jones N, Nakagiri A, Potacharoen W, Suzuki KI (2008) Study of endophytic Xylariaceae in Thailand: diversity and taxonomy inferred from rDNA sequence analyses with saprobes forming fruit bodies in the field. Mycoscience 49: 359–372. https://doi.org/10.1007/S10267-008-0440-6

Posada D (2008) jModelTest: phylogenetic model averaging. Molecular Biology and Evolution 25: 1253–1256. https://doi.org/10.1093/molbev/msn083

Prieto M, Schultz M, Olariaga I, Wedin M (2018) *Lichinodium* is a new lichenized lineage in the Leotiomycetes. Fungal Diversity 94: 23–39. https://doi.org/10.1007/s13225-018-0417-5

Pringle A, Vellinga E, Peay K (2015) The shape of fungal ecology: Does spore morphology give clues to a species' niche? [Commentary]. Fungal Ecology 17: 213–216. https://doi.org/10.1016/j.funeco.2015.04.005

Quijada L, Baral H-O, Jaen-Molina R, Weiss M, Caujapé-Castells J, Beltrán-Tejera E (2014) Phylogenetic and morphological circumscription of the *Orbilia aurantiorubra* group. Phytotaxa 175(1): 1–18. https://doi.org/10.11646/phytotaxa.175.1.1

Rebentisch JF (1805) Index plantarum circum Berolinum sponte nascentium adiectis aliquot fungorum descriptionibus. Fr. Schüppel, 1–46. https://books.google.com/books?vid=HARVARD:32044106330269

Rehm H (1887–1896) Die Pilze Deutschlands, Oesterreichs und der Schweiz. III. Abtheilung: Ascomyceten: Hysteriaceae und Discomyceten. In Dr. L. Rabenhorst's Kryptogamen-Flora von Deutschland, Oesterreich und der Schweiz. 2nd ed. Bd 1: Abt. 3. Leipzig, Verlag von Eduard Kummer, 1275 pp. https://doi.org/10.5962/bhl.title.1356

Rehm H (1904) Revision der Gattungen *Tryblidiella* Sacc., *Rhytidhysterium* Speg., *Tryblidaria* Sacc., *Tryblidium* Rebent., *Tryblidiopsis* Karst. Annales Mycologici 2: 522–526. https://books.google.com/books?id=IfYEAAAAYAAJ

Rehm H (1912) Zur Kenntnis der Discomyceten Deutschlands, Deutsch-Österreichs und der Schweiz. Berichte der Bayerischen Botanischen Gesellschaft zur Erforschung der Heimischen Flora 13: 102–206.

Reynolds AM (2013) Beating the odds in the aerial lottery: Passive dispersers select conditions at takeoff that maximize their expected fitness on landing. The American Naturalist 181: 555–561. https://doi.org/10.1086/669677

Rindlav-Westling Å, Stading M, Hermansson A-M, Gatenholm P (1998) Structure, mechanical and barrier properties of amylose and amylopectin films. Carbohydrate Polymers 36: 217–224. https://doi.org/10.1016/S0144-8617(98)00025-3

Saccardo PA (1883) Sylloge Fungorum omnium hucusque cognitorum (Vol. 2). Padua, 815 pp. https://doi.org/10.5962/bhl.title.80010

Saccardo PA (1889) Sylloge Fungorum omnium hucusque cognitorum (Vol. 8). Padua, 1143 pp. https://biodiversitylibrary.org/page/32882632

Sass JE (1958) Botanical microtechnique (3rd edn). The Iowa State University Press, Ames, 228 pp.

Sequencher (2012) DNA sequence analysis software (Version 5.1) [Software]. Gene Codes Corporation, Ann Arbor, Michigan. http://www.genecodes.com

Schoch CL, Seifert KA, Huhndorf S, Robert V, Spouge JL, Levesque CA, Chen W, Fungal Barcoding Consortium (2012) Nuclear ribosomal internal transcribed spacer (ITS) region as a universal DNA barcode marker for Fungi. Proceedings of the National Academy of Sciences 109: 6241–6246. https://doi.org/10.1073/pnas.1117018109

Sherwood MA (1977) The ostropalean fungi. Mycotaxon 5: 1–277.

Sherwood MA (1980) Taxonomic studies in the Phacidiales: the genus *Coccomyces* (Rhytismataceae). Occasional Papers of the Farlow Herbarium of Cryptogamic Botany 15: 1–120. https://biodiversitylibrary.org/page/7449817

Sherwood MA (1981) Convergent evolution in discomycetes from bark and wood. Botanical Journal of the Linnean Society 82: 15–34. https://doi.org/10.1111/j.1095-8339.1981.tb00948.x

Sherwood-Pike MA (1987) The ostropalean fungi III: the Odontotremataceae. Mycotaxon 28: 137–177.

Sherwood MA, Coppins BJ (1980) *Xerotrema*, a new genus of odontotremoid fungus from Scotland. Notes of the Royal Botanic Garden, Edinburgh 38: 367–371.

Sinclair WA, Lyon HH (2005) Diseases of Trees and Shrubs (2nd edn). Cornell University Press, Ithaca, 660 pp.

Solheim H, Torp TB, Hietala AM (2013) Characterization of the ascomycetes *Therrya fuckelii* and *T. pini* fruiting on Scots pine branches in Nordic countries. Mycological Progress 12: 37–44. https://doi.org/10.1007/s11557-012-0813-2

Stading M, Rindlav-Westling Å, Gatenholm P (2001) Humidity-induced structural transitions in amylose and amylopectin films. Carbohydrate Polymers 45: 209–217. https://doi.org/10.1016/S0144-8617(00)00242-3

Stafleu FA, Cowan RS (1983) Taxonomic literature: a selective guide to botanical publications and collections with dates, commentaries and types (2nd edn) [TL2] (Vol. 4). Scheltema & Holkema, Bohn, 1214 pp. https://www.sil.si.edu/DigitalCollections/tl-2/index.cfm

Staiger B, Kalb K, Grube M (2006) Phylogeny and phenotypic variation in the lichen family Graphidaceae (Ostropomycetidae, Ascomycota). Mycological Research 110: 765–772. https://doi.org/10.1016/j.mycres.2006.05.003

Stearn WT (2010) Botanical Latin (4th edn). Timber Press, Portland, 546 pp.

Talavera G, Castresana J (2007) Improvement of phylogenies after removing divergent and ambiguously aligned blocks from protein sequence alignments. Systematic Biology 56: 564–577. https://doi.org/10.1080/10635150701472164

Tanney JB, Douglas B, Seifert KA (2016) Sexual and asexual states of some endophytic *Phialocephala* species of *Picea*. Mycologia 108: 255–280. https://doi.org/10.3852/15-136

Tanney JB, McMullin DR, Miller JD (2018) Toxigenic foliar endophytes from the Acadian Forest. In: Pirttilä AM, Frank AC (Eds) Endophytes of Forest Trees: Biology and Applications (2nd edn). Springer, Netherlands, 343–381. https://doi.org/10.1007/978-3-319-89833-9_15

Tanney JB, Seifert KA (2019) *Tryblidiopsis magnesii* sp. nov. from Picea glauca in Eastern Canada. Fungal Systematics and Evolution 4: 13–20. https://doi.org/10.3114/fuse.2019.04.02

Taylor JW, Jacobson DJ, Kroken S, Kasuga T, Geiser DM, Hibbett DS, Fisher MC (2000) Phylogenetic species recognition and species concepts in Fungi. Fungal Genetics and Biology 31: 21–32. https://doi.org/10.1006/fgbi.2000.1228

Turland NJ, Wiersema JH, Barrie FR, Greuter W, Hawksworth DL, Herendeen PS, Knapp S, Kusber WH, Li DZ, Marhold K, May TW, McNeill J, Monro AM, Prado J, Price MJ, Smith GF (eds.) (2018) International Code of Nomenclature for algae, fungi, and plants (Shenzhen Code) adopted by the Nineteenth International Botanical Congress Shenzhen, China, July 2017. Regnum Vegetabile 159. Koeltz Botanical Books, Glashütten, 254 pp. https://doi.org/10.12705/Code.2018

Vilgalys R (2018) Conserved primer sequences for PCR amplification of fungal rDNA. Vilgalys Mycology Lab, Duke University. https://sites.duke.edu/vilgalyslab/rdna_primers_for_fungi [Accessed on: 2019-1-15]

Vilgalys R, Hester M (1990) Rapid genetic identification and mapping of enzymatically amplified ribosomal DNA from several *Cryptococcus* species. Journal of Bacteriology 172: 4238–4246. https://doi.org/10.1128/jb.172.8.4238-4246.1990

White TJ, Bruns TD, Lee S, Taylor J (1990) Amplification and direct sequencing of fungal ribosomal RNA genes for phylogenetics. In: Innis MA, Gelfand DH, Sninsky JJ, White TJ (Eds) PCR Protocols, a Guide to Methods and Applications. Academic Press, San Diego, 315–322. https://doi.org/10.1016/B978-0-12-372180-8.50042-1

Zoller S, Scheidegger C, Sperisen C (1999) PCR primers for the amplification of mitochondrial small subunit ribosomal DNA of lichen-forming ascomycetes. Lichenologist 31: 511–516. https://doi.org/10.1006/lich.1999.0220